Kiwifruit Bacterial Canker: Exploring Tolerance Mechanisms and Novel Control Strategies

Marta Alexandra Nunes da Silva

Doutoramento em Ciências Agrárias

Departamento de Geociências, Ambiente e Ordenamento do Território

2021

Supervisor

Susana M. P. Carvalho, Assistant Professor, Faculty of Sciences, University of Porto

Co-supervisor

Marta W. Vasconcelos, Assistant Professor, School of Biotechnology, Catholic University of Portugal

Co-supervisor

Giorgio M. Balestra, Assistant Professor, Department of Agriculture and Forest Sciences, Tuscia University

Acknowledgements

To my supervisor, Prof. Dr. Susana M. P. Carvalho and my co-supervisor Prof. Dr. Marta W. Vasconcelos, for all the support, enthusiasm, and all the interesting and insightful discussions, for always pointing me in the right direction, even when things did not go the best way, for giving me the freedom to follow my own steps and backing me up whenever needed, thank you.

To my co-supervisor, Prof. Dr. Giorgio M. Balestra, for the valuable insights and inputs, and for always welcoming me in the warmest way possible during my visits to Tuscia University, thank you.

To Fundação Portuguesa para a Ciência e a Tecnologia, which financed the work presented in this thesis through the project PSAlert (Ref.: PTDC/AGR-PRO/6156/2014), and through my Individual PhD Scholarship (Ref.: SFRH/BD/99853/2014), thank you.

To my laboratory mates, for all the brainstorming, support, laughs and cries, thank you.

To Carla, whom apart from being my colleague has also become one of my closest friends, for her example, guidance, assurance, and for being in this journey with me during the past 10 years, thank you.

To all my friends, for always supporting me and lifting my spirit in stressful times, thank you.

To my boyfriend, for his relentless support, for never questioning my life decisions, and for always driving me forward, although not fully understanding what I was stressing about half of the time, thank you.

Mais importante de tudo, aos meus pais, por sempre lutarem para me proporcionar a melhor educação possível, por sempre apoiarem o meu modo de vida e as escolhas que faço, por serem minha rede de segurança e por me proporcionarem tudo sem pedir nada em troca, obrigada. Seria impossível fazer isto sem vocês.

Abstract

The kiwifruit bacterial canker (KBC), caused by *Pseudomonas syringae* pv. *actinidiae* (Psa), is currently the most destructive disease of kiwifruit plants (*Actinidia* spp.). Psa is considered a worldwide pandemic pathogen and is present in all main kiwifruit producing countries, including China, New Zealand, Italy, Chile, Portugal, Spain, and France, leading to significant economic impacts. Plant infection occurs through natural and artificial openings, causing leaf spotting, wilting, canker formation, and often leading to plant death. Empirical observations suggest that the genetically close bacterium *P. syringae* pv. *actinidifoliorum* (Pfm) is less virulent to kiwifruit plants, not causing significant production losses, but inducing the appearance of necrotic spots, but this has never been appropriately proven in laboratory conditions. Psa and Pfm must be properly managed for optimal crop performance, but current disease management strategies are only preventive, relying on removing infected plant material and applying antibiotic or cupric formulations, which often have limited efficacy or environmental impacts. Moreover, field evidence points out to a higher susceptibility of *A. chinensis* (green and yellow kiwifruits) to this disease, as compared with *A. arguta* (kiwi berry), but the reasons behind the distinct tolerances to KBC are still poorly understood. These knowledge gaps greatly limit the options to develop novel disease management strategies and to exploit plant genetic and metabolic resources to achieve higher tolerance to this disease. In light of this, the major aims of this PhD thesis were to: i) evaluate the susceptibility of different *Actinidia* species to Psa and Pfm; ii) unravel plant tolerance mechanisms against Psa; and iii) explore novel and sustainable strategies to mitigate the disease.

To assess plant genotypic variability to KBC and evaluate the virulence degree of Psa and Pfm, micropropagated *A. chinensis* and *A. arguta* plants were artificially infected with either pathogen. Following inoculation, a higher endophytic bacterial density was observed in *A. chinensis* (particularly of Psa), which was accompanied by a greater extent of disease symptoms, decreased total chlorophylls and increased lipid peroxidation. Moreover, in this species, Psa infection led to an upregulation of the ammonia assimilation cycle, most likely to exploit plant metabolic resources for its own needs. These results demonstrate for the first time in controlled conditions that *A. arguta* is more tolerant to Psa infection than *A. chinensis*, and that Psa is more virulent than Pfm to kiwifruit plants, thus validating field observations.

To understand plant responses to Psa, targeted gene expression (RT-qPCR), whole transcriptome (RNA-Seq) and metabolomic analysis were carried out. Results revealed that following Psa infection, distinct defence-related responses were activated in *A. chinensis* and *A. arguta*, namely related with pathogen recognition, scavenging of reactive oxygen species, the phenylpropanoids pathway and phytohormone regulation, which may account for the distinct tolerance degree of these plant species. In particular, results suggest that phytohormone regulation (particularly pertaining to jasmonic - JA, salicylic - SA, and abscisic acids - ABA) plays a key role in the distinct tolerance of *A. chinensis* and *A. arguta*. Following Psa infection: JA and SA concentrations increased 2 days post-inoculation (dpi) in *A. chinensis*, but not in *A. arguta*, ABA concentration

decreased 2 dpi in *A. arguta* and 15 dpi in *A. chinensis*, and elicitation of the JA pathway increased ABA concentration and disease susceptibility in *A. chinensis*, whereas elicitation with SA did not. Overall, data suggest that in *A. arguta* defence responses are activated at an earlier stage following infection and/or in a more efficient way than in *A. chinensis*, through faster recognition of the pathogen, a more complex antioxidant response at earlier stages of infection, tissue reinforcement with lignin, and downregulation of the ABA pathway. Moreover, several genes involved in key regulatory and defence pathways were found to be upregulated only in *A. arguta*, including *EDM2*, *FOX1*, *GLOX* and *SN2*, possibly contributing to its higher tolerance to Psa.

In *A. chinensis*, Psa impaired the accumulation of glutamine and ornithine and the expression of genes involved in nitrogen (N) metabolism, such as *GAD1*, *GAD4*, *GLU1* and *GLN1*. Taking into consideration these results and previous studies that showed the influence of N nutrition on plant susceptibility to pests and diseases, it was hypothesized that the manipulation of the N source could lead to higher Psa tolerance. *A. chinensis* plants grown with nitrate (NO_3^-) as the N source and inoculated with Psa showed lower bacterial colonization, improved plant photosynthetic capacity and mineral nutrition, as compared with ammonium (NH_4^+). In plants grown under NH_4^+ supply, total N concentration in shoot tissues was higher, and genes related to the JA and ethylene (ET) pathways were upregulated. These results suggest that: i) NH_4^+ may be unfavourable to *A. chinensis* defence mechanisms by increasing N accumulation in plant tissues (which favours Psa growth), and by promoting JA and ET-related pathways (that negatively affect plant defences), and ii) NO_3^- could provide an adaptative advantage in cases of Psa infection by decreasing N concentration in plant tissues and improving plant mineral nutrition.

Finally, an *in vitro* evaluation of the antimicrobial potential of six plant essential oils (PEOs) (anise, basil, cardamom, cumin, fennel and laurel) against Psa and Pfm revealed that all of them successfully inhibited bacterial growth, with cumin being generally more effective at lower concentrations. Foliar application of cumin PEO at 0.1% 15 days before infection with Psa, led to a 73% decrease of Psa endophytic population (at 15 dpi). These results support the consideration of PEOs as tools for more sustainable disease management strategies, either by complementing or by substituting the currently used treatments.

Taken together, the findings of this thesis provide innovative knowledge on the regulatory pathways triggered by Psa infection in *Actinidia* spp., and demonstrate the relevance of N nutrition in kiwifruit plants susceptibility to Psa. Moreover, they also highlight the potential contribution of PEOs and elicitors to a more successful and sustainable Psa management.

Keywords: *Actinidia chinensis*, *Actinidia arguta*, nitrogen metabolism, phytohormones, plant essential oils, primary metabolism, *Pseudomonas syringae* pv. *actinidiae*, *Pseudomonas syringae* pv. *actinidifoliorum*, tolerance, transcriptome

Resumo

O cancro bacteriano do kiwi (CBK), causado pela *Pseudomonas syringae* pv. *actinidiae* (Psa), é atualmente a doença mais destrutiva da cultura do kiwi (*Actinidia* spp.). A Psa é considerada um patogénio mundialmente pandémico, estando presente em todos os principais países produtores de kiwi (incluindo China, Nova Zelândia, Itália, Chile, Portugal, Espanha e França), causando impactos económicos significativos. A infeção ocorre através de aberturas naturais e artificiais da planta, causando necrose nas folhas, murchidão, formação de cancros e, frequentemente, morte da planta. Observações empíricas sugerem que a bactéria geneticamente próxima *P. syringae* pv. *actinidifoliorum* (Pfm) é menos virulenta para as plantas de kiwi, não causando perdas de produção significativas, mas induzindo o aparecimento de manchas necróticas. No entanto, esta evidência nunca foi devidamente comprovada em condições laboratoriais. A Psa e a Pfm devem ser adequadamente geridas para promover o desempenho ideal da cultura, mas as estratégias atuais de controlo da doença são apenas preventivas, envolvendo a aplicação de antibióticos ou formulações cúpricas, que geralmente têm eficácia limitada ou impactos ambientais. Evidências de campo apontam ainda para uma maior suscetibilidade de *A. chinensis* (kiwi verde e amarelo), em comparação com *A. arguta* (kiwi bebé), mas as razões da distinta tolerância ao KBC são ainda pouco conhecidas. Estas lacunas no conhecimento limitam o desenvolvimento de novas estratégias de gestão da doença, e a compreensão dos fatores genéticos e metabólicos responsáveis pela maior tolerância de determinados genótipos à doença. Assim, os principais objetivos desta tese de doutoramento foram: i) avaliar a suscetibilidade de diferentes espécies de *Actinidia* à Psa e à Pfm; ii) explorar os mecanismos de tolerância da planta contra a Psa; e iii) identificar novas estratégias para o controlo sustentável da doença.

Para avaliar a variabilidade interespecífica ao CBK e o grau de virulência da Psa e Pfm, plantas micropropagadas de *A. chinensis* e *A. arguta* foram artificialmente infetadas com um dos patogénios. Após inoculação, observou-se uma maior densidade bacteriana endofítica em *A. chinensis* (particularmente de Psa), acompanhada por uma maior extensão dos sintomas da doença, diminuição das clorofilas totais e aumento da peroxidação lipídica. Nesta espécie, a infeção por Psa levou ainda a uma regulação positiva do ciclo de assimilação de amónia. Estes resultados demonstram pela primeira vez em condições controladas que *A. arguta* é mais tolerante à infeção por Psa do que *A. chinensis*, e que a Psa é mais virulenta do que a Pfm, validando assim observações de campo.

Por forma a compreender os mecanismos de tolerância à Psa, foram realizadas análises de expressão génica direcionada (RT-qPCR), de transcritoma total (RNA-Seq) e metabolómicas. Após infeção por Psa, respostas distintas relacionadas com a defesa foram ativadas em *A. chinensis* e *A. arguta*, nomeadamente relacionadas com o reconhecimento de patogénios, eliminação de espécies reativas de oxigénio, via dos fenilpropanóides e regulação de fitohormonas. Em particular, os resultados sugerem que a regulação de fitohormonas (particularmente dos ácidos jasmónico - AJ, salicílico - AS e abscísico - ABA) desempenha um papel fundamental na tolerância distinta de *A. chinensis* e *A. arguta* à Psa. Após infeção, as concentrações de AJ e AS aumentaram

em *A. chinensis*, mas não em *A. Arguta*. Já a concentração de ABA diminuiu 2 dias pós infeção (dpi) em *A. arguta* e apenas 15 dpi em *A. chinensis*, e a elicitação da via do AJ aumentou a concentração de ABA e a suscetibilidade à doença em *A. chinensis*, enquanto que a elicitação da via do AS não. Globalmente, os dados sugerem que em *A. arguta* as respostas de defesa são ativadas num estado inicial após a infeção ou de forma mais eficiente do que em *A. chinensis*, através de: um reconhecimento mais rápido do patogénio, uma resposta antioxidante mais complexa nos estados iniciais da infeção, reforço do tecido com lenhina, e regulação negativa da via do ABA. Adicionalmente, vários genes envolvidos nas principais vias regulatórias e de defesa das plantas foram sobre expressos apenas em *A. arguta*, incluindo os genes *EDM2*, *FOX1*, *GLOX* e *SN2*, possivelmente contribuindo para sua maior tolerância à Psa.

Em *A. chinensis*, a Psa diminuiu a acumulação de glutamina e ornitina, e aumentou a expressão de genes envolvidos no metabolismo do azoto (N), tais como como *GAD1*, *GAD4*, *GLU1* e *GLN1*. Tendo em consideração estes resultados e estudos anteriores que mostraram a influência da nutrição de N na suscetibilidade das plantas a pragas e doenças, foi formulada a hipótese de que a manipulação da fonte de N poderia levar a uma maior tolerância à Psa. Plantas de *A. chinensis* crescidas com nitrato (NO_3^-) como fonte de N e inoculadas com Psa apresentaram menor colonização bacteriana, melhor capacidade fotossintética e nutrição mineral, em comparação com amónia (NH_4^+). Nas plantas sob fornecimento de NH_4^+, a concentração total de N aumentou nos tecidos da parte aérea, e genes relacionados com as vias do AJ e do etileno (ET) foram sobre expressos. Estes resultados sugerem que: i) a NH_4^+ pode ser desfavorável aos mecanismos de defesa de *A. chinensis* por aumentar a concentração de N nos tecidos da planta (o que favorece o crescimento de Psa), e por promover vias relacionadas com o AJ e ET (que afetam negativamente as defesas da planta), e ii) o NO_3^- pode constituir uma vantagem adaptativa em casos de infeção por Psa, diminuindo a concentração de N e melhorando a nutrição mineral da planta.

Por fim, o potencial antimicrobiano de seis óleos essenciais (OE) de plantas (anis, basílico, cardamomo, cominho, funcho e louro) foi comprovado *in vitro* contra a Psa e a Pfm, sendo que o cominho foi geralmente mais eficaz. A aplicação foliar de OE de cominho a 0,1% 15 dias antes da infeção, levou a uma diminuição de 73% da população endofítica de Psa (15 dpi). Estes resultados suportam o interesse da utilização dos OEs como ferramenta mais sustentável de gestão da doença, como complemento ou substituição dos tratamentos usados atualmente.

No seu conjunto, os resultados desta tese fornecem conhecimento inovador sobre as vias regulatórias desencadeadas pela infeção por Psa em *Actinidia* spp., e demonstram a importância da fonte de N na suscetibilidade das plantas de kiwi ao patogénio. Estes destacam ainda a potencial contribuição dos OEs e dos elicitadores à base de fitohormonas para uma gestão mais eficaz e sustentável da Psa.

Palavras-chave: *Actinidia chinensis*, *Actinidia arguta*, metabolismo do azoto, fito hormonas, metabolismo primário, óleos essenciais de plantas, *Pseudomonas syringae* pv*. actinidiae*, *Pseudomonas syringae* pv. *actinidifoliorum*, tolerância, transcritoma

Publications and Communications

Publications in international peer-reviewed journals:

Nunes da Silva, M., Vasconcelos, M.W., Pinto, V., Balestra, G.M., Mazzaglia, A., Carvalho, S.M.P. (2021) Role of methyl jasmonate and salicylic acid in kiwifruit plants further subjected to Psa infection: biochemical and genetic responses. *Plant Physiology and Biochemistry*, 162, 258–266. DOI: 10.1016/j.plaphy.2021.02.045.

Nunes da Silva, M., Vasconcelos, M., Gaspar, M., Balestra, G.M., Mazzaglia, A., Carvalho, S.M.P. (2020) Early pathogen recognition and antioxidant system activation contributes to *Actinidia arguta* tolerance against *Pseudomonas syringae* pathovars *Actinidiae* and *actinidifoliorum*. *Frontiers in Plant Science* 11, 1022. DOI: 10.3389/fpls.2020.01022.

Nunes da Silva, M., Machado, J., Balestra, G.M., Mazzaglia, A., Vasconcelos, M.W. Carvalho, S.M.P. (2019) Exploring the expression of defence-related genes in *Actinidia* spp. after infection with *Pseudomonas syringae* pv. *actinidiae* and pv. *actinidifoliorum*: first steps. *European Journal of Horticultural Science*, 84, 206-212. DOI: 10.17660/ejhs.2019/84.4.2.

Under submission:

Nunes da Silva, M., Santos, M.G., Vasconcelos, M.W., Carvalho, S.M.P. (2021) Kiwifruit bacterial canker: current knowledge on disease dynamics and on plant defence mechanisms.

Nunes da Silva, M., Vasconcelos, M.W., Fernandes, A.P.G., Valente, L.M.P., Carvalho, S.M.P. (2021). Nitrogen source impacts mineral accumulation and gene expression in young kiwifruit plants.

Nunes da Silva, M., Carvalho, S.M.P., António, C., Rodrigues, A.M., Gomez-Cadenas, A., Vasconcelos, M.W. (2021). Defence-related pathways, phytohormones and primary metabolism are key players in the distinct tolerance of *Actinidia chinensis* and *A. arguta* to *Pseudomonas syringae* pv. *actinidiae*.

Santos, M.G., Nunes da Silva, M., Vasconcelos, M.W., Carvalho, S.M.P. (2021). Kiwifruit bacterial canker: which paths have been taken for disease management and where are we going next?

Nunes da Silva, M., Fernandes, A.P.G., Valente, L.M.P., Vasconcelos, M.W., Carvalho, S.M.P. (2021). Influence of the nitrogen source on the tolerance of kiwifruit plants to *Pseudomonas syringae* pv. *actinidiae*.

Nunes da Silva, M., Vasconcelos, M.W., Balestra, G.M., Mazzaglia, A., Carvalho, S.M.P. Cumin essential oil reduces *Actinidia chinensis* infection by *Pseudomonas syringae* pv. *actinidiae*.

Oral communications in international conferences:

Nunes da Silva, M., Vasconcelos, M.W., Mazzaglia, A., Gomez-Cadenas, A., Balestra, G.M., Carvalho, S.M.P. (2019) Mechanisms underlying *A. chinensis* var. *deliciosa* defense responses against *Pseudomonas syringae* pv*. actinidiae* after methyl jasmonate and salicylic acid application. *4th International Symposium on Biological Control of Bacterial Plant Diseases*, Viterbo, Italy, 9-11 July 2019.

Nunes da Silva, M., Machado, J.F.F., Balestra, G.M., Mazzaglia, A., Vasconcelos, M.W., Carvalho, S.M.P. (2017) Exploring *Actinidia* spp. defence mechanisms against *Pseudomonas syringae* pv*. actinidiae* strains with distinct virulence. *IX International Symposium on Kiwifruit*, ISHS, Porto, Portugal, 6-9 September 2017.

Poster communications in international conferences:

Nunes da Silva, M., Carvalho, S.M.P., Vasconcelos, M.W. (2021). Defence-related pathways, phytohormones and primary metabolism are key players in the distinct tolerance of *Actinidia* spp. to *Pseudomonas syringae* pv. *actinidiae*. Second Plant Pests and Diseases Forum, Portugal, 24 March 2021.

Nunes da Silva, M., Fernandes, A.P.G., Vasconcelos, M.W.,Carvalho, S.M.P. (2020) Nitrate fertilization increases kiwifruit plant tolerance to *Pseudomonas syringae* pv*. actinidiae*. Encontro Ciência 20, Lisbon, Portugal, 4-5 November 2020.

Nunes da Silva, M., Vasconcelos, M.W., Mazzaglia, A., Balestra, G.M., Carvalho, S.M.P. (2019) Evaluation of the susceptibility *of A. chinensis* var. *deliciosa* and *A. arguta* var. *arguta* to *Pseudomonas syringae* pv*. actinidiae. XVI Spanish Portuguese Congress of Plant Physiology,* Pamplona, Spain, 26-28 June 2019.

Nunes da Silva, M., Machado, J., Balestra, G.M., Mazzaglia, A., Vasconcelos, M.W., Carvalho. S.M.P. (2017) Chemical characterization and antimicrobial activity of 6 plant essential oils against *Pseudomonas syringae* pv*. actinidiae* and *P. syringae* pv. *actinidifoliorum*. *IX International Symposium on Kiwifruit*, ISHS, Porto, Portugal, 6-9 September 2017.

Nunes da Silva, M., Machado, J., Balestra, G.M., Mazzaglia, A., Vasconcelos, M.W., Carvalho, S.M.P. (2017) Kiwifruit bacterial canker: novel insights on an old problem. *UK Council for Graduate Education Annual Conference,* Porto, Portugal, 6-7 July 2017.

Nunes da Silva, M., Nascimento, B., Correia, A., Teixeira, P., Balestra, G.M., Vasconcelos, M.W., Carvalho, S.M.P. (2016) Evaluation of natural antimicrobial agents against *Pseudomonas syringae* pv*. actinidiae*. *Annual Conference COST FA1106 "Quality Fruit*", Porto, Portugal. 6-8 October 2016.

Awards:

2017 - 3th Best Poster Presentation at the UK Council for Graduate Education Annual Conference (held by the UK Council for Graduate Education), 7 July 2017, Porto, Portugal.

2017 - Best Poster Presentation at the IX International Symposium on Kiwifruit (held by the International Society for Horticultural Science), 9 September 2017, Porto, Portugal.

Index

Acknowledgements i
Abstract iii
Resumo v
Publications and Communications vii
Index ix
Table list xv
Figure list xvii
Abbreviations, acronyms and chemical formulas xxi

CHAPTER 1 - GENERAL INTRODUCTION 1

Overview 3
Aim and outline of the thesis 4

Sub-chapter 1.1. Kiwifruit bacterial canker: current knowledge on disease dynamics and on plant defence mechanisms 7

1. Introduction 9
2. Disease dynamics 12
 2.1. Plant infection 12
 2.2. Symptoms and disease cycle 13
 2.3. Biotic and abiotic factors implicated in disease development 14
  2.3.1. Bacterial strain 14
  2.3.2. Plant genotype 15
  2.3.3. Edaphoclimatic conditions 16
  2.3.4. Orchard management practices 17
  2.3.5. Plant nutrition 19
3. Exploring plant tolerance mechanisms 20
 3.1. Plant defences 20
 3.2. Phytohormone regulation 23
 3.3. Primary and secondary metabolism 24
4. Conclusion 26

Sub-chapter 1.2. Kiwifruit Bacterial Canker: which paths have been taken for disease management and where are we going next? 27

1. Introduction 29
2. Antibiotic and copper-based treatments 31
3. Plant breeding 32
4. Forecast models 33
5. Early disease detection 34
6. Plant elicitors 36
7. Emerging molecules and compounds 37
 7.1. Plant extracts and essential oils 37
 7.2. Propolis 39
 7.3. Bacteriophages 39
 7.4. Antimicrobial peptides 40
8. Microbiota and other beneficial microorganisms 41

9. Gene editing 42
10. Conclusion 43

CHAPTER 2 - EVALUATION OF PLANT GENOTYPIC SUSCEPTIBILITY TO PSA 45

Sub-chapter 2.1. Exploring the expression of defence-related genes in *Actinidia* spp. after infection with *Pseudomonas syringae* pv. *actinidiae* and pv. *actinidifoliorum*: first steps 47

1. Introduction 49
2. Materials and methods 50
2.1. Plant maintenance 50
2.2. Bacterial suspension preparation and plant inoculation 51
2.3. Plant sampling 51
2.4. CFUs determination in plant tissues 51
2.5. Defence-related gene expression analysis 51
2.6. Statistical analysis 52
3. Results 53
4. Discussion 54
5. Conclusion 58

Sub-chapter 2.2. Early pathogen recognition and antioxidant system activation contributes to *Actinidia arguta* tolerance against Psa and Pfm 59

1. Introduction 61
2. Materials and methods 64
2.1. Plant maintenance and inoculation 64
2.2. Scoring of foliar symptoms and sampling 65
2.3. Endophytic bacterial population 65
2.4. Malondialdehyde 66
2.5. Primary and secondary metabolites 66
2.6. Gene expression 67
2.7. Statistical analysis 68
3. Results 69
3.1. Symptoms and colony-forming units 69
3.2. Primary and secondary metabolites 71
3.3. Gene expression 73
4. Discussion 76
4.1. Bacterial progression is more restricted in *A. arguta* 76
4.2. Primary and secondary metabolism is less impacted in *A. arguta* than in *A. chinensis* 77
4.3. Plant antioxidant system is activated earlier in *A. arguta* than in *A. chinensis* 78
4.4. *A. arguta* seems to identify and respond to Psa- and Pfm-infection from an earlier stage after plant infection 79
5. Conclusion 80

CHAPTER 3 - UNRAVELLING PLANT TOLERANCE MECHANISMS 81

Sub-chapter 3.1. Defence-related pathways, phytohormones and primary metabolism are key players in the distinct tolerance of *Actinidia chinensis* and *A. arguta* to *Pseudomonas syringae* pv. *actinidiae* 83

1. Introduction 85
2. Materials and Methods 87
2.1. Plant inoculation and sampling 87
2.2. Psa endophytic population in shoot tissues 88
2.3. Phytohormone quantification 88
2.4. GC-TOF-MS primary metabolite profiling 89
2.5. Whole transcriptome sequencing 90
2.6. GO enrichment and differential gene expression analysis 90
2.7. Data and statistical analysis 91
3. Results 91
3.1. Psa endophytic population in shoot tissues 91
3.2. Phytohormone composition 92
3.3. Primary metabolism 92
3.4. Functional classification of differentially expressed genes 94
3.5. Differential gene expression 95
3.5.1. Plant defence 95
3.5.2. Hormonal regulation 98
3.5.3. Primary metabolism 98
4. Discussion 101
4.1. Psa infection differently regulates defence-related pathways in *A. chinensis* and *A. arguta* 101
4.2. The ABA pathway is downregulated in *A. arguta*, whereas the JA and SA pathways are upregulated in *A. chinensis* 103
4.3. Psa infection impairs plant primary metabolism, particularly the ammonia-assimilation cycle 104
5. Conclusion 105
Supplementary Material 107

Sub-chapter 3.2. Role of methyl jasmonate and salicylic acid in kiwifruit plants further subjected to Psa infection: biochemical and genetic responses 115

1. Introduction 117
2. Materials and Methods 120
2.1. Plant maintenance and Psa inoculum 120
2.2. Plant elicitation, inoculation and sampling 120
2.3. Psa endophytic population 121
2.4. Total proteins, primary and secondary metabolites 121
2.5. Phytohormones 121
2.6. Gene expression 122
2.7. Data analysis 124
3. Results 124
3.1. Foliar disease symptoms and Psa endophytic population 124
3.2. Photosynthetic pigments and proteins 124
3.3. Secondary metabolites 126
3.4. Phytohormones 126
3.5. Gene expression 127
3.6. Principal component analysis (PCA) 128
4. Discussion 130
4.1. Biochemical and genetic alterations induced by Psa infection 130
4.2. Kiwifruit plant responses to Psa infection after elicitation with MJ or SA 131
5. Conclusion 134

CHAPTER 4 - DEVELOPING NOVEL CONTROL STRATEGIES 135

Sub-chapter 4.1. Nitrogen source impacts mineral accumulation and gene expression in young kiwifruit plants 137

1. Introduction 139
2. Material and methods 142
   2.1. Plant maintenance 142
   2.2. Plant sampling and biometric analysis 142
   2.3. Quantification of photosynthetic pigments and secondary metabolites 143
   2.4. Total protein, nitrogen and mineral analysis 143
   2.5. Gene expression 144
3. Results 146
   3.1 Plant growth, photosynthetic pigments and secondary metabolites 146
   3.2 Total protein, nitrogen and mineral concentration 147
   3.3. Gene expression analysis 148
4. Discussion 149
   4.1 NH_4^+ reduced total chlorophyll, carotenoids and polyphenolics 149
   4.2 NO_3^- and Mix increased the concentration of several minerals in plant tissues 152
   4.3. The N source influenced the regulation of plant genetic resources 152
5. Conclusion 153

Supplementary Material 155

Sub-chapter 4.2. Influence of the nitrogen source on the tolerance of kiwifruit plants to *Pseudomonas syringae* pv. *actinidiae* 157

1. Introduction 159
2. Material and methods 161
   2.1. Plant maintenance 161
   2.2. Inoculum preparation and plant inoculation 162
   2.3. SPAD scoring, sampling and biometric analysis 162
   2.4. Determination of Psa endophytic population 163
   2.5. Total N, protein and mineral concentrations 163
   2.6. Gene expression 163
   2.7. Statistical analysis 165
3. Results 165
   3.1. Plant growth and SPAD scoring 165
   3.2. Psa endophytic population in plant tissues 167
   3.3. Total protein, total N and mineral concentration 167
   3.4. Gene expression 169
4. Discussion 172
   4.1. Nitrate increased plant tolerance to Psa, preventing the impairment of photosynthetic and metabolic functions 172
   4.2. Nitrogen and mineral composition were affected by the N source, with potential implications to plant responses against Psa infection 173
5. Conclusion 174

Supplementary Material 177

Sub-chapter 4.3. Cumin essential oil reduces *Actinidia chinensis* infection by *Pseudomonas syringae* pv. *actinidiae* **179**

1. Introduction 181
2. Materials and methods 184
   2.1. PEOs chemical characterization 184
   2.2. Preparation of PEO emulsions 184
   2.3. Bacterial strains, culturing media and antibacterial activity 185
   2.4. *In planta* validation of cumin EO antimicrobial activity against Psa 185
   2.5. Statistical analysis 186
3. Results 186
4. Discussion 190
5. Conclusion 191

Supplementary Material 193

CHAPTER 5 - GENERAL DISCUSSION **195**

1. Evaluation of plant genotypic susceptibility to Psa 197
2. Unravelling plant tolerance mechanisms 198
   2.1. Pathogen recognition 199
   2.2. ROS scavenging 200
   2.3. Phenylpropanoids 201
   2.4. Phytohormone regulation 201
3. Developing novel control strategies 202
   3.1. Nitrate fertilization 203
   3.2. PEOs application 204

Conclusions and Future Prospects **207**

Reference List **209**

Table list

CHAPTER 1 - GENERAL INTRODUCTION

Sub-chapter 1.1

Table 1 - Analysis of the Strengths, Weaknesses, Opportunities and Threats (SWOT) of the methods with potential to control *Pseudomonas syringae* pv*. actinidiae*. _____ 30

CHAPTER 2 - EVALUATION OF PLANT GENOTYPIC SUSCEPTIBILITY TO PSA

Sub-chapter 2.1

Table 1 - Primer sequences and annealing temperature (T_{ann}) of housekeeping and target genes used for RT-qPCR analysis._____ 53

Sub-chapter 2.2

Table 1 - Primer sequences (Forward - F and Reverse - R) and annealing temperature (T_{ann}) of housekeeping (H) and target genes used for RT-qPCR analysis. _____ 68

CHAPTER 3 - UNRAVELLING PLANT TOLERANCE MECHANISMS

Sub-chapter 3.2

Table 1 - Primer sequences and annealing temperature (T_{ann}) of housekeeping and target genes used for RT-qPCR analysis._____ 123

Table 2 - Relative fold of expression of target genes in non-elicited (iCTR), MJ-elicited (1.0 mM methyl jasmonate, iMJ) or SA-elicited (2.5 mM salicylic acid, iSA) *A. chinensis* plants, analysed 15 days post-inoculation with *P. syringae* pv. *actinidiae* (Psa), as compared with non-elicited mock-inoculated plants (niCTR). _____ 128

CHAPTER 4 - DEVELOPING NOVEL CONTROL STRATEGIES

Sub-chapter 4.1

Table 1 - Primer sequences and annealing temperature (T_{ann}) of housekeeping and target genes used for RT-qPCR analysis._____ 145

Table 2 - Shoot and root mineral concentration in *A. chinensis* var. *deliciosa* 'Hayward' plants grown with 214 μM NO_3^-, 214 μM NH_4^+ or 107 μM NO_3^- + 107 μM NH_4^+ (Mix) for 21 days. __ 149

Sub-chapter 4.2

Table 1 - Primer sequences and annealing temperature (T_{ann}) of housekeeping and target genes used for RT-qPCR analysis._____ 164

Table 2 - Shoot and root mineral concentration in *A. chinensis* var. *deliciosa* 'Hayward' plants grown with three different nitrogen (N) treatments [214 μM NO_3^-, 214 μM NH_4^+ or 107 μM NO_3^- + 107 μM NH_4^+ (Mix)] for a total of 35 days. At day 21, plants were inoculated with saline solution (mock-inoculated control) or with *P. syringae* pv*. actinidiae* (Psa). _____ 170

Sub-chapter 4.3

Table 1 - Quantitative and qualitative composition (% w/w) of the Top 5 compounds contributing to the chemical composition of essential oils from anise, basil, cardamom, cumin, fennel and laurel. _____ 187

Figure list

CHAPTER 1 - GENERAL INTRODUCTION

Sub-chapter 1.1

Figure 1 - Current dispersion of *Pseudomonas syringae* pv*. actinidiae* (Psa) biovars and *P. syringae* pv. *actinidifoliorum* (Pfm) around the world and year of the first report in each country. 10

Figure 2 - Overview of the factors involved in the crosstalk between pathogen/host which promote the prevalence/severity of the kiwifruit bacterial canker. Full lines indicate aspects inherent to the pathosystem (Psa/kiwifruit plants) and dashed lines refer to the external factors. Abbreviations: Ca, calcium; Mg, magnesium; RH, air relative humidity. 14

Figure 3 - Summary of the pathways affected by *Pseudomonas syringae* pv*. actinidiae* (Psa) in *Actinidia* spp. following infection. 21

CHAPTER 2 - EVALUATION OF PLANT GENOTYPIC SUSCEPTIBILITY TO PSA

Sub-chapter 2.1

Figure 1 - Number of colony-forming units estimated in plant tissues from *A. chinensis* var. *deliciosa* 'Hayward' and *A. arguta* var. *arguta* 'Ken's Red' at 1, 2 and 5 days post-inoculation (dpi) with *P. syringae* pv*. actinidiae* (Psa) or *P. syringae* pv. *actinidifoliorum* (Pfm). 53

Figure 2 - Gene expression analysis of *SOD*, *CAT*, *APX*, *LOX1*, *SAM* and *TLP1* in *A. chinensis* var. *deliciosa* 'Hayward' and *A. arguta* var. *arguta* 'Ken's Red' at 1, 2 and 5 days post-inoculation (dpi) with *P. syringae* pv*. actinidiae* (Psa) or *P. syringae* pv. *actinidifoliorum* (Pfm). 55

Sub-chapter 2.2

Figure 1 - Symptom occurrence rate (percentage of individuals showing disease symptoms) in *A. chinensis* var. *deliciosa* 'Hayward' and *A. arguta* var. *arguta* 'Weiki' plants inoculated with *Pseudomonas syringae* pv*. actinidiae* (Psa) or *P. syringae pv. actinidifoliorum* (Pfm) registered 1, 7, 14 and 21 days post-inoculation (dpi). Foliar symptoms were scored taking into account the percentage of leaf area affected by necrotic spots. 69

Figure 2 - Most typical foliar symptoms observed in *A. chinensis* var. *deliciosa* 'Hayward' and *A. arguta* var. *arguta* 'Weiki' plants inoculated with *P. syringae* pv*. actinidiae* (Psa) or *P. syringae* pv. *actinidifoliorum* (Pfm) observed 21 days post-inoculation. 70

Figure 3 - Number of colony-forming units (CFU, per gram of plant tissue) in *Actinidia chinensis* var. *deliciosa* 'Hayward' and *A. arguta* var. *arguta* 'Weiki' plants inoculated with *Pseudomonas syringae* pv*. actinidiae* (Psa) or *P. syringae* pv. *actinidifoliorum* (Pfm) registered 1, 7, 14 and 21 days post-inoculation (dpi). 70

Figure 4 - Total chlorophylls (A and B) and malondialdehyde (C and D) concentrations in *A. chinensis* var. *deliciosa* 'Hayward' and *A. arguta* var. *arguta* 'Weiki' plants, 1, 7, 14 and 21 days post mock-inoculation (Control), or inoculation with *P. syringae* pv*. actinidiae* (Psa) or *P. syringae* pv. *actinidifoliorum* (Pfm). 71

Figure 5 - Total soluble polyphenols (A and B) and lignin (C and D) concentrations in *A. chinensis* var. *deliciosa* 'Hayward' and *A. arguta* var. *arguta* 'Weiki' plants, 1, 7, 14 and 21 days post mock-inoculation (Control), or inoculation with *P. syringae* pv*. actinidiae* (Psa) or *P. syringae* pv. *actinidifoliorum* (Pfm). 72

Figure 6 - Relative fold of expression of *SOD* (superoxide dismutase), *APX* (ascorbate peroxidase) and *CAT* (catalase) genes in *A. chinensis* var. *deliciosa* 'Hayward' (panels A, C and

E, respectively) and in *A. arguta* var. arguta 'Weiki' plants (panels B, D and F, respectively) inoculated with *P. syringae* pv. *actinidiae* (Psa) or *P. syringae* pv. *actinidifoliorum* (Pfm) registered 1, 2, 7, 14 and 21 days post-inoculation (dpi). 74

Figure 7 - Relative fold of *LOX1* (lipoxygenase 1), *SAM* (S-adenosylmethionine synthetase) and *Pto3* (Pto-like protein kinase 3) genes in *A. chinensis* var. *deliciosa* 'Hayward' (panels A, C and E, respectively) and in *A. arguta* var. arguta 'Weiki' plants (panels B, D and F, respectively) inoculated with *P. syringae* pv. *actinidiae* (Psa) or *P. syringae* pv. *actinidifoliorum* (Pfm) registered 1, 2, 7, 14 and 21 days post-inoculation (dpi). 75

CHAPTER 3 - UNRAVELLING PLANT TOLERANCE MECHANISMS

Sub-chapter 3.1

Figure 1 - Colony-forming units (x 10^4 per gram of fresh plant tissue) in *A. chinensis* and *A. arguta* shoot tissues, 48 hours post-inoculation with *P. syringae* pv. *actinidiae*. 91

Figure 2 - Abscisic acid, jasmonic acid and salicylic acid concentrations in *A. chinensis* and *A. arguta* shoot tissues, 48 hours pos mock-inoculation (Control) or inoculation with *P. syringae* pv. *actinidiae* (Inoculated). 92

Figure 3 - Metabolic pathway reflecting changes in the levels of primary metabolites in *A. chinensis* and *A. arguta* shoot tissues, 48 hours post-inoculation with *P. syringae* pv. *actinidiae*, in relation to mock-inoculated plants. 93

Figure 4 - Total number of contigs and number of contigs with BLAST hits, mapping and GO annotation detected following *de novo* transcriptome assembly of *Actinidia chinensis* and *A. arguta*, number of singular and common genes with GO annotation, and differentially expressed genes 48 hours post-inoculation with *Pseudomonas syringae* pv. *actinidiae*. 94

Figure 5 - Gene Ontology (GO) classification and differential expression of genes identified in *A. chinensis* and *A. arguta*, 48 hours post-inoculation with *P. syringae* pv. *actinidiae*, as compared with mock-inoculated plants. 96

Figure 6 - Heatmap of the fold of expression of statistically significant differentially expressed genes related to plant defence in *A. chinensis* and *A. arguta* plants, 48 hours post-inoculation with *P. syringae* pv. *actinidiae* (Psa, relatively to mock-inoculated plants). 97

Figure 7 - Heatmap of the fold of expression of statistically significant differentially expressed genes related with the abscisic acid, jasmonic acid and salicylic acid pathways identified in *A. chinensis* and *A. arguta* plants, 48 hours post-inoculation with *P. syringae* pv. *actinidiae* (Psa, relatively to mock-inoculated plants). 99

Figure 8 - Heatmap of the fold of expression of statistically significant differentially expressed genes related to primary metabolism identified in *A. chinensis* and *A. arguta* plants, 48 hours post-inoculation with *P. syringae* pv. *actinidiae* (Psa, relatively to mock-inoculated plants). 100

Sub-chapter 3.2

Figure 1 - Colony-forming Units (x 10^7 per gram of fresh plant tissue) 15 days post-inoculation with *Pseudomonas syringae* pv. *actinidiae* (Psa) of kiwifruit plants previously subjected to: no-elicitation (iCTR), elicitation with 1.0 mM methyl jasmonate (iMJ) or with 2.5 mM salicylic acid (iSA). 125

Figure 2 - Total chlorophyll (A), carotenoids (B) and total protein (C) concentrations in mock-inoculated non-elicited plants (niCTR), and in plants previously subjected to: no-elicitation (iCTR), elicitation with 1.0 mM methyl jasmonate (iMJ) or with 2.5 mM salicylic acid (iSA), 15 days post-inoculation with *P. syringae* pv. *actinidiae* (Psa). 125

Figure 3 - Flavonoids (A), total polyphenols (B) and lignin (C) concentrations in mock-inoculated non-elicited plants (niCTR), and in plants previously subjected to: no-elicitation (iCTR), elicitation with 1.0 mM methyl jasmonate (iMJ) or with 2.5 mM salicylic acid (iSA), 15 days post-inoculation with *P. syringae* pv. *actinidiae* (Psa). 126

Figure 4 - Abscisic (A), jasmonic (B) and salicylic (C) acid concentrations in mock-inoculated non-elicited plants (niCTR), and in plants previously subjected to: no-elicitation (iCTR), elicitation with 1.0 mM methyl jasmonate (iMJ) or with 2.5 mM salicylic acid (iSA), 15 days post-inoculation with *P. syringae* pv. *actinidiae* (Psa). _____ 127

Figure 5 - Principal component analyses between: (A) non-elicited mock-inoculated plants (niCTR) and non-elicited Psa-inoculated plants (iCTR); and between (B) non-elicited (iCTR), methyl jasmonate-elicited (iMJ) or salicylic acid-elicited (iSA) Psa-inoculated plants. ____ 129

CHAPTER 4 - DEVELOPING NOVEL CONTROL STRATEGIES

Sub-chapter 4.1

Figure 1 - Shoot and root length (A), fresh weight (B) and shoot to root ratio (C) of *A. chinensis* var. *deliciosa* 'Hayward' plants grown with 214 μM NO_3^-, 214 μM NH_4^+ or 107 μM NO_3^- + 107 μM NH_4^+ (Mix) for 21 days._____ 146

Figure 2 - Total chlorophyll (A) and carotenoids (B) concentrations in shoots of *A. chinensis* var. *deliciosa* 'Hayward' plants grown with 214 μM NO_3^-, 214 μM NH_4^+ or 107 μM NO_3^- + 107 μM NH_4^+ (Mix) for 21 days. _____ 147

Figure 3 - Total soluble polyphenolics (A), flavonoids (B) and lignin (C) concentrations in shoots and roots of *A. chinensis* var. *deliciosa* 'Hayward' plants grown with 214 μM NO_3^-, 214 μM NH_4^+ or 107 μM NO_3^- + 107 μM NH_4^+ (Mix) for 21 days._____ 147

Figure 4 - Total protein (A) and total nitrogen (B) concentrations in shoots and roots of *A. chinensis* var. *deliciosa* 'Hayward' plants grown with 214 μM NO_3^-, 214 μM NH_4^+ or 107 μM NO_3^- + 107 μM NH_4^+ (Mix) for 21 days._____ 148

Figure 5 - Heatmap of the relative fold of expression of genes *SOD*, *APX*, *CAT*, *TLP1*, *F3H*, *LOX1*, *PAL*, *SAM*, *ICS1*, *JIH*, *GLU1*, *GDH1, GAD1, MOT1* and *FER1* in shoots and roots of *A. chinensis* var. *deliciosa* 'Hayward' plants grown with 214 μM NO_3^-, 214 μM NH_4^+ or 107 μM NO_3^- + 107 μM NH_4^+ (Mix) for 21 days._____ 150

Sub-chapter 4.2

Figure 1 - Shoot and root length (cm) (A), and fresh weight (g) (B) of *A. chinensis* var. *deliciosa* 'Hayward' plants grown with three different nitrogen treatments [214 μM NO_3^-, 214 μM NH_4^+ or 107 μM NO_3^- + 107 μM NH_4^+ (Mix)] for a total of 35 days. At day 21, plants were inoculated with saline solution (mock-inoculated control, CTR) or with *P. syringae* pv. *actinidiae* (Psa). ____ 166

Figure 2 - Shoot to root ratio of *A. chinensis* var. *deliciosa* 'Hayward' plants grown with three different nitrogen treatments [214 μM NO_3^-, 214 μM NH_4^+ or 107 μM NO_3^- + 107 μM NH_4^+ (Mix)] for a total of 35 days. At day 21, plants were inoculated with saline solution (mock-inoculated control, CTR) or with *P. syringae* pv. *actinidiae* (Psa)._____ 166

Figure 3 - SPAD values of *A. chinensis* var. *deliciosa* 'Hayward' plants grown with three different nitrogen treatments [214 μM NO_3^-, 214 μM NH_4^+ or 107 μM NO_3^- + 107 μM NH_4^+ (Mix)] for a total of 35 days. At day 21, plants were inoculated with saline solution (mock-inoculated control) or with *P. syringae* pv. *actinidiae* (Psa). _____ 167

Figure 4 - Colony-forming units (x 10^{11} per gram of plant tissue) in *A. chinensis* var. *deliciosa* 'Hayward' plants grown with three different nitrogen (N) treatments [214 μM NO_3^-, 214 μM NH_4^+ or 107 μM NO_3^- + 107 μM NH_4^+ (Mix)] for a total of 35 days. At day 21, plants were inoculated with *P. syringae* pv. *actinidiae* (Psa). _____ 168

Figure 5 - Total protein (A) and nitrogen (B) concentrations in shoots and roots of *A. chinensis* var. *deliciosa* 'Hayward' plants grown with three different nitrogen treatments [214 μM NO_3^-, 214 μM NH_4^+ or 107 μM NO_3^- + 107 μM NH_4^+ (Mix)] for a total of 35 days. At day 21, plants were inoculated with saline solution (mock-inoculated control, CTR) or with *Pseudomonas syringae* pv. *actinidiae* (Psa). _____ 168

Figure 6 - Heatmap of the relative fold of expression of genes *SOD*, *APX*, *CAT*, *PR1*, *TLP1*, *LOX1*, *PAL*, *SAM*, *GLU1, GDH1* and *GAD1* in shoots and roots of *A. chinensis* var. *deliciosa*

'Hayward' plants grown with three different nitrogen treatments [214 µM NO_3^-, 214 µM NH_4^+ or 107 µM NO_3^- + 107 µM NH_4^+ (Mix)] for a total of 35 days. At day 21, plants were inoculated with saline solution (mock-inoculated control) or with *P. syringae* pv*. actinidiae* (Psa). _____ 171

Sub-chapter 4.3

Figure 1 - Diameter of the inhibition halo of *Pseudomonas syringae* pv*. actinidiae* (Psa, strains 1F and 7286) and *P. syringae* pv. *actinidifoliorum* (Pfm, strains 18804 and 19441) cultures exposed to 1, 5, 10, 25, 50, 75 and 90% of anise, basil, cardamom, cumin, fennel and laurel essential oils for 48h. _____ 188

Figure 2 - Colony-forming units (x 10^7 per gram of plant tissue) in *A. chinensis* var. *deliciosa* 'Tomuri' plants, 30 days after foliar treatment with 0.1% of cumin essential oil (EO), and 15 days post-inoculation with *Pseudomonas syringae* pv*. actinidiae* strain 7286. _____ 189

Abbreviations, acronyms and chemical formulas

1-MCP - 1-methylcyclopropene
ABA - abscisic acid
APX - ascorbate peroxidase
ASM - acibenzolar-S-methyl
B - boron
C - carbon
Ca - calcium
$Ca(NO_3)_2$ - calcium nitrate
$CaCl_2$ - calcium dichloride
CAT - catalase
CBK - cancro bacteriano do kiwi
cDNA - complementary deoxyribonucleic acid
CFBP - collection of plant-associated bacteria
CFU - colony-forming unit
$CuSO_4$ - copper(II) sulphate
cv - cultivar
DEG - differentially expressed gene
DEPC - diethylpyrocarbonate
dpi - days post-inoculation
EO - essential oil
EPPO - European and Mediterranean Plant Protection Organization
ET - ethylene
ETI - effector-triggered immunity
Fe - iron
FPKM - reads per kb per million
FW - fresh weight
GABA - gamma-aminobutyric acid
GC-MS - gas chromatography-mass spectrometry
GC-TOF-MS - gas chromatography time of flight mass spectrometry
GFPuv - UV-excited green fluorescent protein
GO - gene ontology
GR - glutathione reductase
H_2O - hydrogen peroxide
H_3BO_3 - boric acid
HNO_3 - nitric acid
hpi - hours post infection
HR - hypersensitive response
ICMP - international collection of microorganisms from plants
ICP-OES - inductively coupled plasma-atomic emission spectrometry
JA - jasmonic acid
K - potassium
KBC - kiwifruit bacterial canker
KCl - potassium chloride
KNO_3 - potassium nitrate
KVH - Kiwifruit Vine Health
LOX - lipoxygenase
LSD - least significant difference
Mg - magnesium
$MgSO_4$ - magnesium sulphate
MJ - methyl jasmonate
MLS - multilocus sequence
Mn - manganese
$MnSO_4$ - manganese(II) sulphate
MoO_3 - molybdenum trioxide
N - nitrogen
NaCl - sodium chloride
NADPH - nicotinamide adenine dinucleotide phosphate
NH_4^+- ammonium
NH_4Cl - ammonium chloride
$NH_4H_2PO_4$ - ammonium dihydrogen phosphate
NH_4NO_3 - ammonium nitrate
$NiSO_4$ - nickel(II) sulphate
NO - nitric oxide
NO_3^-- nitrate
nm - nanometre
NSA - nutrient sucrose agar
O^{2-}- superoxide anion
OD - optical density
OEP - óleo essencial de plantas
P - phosphorous
PAL - phenylalanine ammonia-lyase
PAMP - pathogen-associated molecular pattern
PCA - principal component analysis
PCR - polymerase chain reaction
PEO - plant essential oil
Pfm - *Pseudomonas syringae* pv. *actinidifoliorum*
ppm - parts per million
PR - pathogenesis-related
PRR - pattern recognition receptor
Psa - *Pseudomonas syringae* pv. *actinidiae*
PTI - PAMP-triggered immunity
RH - air relative humidity
RIN - RNA integrity number
RNA - ribonucleic acid
ROS - reactive oxygen species
RT - room temperature
RT-qPCR - reverse transcription quantitative real-time polymerase chain reaction
R-protein - resistance protein
SA - salicylic acid
SAM - S-adenosylmethionine
SAR - systemic acquired resistance
SOD - superoxide dismutase
SPAD - soil plant analysis development
T3E - type III effectors
T3SS - type III secretion system
TCA - tricarboxylic acid
TLP - thaumatin-like protein
var - variety
Zn - zinc
$ZnSO_4$ - zinc sulphate

CHAPTER 1

General Introduction

Overview

Originated from southwestern and central China, plants from the genus *Actinidia* are dioecious perennial vines, with fruits that can be described as berries due to the numerous seeds embedded in a juicy pericarp. Initially, this fruit was called “Chinese gooseberry”, but it was later renamed as “kiwifruit” by the New Zealand fruit handling firm Turners & Growers Ltd. (Auckland, New Zealand). Although for many years the name “kiwifruit” referred only to the fruit of one specific cultivar of *Actinidia chinensis* (cv. ‘Hayward’), nowadays it is used to refer to the fruits of any *Actinidia* species (Ferguson, 2013).

A. chinensis comprises the two most economically important varieties worldwide: *A. chinensis* var. *deliciosa* (green kiwifruit) and *A. chinensis* var. *chinensis* (yellow kiwifruit). The green-fleshed cultivar ‘Hayward’ overwhelmingly dominates the market. In the last decade, *A. chinensis* var. *chinensis* has been increasingly growing in production, with the cultivar ‘Hort16A’, registered by Zespri under the trademark Zespri® Gold, being the second variety with higher international commercial dimension (following ‘Hayward’) (Neves, 2008; Hanley, 2018). More recently *A. arguta*, commonly known as ‘kiwi berry’ or ‘baby kiwi’, has gained some commercial interest, being present in several countries such as the USA, New Zealand, Chile, France, Germany, Italy and Japan. *A. arguta* fruits have a similar taste to the green-fleshed kiwifruit, being inclusively sweeter in some cases, and having a similar nutritional profile, rich in antioxidants, vitamins and minerals (Stefaniak *et al*., 2020). However, its cultivation continues largely limited due to the labour-intensive harvesting procedures, and to its more limited shelf-life (Ferguson, 2013). In 2019, the world's largest kiwifruit producer was China, followed by Italy, New Zealand, Chile, Iran, and Greece, which account for over 90% of the worldwide production. However, countries like Portugal, Turkey, Spain, and France also have increasingly higher production rates, with values ranging between 25000 and 70000 tonnes per year (FAOSTAT, 2021).

In Portugal, the *Actinidia* culture was introduced in 1973, but it was only during the 80s that a greater expansion of the culture became evident, mainly due to its high productive potential, added value and reduced production costs (Félix and Cavaco, 2004; Antunes, 2008). Since 2000, the national kiwifruit planted area and associated production showed an evident growth but, from 2009 until 2014, there was a decrease of 33% in plant productivity, which was not in agreement with the increase in the cultivated area (FAOSTAT, 2021). These production losses were due to unfavourable climatic conditions (e.g., warmer winters not reaching the needed vernalisation period and deficient pollination) but were also related, to a great extent, to the introduction of *Pseudomonas syringae* pv. *actinidiae* (Psa), which causes the kiwifruit bacterial canker (KBC) (DGAV, 2014).

In 2010, characteristic symptoms of CBK similar to the ones observed during the first Psa epidemic outbreaks in Italy (which occurred in 2008), were observed in a Portuguese

orchard of *A. chinensis* var. *deliciosa* 'Summer' located in the region of Entre-Douro e Minho (Balestra *et al*., 2010). Shortly after, several governmental actions were reinforced, aiming to limit the introduction and spread of the disease within the Portuguese territory. These measures led to the creation of a National Action Plan for Psa Control, which provides general management guidelines to mitigate the disease (DGAV, 2014). As a result of the prospecting programs promoted by official entities, in 2011, Psa was detected in the northern region of the country, in plants that had been imported from Italy, and several bacterial outbreaks in other relevant kiwifruit production regions were also recorded (DRAPN, 2013; DRAPC, 2015). Currently, Psa is considered a worldwide pandemic pathogen and is present in all main kiwifruit producing countries, including China, New Zealand, Italy, Chile, Portugal, Spain, and France (EPPO, 2020). Due to its rapid worldwide distribution and severity, Psa integrates the list of pests recommended for quarantine regulatory measures of the European and Mediterranean Plant Protection Organization (EPPO, 2012).

Aim and outline of the thesis

So far, most studies on Psa and Pfm have focused on population structure, origin, detection techniques and disease cycle. Still, little is known about the different tolerance levels between distinct kiwifruit genotypes and the phenotypic and genotypic traits that underpin their contrasting behaviour to Psa infection. Moreover, current disease management strategies are limited, relying on strict phytosanitary measures and application of antibiotic and cupric formulations that frequently show low efficacy and high environmental impacts. Thus, the main goals of this work were to explore plant tolerance mechanisms and novel disease management strategies. The specific goals of this thesis were to:

i) evaluate the responses of different kiwifruit genotypes to Psa and Pfm infection;
ii) confirm the field-reported higher virulence of Psa, as compared with Pfm;
iii) identify key metabolic and genetic networks involved in plant defences against Psa;
iv) understand how the nitrogen source can affect plant tolerance to the disease; and
v) assess the potential of plant essential oils in increasing plant tolerance to Psa.

The present thesis is organized into five Chapters, including a total of nine Sub-chapters formatted as scientific articles (each comprised of an Abstract, Introduction, Materials and methods, Results, Discussion and Conclusion). **Chapter 1** is composed of a General Introduction, followed by two in-depth literature reviews that are focused on: pathogen dissemination and diversity, disease dynamics and plant defence mechanisms (**Chap 1.1**); and currently employed and emergent practices for the control of the disease (**Chap 1.2**). In

Chapter 2, the genotypic variability to Psa and Pfm infection is evaluated between *A. chinensis* and *A. arguta* through: i) short-term disease assessment (**Chap 2.1**), and ii) long-term disease assessment (**Chap 2.2**). For these, we focused on the expression of important defence-related genes through targeted analysis (RT-qPCR) and on the accumulation of primary and secondary metabolites involved in plant-pathogen interactions. **Chapter 3** explores the transcriptomic and metabolic pathways involved in plant responses to Psa infection through: i) the analysis of early responses of *A. chinensis* and *A. arguta* to Psa infection using whole-transcriptome sequencing, phytohormone and primary metabolism profiling (**Chap 3.1**); and ii) the manipulation of *A. chinensis* phytohormone regulation via plant elicitation with methyl jasmonate or salicylic acid (**Chap 3.2**). **Chapter 4** investigates potential tools for a more effective Psa management, including i) nitrogen nutrition on kiwifruit plant susceptibility to Psa (comparing the use of NO_3^-, NH_4^+ or a 1:1 Mix) (**Chap 4.1 and 4.2**), and ii) the antimicrobial efficacy of 6 plant essential oils (anise, basil, cardamom, cumin, fennel and laurel) against Psa and Pfm (**Chap 4.3**). The main achievements, practical applications, limitations, and future prospects of this study are discussed in **Chapter 5**, which is followed by the general list of bibliographical references used throughout this thesis.

CHAPTER 1 - Sub-chapter 1.1

Kiwifruit bacterial canker: current knowledge on disease dynamics and on plant defence mechanisms

Kiwifruit bacterial canker: current knowledge on disease dynamics and on plant defence mechanisms

Abstract

Globalization, which propelled human migration and commercial exchanges at a global level, woefully led to the introduction of non-indigenous organisms into several agroecological systems. One of these cases is the bacterium *Pseudomonas syringae* pv*. actinidiae* (Psa), which can infect several kiwifruit species causing the kiwifruit bacterial canker (KBC), associated with drastic production losses and added costs related to orchard management. All the currently cultivated *Actinidia chinensis* varieties are susceptible to Psa, while species as *A. arguta* and *A. eriantha* seem to be more tolerant to the pathogen. However, information on how these networks are activated and regulated and how they differ between tolerant and susceptible kiwifruit plants is still not fully understood.

Despite the exponential publication of scientific, technical and academic works during the last two decades, data regarding KBC are frequently incomplete or scattered, hindering the dissemination, integration and comparison of the currently available information. Here, we make a critical overview of the currently available data concerning the interaction between kiwifruit plants and Psa.

The extent of the disease seems to be highly influenced by factors inherent to the Psa biovar and kiwifruit plant species, and also by external factors including the orchard edaphoclimatic conditions, agronomic practices adopted, and plant nutrition. Recent findings also point out the importance of defence mechanisms, phytohormone regulatory pathways and secondary metabolism in plant defence against Psa. Although the mitigation of Psa has been extremely challenging, the integration of this data could propel additional research efforts and contribute to a prompter response against the pathogen amongst producers, researchers and policy-makers.

1. Introduction

Pseudomonas syringae pv*. actinidiae* (Psa) was first identified in Japan and China in the 80s, with sporadic outbreaks for over two decades. However, from 2008 on, it rapidly disseminated to several kiwifruit producing countries across the world (e.g., China, New Zealand, Italy, Portugal, Spain and France, Fig. 1), posing significative impacts to the kiwifruit industry (Vanneste, 2017; EPPO, 2020). So far, six Psa populations (or biovars) have been identified and named according to the chronological order they were characterized, taking into consideration several factors including: their geographic distribution, analysis of whole-genome sequencing and multilocus sequence of housekeeping genes, virulence genes for type III effectors (T3E) or toxin production (Chapman *et al*., 2012; Cunty *et al*., 2015; Fujikawa and Sawada, 2016; Sawada *et al*., 2016). Until the present moment, Japan has the most diverse bacterial populations associated with KBC (Sawada and Fujikawa, 2019), whereas in other countries lower diversity has been reported (Fig. 1).

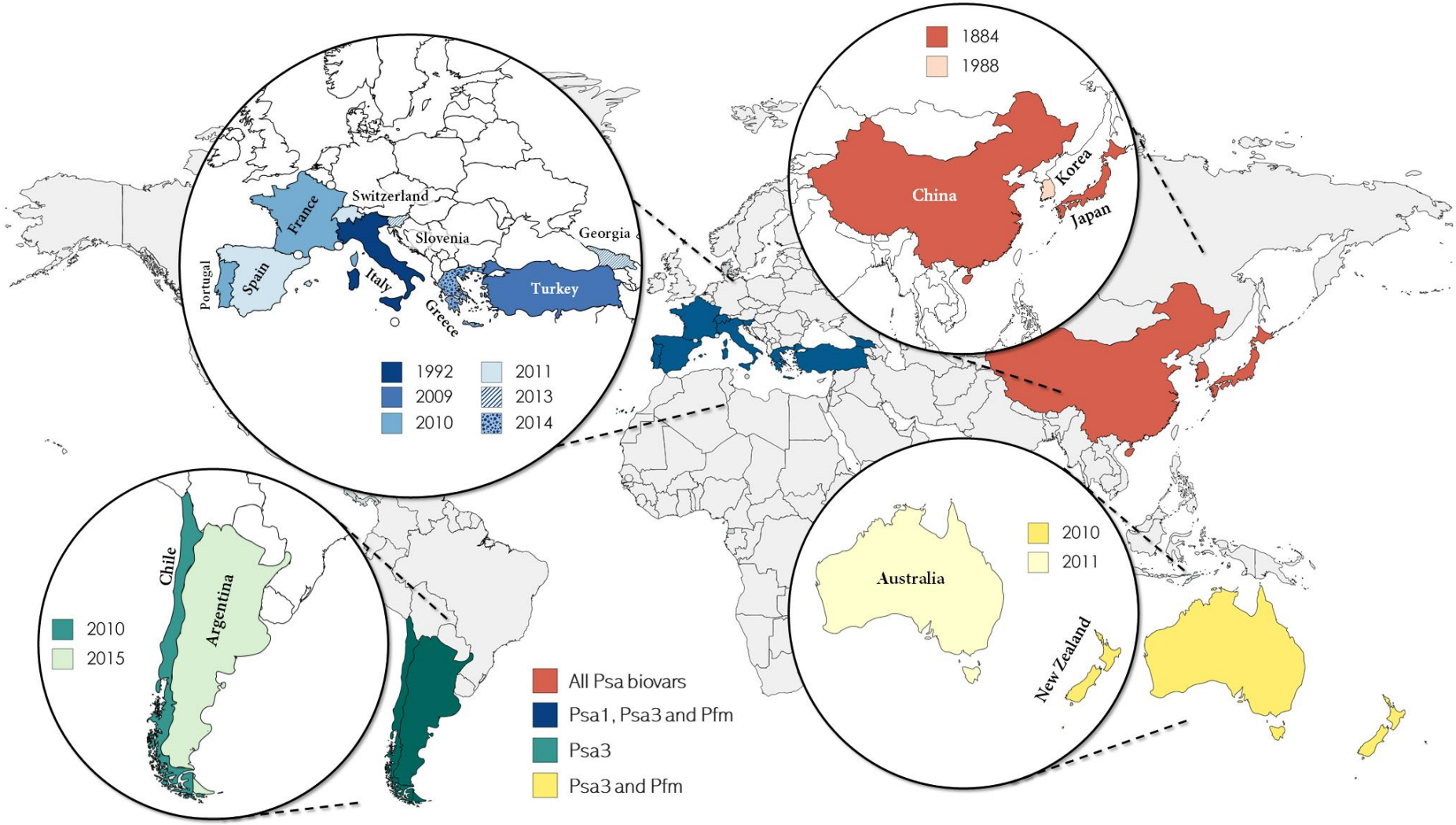

Figure 1 - Current dispersion of *Pseudomonas syringae* pv. *actinidiae* (Psa) biovars and *P. syringae* pv. *actinidifoliorum* (Pfm) around the world and year of the first report in each country.

Psa population 1 (Psa1) was found to be widely distributed in Japan (not only in commercially cultivated kiwifruit plants but also in wild *Actinidia* spp. from mountain regions), in Italy and Korea (Sawada *et al*., 2014; Sawada *et al.*, 2016; McCann *et al*., 2017). It is generally acknowledged that Psa1 presents a genomic island containing an *argK-tox* cluster, which is involved in the production of a phaseolotoxin that induces yellow halos around leaf lesions, and shoot and branch wilting (Tamura *et al*., 2002: Genka *et al*., 2006). However, it was recently demonstrated that not all Psa1 populations can produce this phytotoxin, probably due to mutations in the *argK-tox* cluster or to the lack of its acquisition from their ancestors (Fujikawa *et al*., 2020). Psa2 has only been found in Korea and possesses the gene cluster *cor*, responsible for the synthesis of coronatine, which induces chlorosis, hypertrophy, and stunting of plant tissues (Gnanamanickam *et al*., 1982). Psa biovar 3 is responsible for the most recent and severe outbreaks associated with KBC, being present in all main kiwifruit producing regions. Despite its inability to produce phytotoxins, it is generally acknowledged that it is the most virulent among all biovars (Ferrante and Scortichini, 2009; Koh *et al*., 2010; Donati *et al*., 2014). Recent findings pinpoint that the type III secretion system (T3SS) has an important role in Psa3 virulence. Ishiga *et al*. (2020) observed that kiwifruit seedlings inoculated with Psa3 showed severe necrosis within 1 week after infection, associated with the expression of genes involved in the T3SS *in planta*, which did not occur in seedlings inoculated with a Psa3 T3SS-deficient *hrcN* mutant. A subsequent study reported that among several T3SS genes, *avrE1* and *hopR1* are additively required for Psa3 *in planta* growth and lesion production (Jayaraman *et al*., 2020). Psa3 can also produce exopolysaccharides and N-acyl homoserine lactones, which seem to be toxic to kiwifruit tissues (Andolfi *et al*., 2014; Cellini *et al*., 2020). Moreover, it can be found in syndemic associations with two other kiwifruit pathogens, e.g., *P. syringae* pv. *syringae* and *P. viridiflava*, suggesting that the establishment of a pathogenic consortium enhances Psa3 pathogenesis (Purahong *et al*., 2018). In addition to the Psa biovars previously identified, two novel and distinct populations, Psa5 and Psa6, were described in Japan in subsequent years. Psa5 was only found in *A. chinensis* var. *chinensis* 'Hort16A' in Saga in 2012, following the appearance of symptoms similar to those from KBC. Although being closely related to Psa2, Psa5 does not produce coronatine nor phaseolotoxin and shows lower pathogenicity than biovars 1, 2, and 3. Psa6 was isolated for the first time in 2015 from *A. chinensis* var. *deliciosa* 'Hayward' orchards located in Nagano, and, as reported for Psa5, disease symptoms were less severe than those commonly associated with Psa3. Although this population is genetically close to Psa3, it can produce phaseolotoxin and coronatine (Sawada *et al*., 2016). Due to the severe effects of these pathogens and ability to easily disseminate and infect kiwifruit plants, Psa has been included in the A2 List of organisms recommended for regulation as quarantine pests from the European and Mediterranean Plant Protection Organization (EPPO, 2012).

Psa4, on the other hand, was considered a Psa biovar until 2015, having been reclassified as *Pseudomonas syringae* pv. *actinidifoliorum* (Pfm) (Ferrante and Scortichini, 2014; Cunty *et al*., 2015). This species encompasses the low virulent strains present in Japan, New Zealand, Australia, France, Spain and Switzerland (Chapman *et al*., 2012; Scortichini *et al*., 2012; Abelleira *et al*., 2015; Cunty *et al*., 2015) and has not been linked with significant symptomatology nor production losses (Vanneste *et al*., 2014; Nunes da Silva *et al*., 2020). For these reasons, Pfm has not been subjected to the strict surveying and control measures applied to Psa.

Given that the number of described Psa populations keeps increasing, there may be a vast bacterial diversity still to be identified. This increase is mostly a result of the extensive survey campaigns implemented in several countries as part of local disease mitigation programmes, and the development of novel genotyping technologies (Ochoa-Díaz *et al*., 2018). The still missing pieces regarding the genomes of bacterial pathogens limit the full understanding of their origin and temporal development, hindering the knowledge of the evolutionary processes that lead to the appearance of modern bacterial populations and the prediction of future evolutionary events.

2. Disease dynamics

2.1. Plant infection

Psa infection begins with bacteria entering the host plant through natural openings (e.g., stomata, lenticels, broken trichomes and hydathodes), natural wounds (caused by wind damage) and artificially-made wounds (resulting from e.g., pruning and girdling activities) (Spinelli *et al*., 2011; Ferrante *et al*., 2012; Donati *et al*., 2020). Moreover, Psa can be vectored by contaminated pollen, and its systemic penetration into flowers can occur either from the stigma or via the nectarthodes, due to their humid and nutrient-rich environment, migrating afterwards along the style (Balestra *et al*., 2018; Donati *et al*., 2020). In contrast, pathogen penetration through plant roots seems to be very limited, but Psa is still able to migrate from infected aboveground organs to belowground structures and, at bud break, it can migrate from the overwintering organs to both closed and open buds (Donati *et al*., 2020).

After infection, Psa can colonize and multiply within the apoplastic tissues or it can live epiphytically on leaf surfaces, up to three weeks (Serizawa and Ichikawa, 1993a; Petriccione *et al*., 2014; Donati *et al*., 2020). Migration within the plant from infected to healthy tissues occurs preferentially through the xylem, often leading to plugging of its vessels, or through sieve elements and sclerenchyma fibres in the shoot cortex (Renzi *et al*., 2012; Donati *et al*., 2020). Psa first colonizes leaf tissues without causing visual symptoms (asymptomatic

biotrophic phase), during which the pathogen colonizes and thrives in the apoplast, taking advantage of plant nutrients for its own metabolic needs (Petriccione *et al*., 2013; Donati *et al*., 2020). Thereafter, when it overcomes plant defences (necrotrophic phase), a wide variety of disease symptoms appear.

2.2. Symptoms and disease cycle

Symptoms begin primarily during spring, with the appearance of dark-brown necrotic spots surrounded by a yellow halo in the leaves, which subsequently start to curl, wilt and dry out. Flowers and buds can also wilt and decay, and canker formations can appear in trunks, branches, grafting zones and wounds, frequently accompanied by the presence of reddish-brown discolorations under the bark and white or red-rusty exudates (Ferrante *et al*., 2012; Donati *et al*., 2018). The release of exudates, highly infectious to nearby plants and very characteristic to KBC, results from elevated Psa endophytic populations that occurs during favourable periods. Branch wilting may compromise bud and flower development, sometimes leading to necrotic lesions in sepals, flower abortion and deformed fruits (Donati *et al*., 2020). During summer, due to the increase of average daily temperatures, Psa population gradually decreases in plant tissues, and host infection seems to occur preferentially through stomata and hydathodes (Scortichini *et al*., 2012; Donati *et al*., 2014). As a result of the plant scaring process, callous tissues may become visible (Serizawa *et al*., 1989). During autumn, this process is further accelerated by the increase of air relative humidity (RH) and lower temperatures (Serizawa and Ichikawa, 1993d; Serizawa *et al*., 1994). During this period, Psa takes advantage of both natural (leaf and fruit fall wounds, lenticels and buds) and man-made wounds (related to harvest and pruning activities), aggravating the risk of infection and the release of infectious exudates (Serizawa and Ichikawa, 1993d). During winter bacteria can survive in the cortex of infected tissues, resuming their activity in late winter and early spring, and starting the disease cycle again (Donati *et al*., 2020). During this season, periods of moderate rainfall and high RH can reduce the latency period that precedes the appearance of disease symptoms, which are closely related with the degree of infection present in the fall of the previous year (Serizawa *et al., 1*989; Serizawa and Ichikawa 1993c; Serizawa *et al*., 1994). Recent findings demonstrated that, even with the absence of visual foliar symptoms, Psa is still able to strive in plant sap (Abelleira *et al*., 2015). Therefore, determination of plant infection should rely on microbiological and molecular biology methods, rather than on visual observations alone.

2.3. Biotic and abiotic factors implicated in disease development

As average temperatures, rainfall and RH are distinct between the numerous areas of kiwifruit production worldwide, symptoms may develop at different rates or extents in distinct geographical areas. It has been demonstrated that infection of kiwifruit plants by Psa can occur at any time of the year, probably because the bacterium can live epiphytically in plant leaves (Scortichini *et al*., 2012; Stefani and Giovanardi, 2012), but changes in Psa population structure were observed between epiphytic and endophytic populations, and between seasons (Figueira *et al*., 2020). Ultimately, the main outcome of plant infection by Psa is extremely dependent on several factors, namely: i) inherent to the pathosystem itself (including the Psa biovar and kiwifruit plant species); and ii) external factors (such as local edaphoclimatic conditions, orchard management practices, and plant nutrition). These are summarized in Fig. 2 and are described below.

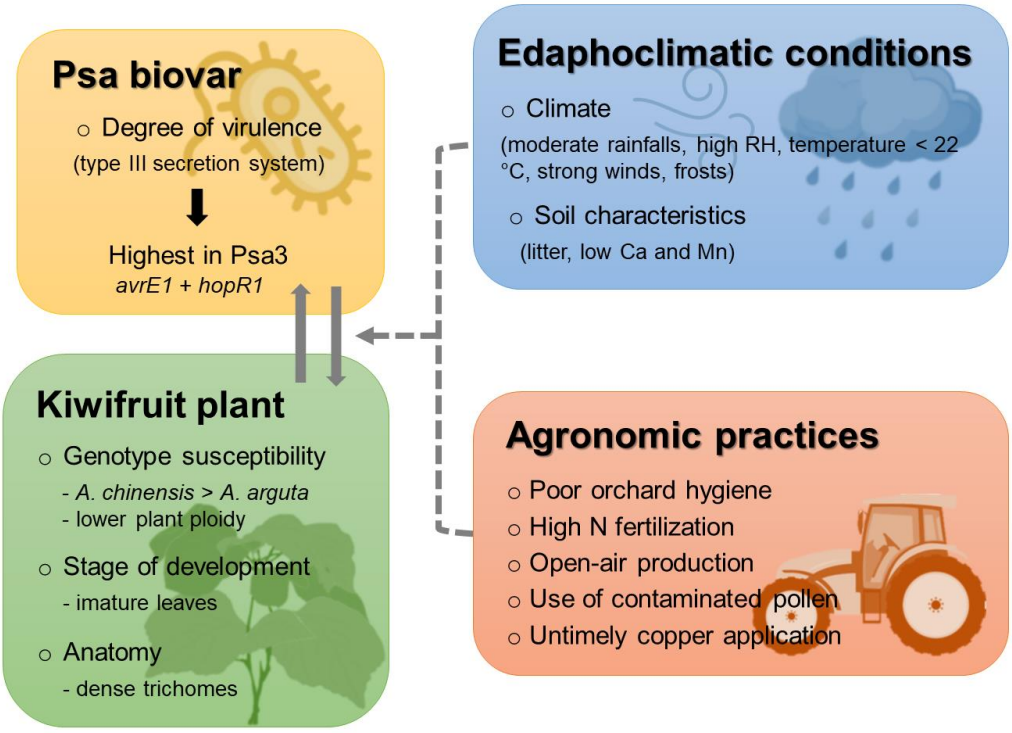

Figure 2 - Overview of the factors involved in the crosstalk between pathogen/host which promote the prevalence/severity of the kiwifruit bacterial canker. Full lines indicate aspects inherent to the pathosystem (Psa/kiwifruit plants) and dashed lines refer to the external factors. Abbreviations: Ca, calcium; Mg, magnesium; RH, air relative humidity.

2.3.1. Bacterial strain

During the last decades, dozens of studies have been published, aiming at confirming Psa identity and understanding plant tolerance mechanisms. Although it is generally acknowledged that Psa3 is the most virulent population to kiwifruit plants, assessing the full

pathogenicity of a given bacterial population is not always straightforward because in numerous studies information on plant maintenance conditions during the experimental period is incomplete, and the highly variable strategies used for plant inoculation and disease evaluation hamper result comparison and elaboration of robust conclusions. Moreover, the use of different bacterial strains, inoculum densities, plant cultivars and developmental stages from study to study also hinders the evaluation of the tolerance degree of a given genotype and also the virulence degree of a given bacterial strain. Divergence in the degree of symptom appearance has also been reported between bacterial strains isolated from different plant species and geographical areas. For example, Psa strain Hs15-41, isolated from wild *A. arguta* plants in the Abashiri region (Japan), only induced weak infection reaction in *A. arguta* 'Issai', whereas the strain S-21 isolated from the same plant species in the Zushi region caused the appearance of large necrotic symptoms. On the other hand, different symptom extent between different plant cultivars has been reported for the same bacterial strain. For example, Hs15-41 caused only a minor infection reaction in 'Issai', but severe necrotic lesions or even bacterial ooze in 'Minakimani'. Similarly, Psa strains isolated from wild *A. arguta* plants caused severe leaf spotting in *A. polygama*, but not in *A. rufa*, and strains isolated from *A. kolomikta* induced limited symptoms on *A. chinensis* var. *deliciosa* (Ushiyama *et al*., 1992). Thus, the extent of disease progression is not related to the Psa strain alone, being a result of its specific interaction with each kiwifruit genotype.

2.3.2. Plant genotype

The identification of plant genotypes with higher tolerance to pests and pathogens has been the cornerstone for a more sustainable disease management. However, this assessment is not easy due to the complex genotypic variability of the host plant, as well as the lack of standardized methods for tolerance screening. Although all species of the genus *Actinidia* can be infected with Psa, there seems to be a considerable variation in their tolerance degree to this bacterium. Field and laboratory pieces of evidence have shown that cultivars of *A. chinensis* var. *chinensis* (such as 'Hort16A' and 'Jin Tao') present the highest susceptibility to Psa, *A. chinensis* var. *deliciosa* cultivars (such as 'Hayward') have shown moderate susceptibility, and *A. arguta* cultivars (including 'Enza Red' and 'Hongyang') were found to be the most tolerant ones (Vanneste *et al*., 2014; Nardozza *et al*., 2015; Saei *et al*., 2018; Nunes da Silva *et al*., 2020; Wang *et al*., 2020a). Several studies, including a screening of a large number of orchards in New Zealand, also suggested a higher tolerance to Psa with an increase in plant ploidy level: i) tetraploid genotypes (*A. arguta*, *A*. *chrysantha, A*. *kolomikta*, *A*. *macrosperma*, *A*. *polygama*, *A*. *tetramera*, and *A*. *valvata*) had a higher tolerance to Psa, and ii) tetraploid and hexaploid genotypes of *A. chinensis* had a generally higher tolerance than diploid genotypes of the same species (Cotrut *et al*., 2013; Nardozza

et al., 2015; Saei *et al*., 2018; Wang *et al*., 2020a). Additionally, it has been shown that male cultivars of *A. chinensis* also seem more prone to Psa infection than female cultivars, showing higher levels of Psa endophytic density (Donati *et al*., 2020). Nevertheless, despite these reports consistently attested for the higher tolerance of some kiwifruit species and varieties over others, it was recently demonstrated that some genotypes of a given species considered as tolerant can have drastic differences in their response to Psa infection. For example, distinct genotypes of *A. eriantha*, considered a tolerant species, behaved from highly tolerant to highly susceptible in *in vitro* assays (Wang *et al*., 2020a).

The full characterization of the vast array of currently existing commercial, wild and crossbred plant genotypes according to their susceptibility to a specific pathogen may seem a never-ending work, but it has already proven successful in overcoming Psa limitations to the commercial exploration of kiwifruits. After the first devastating outbreaks occurred in New Zealand orchards of *A. chinensis* var. *chinensis* 'Hort16A' in 2011, trials were conducted using the library of cultivars already available to find equally interesting commercial ones, but with increased tolerance to Psa. Based on the observation of less prevalent and less severe KBC symptoms, as well as to decreased bud rot incidence and production of bacterial exudate, affected orchards of 'Hort16A' began to be replaced by 'Gold3' (Vanneste, 2017).

Crop improvement through the identification of tolerant genotypes is certainly one of the foundations for a more successful management of agronomical pathogens, but potential limitations on e.g., fruit organoleptic properties, should be thoroughly addressed previously to their large-scale cultivation. Moreover, one should consider that most of the screening programmes are developed under greenhouse or microcosm conditions (which allow screening a larger number of cultivars at the same time), not accounting for outcomes regarding plant productivity and adaptability to more challenging environmental conditions.

2.3.3. Edaphoclimatic conditions

Orchard edaphoclimatic conditions, mainly concerning rainfall, RH, temperature and occurrence of frosts, have been considered key modulators in plant responses against Psa infection (Fig. 2). For example, it has been observed that rainfall plays a major role in long-term Psa prevalence in open-air orchards, whereas in protected orchards (i.e., installed under covering structures with no exposure to rainfall) successful pathogen eradication was accomplished with the removal of infected plants (Ko *et al*., 2002). However, this climatic parameter seems to have a dual effect depending on its intensity, as it can promote Psa dispersion and penetration into plant tissues when in small amounts, whereas heavy rainfalls can lead to inoculum washing from the leaf canopy, thus decreasing Psa penetration (Hirano and Upper, 2000). Long-term high RH also seems to favour bacterial multiplication and movement inside plant tissues. Vanneste *et al*. (2015) showed that maintaining Psa-infected

kiwifruit seedlings at RH above 95% for 21 days can lead to extensive symptoms, including necrosed stem tissues, dead leaves, wilting of plant tips, and to the colonisation of the vascular system (with Psa being detected throughout the stem). However, if the high RH was maintained for only two days and followed by 19 days at 60% RH, bacterial dispersal and visual symptoms were mostly restricted to the point of inoculation (Vanneste *et al*., 2015). More recently, it has been demonstrated that the predicted optimal RH for Psa epiphytic and endophytic growth was 60% and 80%, respectively. Besides, RH significantly influenced Psa maximum population size during its endophytic phase, but not in the epiphytic phase (Donati *et al*., 2020). Along with rainfall and RH, average daily temperatures may also affect the extent of disease symptoms. Reports from several countries have described decreased Psa symptoms during the summer months (Li *et al*., 2001; Vanneste, 2013; Antoniacci *et al*., 2019). For instance, it was shown that Psa strains from different geographic origins have unique growth patterns at different temperatures, with Psa3 strains being completely inhibited above 30 °C (Choi *et al*., 2014). Other environmental events, such as frost and strong winds, also favour the development of the disease, mostly due to the appearance of injuries in plant tissues that allow bacterial entry (Serizawa *et al*., 1989; Ferrante and Scortichini, 2014). Water deficit can also promote symptom development, since it has been demonstrated that soil moisture maintenance at field capacity resulted in lower plant infection than with lower irrigation rates (Mauri *et al*., 2016).

To decrease the influence of environmental conditions that favour pathogen growth, several solutions have been suggested during the last decade, such as the use of fans, under-vine shelters and overhead irrigation (KVH, 2016, 2018). Protection against rain, wind and hail can be provided by the installation of wind-breaks (either artificial or natural) and coverings (made of plastic or cloth) to diminish bacterial spread and the incidence of plant wounding (Black *et al.,* 2015; KVH, 2018; Chiabrando and Giacalone, 2018). However, these structures pose added costs to orchard management, and still very little is known on how they may affect plant productivity. Nevertheless, despite the undeniable importance of orchard edaphoclimatic conditions in the outcome of bacterial infections, the agronomical practices employed is also of utmost importance in the extent of Psa infection.

2.3.4. Orchard management practices

The spread of Psa within and between orchards mainly results from the presence of epiphytic bacterial populations, bacterial exudates, and the accumulation of infected plant material in the orchard. Therefore, the removal of infected material should be dully pursued, and comprise not only plants showing disease symptoms but also their surrounding plants, as these may also harbour bacteria without showing disease symptoms (Abelleira *et al*., 2015). Psa was found to survive in fallen leaves and pruning wood litter for up to 6 months,

especially under climatic conditions of high precipitation and mild temperatures (Aguín *et al.,* 2015; Donati *et al.,* 2020). As this represents a potential source of inoculum for the next growing season, plant litter should be promptly removed from the orchards (Tyson *et al*., 2012; Tyson *et al.,* 2016). Given the inexistence of curative methods to KBC, during the last decades, the use of copper-based compounds has been adopted as a prophylactic measure against Psa (DGAV, 2014; KVH, 2016; Lamichhane *et al*., 2018; Sciubba *et al*., 2019). Moreover, overhead irrigation is not recommended, as it may facilitate pathogen dissemination between plants, and should be replaced by drip irrigation systems (EPPO, 2012). Pruning activities also proved to be of paramount importance in disease incidence, because wounds can greatly favour the penetration of the pathogen within plant tissues. For example, higher KBC incidence was observed in *A. chinensis* orchards of 'Hayward' (female), as compared with 'Matua' (male), potentially because the female cultivar is more frequently subjected to summer and winter pruning programmes (Koh *et al.,* 1996; Kennelly *et al.,* 2007). Psa spread from plant to plant was also related to the pruning equipment, especially when contaminated shears were used for winter pruning practices (Koh *et al.,* 2010). Therefore, during pruning or harvesting procedures, tools should be sanitized between plants using, e.g., 70% ethanol (DGAV, 2014). The use of wound protectants is also of great importance in controlling wound-infecting pathogens, such as Psa, by constituting a physical barrier, promoting healing and preventing bacterial dispersal (Cornish *et al.,* 2015; Everett *et al.,* 2016; Everett *et al.,* 2017).

Vine architectures favouring open canopies have been proposed to substitute the most traditional pergola structures in areas with higher pressure of bacterial infection (Scortichini, 2014; Mauri *et al.,* 2016). Implementation of multiple leaders, either through training new plants or through grafting bud sticks into well-established trunks, is also a promising approach to obtain less dense canopies, with a lower proportion of woody material, thus hampering the spread of bacterial pathogens, including Psa (Currie *et al.,* 2014; KVH, 2016). Binding sites of plant branches to poles and touching points of irrigation tubes and shoots also seem to facilitate bacterial colonization and increase the risk of disease outbreaks, as well as plant production under high density (Scortichini *et al.,* 2012; McCann *et al.,* 2013). Improved management of plant canopies and cultivation density, could, therefore, be adopted as a way to disrupt the favourable conditions of bacterial growth, by promoting aeration, light penetration, low overlapping of canes and foliage, and facilitating the penetration and uniformization of chemical treatments (Gaskin *et al.,* 2016). Besides, special attention should also be paid to other plant species present in and around infected orchards, as they can also constitute a source of inoculum. Psa was found living epiphytically on *Cryptomeria japonica*, often used as shelterbelts in kiwifruit orchards in New Zealand, surviving up to 14 days when artificially inoculated (Vanneste *et al.,* 2012). Psa was also isolated from *Setaria viridis*, *Alternanthera philoxeroides* and *Paulownia tomentosa* located

under or nearby kiwifruit plants, which inclusively presented the same characteristic disease symptoms (Liu *et al.,* 2016). Several non-host plants collected in the proximity of infected kiwifruit plants, including *Calystegia sylvatica* and *Capsella bursa-pastoris*, have also shown potential for harbouring Psa (Donati *et al., 2*020). In addition, although artificial pollination is frequently used to overcome potential limitations in plant productivity, flower pollen and the pollinators *Apis mellifera* and *Bombus terrestris* are passible for Psa contamination, raising questions on the possibility of pollinators representing a risk factor for pathogen dissemination (Pattemore *et al.,* 2014).

2.3.5. Plant nutrition

Nutrition has also been implicated in plant tolerance against several pathogens, mainly due to alterations in growth, tissue composition and expression of disease tolerance-related genes (Gupta *et al*., 2017). On the other hand, pathogens may interfere with plants' nutrient translocation or utilization efficiency, potentially causing nutrient deficiency, hyperaccumulation, or even toxicity (Cesco *et al*., 2020). So far, there is still a limited number of studies that have addressed the importance of plant nutrition/fertilization in mitigating kiwifruit pathogens such as Psa. For example, the role of N in plant defence against Psa is not straightforward. It has been suggested that high nitrogen fertilization favours the microclimatic conditions needed for Psa epiphytic growth, also leading to reduced penetration of the copper treatments due to denser canopies (Gaskin *et al*., 2016). Exogenous N-supply (as 0.5 mM urea) enhanced plant sensitivity to Psa, increasing bacterial endophytic density (Li *et al*., 2020). On the other hand, its deficiency also seems to promote Psa growth *in planta*, probably due to induction of early leaf senescence, impairment of plant defences and depletion of nutrient storage (Groen and Whiteman, 2014). Besides, the type of N source also seems to impact the extent of disease progression. For instance, it was found that in *A. chinensis* var. *deliciosa* 'Hayward' higher nitrate rates positively influenced plant responses against Psa, whereas ammonium nitrate showed higher disease incidence and severity, increasing endophytic Psa populations (Mowat *et al.*, 2015; Mauri *et al*., 2016). It was also demonstrated that depletion of calcium (Ca) and manganese (Mn) in Psa-inoculated *chinensis* var. *deliciosa* 'Hayward' micropropagated plants led to a slight increase of symptoms severity, whereas deficiency of Ca, iron (Fe) and boron (B) significantly increased Psa endophytic population. Moreover, a surplus of B and Ca slightly increased symptom severity, and excess of B and Mn significantly reduced plant photosynthetic quantum yield (Mauri *et al*., 2016). Iodine (I) application to *A. chinensis* var. *chinensis* 'Hort16A' seedling media also resulted in lower disease incidence, which is attributed by the authors to its antioxidant activity, but in 'Hayward' seedlings, it led to phytotoxicity symptoms (Holmes, 2012; Gupta *et al*., 2015). The optimization of I supply regimens to kiwifruit plants

may be successful in increasing plant tolerance to bacterial pathogens, and should, therefore, be subject to further investigation. Also, as regular copper foliar spraying is currently a staple in orchard management for the control of several fungal and bacterial diseases, including KBC (Cameron and Sarojini, 2014), its application for nutritional purposes should ideally take into consideration the already undertaken phytosanitary treatments to avoid potential phytotoxic or bleaching events. Nevertheless, the role of copper in plant nutrition and response against bacterial infection has been poorly explored. For example, copper application (10 ppm, two times/week) to 'Hort16A' and 'Hayward' seedling reduced the levels of disease incidence, but resulted in copper accumulation in plant tissues, whereas treatment with copper phosphite produced a marked phytotoxic effect on 'Hort16A' (Holmes, 2012). It is clear that the relationship between plant fertilization and tolerance is highly complex, since, besides the studied mineral concentrations, the mode and frequency of application, as well as possible interactions with the edaphoclimatic conditions of the orchard could result in different disease incidence. A deeper understanding of the environmental conditions associated with bacterial epidemics is a key aspect in the development of effective disease mitigation strategies, reason why they should be better explored by the scientific community.

3. Exploring plant tolerance mechanisms

Breeding for resistance is an integral part of any crop protection approach, as it is easy to implement with little environmental impact. However, a good comprehension of the plant defence mechanisms is essential for identifying tolerance traits and supporting genotype selection. So far, several groups of transcripts, specific genes and metabolites were found to be affected in kiwifruit plants during Psa infection, which could be used to propel the understanding of plant tolerance mechanisms (Fig. 3).

3.1. Plant defences

The first line of plant defence against pathogenic bacteria, called PAMP-triggered immunity (PTI), is activated through plant cell Pattern Recognition Receptors (PRRs) that recognize specific Pathogen-Associated Molecular Patterns (PAMP) characteristic to each pathogen. These can include flagellin, lipopolysaccharides or nucleotide-binding site leucine-rich repeats (NBS-LRR) proteins (Clay *et al*., 2009; Wurms *et al*., 2017a; Michelotti *et al.,* 2018; Wang *et al*., 2018a).

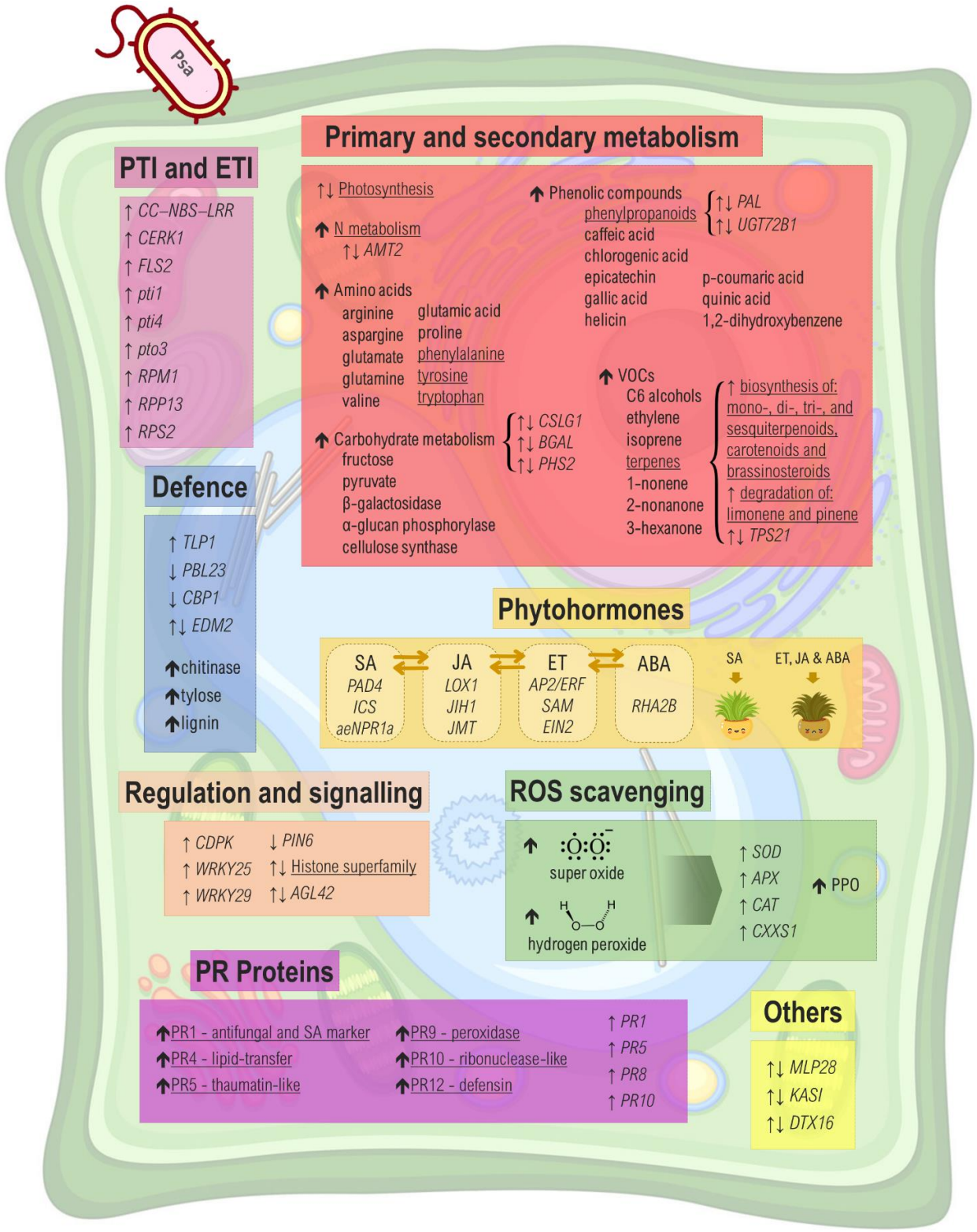

Figure 3 - Summary of the pathways affected by *Pseudomonas syringae* pv. *actinidiae* (Psa) in *Actinidia* spp. following infection. Arrows indicate: ↑ increase, ↓ decrease, or ↑↓ distinct responses between genotypes within the same study. Metabolites appear in bold case, families of transcripts are underlined, and *differentially expressed genes* are in italics. Abbreviations: ABA (abscisic acid), ET (ethylene), ETI (effector-triggered immunity), JA (jasmonic acid), PPO (peroxidase), PR (pathogenesis-related), PTI (pattern-triggered immunity), ROS (reactive oxygen species), SA (salicylic acid). (References: Miao *et al*., 2005; Miao *et al*., 2009; Spinelli *et al*., 2011; Petriccione *et al*., 2013; Reglinski *et al*., 2013; Cellini *et al*., 2014; Petriccione *et al*., 2014; Petriccione *et al*., 2015; Wurms *et al*., 2017a, 2017b; Michelotti *et al*. 2018; Wang *et al*., 2018; Nunes da Silva *et al*., 2019; Tahir *et al*., 2019; Li *et al*., 2020; Nunes da Silva *et al*., 2020; Sciubba *et al.,* 2020; Sun *et al*., 2020; Wang *et al*., 2020b)

A recent study identified 16 NBS-LRR genes differentially regulated in the genome of *A. chinensis* 2 days post infections (dpi) with Psa (Wang *et al*., 2020b). Moreover, genes directly involved in PTI and ETI, such as *FLS2*, *CC-NBS-LRR, Pti1, Pti4*, *RPP13*, *RPM1* and *RPS2*, were also found to be upregulated just 2 dpi with Psa (Wurms *et al*., 2017b; Wang *et al*., 2018a). *Pto3*, also involved in pathogen recognition and activation of plant defences, was found to increase 2 dpi with Psa in *A. arguta* (more tolerant), but only at 14 dpi in *A. chinensis* (more susceptible) (Nunes da Silva *et al*., 2020). The expression of specific genes involved in pathogen recognition in the early stages of infection may underpin the higher tolerance of some kiwifruit genotypes, resulting in a more effective activation of plant defence mechanisms.

The second line of plant defence mechanisms, called effector-triggered immunity (ETI), is activated after the recognition by plant resistance (R) proteins of bacterial effectors injected by the pathogen into the cytoplasm of plant cells. PTI and ETI can subsequently develop into an hypersensitive response (HR) at the infection site, which involves e.g., production of reactive oxygen species (ROS), increased enzymatic activity, changes in structural defences, and overexpression of R-genes (Michelotti *et al*., 2018). It was recently observed that genes *EDM2*, required for RPP7-dependent disease tolerance against pathogens, and *CSLG1*, a putative cellulose synthase-encoding gene, were upregulated in tolerant kiwifruit genotypes (but not in susceptible ones), possibly playing a role in the strengthening of the vascular system (Tahir *et al*., 2019). Moreover, the formation of reactive oxygen species (ROS) and lipid peroxidation, which may pose a threat to cell homeostasis, was found to occur after Psa infection of the susceptible *A. chinensis*, but not of the more tolerant *A. arguta* (Cellini *et al*., 2014; Nunes da Silva *et al*., 2020). To counteract the potentially harmful effects of these molecules, plants produce several antioxidant enzymes, such as peroxidases, to a higher extent in more tolerant varieties than in susceptible ones (Miao *et al*., 2005). Also, following Psa infection *APX*, *SOD* and *CAT* transcriptional levels were upregulated earlier in the tolerant *A. arguta* than in *A. chinensis* (Petriccione *et al*., 2015; Nunes da Silva *et al*., 2019, 2020). Tahir *et al*. (2019) also observed upregulation of a gene encoding a putative thioredoxin-like protein (*CXXS1*) in several kiwifruit genotypes with higher tolerance to Psa infection, but not in less tolerant ones. Taken together, these pieces of evidence suggest that in tolerant genotypes the antioxidant system is more complex, potentially preventing imbalances in cellular homeostasis and promoting plant fitness shortly following infection.

The content of soluble proteins in annual branches of tolerant cultivars was also found to be significantly higher than in susceptible ones before natural infection and, besides, protein content increased in susceptible cultivars and decreased in tolerant cultivars after infection (Miao *et al*., 2005). Proteomic analysis revealed that plant responses against Psa include proteins involved in basal plant defence, oxidative stress tolerance, heat shock, pathogenesis, transport and general signalling processes (Petriccione *et al*., 2013;

Petriccione *et al*., 2014; Wurms *et al*., 2017a; 2017b, Wang *et al*., 2018a; Nunes da Silva *et al*., 2019).

3.2. Phytohormone regulation

Plant responses against pathogens are regulated by complex phytohormone-mediated networks in which salicylic acid (SA), jasmonic acid (JA), abscisic acid (ABA) and ethylene (ET) counteract and interact with each other, modulating defence responses according to the type of pathogen and plant species (Pieterse *et al*., 2012). Genes involved in ET biosynthesis, such as *AP2*/*ERF* and *SAM*, were found to be upregulated just 2 dpi in *A. chinensis* plants inoculated with Psa (Wurms *et al*., 2017a, Nunes da Silva *et al*., 2020). Psa inoculation also induced the overexpression of *LOX1*, involved in the first step of the JA pathway, just 1 day after inoculation of *A. arguta* with Psa (Nunes da Silva *et al*., 2020). *LOX1* increased activity in *A. chinensis* Psa-inoculated plants is regarded as a strategy used by the pathogen to antagonize SA responses through the enhancement of the JA pathway, or as a consequence of the activation of other metabolic pathways, such as ET, through a positive feedback (Cellini *et al*., 2014). Other genes involved in ET and SA signalling pathways, such as *EIN2* and *PAD4*, respectively, were also upregulated in *A. chinensis* plants just 2 dpi after inoculation with Psa (Wurms *et al*., 2017b). In addition, an NPR1-like gene (*AeNPR1a*), a key component of the SA-dependent signalling pathway, was overexpressed in *A. eriantha* only 12 hours post infection (hpi) with Psa (Sun *et al*., 2020). Constitutive expression of this gene in transgenic tobacco plants induced the expression of PR-genes and promoted tolerance against bacterial infection, also restoring basal tolerance against *P. syringae* pv. *tomato* DC3000 in an *Arabidopsis thaliana npr1-1* mutant. As such, these authors suggest that *AeNPR1a*, and, by extent, the SA pathway, may have a central role in kiwifruit defence responses against Psa (Sun *et al*., 2020). In fact, several studies have demonstrated that *Actinidia* spp. defence responses against Psa are mainly SA-mediated, whereas the JA and ET pathways negatively affect plant tolerance to the pathogen (Reglinski *et al*., 2013; Petriccione *et al*., 2013, 2014; Cellini *et al*., 2014). In *A. chinensis*, inoculation with Psa and Pfm increased the concentrations of SA, to a greater extent than JA (Wurms *et al*., 2017b), and treatment with the SA inducer acibenzolar-S-methyl (ASM) reduced the incidence of plant disease caused by Psa (Cellini *et al*., 2014). Histological analysis also suggested that after treatment with ASM, bacterial colonization of plant tissues is greatly impaired (Spinelli *et al*., 2011). Contrastingly, a significant increase in disease development was observed in plants treated with methyl jasmonate (MJ), an inducer of the JA pathway (Reglinski *et al*., 2013; Cellini *et al*., 2014). Also, treatment with ET increased disease development, while application of the ET receptor blocker 1-methyl cyclopropane (1-MCP) decreased disease

incidence (Cellini *et al*., 2014). Pathogenesis-related (PR)-proteins transcriptional profiles also seem to be regulated by a complex interaction with plant hormones (Cellini *et al*., 2014; Wurms *et al*., 2017b). Transcriptional analysis of ASM-treated plants revealed the induction of *PR1* and *PR8* in *A. chinensis* var. *deliciosa* and of *PR1* in *A. chinensis* var. *chinensis*, whereas the expression of *PR5* and *PR10* were found to be little affected (Cellini *et al*., 2014). While *PR1* plays an antifungal role in plant defence and is frequently used as a molecular marker of SAR, *PR8* has shown chitinase and lysozyme functions, and *PR10* has ribonuclease-like activity and structure. Interestingly, the exposure of healthy *A. chinensis* var. *deliciosa* plants to Psa-inoculated neighbours significantly increased the transcription of *PR10*, which tended to decrease following subsequent inoculation of pre-exposed plants. The authors hypothesise that the exposure of healthy plants to volatile organic compounds from infected ones can induce differential gene expression and promote the activation of SA-dependent defences and enzymatic activity (Cellini *et al*., 2014).

A gene involved in the positive regulation of ABA, *RHA2B*, was also found to be upregulated 2 dpi with Psa, pinpointing that ABA regulation may be important in the first stages of plant infection (Wurms *et al*., 2017b). Stomatal closure, regulated through the ABA pathway, frequently acts as a mechanical barrier against several pathogens (Melotto *et al*., 2006, Ton *et al*., 2009; Hossain *et al*., 2011). However, exogenous application of ABA slightly increased disease development in several *A. chinensis* varieties (Cellini *et al*., 2014). Thus, the tolerant character of some kiwifruit genotypes to Psa probably results from the upregulation of the SA pathway which, in turn, negatively regulates the JA, ET and ABA pathways. These pieces of evidence have already propelled the use of plant elicitors composed by the SA-inducer ASM, commercialized as Bion® or Actigard®, although their efficacy against Psa seems to be highly dependent on the kiwifruit genotype (Cellini *et al.,* 2014). Further understanding of plant hormonal regulation in plant responses to bacterial pathogens would greatly benefit the development of tailored elicitor formulations for each plant genotype and/or pathogen, including the pathosystem *Actinidia*/Psa.

3.3. Primary and secondary metabolism

Plant infection by pathogenic agents frequently leads to impairments of both primary and secondary metabolism. For example, loss of chloroplast functions often occurs following pathogen invasion, consequently leading to tissue chlorosis or necrosis and changes in the photosynthetic metabolism of the host plant, further contributing to the development of disease (Lu and Yao, 2018). In kiwifruit plants, transcripts related to photosynthesis were downregulated in susceptible *A. chinensis* cultivars, but highly expressed in the more tolerant *A. eriantha* ones (Wang *et al*., 2017a, 2017b). This phenomenon can be related to structural

damages caused by higher bacterial multiplication rates inside the tissues of susceptible species. A subsequent study also demonstrated that Psa infection resulted in several amino acid impairments, leading to extensive reprogramming of carbon (C) and N cycling in various metabolic pathways, including photosynthesis, C fixation, and the tricarboxylic acid cycle (Li *et al*., 2020). Several sugars e.g., sucrose and fructose, were differently impaired in plant leaves, stems or bleeding-saps following Psa infection (Li *et al*., 2020). Although carbohydrates serve as signalling molecules and provide energy to support the demanding defence-related pathways, the authors suggested that the high concentration of sugars may propel bacterial proliferation and progression inside plant tissues (Li *et al*., 2020). Transcriptome analysis also revealed that a gene encoding a putative beta-galactosidase (*BGAL*), linked to carbohydrate metabolism, was upregulated in moderately tolerant genotypes, but downregulated in highly tolerant ones (Tahir *et al*., 2019), indicating that carbohydrate metabolism is impaired to different extents depending on the tolerance degree to Psa. Higher concentrations of gamma-aminobutyric acid, caffeic acid, and chlorogenic acid have also been proposed to provide a defensive advantage to *A. arguta* against Psa (Sciubba *et al.,* 2020).

The phenylpropanoid pathway, responsible for synthesizing a wide variety of phenolic compounds, such as lignins, phenolic acids, stilbenes, and flavonoids, seems to be of particular importance for plant tolerance against bacterial pathogens, including Psa (Wang *et al*., 2018a). Miao *et al*. (2009) compared the content of phenolic compounds in shoots and leaves of kiwifruit cultivars with different tolerance to Psa and observed that, before inoculation, phenolic compounds in tolerant cultivars were significantly higher than in susceptible ones, and that, after inoculation, their concentration increased in tolerant and susceptible cultivars. Concordantly, the expression of genes related to phenylpropanoids biosynthesis, including *UGT72B1 and PAL*, were upregulated in *A. chinensis* following inoculation with Psa (Wang *et al*., 2017a; Tahir *et al*., 2019). However, a recent study reported that PAL activity decreased in a more tolerant *A. chinensis* var. *deliciosa* cultivar (‘Jinkui’), but rapidly increased in a more susceptible cultivar (‘Hongyang’), also leading to a higher concentration of phenolics, gallic acid and chlorogenic acid in this genotype (Li *et al*., 2020). Besides, several phenolic compounds were found to be differently affected among these two cultivars. In the cultivar with higher tolerance, the main phenolic compounds identified included 1,2-dihydroxybenzene, epicatechin, and trans-cinnamic acid, whereas in the cultivar with lower tolerance epicatechin, trans-cinnamic acid and p-coumaric acid represented the major phenolic compounds (Li *et al*., 2020). It has also been demonstrated that tissue reinforcement by tyloses can restrict to a certain degree Psa migration through the xylem (Renzi *et al*., 2012). Lignin, also involved in plant defence through cell wall reinforcement: i) drastically increased after Psa inoculation in a more tolerant *A. chinensis* cultivar (‘Jinkui’), but not in a susceptible one (‘Hongyang’), and ii) was consistently higher

following Psa infection in *A. arguta*, but not in *A. chinensis*, demonstrating that it may contribute to plant tolerance against infection (Li *et al*., 2020; Nunes da Silva *et al*., 2020). These findings suggest that metabolic pathways associated with carbohydrates and phenolic compounds may play a central role in plant tolerance against Psa. The still scarce knowledge regarding the genetic and metabolic traits that underpin the higher tolerance of certain plant genotypes against bacterial pathogens, such as Psa, greatly hinders the possibility of identifying resistance markers and developing novel genotypes (through e.g., targeted breeding). However, this path should be pursued with caution, as breeding for resistance may propel bacterial evolutionary events, leading to the appearance of more virulent strains. Moreover, the cultural environment may modify the resistance degree of the plant genotype, posing additional challenges for producers and researchers.

4. Conclusion

Until very recently, studies on Psa were mostly focused on population structure, origin and adaptation to *Actinidia* spp., detection techniques and basic disease management strategies. In the last years, however, research efforts also aimed at understanding Psa pathogenesis and plant defence mechanisms. These have demonstrated the distinct virulence degrees of the several Psa populations identified so far, with Psa3 being the most damaging to kiwifruit plants, and that several phenotypic and genotypic traits may be responsible for the increased tolerance of some *Actinidia* genotypes, such as *A. eriantha* and *A. arguta* (in comparison with e.g., *A. chinensis*). Adequate crop protection should take into consideration not only the genotype of the cultivated plant, but also the particular strain of the pathogen, local orchard edaphoclimatic conditions and the agronomical practices employed. Overall, host resistance seems to be the best long-term approach to control plant diseases, but it will only be attainable when sufficient knowledge on plant regulatory mechanisms against pathogenic bacteria is available. In this regard, recent transcriptomic and proteomic approaches have shown that plant responses against Psa include: activation of pathogen recognition mechanisms, basal plant defence mechanisms, ROS scavenging, phytohormone regulation and activation of distinct PR-proteins. Also, primary and secondary metabolic pathways, such as phenols and carbohydrates, seem to modulate the response of kiwifruit plants during the development of KBC, but knowledge on the key aspects involved in increased tolerance against Psa is still currently very limited. Most importantly, plant disease management must be temporally and spatially dynamic to accompany the constantly shifting genetics of bacterial populations and respective plant hosts.

CHAPTER 1 - Sub-chapter 1.2

Kiwifruit Bacterial Canker: which paths have been taken for disease management and where are we going next?

Kiwifruit Bacterial Canker: Which paths have been taken for disease management and where are we going next?

Abstract

In the last decades, kiwifruit production has been severely impaired by the pandemic bacterium *Pseudomonas syringae* pv*. actinidiae* (Psa), which causes the kiwifruit bacterial canker (KBC), that currently affects all main producing countries. Given the lack of effective methods for controlling KBC, largely based on prophylactic antibiotic and copper-based formulations, several attempts have been made to find more effective and sustainable solutions. This prompted a slow recovery in the kiwifruit sector, with the substitution of sensitive cultivars for more tolerant ones and to the development of forecast models and technologies based on plant optical properties for early disease detection. Elicitors, such as acibenzolar-*S*-methyl, chitosan, and beneficial microorganisms have already been used in the field with some degree of success. On the other hand, other molecules and compounds, including phages, antimicrobial peptides, plant essential oils and propolis, have shown potential against Psa in laboratory trials. This review aims to provide a critical overview of the progress of the distinct approaches being developed to control Psa, discussing their potential and limitations, which may propel the design of integrated and improved control strategies for the successful management of plant diseases such as KBC.

1. Introduction

The kiwifruit bacterial canker (KBC), caused by the bacterium *Pseudomonas syringae* pv*. actinidiae* (Psa) is currently a worldwide epidemic, being present in all main kiwifruit producing countries, such as China, New Zealand, Italy, Chile, Spain, Portugal and South Korea, where it has been causing important economic impacts (Vanneste, 2017; EPPO, 2020). Owed to the severe effects of the pathogen and its ability to easily disseminate and infect kiwifruit plants, Psa was included in the A2 List of organisms recommended for regulation as quarantine pests from the European and Mediterranean Plant Protection Organization (EPPO, 2012). The conjugation of antibiotic and copper treatments with the implementation of strict orchard management routines proved to be of utmost importance in restricting Psa dispersion within and between orchards in several countries. However, its effectiveness in preventing disease appearance and further development is frequently unpredictable and highly related to the care taken in the operational processes involved. In the last decades, research efforts have focused on breeding for higher tolerance, developing forecast models and disease detection technologies, and identifying plant elicitors or microbial inhibitory agents. Other strategies employed to crops other than kiwifruits, such as gene-editing, may also have potential in the control of KBC. Nevertheless, all these methodologies present distinct strengths, weaknesses, opportunities and threats, which should be considered for the effective management of this disease (Table 1).

Table 1 - Analysis of the Strengths, Weaknesses, Opportunities and Threats (SWOT) of the methods with potential to control *Pseudomonas syringae* pv. *actinidiae*.

Strategies	Strengths	Weaknesses	Opportunities	Limitations
Antibiotics	• High antimicrobial activity • High specificity	• Use restriction • Environmental burden	• Novel antibiotics	• Bacterial resistance • Human health concerns
Copper compounds	• High antimicrobial activity • Cost-effectiveness	• Non-long-lasting protection under rainy conditions	• Novel formulations	• Environmental impact • Human health concerns
Plant breeding	• Long-term strategy • Chemical-free	• Time-consuming • Imprecise	• Genetic wealth of *Actinidia* germplasm	• Risk of losing relevant traits • Lack of suitable breeding lines
Forecast models	• Non-invasive • Chemical-free	• Technical knowledge required • Need for calibration and revalidation	• Combination with sensing systems • Availability of databases	• Unpredictability of climate change
Early disease detection	• Non-invasive • More efficient action • Chemical-free	• High cost • Technical knowledge required • Variable effectiveness during crop cycle	• Improvement with machine learning • Combination with unmanned vehicles • Poorly explored for Psa	• Unpredictability of climate change
Elicitors	• Promote early response • Can be from natural origin	• May have a fitness cost • Uncertain stability	• Few tested for Psa control	• Risk of phytotoxicity • Costs
Plant essential oils	• Highly abundant • Can act synergistically	• Uncertain stability • Poor curative action	• Improvement of EO products through nanotechnology	• Risk of phytotoxicity
Bacteriophages	• High abundancy of phages • Chemical-free	• Uncertain stability of phage-based products	• Screening for novel phages and combinations	• Legislation • Difficulties in upscaling
Antimicrobial peptides	• Can be polyfunctional • Promote early response	• Uncertain stability	• Highly abundant • Poorly explored strategy	• Low efficiency against Psa • Risk of phytotoxicity
Microorganisms	• High abundancy of organisms • Chemical-free	• May be affected by other treatments	• Screening for novel candidate organisms	• Risk of ecological imbalances • Legislation • Difficulties in upscaling
Gene-editing	• Long-term strategy • Precise genetic modifications • Faster than conventional breeding	• Poor understanding of tolerance mechanisms • Need for high technical knowledge • Resistance likely a polygenic trait	• Technological development • Poorly explored in *Actinidia* • Availability of information technology	• Restriction of GMOs • Low public acceptance

2. Antibiotic and copper-based treatments

The absence of curative measures against Psa propelled the use of prophylactic treatments at strategic moments of plant growth to prevent infection. The use of antibiotics for plant disease control is still allowed in several countries, such as China, the USA and New Zealand, although the options for their use are generally limited and strongly regulated (KVH, 2016). Despite being effective in controlling plant pathogenic bacteria, including Psa, long-term exposure to antibiotics may lead to bacterial resistance (Cameron *et al.,* 2014; Zoysa *et al.,* 2015; Daranas *et al.,* 2018). The discovery of novel antibiotics for agricultural purposes is still a subject of research, but due to the great limitations involving their use, linked to environmental and human health concerns, their use in fruit plantation, including kiwifruit, has become obsolete over the years.

During the last decades, the use of copper-based compounds to control microbial pathogens has been substituting antibiotics, mostly due to their high antibacterial activity, broad-spectrum, cost-effectiveness, chemical stability and prolonged effect after application (Lamichhane *et al.,* 2018). Until the first Psa outbreaks in Italy and New Zealand, kiwifruit orchards did not require regular application of phytosanitary products. However, since then, copper application has been adopted as a prophylactic measure against Psa worldwide. In Portugal, for example, governmental guidelines advise at least six applications of copper-based formulations at strategic moments during the kiwifruit growing season (e.g., after harvest, at flowering and after winter pruning) (DGAV, 2014). Nevertheless, several factors affect the efficacy of copper treatments, mostly pertaining to the form of copper used, particle size, degree of retention on the plant surface and solubility (KVH, 2016; Sciubba *et al.,* 2019). More soluble forms (e.g., copper sulphates) pose increased problems because they are more easily washed out after raining, leading to less plant protection and greater propensity to cause soil pollution (Ashrafzadeh and Leung, 2019). Combination with other compounds has been shown to increase Psa control while decreasing the amount of copper needed. For example, Scortichini (2016) showed increased effectiveness of a mixture of hydracid of citric acid (21.4%), zinc (4.7%) and copper (2.6%) on the reduction of bacterial oozing from infected kiwifruit vines, when compared with Bordeaux mixture (copper sulphate pentahydrate and lime, with 25% active copper), presumably due to higher penetration into plant tissues. Despite their undeniable effectiveness as a prophylactic measure, copper compounds do not have curative properties and show no systemic transport within plant tissues, thus failing in the broad protection of the infected plant (Lamichhane *et al.,* 2018). Combinations with other compounds, such as humic acids, amino acids or nitrates, could improve copper efficiency against systemic bacteria, such as Psa, while ensuring low environmental impacts (Monchiero *et al.,* 2015).

3. Plant breeding

Crop improvement is probably the foundation of an integrated approach to mitigate agronomical pathogens, including Psa. Whereas previous breeding programs were mainly oriented to fruit organoleptic properties, after the complete collapse of the most sensitive *A. chinensis* var. *chinensis* 'Hort16A' (yellow kiwifruit) worldwide, Psa tolerance became one of the main criteria to be used for developing new *Actinidia* genotypes (Debenham *et al.,* 2013; Beatson *et al.,* 2014; Wang *et al.,* 2019). As a result, susceptible cultivars (e.g., 'Hort16A') have been gradually replaced by more tolerant ones, including var. *chinensis* 'Gold3', developed by the breeding program from Plant and Food Research and Zespri (Ashrafzadeh and Leung, 2019). Although the initial responses to Psa were conditioned by the lack of reliable procedures for assessing cultivar susceptibility to Psa, improvements were made through the development of methodologies for symptom analysis and assessment on bacterial dispersion in plant tissues. These, in combination with field observations, resulted in the categorization of numerous species, cultivars and progeny of novel crosses in terms of their susceptibility (Nardozza *et al.,* 2015; Hoyte *et al.,* 2015; Wang *et al.,* 2019). Nevertheless, there is still an enormous genetic wealth in *Actinidia* spp. germplasm to be explored by, e.g., introgression breeding (Huang and Liu, 2014). Introgressions from the wild *A. eriantha* first aimed at desirable appealability to increase fruit consumption convenience (Atkinson *et al.,* 2009). Later, *A. eriantha* was used as the male parent in the crossing with *A. chinensis* var*. chinensis* for the commercial release of 'Jinyan' (Huang and Liu, 2014) which, apart from other agronomically interesting traits, also showed lesser susceptibility to Psa (Lei *et al.,* 2015). Another aspect to explore is the large variation in ploidy within the genus *Actinidia*, including diploids, tetraploids, hexaploids, heptaploids and octaploids species (Huang *et al.,* 2004; Zhang *et al.,* 2017; Asakura and Hoshino 2018). In fact, higher ploidy has been associated with higher tolerance to Psa (Cotrut *et al*., 2013; Wang *et al*., 2020a). Disease incidence was observed to be higher in diploid and tetraploid *A. chinensis* var. *chinensis* genotypes. In contrast, *A. arguta* diploid individuals registered higher susceptibility to Psa and tetraploid individuals showed a lower degree of susceptibility, which was similar to hexaploids of 'Hayward' (Cotrut *et al*., 2013). Techniques of random genetic modification by using mutagenic agents (e.g., ethyl methane sulfonate) are still applied in the development of new genotypes, including *Actinidia* cultivars (Sartori *et al.,* 2015). However, the process is very laborious and expensive, involving the need to analyse the genetic changes that could be incorporated into elite lines.

4. Forecast models

Forecast modelling has long been used to predict the spread and incidence of several plant pathogens, allowing to better plan and anticipate the necessary measures for a more effective control. Concerning Psa management, the 'OsiriS' (Marcon *et al.,* 2015) and 'OttaviO' (Cacioppo *et al.,* 2015) sensing systems were successfully tested in field trials. The systems measured several pedoclimatic parameters that can be remotely accessed for decision-making, including air temperature, relative humidity (RH), leaf wetness, wind speed, photosynthetically active radiation, soil tension, pH and electrical conductivity. This integrated approach was used to predict Psa infection and decide when to apply copper treatments, resulting in a 60% decrease in Psa symptoms and the reduction of costs associated with copper application (Cacioppo *et al*., 2015; Marcon *et al*., 2015). Models used for the prediction of fire blight of apple and pear were also used as a basis for a Psa infection risk model. These began to be developed in 2011 by a New Zealander consortium, and were further fine-tuned and tested in New Zealand, Italy and Korea (Psa-V risk model) (Antoniacci *et al.,* 2019; Beresford *et al.,* 2017; Kim *et al.,* 2018). The model is weather-based and conjugates the concept of multiplication capacity (M index) and Psa dispersal. The M index, which estimates the pathogen population growth, is determined by the accumulated air temperature for 72 h, during the hours when plant canopies are wet, either considering leaf surface wetness (>50%) or air relative humidity (>81%) as surrogate parameters. The risk of infection (R index) is determined daily, but it depends on the total rainfall of the last 24 h, which should be above 1 mm (otherwise the R index, i.e., risk of infection, would be considered null) (Beresford *et al.,* 2017). This model showed high accuracy in predicting leaf infection mainly in spring and summer seasons, but its application in Korea pointed to its sensitiveness regarding the absence/presence of rainfall (Kim *et al.,* 2018). In this case, the original model resulted in false positives during the summer due to high temperatures that, not being favourable to Psa growth, were not considered on the risk estimation. Accumulation of rain also had to be reconsidered, not only because of inoculum reductions during heavy rainfalls but also due to the influence of temperature on humidity persistence in the plant surface. Kim and co-workers (2018) addressed this question by introducing a maximum threshold of 27 °C for temperature and 100 mm for accumulated rainfall, resulting in increased suitability of the Psa-V model to be applied to the reality of Korea, with an 85.7% accuracy in predicting disease incidence (Kim *et al.,* 2018).

Other models, such as CLIMEX and MaxEnt, were also used to predict the global spread and distribution of Psa (Khandan *et al.,* 2013). Using CLIMEX the authors generated ecoclimatic indices to predict the favourableness of a specific region to be colonized by Psa, and with MaxEnt Psa distribution was predicted using a set of selected bioclimatic variables combined with geo-referencing. However, discrepancies between both models were

observed for regions with different climatic conditions than those in which the models were originally trained (Khandan *et al.,* 2013), reinforcing the importance of calibration and revalidation in forecast modelling. Regarding modelling for Psa infection and spread, considerations must be taken on factors that could exacerbate disease development, such as frost, wind or genotypic susceptibility (KVH, 2016). Freezing temperatures and duration were considered in the model from Do *et al.* (2016) to predict damage accumulation in Psa-infected canes from *A. chinensis* var. *deliciosa* 'Hayward' and *A. chinensis* var. *chinensis* 'Hort16A'. However, this model was only accurate in predicting accumulated damage (lesion extension and rate of necrosis) in the less susceptible cultivar ('Hayward') but not in the most susceptible one ('Hort16A') (Do *et al.,* 2016).

One of the biggest challenges in forecast modelling is adjusting to new realities for reliable extrapolation, further aggravated under climate change scenarios. Considering future climatic circumstances, MaxEnt was used in combination with ArcGIS® (ESRI, 2014) for modelling Psa distribution in China, resulting in mapping regions according to four categories of suitability to harbour the pathogen (Wang *et al.,* 2018c). More recently, Qin *et al*. (2020) presented their projections of Psa distribution in China by 2050, using an ensemble model resulting from three modelling algorithms combining a set of bioclimatic variables. The authors highlighted several aspects (such as precipitation from late winter to early spring, and average temperature during the warmest quarter), further indicating that environmental variables contribute to a greater extent to model accuracy when translated into bioclimatic features with higher influence (Qin *et al., 2*020). These projections should be extended to other regions for a better action plan against Psa at both regional and global levels. The growing sophistication in sensing systems, larger availability of databases and better understanding of Psa epidemiology, will certainly result in either refining existing forecasting models or the creation of novel ones.

5. Early disease detection

More options with increased reliability are now available for early detection of plant disease through non-invasive methodologies. By analysing spectral characteristics (reflectance, transmittance, and absorbance) of plant tissues, physiological and nutritional alterations can be assessed and used for disease detection without direct physical contact (Bergsträsser *et al.,* 2015). These optical sensing systems explore different imaging techniques including Red-Green-Blue colour model (RGB), thermal, multi- and hyperspectral, chlorophyll fluorescence and 3-D, and current technological sophistication allows to measure data by a spectral range from 350 to 2 500 nm, with very high resolution (Mahlein, 2016). Depending on the purpose, they can be used for analysis at leaf-, plant-, or

orchard-level and be installed in fixed or mobile platforms, including e.g., farm tractors, robots, crewless aerial vehicles, aircraft or satellites (Mahlein, 2016, Maes *et al.,* 2016, Xue *et al.,* 2019).

Satellite imagery has also been tested for monitoring Psa incidence in kiwifruit orchards, and a series of vegetation indices that could be related to disease development were identified (Taylor *et al.,* 2014). Multi-spectral imagery using light bands ranging from the visible to near-infrared region (NIR) of the electromagnetic spectrum were analysed and compared with shapefiles, resulting from precise mapping of Psa-positive samples collected along orchards in Bay of Plenty, New Zealand. The authors achieved reasonable detection accuracies, ranging from 75% to 79%, by using binomial logistic regression in the modelling of the vegetation indices. However, the method had limitations during stages when vine vigour was more stationary (Taylor *et al.,* 2014).

Thermal imagery (or infrared thermography) can be used to assess plant tissue temperature, which is correlated to evapotranspiration (Mahlein, 2016). Therefore, slight modifications in transpiration caused by Psa infection can be detected with infrared cameras before symptoms can be visualized in the field. However, this approach cannot discriminate Psa infection from other stresses that induce changes in evapotranspiration (e.g., heat). Maes *et al*. (2014) showed that Psa could be detected at leaf level by thermal imaging as early as two days after exposure by identifying cold spots on leaf surface not showing visual symptoms. Moreover, the suitability of thermal imaging in identifying two distinct stages of the infection process was demonstrated (Maes *et al.,* 2014). At the orchard level, this technology was also validated in the mapping of affected zones. Psa-infected areas could be identified in colder canopies (from 1 °C to 3 °C, approximately), and a tendency for higher Psa incidence in outer parts of the canopies was also observed (Maes *et al.,* 2014).

Given that numerous factors can impair plant physiological and anatomical status, several authors have developed spectral indices (or signatures) to differentiate distinct diseases in sugar beet (Mahlein *et al.,* 2013), leaf rust in wheat (Ashourloo *et al.,* 2014) or *flavescence dorée* in grapevine (Al-Saddik *et al.,* 2017). While such signatures are not yet available for detecting Psa infection, their creation would represent a step forward in optimizing early detection of this pathogen (Al-Saddik *et al.,* 2019). These, together with the use of emerging techniques of deep machine-learning (convolutional neuronal networks) may significantly improve the application of early disease detection techniques to mitigate KBC (Mohanty *et al.,* 2016; Toda and Okura, 2019; Boulent *et al.,* 2019).

6. Plant elicitors

One alternative strategy to the use of conventional pesticides relies on inducing plant resistance through elicitors (also known as defence inducers, plant activators or priming agents) (Ramírez-Carrasco *et al.,* 2017). Numerous chemical compounds have been reported as plant elicitors, including phytohormones and their analogues, carbohydrate polymers, lipids, glycoproteins, vitamins and polysaccharides (Bektas and Eulgem, 2015; Mauch-Mani *et al.,* 2017; Tripathi *et al.,* 2019). Salicylic acid (SA) and its functional analogues benzothiadiazole (BTH) and β-aminobutyric acid (BABA) are among the most studied for their action as broad-spectrum defence inducers through systemic acquired resistance (SAR) (Tripathi *et al.,* 2019; Li *et al*., 2020). The most used BTH in kiwifruit protection is acibenzolar-*S*-methyl (ASM), commercialized as Bion® or Actigard®. Several works have shown the effectiveness of ASM on controlling Psa in *Actinidia* spp., despite their effectiveness being genotype-dependent. Cellini *et al.* (2014) showed that *A. chinensis* var. *deliciosa* plants with lower Psa incidence were more prone to form necrotic spots, callose deposition and superoxide burst after ASM application, while the same was not observed in *A. chinensis* var. *chinensis*. Nevertheless, the protective effect of ASM was maintained for several weeks in both species (Cellini *et al.,* 2014). Additionally, Wurms *et al.* (2017b) observed that ASM significantly reduced lesion length of Psa infection by 50%, indicating that primed plants could respond more strongly to the infection. Interestingly, elicitation of the ethylene (ET) and jasmonic acid (JA) pathways was associated to worsening of disease incidence, most likely owed to SA pathway suppression and promotion of stomatal opening, which facilitate Psa invasion into the host tissues (Bektas and Eulgem, 2015; Michelotti *et al.,* 2018; Brunetti *et al*., 2020). Beta-aminobutyric acid (BABA) is a plant metabolite that tends to accumulate in sites of bacterial or fungal infection, and has been shown to have potential in controlling pathogens and pests in several plant species (Baccelli and Mauch-Mani, 2016; Li *et al.,* 2019). In kiwifruit, BABA was successfully tested to control postharvest infections caused by *Botrytis cinerea* and *Alternaria alternata*, inducing gene expression and enzymatic activity in treated fruits. The authors also showed that BABA protective effect increased when it was applied in combination with the antagonistic yeast *Hanseniaspora uvarum* (Cheng *et al.,* 2019). Brunetti *et al*. (2020) have recently presented promising results in leaf disk assays, with BABA reducing Psa-induced symptoms, probably due to a direct bactericidal effect (Brunetti *et al., 2*020).

Apart from SA-analogues, chitosan is one of the most studied elicitors and has already been included in commercial products for field applications in kiwifruit orchards (Collina *et al.,* 2016; Brunetti *et al*., 2020). This compound is believed to be bacteriostatic, affecting the biochemistry of the bacteria surface (Shanmugam *et al.,* 2016), and may also hamper pathogen access to nutrients and minerals (Beatrice *et al.,* 2017). Chitosan field efficacy to

control Psa was demonstrated in a three-year trial with *A. chinensis* var. *deliciosa* 'Hayward', in which leaf spots, twig wilting and the number of exudates were significantly reduced (Scortichini, 2014). This possibly occurs due to an enhanced expression of genes encoding pathogenesis-related (PR) proteins, which have been described in chitosan-elicited kiwifruit plants during Psa infection (Beatrice *et al.,* 2017). Numerous positive attributes have been pointed to chitosan, including its broad activity spectrum, biodegradability, and biocompatibility (Scortichini, 2014; Beatrice *et al.,* 2017; Yang and Zhong, 2017); however, an important drawback for field application of chitosan is its insolubility in water. Several water-soluble chitosan derivatives have been obtained by chemical modifications and tested for their protection against pathogenic bacteria to overcome this limitation. Besides, several chitosan derivatives have been reported as having higher antibacterial activity than chitosan itself, especially against Gram-negative bacteria, possibly due to differences in the bacteriostatic effect and interference with the pathogen homeostasis (Yang and Zhong, 2017). Plant elicitors are a viable alternative to substitute, at least in part, conventional pesticides, and current research points to an increment in their use in the coming years. Notwithstanding, care must be taken so that the physiological costs of elicitation do not compromise plant fitness and productivity (van Hulten *et al.,* 2006).

7. Emerging molecules and compounds

7.1. Plant extracts and essential oils

Plants produce a wide diversity of substances used for signalling and defence processes against invaders, which include bioactive molecules/compounds present in plant extracts (*latu sensu*) and, more specifically, in plant essential oils (EOs) (Song *et al.,* 2016; Sciubba *et al.,* 2019; Mori *et al.,* 2019). EOs antibacterial activity has been attributed to e.g., alterations in the permeability of pathogen cell surface, loss of intracellular contents, and impairments in quorum sensing mechanisms (Chouhan *et al.,* 2017; Pucci *et al.,* 2018).

Activity against Psa, *P. syringae* pv. *syringae* and *P. viridiflava* was found in extracts from plants from the Liliales and Urticales orders, which inhibited bacterial multiplication for, at least, two weeks after leaf spraying (Balestra, 2007). Antimicrobial activity against Psa was also demonstrated for extracts and EOs from plants belonging to the families Myrtaceae (*Pimenta* spp., *Melaleuca* spp. and *Syzygium aromaticum*), Lauraceae (*Cinnamomum* spp. and *Laurus* spp.), Lamiaceae (*Mentha suaveolens*, *Rosmarinus* spp., *Salvia* spp., *Monarda* spp., *Thymus vulgaris* and *Origanum vulgare*), Poaceae (*Phyllostachys heterocycla f. pubescens*), Euphorbiaceae (*Sapium baccatum*), Amaryllidaceae (*Allium sativum*), Theaceae, Hypericaceae (*Hypericum perforatum*), Polygonaceae (*Polygonum cuspidatum*)

and Vitaceae (*Vitis vinifera*) (Vavala *et al.,* 2016; Song *et al.,* 2016; Vu *et al.,* 2017; Mattarelli *et al.,* 2017; Pucci *et al.,* 2018; Mori *et al.,* 2019; Lovato *et al.,* 2019; Simonetti *et al*., 2020). Laboratory trials indicated that the most effective EOs against Psa are those rich in phenolic compounds, stilbenes, xanthones, olefinic compounds, cinnamaldehyde and tannins (Song *et al.,* 2016; Vu *et al.,* 2017; Mori *et al.,* 2019; Simonetti *et al*., 2020). Song *et al.* (2016) showed the inhibitory effect against Psa of the constituents eugenol, methyl eugenol and estragole, from *Pimenta* spp. EO, and cinnamaldehyde, from *Cinnamomum cassia* EO. Activity against Psa and other bacteria was also demonstrated *in vitro* for several constituents of EOs isolated from the medicinal plant *Sapium baccatum*, including, methyl gallate, corilagin, tercatain, chebulagic acid, chebulinic acid, quercetin 3-O-α-L-arabinopyranoside and gallic acid (Vu *et al.,* 2017).

Lovato *et al.* (2019) demonstrated the suppression of Psa virulence after exposure to green tea extracts (*Camellia sinensis*) by reducing pathogen motility and biofilm production. Despite the promising ability of EOs to inhibit Psa, their composition is strongly influenced by the plant growth conditions, chemotype, plant age and organ used (Pucci *et al.,* 2018). Moreover, the extraction method is decisive relatively to what can be maintained or lost in EOs preparation (Mori *et al.,* 2019). For example, Mori *et al.* (2019) showed that the antimicrobial activity of EOs from *P. h.* f. *pubescens* against Psa and other plant pathogens was considerably higher for EOs extracted by super-heated steam, as compared with EOs extracted with ethanol or hot water. Besides, Mattarelli *et al.* (2017) observed marked differences in the composition of EOs extracted from the closely related species *Monarda didyma* and *M. fistulosa*, not only in terms of the diversity of their constituents, but also in their relative abundance. Despite this fact, their activity against Psa was similar, presumably because of a higher carvacrol content, observed in the EO with less thymol. Plant elicitation may also be considered to obtain more effective bioactive compounds. For example, root extracts from *H. perforatum* plants elicited with chitosan oligosaccharides showed higher activity against Psa than an extract from roots of non-elicited plants (Simonetti *et al*., 2020).

Despite the clear advantages pointed to the use of EOs in plant protection, factors such as phytotoxicity, difficulties in the uniformization and perishability of the products, low solubility and chemical instability, are constraints to their inclusion in commercial formulations (Rossetti *et al.,* 2017; Pucci *et al.,* 2018). Additionally, EOs can act synergistically, which might lead to the need for lower doses to maintain their efficacy against plant pathogens (Vavala *et al.,* 2016). Nevertheless, little is known about the interactions leading to synergism or antagonism between EOs or their constituents (Chouhan *et al.,* 2017). Nanotechnology can be a promising strategy to address some of these limitations, as already demonstrated for microencapsulated gallic acid and ellagic acid to control bacterial pathogens, including Psa (Rossetti *et al.,* 2017). Nevertheless, the antimicrobial activity of integral EOs and their constituents, either in combination or applied alone, should be subject to further investigation

and thoroughly validated in field conditions. As these limitations are overcome and further research is developed, more EOs-based products are likely to emerge in the market in the near future.

7.2. Propolis

Propolis, a mixture of resins, balsams, essential and aromatic oils, and pollen, is another interesting option for controlling plant bacterial pathogens, such as Psa. Until now, more than 400 substances have been identified in propolis, including phenolic compounds, aromatic acids, diterpenic acids, aldehydes, monoterpene, amino acids, steroids and inorganic compounds (Bulman *et al.,* 2011; Gavanji *et al.,* 2012; Pobiega *et al.,* 2019). Despite the major differences commonly observed in the composition of different types of propolis, they are consistently referred to as having a broad range of biological activities against bacteria (Bulman *et al.,* 2011; Pobiega *et al.,* 2019). However, studies on their potential in agriculture remain quite discrete and often related to post-harvest diseases in marketable fruits (Yang *et al.,* 2010; Ordóñez *et al.,* 2011). Propolis extracts have shown activity against phytopathogens such as the fungi *Phytophthora infestans* (Yusuf *et al.,* 2005), *Penicillium* spp. (Yang *et al.,* 2010), *Podosphaera fuliginea* (Guginski-Piva, 2015) and the bacteria *Erwinia carotovora*, *P. syringae* pv. *tomato*, *Xanthomonas campestris* pv. *vesicatoria* (Ordóñez *et al.,* 2011), *X. axonopodis* pv. *phaseoli* and *P. syringae* pv. *tabaci* (Jaski *et al.,* 2019). Until recently, the use of propolis for Psa control was considered as a desperate attempt to find solutions in the face of an uncontrolled situation (Youn*,* 2012). Thus, the lack of research on this particular topic might result from scepticism related to the discrete results reported in the very few articles where propolis was tested against Psa (Monchiero *et al.,* 2015). Notwithstanding, given the complexity of propolis matrices, it is certainly too early to disregard this natural product as a possibility in Psa control. Further studies to investigate the composition of propolis and the mode of action of their constituents, may change the current perspective on its use in disease management.

7.3. Bacteriophages

Bacteriophages (or phages) are viruses that infect bacteria causing cell lysis following replication of the viral RNA, and can be found in virtually all environments (Di Lallo *et al.,* 2014; Frampton *et al.,* 2014). In the last years, many researchers have dedicated their efforts to isolate and characterize phages for crop protection. An extensive list of phages has been proposed as promising candidates for Psa control in the field after positive laboratorial (Pinheiro *et al.,* 2019) and greenhouse results (Flores *et al.*, 2020). Phages active against

Psa have been isolated not only from *Actinidia* spp., but also from other sources such as the orchard environment, water bodies, or even from public sewage (Di Lallo *et al.,* 2014; Yu *et al.,* 2016; Yin *et al.,* 2019; Flores *et al*., 2020). After an exhaustive screening of phage-host combinations, Frampton *et al.* (2014) selected 24 from more than 250 phages active against Psa, including both narrow and broad host range. This assessment used Psa strains and other pseudomonads (collected in kiwifruit orchards from several countries) and showed that the majority of the phages with higher activity against Psa belong to the Caudovirales order. These phages have a narrow host range and seem to use several strategies in the infection process (Frampton *et al.,* 2014). Furthermore, their capability to survive in a wide range of temperatures, pH and UV light conditions, makes them suitable for storage and field applications (Frampton *et al.,* 2014; Yu *et al.,* 2016).

To ensure phage effectiveness in plant protection, the maintenance of their lytic activity throughout the shelf-life of phage-based products is of utmost importance (Park *et al.,* 2018). Other important features that must be considered in screening phages to be used as biological control agents against plant diseases is the lack of incorporation of genetic information from the phage to the bacterial host (lysogeny and transduction), the efficiency of their action against the pathogen (e.g., time of death) and specificity (Di Lallo *et al.,* 2014; Frampton *et al.,* 2014; Flores *et al., 2*020). Moreover, combinations of phages must be tested for their suitability to incorporate cocktails with increased antibacterial action, and their compatibility with other products must also be assessed. Recently, phage cocktails were validated *in vivo* against Psa, resulting in reduced bacterial load and symptomatology in *A. chinensis* plants grown under greenhouse conditions (Flores *et al*., 2020), thus confirming their potential to integrate novel disease control strategies.

7.4. Antimicrobial peptides

Antimicrobial peptides (AMPs) are extremely abundant in plants, and their cationic activity interferes with bacterial membranes, constituting an alternative to conventional antibiotics and pesticides (Cameron *et al.,* 2014; van Esse *et al.,* 2019). Cameron *et al.* (2014) were among the firsts to point out candidate AMPs to be used in KBC mitigation, reporting short cationic AMPs with activity against Psa (the dodecapeptide amide, KYKLFKKILKFL-NH2, and the hexapeptide amide, WRWYCR-NH2), which showed similar effectiveness in controlling Psa to that of streptomycin. The authors also showed that conjugation with the toxic moiety 5-nitro-2-furaldehyde (NFA) may be used for designing novel AMPs against Psa. However, in this case, acylation diminished the antimicrobial activity of the tested AMPs. In addition, analogues of the cyclic lipopeptide battacin, produced by the bacterium *Paneibacillus tianmunesis* and with described antimicrobial activity against

several plant pathogens, have demonstrated enhanced activity when their synthesis includes linearization of the original structure. The most active was further tested for its capability against Psa, proving to be highly effective either in preventing biofilm formation or eradicating preformed biofilms (Zoysa *et al.,* 2015). Activity against Psa and other bacterial and fungal pathogens was also demonstrated for a collection of 36 linear lipopeptides from the cecropin A-melittin hybrid undecapeptide (BP100). In general, it was observed that lipopeptides bearing a hexanoyl chain were more effective against both Psa and *P. syringae* pv. *syringae* (Oliveras *et al.,* 2018).

It is interesting to note that, although dozens of AMPs have shown activity against Psa, very few were collected from plants. A small number of AMPs extracted from *Actinidia* spp. have been registered in the available databases but, to the best of our knowledge, to date none have shown to be detrimental to Psa. In the few studies on the activity of AMPs against Psa, the tested peptides were synthesized by the research team (Cameron *et al.,* 2014; Oliveras *et al.,* 2018; Camó *et al.,* 2019), which might be the reflex of lack of preference for natural AMPs. Moreover, despite many laboratory studies on the activity of AMPs, *in planta* trials are still scarce, as is the case of Psa-infected *Actinidia* plants. This is particularly pertinent because the biocide effect of AMPs is often lower *in planta*, when compared to *in vitro* observations, presumably due to their degradation by plant proteases (Jung and Kang, 2014; Holaskova *et al.,* 2015).

Considering the natural sources of AMPs and the structural and biochemical modifications that can be performed in the synthesis of novel peptides, possibilities are vast, but several limitations such as toxicity, instability of the substances and production costs are major obstacles to their use (Tang *et al.,* 2018). These constraints need to be further addressed so that AMP-based products can emerge in the market and be implemented in crop management, particularly in cases of pandemic phytopathogens, such as Psa.

8. Microbiota and other beneficial microorganisms

In addition to the predatory character of bacteriophages, other ecological aspects of microbial resources have been explored for plant disease management. These include antibiosis, lysis, production of pathogen-inhibiting volatile compounds and siderophores, and competition for space and nutrients (Tontou *et al.,* 2016a, 2016b; Compant *et al.,* 2019). An increasing list of beneficial fungi and bacteria applied to control Psa in kiwifruit orchards has been made available in recent years, including the fungi *Aureobasidium pullulans*, *Trichoderma* spp. and *Ulocladium oudemansii* and the bacteria *Bacillus subtilis*, *P. fluorescens* and *Pantoea agglomerans* (Stewart *et al.,* 2011; Hill *et al.,* 2015; KVH, 2016; de Jong *et al.,* 2019). Lactic acid bacteria (e.g., *Lactobacillus plantarum*) have also been

considered a promising group because they produce acidifying metabolites (organic acids), antimicrobial peptides (e.g., bacteriocins) and other bioactive compounds (Purahong *et al.,* 2018; Daranas *et al.,* 2018). The endophyte *P. synxantha*, isolated from *A. chinensis* var. *chinensis*, was proposed for further investigation due to its antagonistic activity against Psa, possibly due to the presence of genes involved in the synthesis of nonribosomal peptide synthetases, which may antagonise Psa (Tontou *et al.,* 2016a, 2016b). Endophytic bacteria from the New Zealand native *Leptospermum scoparium* also showed activity against Psa both *in vitro* and *in planta* (Wicaksono *et al.,* 2018). While these endophytes can be used to patrol plant tissues from the inside, due to their systemic character, the epiphytic stage of Psa opens a window of opportunity to use beneficial epiphytic microorganisms for its control (Purahong *et al.,* 2018). Despite these promising pieces of evidence, a satisfactory level of protection has not yet been accomplished with these strategies. Low mobility within the plant and the lack of knowledge on the persistence of the inoculated organisms are among the reasons why the long-term efficacy of using beneficial microorganisms is still seen with some reservations when considering field applications (Wicaksono *et al.,* 2018).

9. Gene editing

Traditional breeding techniques are frequently expensive, lengthy and imprecise (Wang *et al.,* 2018b; Borrelli *et al.,* 2018). The growing need for new crop genotypes in a faster, more efficient and cost-effective way, has propelled the development of new breeding techniques. These allow the possibility of introducing precise modifications into the genome of an organism, through gene-editing, being a major opportunity in state-of-the-art plant breeding (Dong and Ronald, 2019). Nevertheless, these technologies have not been properly explored in *Actinidia* spp..

The first-generation gene-editing techniques included the zinc finger nucleases (ZFNs) and transcription activator-like effector nucleases (TALENs). These techniques were effectively used for disease resistance in several plant species such as rice, for example, in which increased resistance against *Xanthomonas oryzae* pv. *oryzae* was achieved after genetic modifications in the susceptibility gene *Os11N3*, through the inability of the bacterial effector to bind to its target (Li *et al.,* 2012). Nevertheless, despite being powerful techniques, utilization of ZNFs and TALENs is often costly, laborious and complex due to the need for protein engineering (Rinaldo and Ayliffe, 2015; Jaganathan *et al.,* 2018). The clustered regularly interspaced short palindromic repeats (CRISPR)/CRISPR-associated protein 9 (Cas9) system is the most recent gene-editing technique revolutionizing biotechnology and has already been applied in numerous crop species to enhance their tolerance against pests and pathogens (Peng *et al.,* 2017; Fister *et al.,* 2018; Ortigosa *et al.,* 2019). Ortigosa *et al.*

(2019), in particular, edited a gene targeted by coronatine, a phytotoxin used by *P. syringae* bacteria to promote leaf colonization, optimizing gene-edition in *Actinidia* spp. by developing an alternative strategy to CRISPR/Cas9. This strategy consisted of designing a Polycistronic tRNA-gRNA (PTG) to target *AcPDS* in different sites and, comparing the PTG/Cas9 gene-editing approach with CRISPR/Cas9, the authors showed a remarkable 10-fold higher target-editing efficiency, thus demonstrating optimization of gene-editing in kiwifruit plants. Varkonyi-Gasic *et al.* (2019) utilized the CRISPR/Cas9 technique with two polycistronic PTG cassettes bound to promoters from *Arabidopsis* sp. to introduce modifications in target sites of genes *AcCEN* and *AcCEN4* from *A. chinensis*, producing smaller and more compact plants, with increased precocity (Varkonyi-Gasic *et al.,* 2019).

Several resources have been made available to assist the use of gene-editing techniques in increasing plant tolerance to Psa. They include a database with genomic information of *Actinidia* spp. (Wang and Lin-Wang, 2007), online tools such as the CRISPRCasFinder, computer programs for Cas designing (e.g., Cas-Designer) or off-target identification using machine-learning approaches (e.g*.,* VARSCOT) (Park *et al.,* 2015; Couvin *et al.,* 2018; Wilson *et al.,* 2019). Naturally, the knowledge of the genes to be manipulated is the fundamental basis for developing kiwifruit genotypes tolerant to Psa using gene-editing techniques. In this respect, much remains to be unravelled about the genetic bases underlying tolerance traits, but progress has been made with kiwifruit genome sequencing (Huang *et al.,* 2013; Tang *et al.,* 2019a, 2019b) and greater knowledge on functional genomics of kiwifruit plants infected by Psa (Wang *et al.,* 2018a; Nunes da Silva *et al*., 2019; Tahir *et al*., 2019; Nunes da Silva *et al*., 2020).

Regardless of the positive features in gene-editing, several operational constraints related to the commercial release of genetically modified organisms (GMOs) still occur, limiting the use of for gene-editing applications, particularly in areas with stricter regulations (as, e.g., Europe) (Callaway, 2018).

10. Conclusion

To decrease the use of environmentally-harmful phytosanitary products in disease management routines, the search for novel strategies to increase plant tolerance to Psa has been giving clear preference for substances of natural origin, motivated by the need to meet the global compromise of reducing the environmental impact of agriculture and, more importantly, consumers expectations. In this respect, elicitors, plant essential oils, propolis, phages, antimicrobial peptides and beneficial microorganisms have shown potential to be used against Psa, and the complexity of their matrices and the enormous possibilities of combination of active ingredients represent a very appealing basis of work for researchers.

Emergent technologies, such as nanotechnology and artificial intelligence, will allow the development of innovative formulations and the analysis of large amounts of data. This will undoubtedly promote more efficient management strategies against pathogens of agronomic importance, such as Psa. Nevertheless, these novel trends are currently at different stages in terms of testing, validation and implementation in the field and, more importantly, none of them can be considered effective yet, reason why further research should be greatly reinforced.

CHAPTER 2

Evaluation of plant genotypic susceptibility to Psa and Pfm

CHAPTER 2 - Sub-chapter 2.1

Exploring the expression of defence-related genes in *Actinidia* spp. after infection with *Pseudomonas syringae* pv. *actinidiae* and pv. *actinidifoliorum*: first steps

The contents of this chapter have been published as:
Nunes da Silva, M., Machado, J., Balestra, G.M., Mazzaglia, A., Vasconcelos, M.W. and Carvalho, S.M.P. (2019) Exploring the expression of defence-related genes in *Actinidia* spp. after infection with *Pseudomonas syringae* pv. *actinidiae* and pv. *actinidifoliorum*: first steps. *European Journal of Horticultural Science*, 84, 206-212. DOI: 10.3389/fpls.2020.01022.

Exploring the expression of defence-related genes in *Actinidia* spp. after infection with *Pseudomonas syringae* pv*. actinidiae* and pv. *actinidifoliorum*: first steps

Abstract

Kiwifruit bacterial canker (KBC), caused by *Pseudomonas syringae* pv*. actinidiae* (Psa), is currently the most destructive disease of kiwifruit worldwide. Conversely, a closely related bacterial strain, *P. syringae* pv. *actinidifoliorum* (Pfm), only causes necrotic spots and has not been associated with plant mortality. Moreover, there is some evidence on the higher susceptibility of the *Actinidia chinensis var. deliciosa* kiwifruit species to KBC, compared with *A. arguta*, but the reasons behind it are still largely unknown. In this work, micropropagated plants of *A. chinensis* var. *deliciosa* 'Hayward' and *A. arguta* var. *arguta* 'Ken's Red' were inoculated with Psa or with Pfm (10^7 CFUs mL^{-1}). Disease development was monitored 1, 2 and 5 days post-inoculation (dpi) through the determination of colony-forming units (CFUs) and the expression analysis of six plant defence-related genes (*APX*, *CAT*, *SOD*, *LOX1*, *SAM* and *TLP1*). At 5 dpi, CFUs in plant tissues inoculated with Psa and Pfm were, respectively, 17.4-fold and 2.8-fold higher in *A. chinensis* compared with *A. arguta*. Expression of antioxidant enzyme-related genes was very distinct between the two kiwifruit species: *SOD* expression was drastically increased in *A. chinensis* (up to 2.1- fold, 5 dpi), whereas in *A. arguta CAT* was the most upregulated gene (up to 1.7-fold, 2 dpi). *LOX1*, involved in jasmonic acid biosynthesis, was upregulated in both species, however reaching the highest values at 2 dpi in *A. chinensis* (2.2-fold) and 1 dpi in *A. arguta* (1.9-fold). It is concluded that *A. arguta* is much more tolerant to Psa than *A. chinensis* and that the molecular mechanisms between the two kiwifruit species involve specific defence pathways being triggered at distinct moments after plant infection.

1. Introduction

Kiwifruit bacterial canker (KBC) is currently the most destructive disease of kiwifruit worldwide. It is caused by *Pseudomonas syringae* pv*. actinidiae* (Psa) and it affects all kiwifruit species, including the green fleshed kiwifruit *A. chinensis* var. *deliciosa* and the kiwi berry *A. arguta* var. *arguta*. *A. chinensis* orchards are, in general, more affected than *A. arguta* (Vanneste *et al*., 2014). Nevertheless, the reasons behind this differential susceptibility remain unknown. After Psa infection through stomata, lenticels and wounds, disease symptoms range from leaf spotting, shoot wilting, twig dieback, blossom necrosis and lenticels reddening. Systemic migration from leaves to shoots through xylem vessels induces extensive canker formation and further bacterial dispersal into the environment through the release of exudates (Ferrante *et al*., 2012). Interestingly, the closely related strain *P. syringae* pv. *actinidifoliorum* (Pfm) can infect kiwifruit plants but does not cause systemic infection nor plant death (Vanneste *et al*., 2013; Cunty *et al*., 2014). It is presumed that during

the early colonization stages plants can restrain their endophytic bacterial populations through the activation of basal defence mechanisms, such as increased synthesis of oxidative stress-related proteins (Petriccione *et al*., 2013). In fact, one of the earliest cellular responses succeeding an effective pathogen recognition by the host plant is the production of reactive oxygen species (ROS) through the consumption of oxygen in a cascade of reactions called oxidative burst. During this process, superoxide dismutase (SOD), ascorbate peroxidase (APX), and catalase (CAT) play very important roles in ROS detoxification, protecting plant cells from oxidative burst induced by pathogen invasion (Mittler *et al*., 2004). While SOD catalyses the dismutation of superoxide (O^{2-}) to hydrogen peroxide (H_2O_2), APX reduces H_2O_2 to water (H_2O) by utilizing ascorbate as an electron donor and CAT dismutates H_2O_2 to oxygen (O_2) and water. In a recent study, it was shown that the expression of genes encoding antioxidant enzymes, such as *SOD*, *APX*, and *CAT*, increased after *A. chinensis* inoculation with Psa from as early as 1 day post-inoculation (Petriccione *et al*., 2015). Nevertheless, information on other molecular pathways that may be involved in plant defence mechanisms and on how different *Actinidia* spp. respond to infection with *P. syringae* strains with distinct virulence are still very scarce. This work aimed to evaluate how Psa (highly virulent) and Pfm (less virulent) bacterial populations perform in *A. chinensis* var. *deliciosa* 'Hayward' (more susceptible) and *A. arguta* var. *arguta* 'Ken's Red' (more tolerant) plant tissues after artificial infection, and how these species with reported distinct susceptibility to KBC respond to the infection in terms of expression of defence-related genes.

2. Materials and methods

2.1. Plant maintenance

Micropropagated *A. chinensis* var. *deliciosa* 'Hayward' and *A. arguta* var. *arguta* 'Ken's Red' plants were purchased from QualityPlant, Investigação e Produção em Biotecnologia Vegetal, Lda. (Castelo Branco, Portugal). A modified Murashige and Skoog (MS) agarized medium was used for plant maintenance during the trial period and consisted of sucrose (30 g L^{-1}), *myo*-inositol (100 mg L^{-1}), thiamine-HCl (1 mg L^{-1}), nicotinic acid (1 mg L^{-1}), pyridoxine (1 mg L^{-1}), glycine (1 mg L^{-1}) and benzyl aminopurine (0.5 mg L^{-1}), adjusted to pH 5.7 with KOH. Plants were kept in sets of three plants per OS140 box container (Duchefa Biochemie B.V., Haarlem, The Netherlands) in a climate chamber (Aralab Fitoclima 5 000EH, Aralab, Rio de Mouro, Portugal) with 16-h day photoperiod with 200 µmol s^{-1} m^{-2} of photosynthetic photon flux density at the plant level. Temperatures were set to 22 °C during the light period and to 19 °C during the dark period and relative humidity was maintained at 80%.

2.2. Bacterial suspension preparation and plant inoculation

A virulent Psa strain (CFBP7286, isolated in 2008 in Italy from *A. chinensis*) and a less virulent Pfm strain (ICMP18804, isolated in 2010 in New Zealand from *A. chinensis*) were grown for 48 h on nutrient agar with 5% sucrose (NSA) at 27 °C in the dark. In the day of inoculation, a fresh 1-2×10^7 CFU mL^{-1} inoculum was prepared in sterile Ringer's solution (NaCl 0.72%, $CaCl_2$ 0.017% and KCl 0.037%, pH 7.4). Plants were inoculated with bacterial suspension by gently rubbing a sterile swab impregnated with one of the solutions on the abaxial surface of each leaf. For each kiwifruit species (*A. chinensis* and *A. arguta*) and *P. syringae* strain (Psa and Pfm), 27 plants were inoculated (i.e., nine containers with three plants each). Mock-inoculated control plants were treated with Ringer's solution alone.

2.3. Plant sampling

One, 2 and 5 days post-inoculation (dpi), three containers of each kiwifruit species and type of inoculum (with three plants per container) were randomly selected for plant sampling. Plants were removed from the culturing medium and the tip (*ca*. 0.5 cm length) of every leaf was cut with sterile scissors and placed in a sterile container for CFUs determination. The remaining plant was flash-frozen in liquid nitrogen and stored at -80 °C for gene expression analysis. Each biological replicate was obtained by pooling the three plants per container, and three independent biological replicates were analysed per treatment at each time-point.

2.4. CFUs determination in plant tissues

Estimation of bacterial colony-forming units (CFU) was performed using an adapted method from Cellini *et al*. (2014). Samples were surface sterilised by washing in 70% ethanol for 1 min, followed by a 1-min treatment with 1% sodium hypochlorite, after which they were rinsed twice in sterile water for 1 min. Plant samples were then homogenised in 10 mL Ringer's solution. This extract was sequentially diluted ten-fold up to 10^{-5}, and three replicates of 100 µL from each ten-fold dilution were plated on nutrient sucrose agar (NSA) medium. After plate incubation at 27 °C for 48 h in the dark, the number of colonies in each plate was counted and CFU estimated.

2.5. Defence-related gene expression analysis

Plant RNA was extracted according to an adapted protocol from Cellini *et al*. (2014). After tissue homogenization with liquid nitrogen, 1 mL of warm (70 °C) extraction buffer (100

mM Tris-HCl, pH 8.0, cetyltrimethylammonium bromide 4%, polyvinylpyrrolidone K40 4%, 30 mM ethylenediaminetetraacetic, 2.0 M NaCl, spermidine 0.1%, *β*-mercaptoethanol 2%) was added to *ca*. 100 mg of sample. Samples were mixed vigorously and incubated at 65 °C for 10 min. Subsequently, 1 mL of chloroform-isoamyl alcohol (24:1, v/v) was added, and samples were centrifuged for 15 min at 15 000 g. The upper phase was collected to a new tube and combined with 250 µL of 12 M LiCl by gentle pipetting. Samples were incubated overnight at -20 °C, after which they were centrifuged at 15 000 g for 35 min at 4 °C. The supernatant was discarded and the pellet was washed in cold 70% ethanol, dried, and resuspended in 40 µL sterile DEPC water. Single-stranded cDNA was synthesized using iScript cDNA Synthesis Kit (Bio-Rad, California, USA) according to the manufacturer's instructions in a Doppio Thermal Cycler (VWR, Oud-Heverlee, Belgium). Primers for *LOX1*, *SAM* and *TLP1* were designed using Primer3 (Frodo.wi.mit.edu) for an expected PCR product of 100-200 bp and primer annealing temperatures between 58 and 62 ºC, whereas primer sequences for *APX*, *CAT* and *SOD* were obtained from Petriccione *et al*. (2015) (Table 1). Reverse transcription quantitative real-time polymerase chain reactions (RT-qPCR) were performed on a StepOne™ Real-Time PCR System (Applied Biosystems, California, USA) with the following reaction conditions: 2 min at 50 °C, 2 min at 95 °C and 40 cycles with: 15 s at 95 °C, 15 s at each primer pair optimal annealing temperature (Table 1) and 1 s at 72 °C. Amplifications were carried out using a final volume of 20 µL which consisted of 1 µL of the specific primers at 6 µM, 10 µL of 2× iQ SYBR® Green Supermix (Bio-Rad, California, USA) and 8 µL of a 1:100 dilution of the template cDNA. Melt curve profiles were analysed for each tested gene. The comparative CT method (ΔΔCT, Livak and Schmittgen, 2001) was used for the relative quantification of gene expression values using actin (*ACT*) and protein phosphatase 2A (*PP2A*) genes as control transcript (Petriccione *et al*., 2015) and the plants inoculated with Ringer's solution (mock-inoculated controls) as the reference sample. For each sample and target gene, two technical replicates were analysed.

2.6. Statistical analysis

Data were analysed with GraphPad Prism version 6.0 (GraphPad Software, Inc., California, USA). Significant differences between treatments were determined by analysis of variance (ANOVA) followed by Fisher's LSD test ($p < 0.05$).

Table 1 - Primer sequences and annealing temperature (T_{ann}) of housekeeping and target genes used for RT-qPCR analysis.

Gene (Accession number)	**Primer sequence (5′-3′)**		T_{ann} (°C)	**Reference**
	Forward	**Reverse**		
ACT (FG440519)	CCAAGGCCAACAGAGAGAAG	GACGGAGGATAGCATGAGGA	56.0	Ledger *et al*., 2010
PP2A (FG522516)	GCAGCACATAATTCCACAGG	TTTCTGAGCCCATAACAGGAG	55.2	Nardozza *et al*., 2013
APX (FG408540)	GGAGCCGATCAAGGAACAGT	AACGGAATATCAGGGCCTCC	57.8	Petriccione *et al*., 2015
CAT (FG470670)	GCTTGGACCCAACTATCTGC	TTGACCTCCTCATCCCTGTG	56.9	
SOD (FG471220)	CACAAGAAGCACCACCAGAC	TCTGCAATTTGACGACGGTG	57.8	
LOX1 (DQ497792)	GTTAGAGGGGTGGTGACTCT	CTTTAGCACTGCTTGGTTGC	53.5	This study
SAM (U17240)	GAATAGTACTTGCCCCTGGC	TACAAATCGACCAGAGGGGT	55.1	
TLP1 (JX905282)	CAACCCCCTAACACACTAGC	ATTTCCGGAGTTGCAACAGT	54.6	

3. Results

At 2 dpi *A. chinensis* plants had *ca*. 235 ± 23 × 10^3 CFU mL^{-1} for the highly virulent Italian Psa strain (Fig. 1), whereas in *A. arguta* Psa CFU values remained *ca*. 6.7-fold lower (35 ± 12 × 10^3 CFU mL^{-1}). At 5 dpi, *A. chinensis* had 17.4 times higher Psa CFUs count than *A. arguta*, which presented only *ca*. 75 ± 7 × 10^3 CFU mL^{-1}.

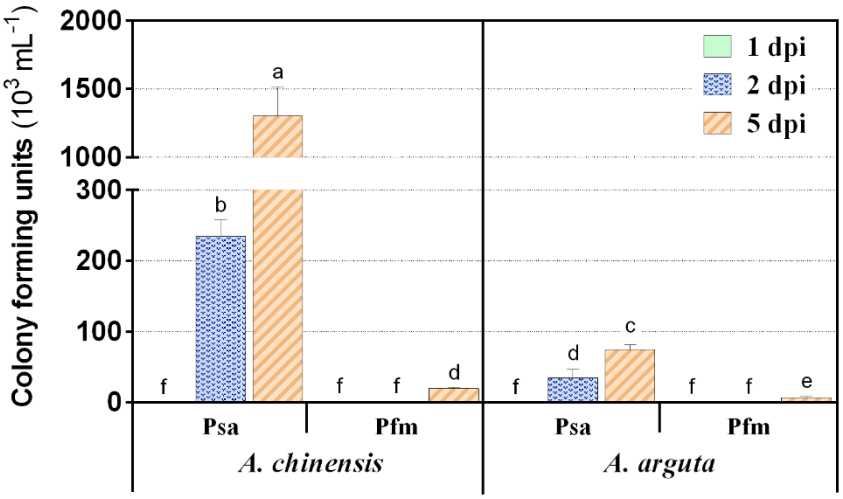

Figure 1 - Number of colony-forming units estimated in plant tissues from *A. chinensis* var. *deliciosa* cv 'Hayward' and *A. arguta* var. *arguta* cv 'Ken's Red' at 1, 2 and 5 days post-inoculation (dpi) with *P. syringae* pv. *actinidiae* (Psa) or *P. syringae* pv. *actinidifoliorum* (Pfm). Each value represents the mean of three biological replicates ± standard error of the mean. Columns with different letters are significantly different at $p < 0.05$.

SOD transcriptional levels significantly increased by 2.1- and 1.7-fold from 1 to 5 dpi after *A. chinensis* inoculation with Psa and Pfm, respectively. In *A. arguta* inoculated plants no variation in *SOD* transcriptional levels was observed over time, but there was a significant downregulation of this gene in inoculated plants compared with non-infected plants (as the relative fold change was lower than 1), regardless of the bacterial strain (Fig. 2). Contrarily to *SOD*, *CAT* transcriptional profile in *A. chinensis* plants did not show significant alterations during the experimental period. In *A. arguta*, on the other hand, *CAT* was upregulated by 1.6- and 1.7-fold from 1 to 2 dpi, after inoculation with Psa and Pfm, respectively.

Psa inoculation induced a 0.4-fold decrease in *APX* expression in *A. chinensis* from 1 to 5 dpi, whereas in *A. arguta* it remained constant during the experimental period, being *ca*. 0.25-fold higher than in mock-inoculated plants (Fig. 2). From 1 to 2 dpi with the less virulent strain (Pfm) *A. chinensis* responded with *APX* overexpression (*ca*. 1.3-fold), whereas *A. arguta* was not significantly affected. Moreover, when *A. arguta* plants were inoculated with Pfm, *APX* was downregulated by up to 0.4-fold, compared with Psa, in all time-points. Compared with mock-inoculated plants, *LOX1* relative expression was 2.2- and 1.8-fold higher in Psa-inoculated *A. chinensis* and *A. arguta* plants 2 dpi and 1 dpi, respectively, being drastically reduced afterwards in both species (Fig. 2). Also, *SAM* was upregulated in *A. chinensis* by 1.4-fold after inoculation with Psa from 1 to 2 dpi, and from 1 to 5 dpi in Pfm-inoculated plants. In *A. arguta*, compared with mock-inoculated plants, this gene was upregulated by 2.2-fold 1 day after Psa inoculation, whereas no significant alterations in *SAM* transcriptional levels were observed after Pfm inoculation. Moreover, Psa-inoculated plants showed significantly higher *LOX1* and *SAM* transcriptional levels than Pfm at 1 dpi in *A. arguta* (1.6- and 2.0-fold, respectively) and at 2 dpi in *A. chinensis* (1.6-fold for both genes). Finally, *TLP1* was significantly upregulated in Psa-inoculated plants from 1 to 5 dpi in *A. chinensis* and from 1 to 2 dpi in *A. arguta* by *ca*. 1.4-fold (Fig. 2).

4. Discussion

After Psa infection through natural openings and wounds, bacteria start to migrate within the vascular system inducing a wide variety of disease symptoms that range from leaf spotting to cankers formation (Ferrante *et al*., 2012). Contrarily, Pfm has lower virulence in kiwifruit plants since it causes a non-systemic infection, only being associated with leaf symptoms (Cunty *et al*., 2014). In this work, CFUs determination showed rapid Psa colonization in kiwifruit plant tissues, especially in *A. chinensis*. Rapid Psa population increase in artificially inoculated *A. chinensis* plants was already observed during the first days after inoculation by Petriccione *et al*. (2014).

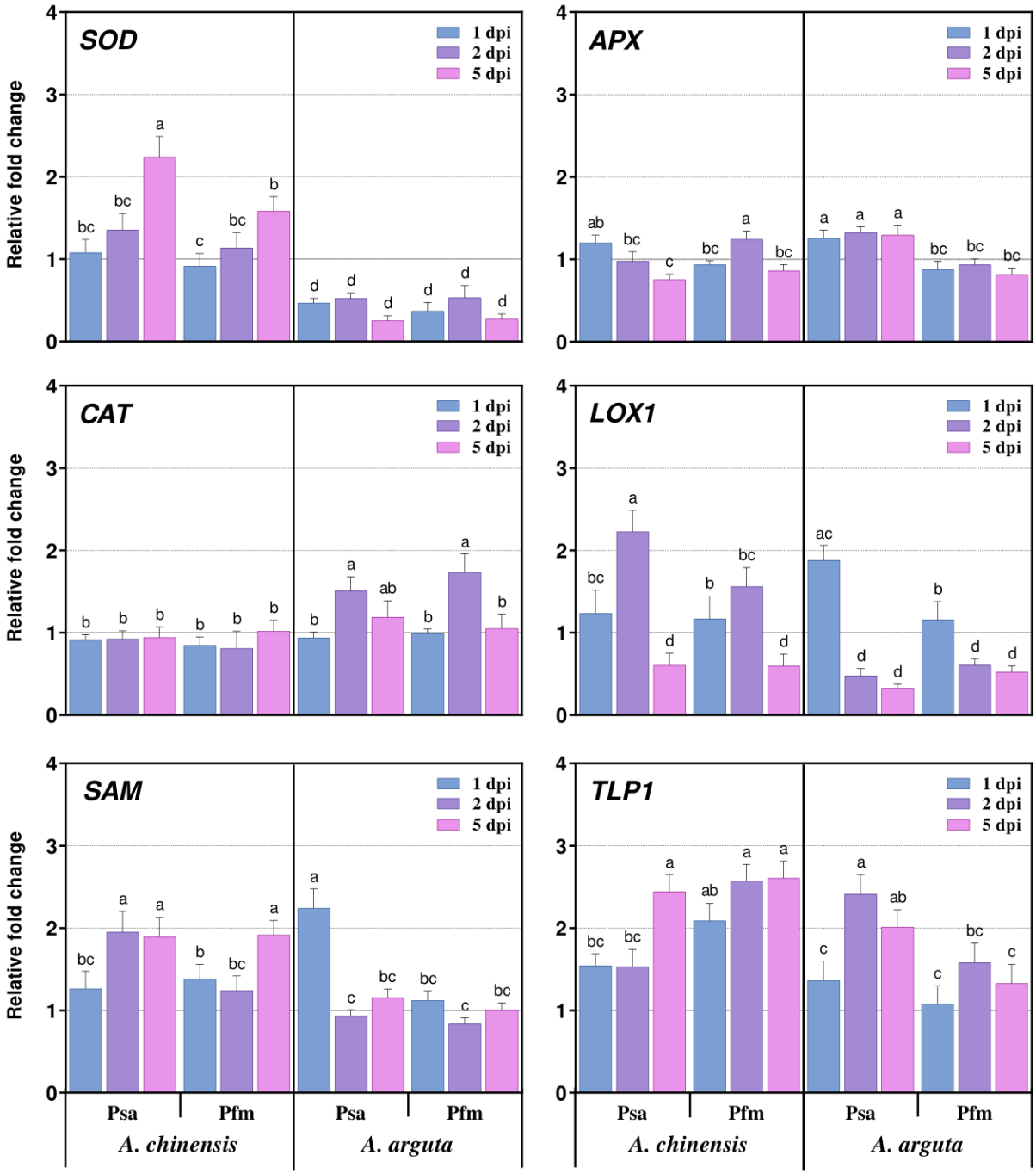

Figure 2 - Gene expression analysis of *SOD*, *CAT*, *APX*, *LOX1*, *SAM* and *TLP1* in *A. chinensis* var. *deliciosa* 'Hayward' and *A. arguta* var. *arguta* 'Ken's Red' at 1, 2 and 5 days post-inoculation (dpi) with *P. syringae* pv. *actinidiae* (Psa) or *P. syringae* pv. *actinidifoliorum* (Pfm). Each symbol represents the mean of three biological replicates ± standard error of the mean. One-fold change represents no relative change in gene expression, as compared with mock-inoculated control plants. Columns with different letters are significantly different at $p < 0.05$.

Here, it is shown for the first time that the less virulent strain Pfm seems to take a longer period to infect plant tissues, as this strain was only detected at 5 dpi, and in significantly lower numbers compared to Psa (representing only 1.5% and 9.3% CFU for *A. chinensis* and *A. arguta* respectively, when comparing to Psa). Similarly to Psa, Pfm endophytic population was higher in *A. chinensis* than in *A. arguta* at 5 dpi (*ca*. 2.8-fold, Fig. 1). Although *A. arguta*'s

susceptibility to Psa was already demonstrated in 1989 through artificial inoculation of nursery plants, it was only more recently that Psa was identified in *A. arguta* field plants for the first time (Vanneste *et al*., 2014). *A. chinensis*, on the other hand, is more commonly associated with Psa infection, frequently accompanied by extensive infection symptoms, such as cane dieback, cankers formation, release of bacterial exudates, and fruit production losses (Balestra *et al*., 2009a). Results presented here corroborate that *A. chinensis* is more susceptible to Psa infection than *A. arguta*. Moreover, Psa and Pfm establishment in plant tissues does not occur immediately after inoculum application and the rate of bacterial colonization is highly dependent on plant species and bacterial strain. It is hypothesised that leaf trichomes play a very important role as an entry route for Psa to the host tissues (Spinelli *et al*., 2011). These authors reported that *A. chinensis* var. *chinensis* had higher trichome density in comparison to *A. chinensis* var. *deliciosa*, which could contribute to the higher susceptibility of var. *deliciosa* once they could provide a more favourable environment for bacterial growth. As *A. chinensis* leaves have higher trichome density than *A. arguta*, Psa and Pfm could strive better in the first species than in the latter, therefore explaining the higher CFU estimation in *A. chinensis*, regardless of the bacterial strain or time-point. In addition, the fact that Psa was able to colonize plant tissues from an earlier stage after inoculation and to a greater magnitude, comparing with Pfm, may be due to its systemic activity. In fact, as Psa can penetrate and migrate within plant leaf veins to the shoot (Petriccione *et al*., 2013), it can then multiply more rapidly, thus arising to greater numbers than Pfm.

It has been recently shown that the expression of antioxidant enzymes-encoding genes plays an important role in *A. chinensis* defence against Psa infection (Petriccione *et al*., 2015). These authors found that the upregulation of *SOD*, *APX* and *CAT* genes was influenced not only by the bacterial concentration used for plant inoculation, but also by the time-point analysed. *SOD* was shown to be significantly upregulated in *A. chinensis* plants 7 dpi after artificial inoculation with Psa (Petriccione *et al*., 2015). In the present study, the expression of these antioxidant enzymes-encoding genes was investigated not only in *A. chinensis* but also in *A. arguta*, following inoculation with two closely related but pathogenically distinct *P. syringae*. As *SOD* catalyses the dismutation of O^{2-} to H_2O_2, the gradual increase in *SOD* transcription following the inoculation of *A. chinensis* may be due to the cumulative concentration of H_2O_2 in plant cells in response to the increased Psa population (Fig. 2). *CAT* transcriptional profile in *A. chinensis* plants did not show significant alterations during the experimental period, which seems to be in accordance with the results from Petriccione *et al*. (2015), where significant up-regulation of *CAT* expression in Psa-inoculated plants was only observed 7 dpi. However, in *A. arguta*, *CAT* overexpression was observed from 1 to 2 dpi, after inoculation with both Psa and Pfm. Perhaps in this plant species *CAT* plays a more determinant role in the prevention of oxidative stress, whereas in

A. chinensis SOD seems to have a more active role. Petriccione *et al*. (2015) reported a slight up-regulation in *APX* transcriptional levels 1 and 4 dpi in *A. chinensis* var. *deliciosa* 'Hayward' following inoculation with Psa. Moreover, in the present study, Psa inoculation decreased *APX* expression, whereas Pfm inoculation slightly increased its transcriptional levels in *A. chinensis*. In contrast, in *A. arguta APX* relative expression after Psa and Pfm inoculation remained constant during the experimental period, with Psa-inoculated plants presenting significantly higher *APX* transcriptional levels. Therefore, it is clear that plant infection with bacterial pathovars with distinct virulence induces differentiated responses regarding the expression of genes related to the antioxidant pathways, which also differed between plant species.

LOX1 encodes a lipoxygenase involved in the synthesis of oxygenated fatty acids, including jasmonic acid (JA) and aldehydes, which play important functions in plant defence against pathogens and herbivores (Kolomiets *et al*., 2000). The relative expression of this gene significantly increased in Psa-inoculated plants of both species, being drastically reduced afterwards. Interestingly, lipoxygenases convert α-linolenic acid into 13-hydroperoxy-octadecatrienoic acid during JA biosynthesis, a known antagonist to *Actinidia* spp. defence mechanisms. In fact, previous studies showed that exogenous application of methyl jasmonate, a synthetic analogue of JA, increased *A. chinensis* plants disease index after inoculation with Psa (Reglinski *et al*., 2013), and seemed to impair the salicylic acid (SA) pathway, thus increasing *Actinidia* spp. susceptibility to Psa (Cellini *et al*., 2014). What is more, several *P. syringae* strains can produce the toxin coronatine, which disrupts plant defences by impairing plant ethylene (ET) and JA pathways (Zheng *et al*., 2012). *LOX1* increased activity was reported in *A. chinensis* Psa-inoculated plants, and is regarded as a strategy used by the pathogen to antagonize SA responses through the enhancement of the JA pathway, or as a consequence of the activation of other metabolic pathways, such as ET (Cellini *et al*., 2014). In fact, in the present study, S-adenosylmethionine synthetase encoding gene, *SAM*, a precursor of ET biosynthesis and was upregulated in *A. chinensis* after inoculation with Psa from 1 to 2 dpi and from 1 to 5 dpi in Pfm-inoculated plants. In *A. arguta*, *SAM* was upregulated by 1 day after Psa inoculation, as compared with mock-inoculated plants. Exogenous application of ET was found to enhance disease index after Psa inoculation, probably because it antagonises the SA pathway (Cellini *et al*., 2014). Contrarily, exogenous application of an ET receptor blocker, 1-MCP, decreased disease severity, thus supporting the evidence that ET may enhance the noxious effects of the pathogen, as was already demonstrated in other plant-pathogen systems (Weingart *et al*., 2001). In this work, genes involved in the JA and ET biosynthesis pathways (*LOX1* and *SAM*) seemed to be triggered later in *A. chinensis*, compared to *A. arguta*, since in the latter cultivar the upregulation of these genes peaked at 1 dpi, compared with mock-inoculated plants. Moreover, the fact that *A. chinensis* and *A. arguta* Psa-inoculated plants showed higher

LOX1 and *SAM* transcriptional levels than Pfm at 2 dpi and 1 dpi, respectively, clearly demonstrates that plants' defence mechanisms are highly influenced by the bacterial strain. Early deactivation of these pathways in *A. arguta* can be a coping mechanism against invasion by pathogenic bacteria, and underpin its higher tolerance to Psa and Pfm. Finally, *TLP1* encodes a thaumatin-like protein, which belongs to the family of pathogenesis-related (PR) proteins, and is involved in acquired resistance and stress response in plants. These PR proteins were already shown to be upregulated in Psa-infected *A. chinensis* plants as soon as 1 dpi (Cellini *et al*., 2014). In the present work, *TLP1* was significantly upregulated in Psa-inoculated plants from 1 to 5 dpi in *A. chinensis* and from 1 to 2 dpi in *A. arguta*, thus attesting their active role in kiwifruit plant defence against the pathogen. Several studies have already demonstrated that TLPs have strong antifungal properties, probably due to their ability to inhibit the activity of microbial enzymes, such as β-glucanase, xylanase, α-amylase and trypsin, and also due to their ability to rupture pathogen membrane by pore formation (Misra *et al*., 2016). The fact that this gene was upregulated at earlier stages of the infection in *A. arguta* may reinforce its higher tolerance to Psa, compared with *A. chinensis*, or perhaps in *A. chinensis* other PR-proteins play a more preponderant role, at least in the time-points selected in this study.

5. Conclusion

A. chinensis var. *deliciosa* 'Hayward' proved to be much more susceptible to Psa infection *than A. arguta* var. *arguta* 'Ken's Red'. Moreover, Psa tolerance seems to be a result of several plant resistance mechanisms acting together against the pathogen, as distinct defence-related genes were triggered at different moments after plant infection. Whereas *SOD* expression was drastically increased in *A. chinensis*, in *A. arguta CAT* was the most upregulated antioxidant enzyme-encoding gene. Moreover, *LOX1* and *SAM*, involved in JA and ET biosynthesis, respectively, were upregulated 2 dpi in *A. chinensis* and already at 1 dpi in *A. arguta* and, more importantly, their transcriptional levels were higher in Psa-inoculated plants, compared with Pfm. Psa may induce the upregulation of these pathways as part of its infection mechanism, impairing plant defence through negative feedback of the SA pathway. Although these findings provide key evidence on the species-specific relation between *Actinidia* plants and *P. syringae* strains with different virulence, additional studies are needed to fully understand the molecular and metabolomic pathways involved in kiwifruit plants defence against Psa and Pfm. Additionally, these results derive from *in vitro* grown *Actinidia* spp. plants and their reproducibility in fully grown field plants still needs to be confirmed. Nevertheless, this work has potential to contribute to the understanding of the mechanisms involved in plant tolerant to Psa.

CHAPTER 2 - Sub-chapter 2.2

Early pathogen recognition and antioxidant system activation contributes to *Actinidia arguta* tolerance against Psa and Pfm

The contents of this chapter have been published as:
Nunes da Silva, M., Vasconcelos, M., Gaspar, M., Balestra, G.M., Mazzaglia, A. and Carvalho, S.M. (2020) Early pathogen recognition and antioxidant system activation contributes to *Actinidia arguta* tolerance against *Pseudomonas syringae* pathovars a*ctinidiae* and *actinidifoliorum*. *Frontiers in Plant Science* 11, 1022. DOI: 10.17660/ejhs.2019/84.4.2.

Early pathogen recognition and antioxidant system activation contributes to *Actinidia arguta* tolerance against Psa and Pfm

Abstract

Actinidia chinensis and *A. arguta* have distinct tolerances to *Pseudomonas syringae* pv*. actinidiae* (Psa), but the reasons underlying the inter-specific variation remain unclear. This study aimed to integrate the metabolic and molecular responses of these two kiwifruit species against the highly pathogenic Psa and the less pathogenic *P. syringae* pv. *actinidifoliorum* (Pfm) bacterial strains. Disease development was monitored weekly till 21 days post-inoculation (dpi), analysing a broad number and variety of parameters including: colony-forming units (CFU), foliar symptoms, total chlorophylls, lipid peroxidation, soluble polyphenols, lignin and defence-related gene expression. At the end of the experimental period, *A. chinensis* inoculated with Psa presented the highest endophytic bacterial population, whereas *A. arguta* inoculated with Pfm showed the lowest values, also resulting in a lower extent of leaf symptoms. Metabolic responses to infection were also more pronounced in *A. chinensis* with decreased total chlorophylls (up to 55%) and increased lipid peroxidation (up to 53%), compared with mock-inoculated plants. Moreover, at 14 dpi soluble polyphenols and lignin concentrations were significantly higher (112 and 26%, respectively) in Psa-inoculated plants than in mock-inoculated plants, while in *A. arguta* no significant changes were observed in those metabolic responses, except for lignin concentration which was, in general, significantly higher in Psa-inoculated plants (by at least 22%), compared with mock- and Pfm-inoculated plants. Genes encoding antioxidant enzymes (*SOD*, *APX* and *CAT*) were upregulated at an earlier stage in Psa-inoculated *A. arguta* than in *A. chinensis*. In contrast, genes related to the phenylpropanoids (*LOX1*) and ethylene (*SAM*) pathways were downregulated in *A. arguta*, but upregulated in *A. chinensis* in the later phases of infection. Expression of *Pto3*, responsible for pathogen recognition, occurred 2 dpi in *A. arguta*, but only 14 dpi in *A. chinensis*. In conclusion, we found that *A. arguta* is more tolerant to Psa and Pfm infection than *A. chinensis* and its primary and secondary metabolism is less impacted. *A. arguta* higher tolerance seems to be related to early pathogen recognition, the activation of plant antioxidant system, and to the suppression of ET and JA pathways from an earlier moment after infection.

1. Introduction

Pseudomonas syringae pv*. actinidiae* (Psa) is a Gram-negative bacterium that infects several *Actinidia* species, being responsible for the kiwifruit bacterial canker (KBC) (Vanneste *et al*., 2014; Kisaki *et al*., 2018). Following the first outbreaks of Psa in *A. chinensis* var. *deliciosa* 'Hayward' in Japan during the 1980s, the disease spread to other important kiwifruit producing countries, such as South Korea and China (Serizawa *et al*., 1989; Koh, 1994; Cheng *et al*., 1995). Thereafter, epidemic outbreaks associated with a more pathogenic Psa strain were reported for the first time in several *A. chinensis* var. *chinensis* orchards located in South Korea (in 2006) and Italy (in 2008) (Ferrante and Scortichini, 2009; Koh *et al*., 2010).

From then on, Psa quickly disseminated to several countries where kiwifruit production is highly relevant (such as New Zealand, France, Portugal, Spain, Switzerland) rendering KBC a worldwide epidemic (EPPO, 2018). KBC symptoms include leaf spotting, cane dieback, canker formation and fruit shrivelling, resulting in significant economic losses to the kiwifruit industry (Vanneste, 2017).

The pathovar *actinidiae* constitutes a genetically diverse group of bacteria with the capacity to infect several *Actinidia* spp., especially regarding genes responsible for type III effectors and phytotoxin production (Chapman *et al*., 2012). From the six Psa biovars identified until now, biovar 3, also known as Psa3 or Psa-V, seems to be the most pathogenic and the most widely disseminated, having been identified in Europe, New Zealand, Chile and China (Chapman *et al*., 2012; Vanneste *et al*., 2013; Dreo *et al*., 2014). Due to its rapid worldwide distribution, Psa3 is now considered a pandemic pathogen and has been included in the list for quarantine pests of the European and Mediterranean Plant Protection Organization (EPPO, 2014). Contrarily, the genetically close bacterial strain *P. syringae* pv. *actinidifoliorum* (Pfm), formerly known as Psa biovar 4 or Psa-LV (Cunty *et al*., 2015), is a less pathogenic population present in New Zealand, Australia and France (Chapman *et al*., 2012; Scortichini *et al*., 2012; Cunty *et al*., 2015). Whereas Psa3 can induce the formation of cankers in stems and conductive branches, compromising the vascular system of the infected plants, Pfm is characterized by its low severity, with the infection not progressing beyond foliar necrotic spots, and not causing important economic and production losses (Scortichini *et al*., 2012; Vanneste *et al*., 2013; Cunty *et al*., 2015). However, although their effector repertoire has been under analysis during the last decade with distinct bacterial virulence being attributed to differences in effector patterns, the full understanding of how bacteria can penetrate plant tissue and how plants activate their defence mechanisms is far from being achieved.

Generally, all plants of the genus *Actinidia* are affected by Psa, but there seems to be considerable variation in their tolerance to this pathogen. Field evidence has shown that cultivars of *A. chinensis* var. *chinensis*, such as ‘Hort16A’ and ‘JinTao’, present high susceptibility to Psa compared to cultivars of *A. chinensis* var. *deliciosa*, such as ‘Hayward’ (Balestra *et al*., 2009b). In addition, *A. arguta*, *A. macrosperma*, *A. polygama* and *A. rufa* were classified as tolerant to Psa (Nardozza *et al*., 2015; Kisaki *et al*., 2018; Michelotti *et al*., 2018), but the molecular and biochemical mechanisms responsible for this tolerance are not fully known (Wang *et al*., 2018a; Nunes da Silva *et al*., 2019).

The basal plant resistance mechanisms, also called innate immunity, are the first line of defence against various pathogens, including bacteria, and are triggered via plant cells pattern recognition receptors (PRR), which recognize specific pathogen-associated molecular patterns (PAMPs) characteristic to each pathogen (Wurms *et al*., 2017a; Michelotti *et al*., 2018; Wang *et al*., 2018a). As such, microorganism recognition by host plants involves

a complex physiological and molecular reprogramming that encompasses overregulation of pathogenesis-related genes (PR-genes) and defence-related proteins (Michelotti *et al*., 2018). If a pathogen overcomes basal defences, plants may respond with a secondary line of defence, the hypersensitive response (HR), in which plants can become tolerant to a wide range of pathogens over a long period of time in a phenomenon called systemic acquired resistance (SAR) (Cellini *et al*., 2014). This phenomenon includes changes in structural defences, such as strengthening of the cell wall through the deposition of callus and lignin, increased enzymatic activity, and overexpression of the aforementioned PR-genes (Michelotti *et al*., 2018).

Plant defence against pathogens is also associated with molecular networks based on the activity of reactive oxygen species (ROS), such as superoxide (O^{2-}) and hydrogen peroxide (H_2O_2), and phytohormone signalling, including the jasmonic (JA) and salicylic acids (SA) (Petriccione *et al*., 2014; Wurms *et al*., 2017b). Increased production of ROS during stress, in particular, may pose a threat to cell homeostasis due to subsequent lipid peroxidation, protein oxidation, nucleic acid damage, and enzyme inhibition, ultimately resulting in cell death (Sharma *et al*., 2012). Therefore, to avoid oxidative damage, plants synthesize antioxidant enzymes directly involved in ROS detoxification, such as superoxide dismutase (SOD), catalase (CAT), and ascorbate peroxidase (APX). Along with antioxidant enzymes, phenolic compounds are among the most important defence-related molecules produced by plants, and include flavonoids, anthocyanins, phytoalexins, tannins and lignin (Lattanzio, 2013). Miao *et al*. (2009) compared phenolic compounds content in shoots and leaves of kiwifruit cultivars with different tolerance to KBC and observed that before inoculation phenolic compounds in tolerant cultivars were significantly higher than in susceptible ones, and that after inoculation their concentration increased in both tolerant and susceptible cultivars, suggesting that this metabolic pathway may play an important role in plant defence. Lignin, a complex phenolic polymer, is known to accumulate in plant tissues after infection by pathogenic fungi or bacteria, acting by diminishing the mechanical pressure resulting from pathogen penetration and reproduction (Gallego-Giraldo *et al*., 2018). Inoculation of *Brassica rapa* with *Erwinia carotovora*, for example, induced the activation of genes that regulate lignin biosynthesis, leading to increased concentration of p-coumaryl, one of the three lignin monolignols, and to a 43% increase in lignin concentration in plant tissues just 3 days post-inoculation (dpi) (Zhang *et al*., 2007). Despite being key players in plant defence against pathogens, how phenolic compounds are regulated in Psa- and Pfm-infected kiwifruit plants is still poorly understood.

The interaction between kiwifruit plants and Psa and Pfm is highly complex, with multiple bacterial factors and signalling events occurring simultaneously in the host plant tissues, which ultimately defines the susceptibility or tolerance of the plant exposed to the pathogen (Petriccione *et al*., 2015; Wurms *et al*., 2017a; Wang *et al*., 2018a; Tahir *et al*., 2019). In a

preliminary study, focused on the short-term analysis of the expression of key defence-related genes, we have found that *A. arguta* is more tolerant than *A. chinensis* to Psa and Pfm infection by limiting bacterial endophytic population probably through inhibition the of JA and ethylene (ET) pathways (Nunes da Silva *et al*., 2019). However, that study was limited to the early stages of the plant infection (up to 5 dpi) and only addressed the expression of plant-defence related genes, limiting the possibilities of interpretation. Although it has been suggested that the antioxidant system, phytohormone regulatory pathways and pathogen recognition mechanisms play important roles in plant defence against Psa (Petriccione *et al*., 2013; Reglinski *et al*., 2013; Cellini *et al*., 2014; Petriccione *et al*., 2014; Nunes da Silva *et al*., 2019), information on how these networks are activated and regulated and how they differ between tolerant and susceptible kiwifruit plants is still very scarce. This greatly hinders the possibility to identify new metabolic and/or genotypic traits that could be used as markers for kiwifruit plant breeding and for identifying novel plant protection strategies. This work aimed to analyse the dynamics of *Actinidia*/Psa and *Actinidia*/Pfm pathosystems, by identifying and integrating key metabolic and genotypic traits that might account for the higher tolerance of some *Actinidia* spp. To that end, we evaluated weekly (for 21 days post-inoculation with Psa and Pfm) how two kiwifruit species with reported distinct tolerance to KBC (*A. chinensis* and *A. arguta*) responded to a large number and variety of parameters including: bacterial endophytic population in plant tissues, leaf symptoms, primary and secondary metabolism, antioxidant system and pathogen recognition.

2. Materials and methods

2.1. Plant maintenance and inoculation

Micropropagated plants of *A. chinensis* var. *deliciosa* ‘Hayward’ and *A. arguta* var. *arguta* ‘Weiki’ were purchased from QualityPlant - Investigação e Produção em Biotecnologia Vegetal, Lda. (Castelo Branco, Portugal). A modified Murashige and Skoog (MS) agar medium was used for plant maintenance during the trial period, and consisted of sucrose (30 g L^{-1}), *myo*-inositol (100 mg L^{-1}), thiamine-HCl (1 mg L^{-1}), nicotinic acid (1 mg L^{-1}), pyridoxine (1 mg L^{-1}), glycine (1 mg L^{-1}) and benzyl aminopurine (0.5 mg L^{-1}), adjusted to pH 5.7 with KOH. Plants were kept in sets of three plants in 200 mL containers in a climate chamber (Aralab Fitoclima 5 000EH, Aralab, Rio de Mouro, Portugal) with a 16 h day photoperiod and 200 µmol s^{-1} m^{-2} of photosynthetic photon flux density at the plant level. Temperatures were set to 21°C during the light period and to 19 °C during the dark period, and relative humidity was maintained at 80%.

A pathogenic Psa strain (CFBP7286, isolated in 2008 in Italy from *A. chinensis* var. *chinensis*) and a less pathogenic Pfm strain (CFBP18804, isolated in 2010 in New Zealand from *A. chinensis* var. *chinensis*) were grown for 48 h on nutrient agar with 5% sucrose (NSA) at 27 °C in the dark. In the day of inoculation, a fresh 1-2× 10^7 CFU mL^{-1} inoculum was prepared in sterile Ringer's solution (NaCl 0.72%, $CaCl_2$ 0.017% and KCl 0.037%, pH 7.4).

A total of 135 plants (45 plants per treatment) were inoculated with one of the bacterial suspensions or with Ringer's solution alone (mock-inoculated control) by dipping plant shoots in the solution for 15 sec. A set of parameters were evaluated 1, 2, 7, 14 and 21 days post-inoculation (dpi), including: i) endophytic bacterial population in plant tissues and leaf symptoms occurrence rate; ii) primary and secondary metabolism (total chlorophylls, soluble polyphenols, lignin, and reporter genes for the JA- and ET- pathways); iii) antioxidant system (lipid peroxidation, expression of genes *SOD*, *APX* and *CAT*); and iv) pathogen recognition (expression of gene *Pto3*, which interacts with pathogen virulence effectors and activates plant defences). The experiment was concluded at 21 dpi to allow the appearance of disease symptoms but also ensuring that plant tissues were still viable to guarantee a proper RNA extraction.

2.2. Scoring of foliar symptoms and sampling

Foliar symptoms were evaluated taking into account the percentage of leaf area affected by necrotic spots, according to the following scale: 0: no symptoms, healthy plant; I: <5% of the leaf area affected; II: 5-9% of affected leaf area; III: 10-14% of affected leaf area; IV: 15-19% of affected leaf area; V: ≥20% of affected leaf area (adapted from Cellini *et al*., 2014). Sampling was performed at each time-point of analysis by removing plants from the culturing medium and cutting the tip (*ca*. 0.5 cm length) of every leaf with sterile scissors for CFU determination. The remaining plant was flash-frozen in liquid nitrogen, macerated with mortar and pestle and stored at -80°C for metabolites and gene expression analysis. Each biological replicate was obtained by pooling three plants from the same container and three independent biological replicates were analysed per treatment and time-point.

2.3. Endophytic bacterial population

Estimation of Psa and Pfm colony-forming units (CFU) in plant tissues was performed using an adapted method from Cellini *et al*. (2014). Samples were surface sterilized by washing in 70% ethanol for 1 min, followed by a 1-min treatment with 1% sodium hypochlorite, after which they were rinsed twice in sterile water for 1 min. After maceration in 10 mL Ringer's solution, samples were sequentially diluted ten-fold up to 10^{-4}, and three

replicates of 100 µL from each ten-fold dilution were plated on NSA medium. After plate incubation at 27 °C for 48 h in the dark, the number of colonies in each plate was counted and CFU estimated taking into consideration the fresh weight (FW) of each sample.

2.4. Malondialdehyde

An adapted protocol from Li (2000) was used for malondialdehyde (MDA) quantification. Fifty milligrams of plant sample were added to 500 µL of 0.1% trichloroacetic acid (w/v) and mixed vigorously for 90 s. After sample centrifugation for 5 min at 10 000 g, 250 µL of the supernatant were transferred to a new microcentrifuge tube and mixed with 1 mL of 0.5% thiobarbituric acid in 20% trichloroacetic acid. The mixture was incubated at 100 °C for 30 min, after which the reaction was stopped by rapidly transferring the samples to ice. Samples were centrifuged at 10 000 g for 10 min and the supernatant was used to measure absorbances spectrophotometrically at 532 and 600 nm in a nanophotometer (Implen GmbH, München, Germany). MDA (nmol g^{-1} FW) was determined by the following formula:

$$MDA = \frac{(\mathrm{Abs}_{532} - \mathrm{Abs}_{600}) \times \mathrm{volume}}{\varepsilon = 155\mathrm{mM/cm} \times \mathrm{biomass}}$$

2.5. Primary and secondary metabolites

Lyophilized plant tissues (50 mg) were extracted with 1.5 mL of 80% aqueous methanol (v/v) in an ultrasonic bath for 30 min. Samples were centrifuged for 15 min at 15 000 g and the supernatant was transferred to a new microcentrifuge tube, which was kept on ice during the analysis. The methanolic extract was used for total chlorophyll and total soluble polyphenols quantification. The solid biomass that remained in the original microcentrifuge tube was successively extracted with water, acetone and hexane in the conditions previously described, after which it was dried at 70 °C for 48 h and used for lignin quantification.

Total chlorophyll was quantified as in Sumanta *et al*. (2014) by recording samples absorbances at 470, 652 and 665 nm in a nanophotometer (Implen GmbH, München, Germany). Pigments (µg g^{-1} dry weight) were quantified as:

$$Chlorophyll\ a = (16.72\mathrm{Abs}_{665} - 9.16\mathrm{Abs}_{652}) \times \mathrm{volume/biomass}$$

$$Chlorophyll\ b = (34.09\mathrm{Abs}_{652} - 15.28\mathrm{Abs}_{665}) \times \mathrm{volume/biomass}$$

$$Carotenoids = (1000\mathrm{Abs}_{470} - 1.63\mathrm{Chla} - 104.96\mathrm{Chlb})/(221 \times \mathrm{biomass})$$

Total soluble polyphenols were quantified according to the Folin method adapted from Marinova *et al*. (2005). To 100 µL of the methanolic extract, 4.5 mL of ultrapure water and 500 µL of Folin-Denis' reagent were added. The reaction was allowed to occur for 5 min at room temperature, after which 5 mL of 7% sodium carbonate were added. After incubation

for 1 h at RT in the dark, 2 mL of ultrapure water were added. Sample absorbance was recorded at 750 nm and total soluble polyphenols were determined in each sample through a gallic acid standard curve.

Lignin quantification was performed through an adapted method from Hatfield *et al*. (1999). Ten milligrams of dried sample obtained as previously described were mixed with 1 mL of 12.5% acetyl bromide (in acetic acid, v/v) and incubated for 1 h at 50 °C with vigorous stirring. After centrifugation for 5 min at 15 000 g, 100 µL of sample were transferred to a new microcentrifuge tube with 200 µL of acetic acid and 150 µL of 0.3 M sodium hydroxide. After adding 50 µL of 0.5 M hydroxylamine hydrochloride and 500 µL of acetic acid, sample absorbance was recorded at 280 nm in a nanophotometer, and a lignin calibration curve was used for soluble lignin estimation in each sample.

2.6. Gene expression

Total RNA was extracted according to an adapted protocol from Cellini *et al*. (2014). After tissue homogenization with liquid nitrogen, 1 mL of warm (70 °C) extraction buffer (100 mM Tris-HCl, pH 8.0, cetyltrimethylammonium bromide 4% w/v, polyvinylpyrrolidone K40 4% w/v, 30 mM ethylenediaminetetraacetic acid, 2.0 M NaCl, spermidine 0.1% w/v, β-mercaptoethanol 2% v/v) was added to *ca*. 200 mg of sample. Samples were mixed vigorously and incubated at 70 °C for 10 min. Subsequently, 1 mL of chloroform-isoamyl alcohol (24:1, v/v) was added, and samples were centrifuged for 15 min at 15 000 g. The upper phase was collected to a new tube, washed with chloroform-isoamyl alcohol (24:1, v/v), centrifuged for 15 min at 15 000 g and the supernatant combined with 250 µL of 12 M LiCl by gentle pipetting. Samples were incubated overnight at -20 °C, after which they were centrifuged at 15 000 g for 35 min at 4 °C. The supernatant was discarded and the pellet was washed in cold 70% ethanol, dried, and resuspended in 50 µL sterile DEPC water. Single-stranded cDNA was synthesized using iScript cDNA Synthesis Kit (Bio-Rad, California, USA) according to the manufacturer's instructions in a Doppio Thermal Cycler (VWR, Oud-Heverlee, Belgium).

Primers for *LOX1*, *SAM* and *Pto3* were designed using Primer3 for an expected PCR product of 100-200 bp and primer annealing temperatures between 56 and 58 °C, whereas primer sequences for *ACT* were obtained from Ledger *et al*. (2010), *PP2A* from Nardozza *et al*. (2013) and *APX*, *CAT* and *SOD* from Petriccione *et al*. (2015). Reverse transcription quantitative real-time polymerase chain reactions (RT-qPCR) were performed on a StepOne Real-Time PCR System (Applied Biosystems, California, USA) with the following reaction conditions: 3 min at 95 °C and 40 cycles with: 15 s at 95 °C, 30 s at each primer pair optimal annealing temperature (Table 1) and 30 s at 72 °C. Amplifications were carried out using a

final volume of 20 µL which consisted of 1 µL of the specific primers at 6 µM, 10 µL of 2× iQ SYBR Green Supermix (Bio-Rad, California, USA) and 8 µL of a 1:50 dilution of the template cDNA. Melt curve profiles were analysed for each tested gene. The comparative CT method (ΔΔCT, Livak and Schmittgen, 2001) was used for the relative quantification of gene expression values using actin (*ACT*) and protein phosphatase 2A (*PP2A*) genes as control transcript (Petriccione *et al*., 2015) and the plants inoculated with Ringer's solution (mock-inoculated controls) as the reference sample. For each biological replicate and target gene, two technical replicates were analysed.

Table 1 - Primer sequences (Forward - F and Reverse - R) and annealing temperature (T_{ann}) of housekeeping (H) and target genes used for RT-qPCR analysis.

Gene Name *(Accession number)*	**Primer sequence (5′-3′)**		T_{ann} (°C)	**Reference**
ACT FG440519	**Actin** (H)			
	F	CCAAGGCCAACAGAGAGAAG	56.0	Ledger *et al*., 2010
	R	GACGGAGGATAGCATGAGGA		
PP2A FG522516	**Protein phosphatase 2A** (H)			
	F	GCAGCACATAATTCCACAGG	55.2	Nardozza *et al*., 2013
	R	TTTCTGAGCCCATAACAGGAG		
APX FG408540	**Ascorbate peroxidase**			
	F	GGAGCCGATCAAGGAACAGT	57.8	
	R	AACGGAATATCAGGGCCTCC		
CAT FG470670	**Catalase**			
	F	GCTTGGACCCAACTATCTGC	56.9	Petriccione *et al*., 2015
	R	TTGACCTCCTCATCCCTGTG		
SOD FG471220	**Superoxide dismutase**			
	F	CACAAGAAGCACCACCAGAC	57.8	
	R	TCTGCAATTTGACGACGGTG		
LOX1 DQ497792	**Lipoxygenase 1**			
	F	GTTAGAGGGGTGGTGACTCT	53.5	
	R	CTTTAGCACTGCTTGGTTGC		
SAM U17240	**S-adenosylmethionine synthetase**			
	F	GAATAGTACTTGCCCCTGGC	55.1	This study
	R	TACAAATCGACCAGAGGGGT		
Pto3 KR054654	**Pto-like protein kinase 3**			
	F	TACCACTGTCGCCATTAAGC	56.6	
	R	CCAGCGAACCATTGACCATA		

2.7. Statistical analysis

Data were analysed with GraphPad Prism version 6.0 (GraphPad Software, Inc., California, USA). Significant differences between treatments were determined by analysis of variance (ANOVA) followed by Fisher's LSD test ($p < 0.05$). For CFU and relative gene expression analysis, mean comparison was carried out within the same plant species (i.e., having the time-point and the two *P. syringae* pathovars as factors), whereas for total

chlorophylls, MDA, soluble polyphenols and lignin concentrations significant differences among treatments were analysed within each plant species and time-point.

3. Results

3.1. Symptoms and colony-forming units

Mock-inoculated *A. chinensis* and *A. arguta* plants (plants inoculated with a saline solution without bacteria) did not show visual symptomatology throughout the experimental period. On the contrary, *A. chinensis* plants began to show foliar necrosis as soon as 1 day post-inoculation (dpi), whereas in *A. arguta* foliar symptoms started to appear 7 dpi, regardless of the bacterial strain (Fig. 1). The percentage of *A. arguta* plants showing leaf necrotic spots was always smaller than in *A. chinensis*. In fact, in *A. chinensis*, at 21 dpi, 91% of plants had symptoms of Psa infection, with 41% of the plants having leaf symptoms of grade III or grade IV, whereas in *A. arguta* 83% of Psa-inoculated plants had necrotic spots, but these did not progress beyond grade II. In Pfm-inoculated plants, disease symptoms were slightly milder than in Psa-infected plants, reaching grade III in *A. chinensis*, and only grade II in *A. arguta*.

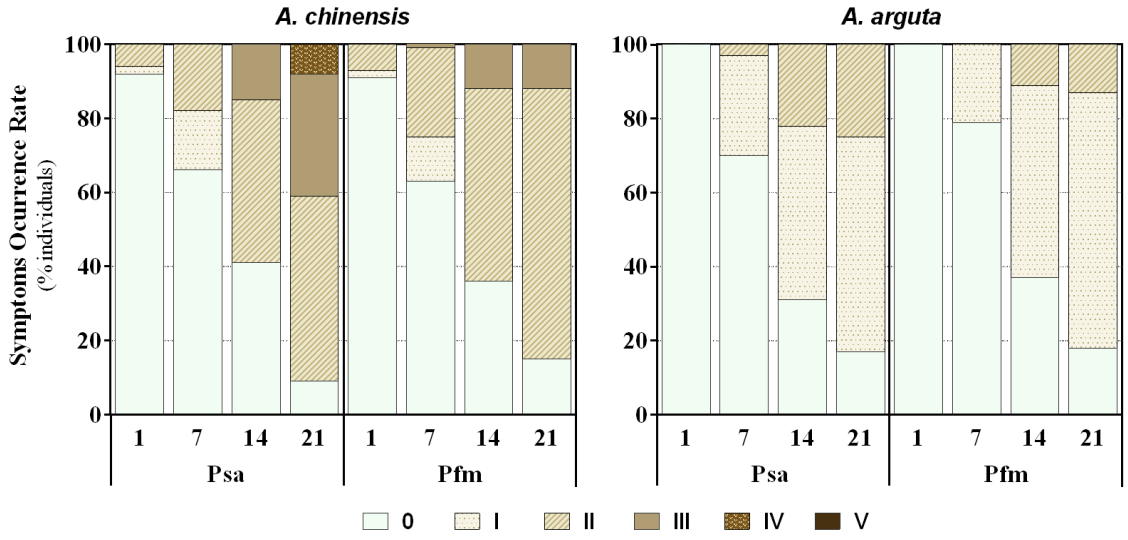

Figure 1 - Symptom occurrence rate (percentage of individuals showing disease symptoms) in *A. chinensis* var. *deliciosa* 'Hayward' and *A. arguta* var. *arguta* 'Weiki' plants inoculated with *P. syringae* pv. *actinidiae* (Psa) or *P. syringae pv. actinidifoliorum* (Pfm) registered 1, 7, 14 and 21 days post-inoculation (dpi). Foliar symptoms were scored taking into account the percentage of leaf area affected by necrotic spots.

At 21 dpi, the most common symptoms in *A. chinensis* included pronounced dark-brown areas of necrotic tissues with varying diameter when inoculated with Psa and smaller light-

brown necrotic areas (up to 5 mm) in Pfm-inoculated plants, whereas in *A. arguta* leaf spot appearance was rare and fainter (Fig. 2).

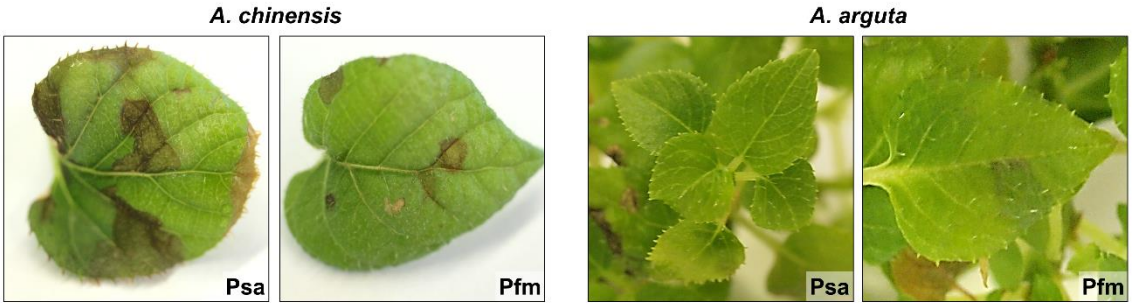

Figure 2 - Most typical foliar symptoms observed in *A. chinensis* var. *deliciosa* 'Hayward' and *A. arguta* var. *arguta* 'Weiki' plants inoculated with *P. syringae* pv. *actinidiae* (Psa) or *P. syringae* pv. *actinidifoliorum* (Pfm) observed 21 days post-inoculation.

In *A. chinensis*, a significant increase in bacterial colonization was observed throughout the experimental period (Fig. 3), reaching a maximum level of 34.0 ± 7.0 × 10^6 CFU g^{-1} at 21 dpi with Psa and 13.1 ± 4.8 × 10^6 CFU g^{-1} with Pfm. Contrastingly, *A. arguta* Psa-inoculated plants presented a colonization peak at 7 dpi, with 6.0 ± 0.5 × 10^3 CFU g^{-1}, after which CFU significantly decreased by 0.8- fold until reaching 0.9 ± 0.2 × 10^3 CFU g^{-1} at 21 dpi. The evolution pattern of endophytic bacterial populations was identical between Psa and Pfm, regardless of plant species, with Psa bacterial density within plant tissues being always higher than Pfm, up to 4.9-fold in *A. chinensis* (7 dpi) and 29.8-fold in *A. arguta* (21 dpi).

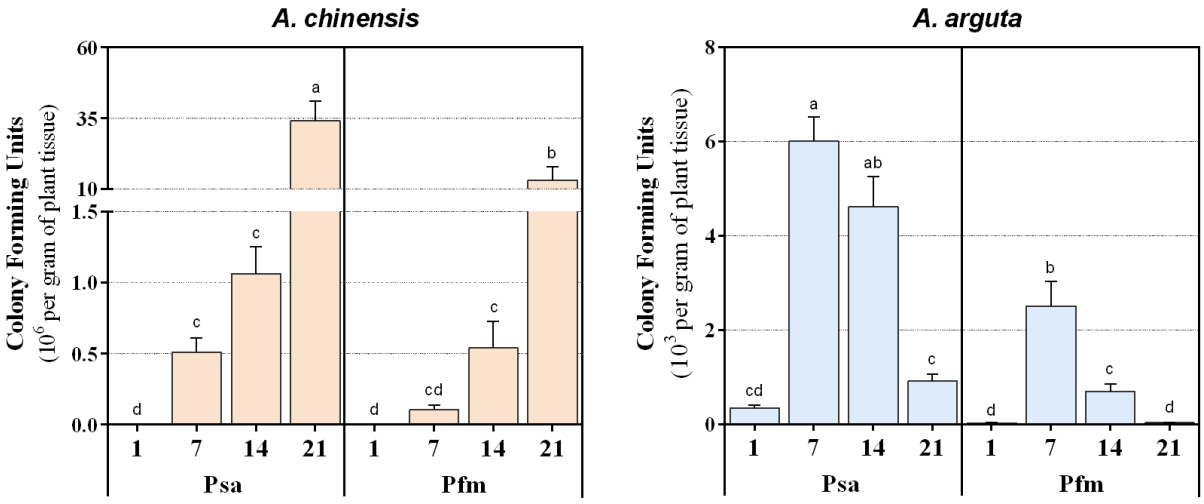

Figure 3 - Number of colony-forming units (CFU, per gram of plant tissue) in *A. chinensis* var. *deliciosa* 'Hayward' and *A. arguta* var. *arguta* 'Weiki' plants inoculated with *P. syringae* pv. *actinidiae* (Psa) or *P. syringae* pv. *actinidifoliorum* (Pfm) registered 1, 7, 14 and 21 days post-inoculation (dpi). For each kiwifruit species, columns represent the mean of three independent replicates (consisting of the pool of three plants each) ± standard error of the mean. Within each plant species, columns with different letters are significantly different at $p < 0.05$. Note that the CFU scale (left x-axis) is different in the two panels.

3.2. Primary and Secondary Metabolites

A. chinensis inoculation led to a significant decrease in total chlorophyll concentration as soon as 7 dpi, regardless of the bacterial strain (Fig. 4A). At the end of the experimental period, Psa and Pfm inoculation induced, respectively, 55 and 39% of chlorophyll loss comparing with the initial values (1 dpi). Contrastingly, no significant alterations were found in total chlorophyll concentration in *A. arguta*-inoculated plants throughout the experimental period (Fig. 4B).

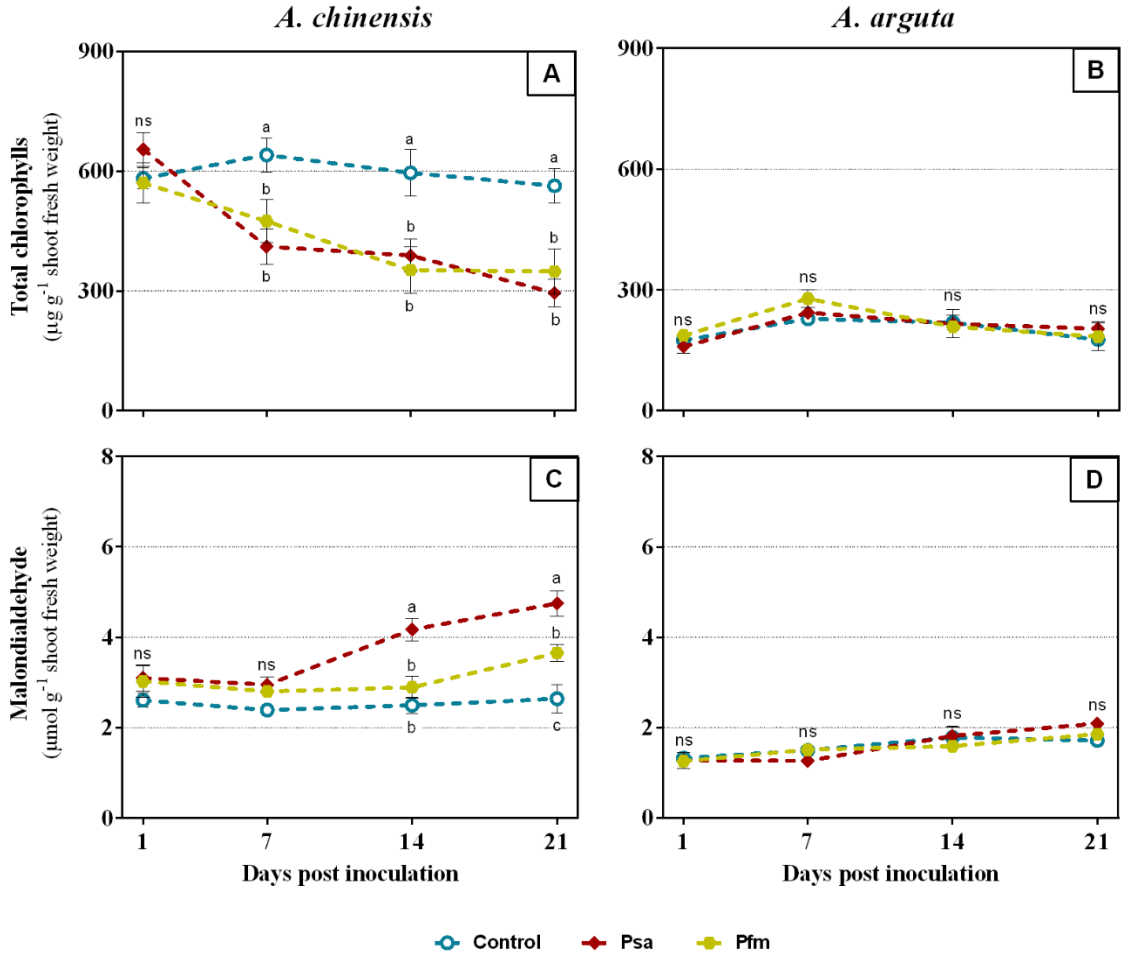

Figure 4 - Total chlorophylls (A and B) and malondialdehyde (C and D) concentrations in *A. chinensis* var. *deliciosa* 'Hayward' and *A. arguta* var. *arguta* 'Weiki' plants, 1, 7, 14 and 21 days post mock-inoculation (Control), or inoculation with *P. syringae* pv. *actinidiae* (Psa) or *P. syringae* pv. *actinidifoliorum* (Pfm). Symbols represent the mean of three independent replicates (consisting of the pool of three plants each) ± standard error of the mean. Within each time-point, symbols with different letters are significantly different at $p < 0.05$ ("ns" indicates no significant differences).

MDA concentration significantly increased after 14 dpi in Psa- and 21 dpi in Pfm-inoculated *A. chinensis* plants when compared with control plants (Fig. 4C). By the end of the experimental period, MDA concentration was 53 and 23% higher in Psa- and Pfm-inoculated plants, respectively, resulting in 4.8 ± 0.3 and 3.7 ± 0.2 µmol g^{-1} MDA, whereas in

control plants this value was significantly lower (2.6 ± 0.3 µmol g^{-1} MDA). Similarly to what was observed for total chlorophyll concentration, in *A. arguta* MDA concentration did not differ significantly between mock- and inoculated-plants (Fig. 4D).

Total soluble polyphenols were only significantly different among inoculated and control plants of *A. chinensis* at 14 dpi, where Psa-inoculated plants had a significantly higher concentration (156.4 ± 10.0 mg g^{-1}) than Pfm (33%) and control plants (112%) (Fig. 5A).

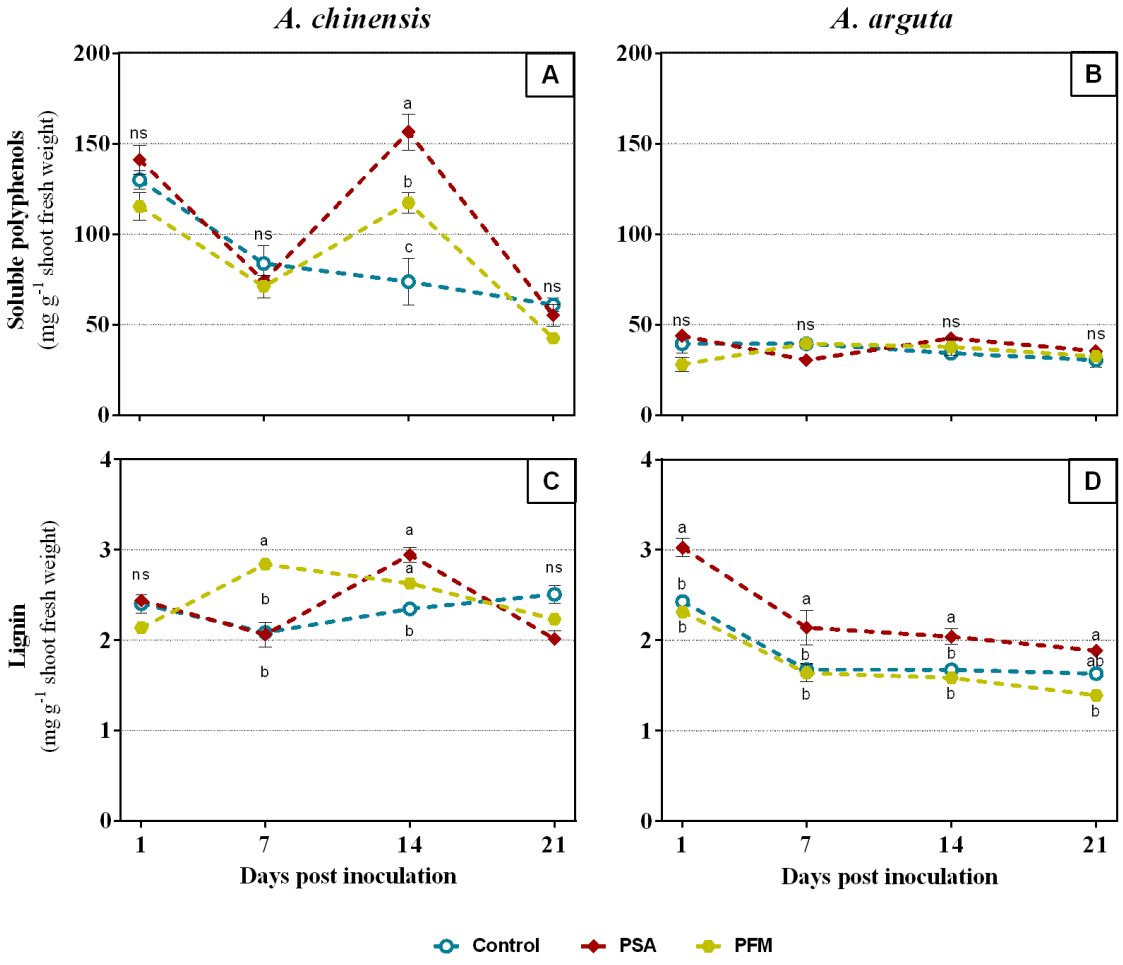

Figure 5 - Total soluble polyphenols (A and B) and lignin (C and D) concentrations in *A. chinensis* var. *deliciosa* 'Hayward' and *A. arguta* var. *arguta* 'Weiki' plants, 1, 7, 14 and 21 days post mock-inoculation (Control), or inoculation with *P. syringae* pv. *actinidiae* (Psa) or *P. syringae* pv. *actinidifoliorum* (Pfm). Symbols represent the mean of three independent replicates (consisting of the pool of three plants each) ± standard error of the mean. Within each time-point, symbols with different letters are significantly different at $p < 0.05$ ("ns" indicates no significant differences).

At the end of the experimental period, total soluble polyphenols were up to 63% lower in all treatments, averaging 53 mg g^{-1}, comparing with 1 dpi. Contrastingly, once more no significant differences were observed in soluble polyphenols in *A. arguta* when comparing control and inoculated plants (Fig. 5B). Concerning lignin concentration, it was found that *A. chinensis* Pfm-inoculated plants had a significantly higher value at 7 dpi (36%) and 14 dpi

(12%) when compared with mock-inoculated plants (Fig. 5). In *A. chinensis* Psa-inoculated plants, lignin concentration only differed from control plants at 14 dpi, being 26% higher. In *A. arguta*, contrastingly to what was observed for the other parameters analysed, a significant variation in lignin concentration occurred between different treatments throughout the experimental period. One dpi, Psa-inoculated plants presented 3.0 ± 0.1 mg g^{-1} lignin, which was 24 and 31% higher than control and Pfm-inoculated plants, respectively. After this time-point, lignin concentration decreased in all treatments and, in general, Psa-inoculated plants remained with a significantly higher lignin concentration compared with control and Pfm-inoculated plants (up to 14%).

3.3. Gene expression

In *A. chinensis* infected plants, *SOD* relative expression only started to be significantly upregulated at 21 (Psa) and 14 dpi (Pfm), reaching a 4.5- and a 3.1-fold increase (respectively) compared to mock-inoculated control plants (Fig. 6). On the other hand, in *A. arguta SOD* overexpression occurred as soon as 1 dpi, and it significantly decreased from 1 to 2 dpi, by 0.46-fold in Psa-inoculated plants and by 0.58-fold in Pfm, being further downregulated by the end of the experimental period. A similar trend was observed in *APX* regulation, since *A. chinensis* infected plants only showed overexpression of this gene at 14 dpi, being 2.4-fold higher compared with mock-inoculated plants, regardless of the bacterial strain. In *A. arguta*, plant inoculation induced *APX* overexpression already at 2 dpi (1.8-fold for Psa and 1.9-fold for Pfm), decreasing thereafter and becoming downregulated at 21 dpi. In *A. chinensis CAT* overexpression was observed at 2 dpi in plants inoculated with both bacterial strains, decreasing until the end of the experimental period. Contrastingly, in *A. arguta CAT* overexpression occurred as soon as 1 dpi, particularly in Pfm-inoculated plants, which reached a 2.5-fold increase relative to mock-inoculated plants. From 14 dpi on, *CAT* expression further decreased to basal levels in plants inoculated with either bacterial strain.

Within each plant species, a similar trend in the relative fold of expression of *LOX1* and *SAM* was observed throughout the experimental period, with little variation being observed between Psa- and Pfm-inoculated plants (Fig. 7). In *A. chinensis*, both transcripts were overexpressed in Psa-inoculated plants at 1 dpi, but returned to basal values at 2 and 7 dpi, significantly increasing thereafter. After Pfm inoculation, *LOX1* and *SAM* relative expression remained unaltered until 21 dpi, where a 2.4- and 3.6-fold overexpression was observed, compared with mock-inoculated plants. In *A. arguta*, *LOX1* and *SAM* relative fold of expression was increased 1 dpi, independently of the bacterial strain, significantly decreasing throughput out the experimental period, by *ca*. 0.94-fold in both inoculums, being inclusively downregulated at 14 and/or 21 dpi.

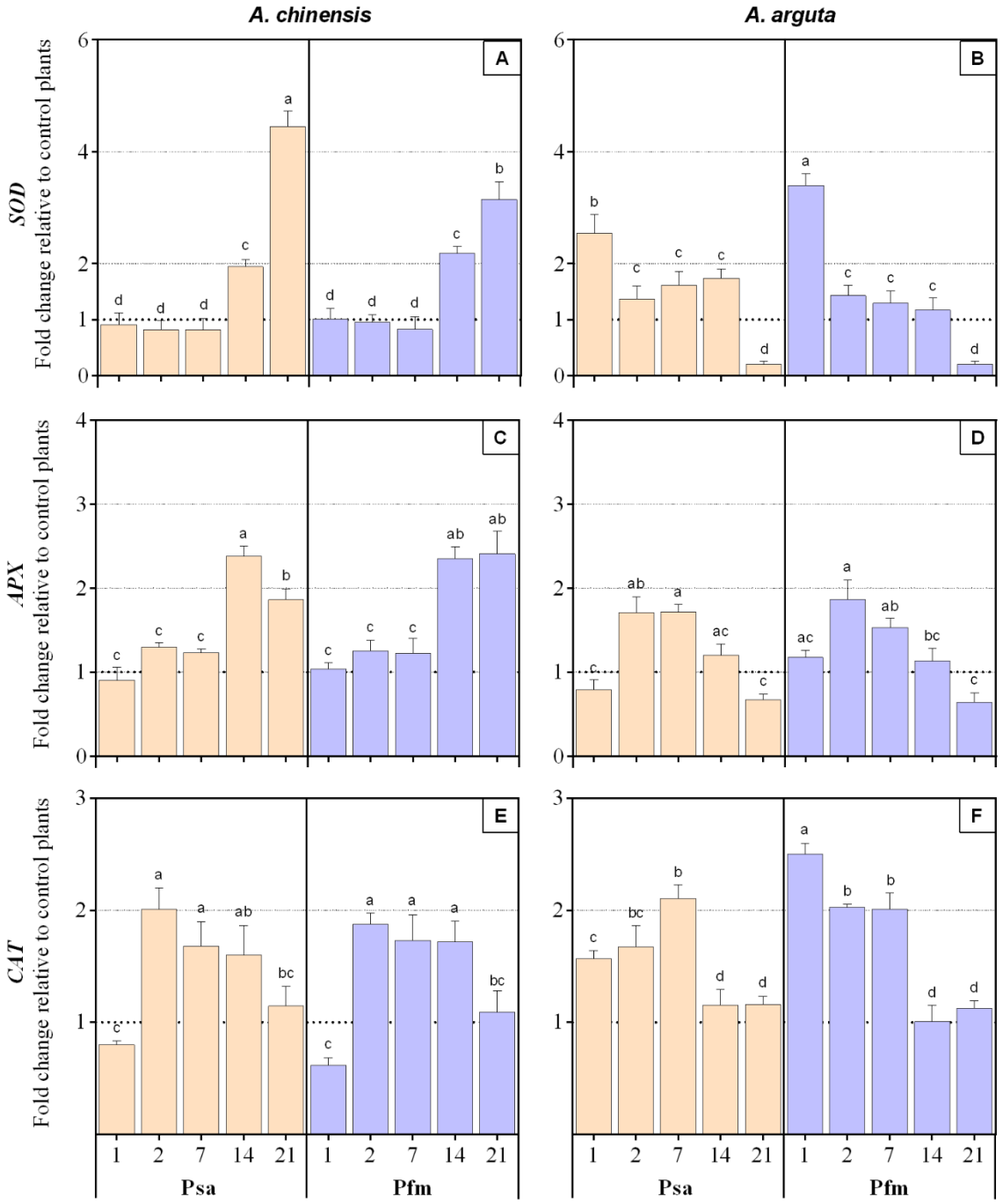

Figure 6 - Relative fold of expression of *SOD* (superoxide dismutase), *APX* (ascorbate peroxidase) and *CAT* (catalase) genes in *A. chinensis* var. *deliciosa* 'Hayward' (panels A, C and E, respectively) and in *A. arguta* var. arguta 'Weiki' plants (panels B, D and F, respectively) inoculated with *P. syringae* pv. *actinidiae* (Psa) or *P. syringae* pv. *actinidifoliorum* (Pfm) registered 1, 2, 7, 14 and 21 days post-inoculation (dpi). Columns represent the mean of three independent replicates (consisting of the pool of three plants each) ± standard error of the mean. Within the same plant species, columns with different letters are significantly different at $p < 0.05$. One-fold change represents no relative change in gene expression, as compared with mock-inoculated control plants.

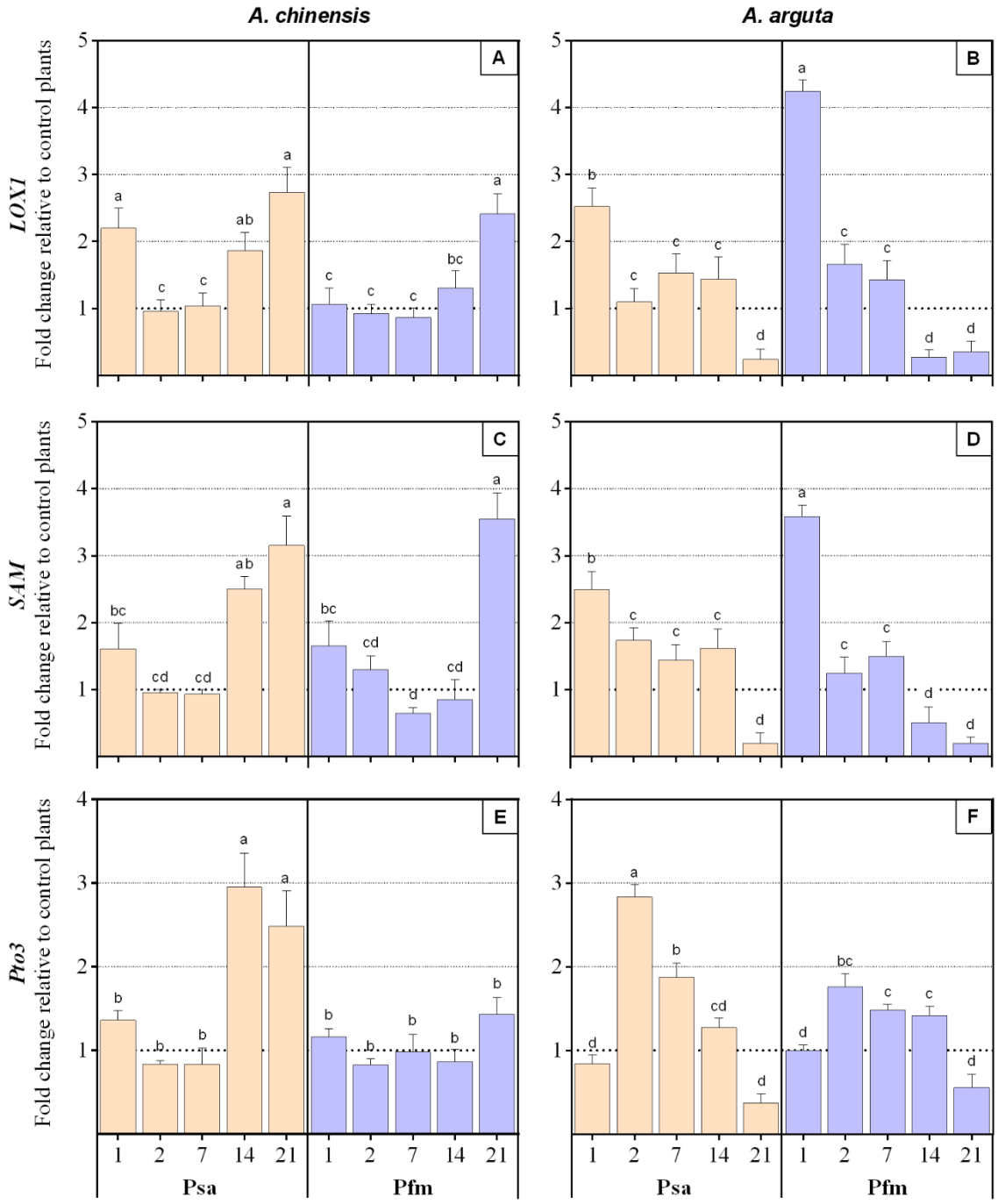

Figure 7 - Relative fold of *LOX1* (lipoxygenase 1), *SAM* (S-adenosylmethionine synthetase) and *Pto3* (Pto-like protein kinase 3) genes in *A. chinensis* var. *deliciosa* 'Hayward' (panels A, C and E, respectively) and in *A. arguta* var. arguta 'Weiki' plants (panels B, D and F, respectively) inoculated with *P. syringae* pv. *actinidiae* (Psa) or *P. syringae* pv. *actinidifoliorum* (Pfm) registered 1, 2, 7, 14 and 21 days post-inoculation (dpi). Columns represent the mean of three independent replicates (consisting of the pool of three plants each) ± standard error of the mean. Within the same plant species, columns with different letters are significantly different at $p < 0.05$. One-fold change represents no relative change in gene expression, as compared with mock-inoculated control plants.

Finally, in *A. chinensis* the relative fold of expression of *Pto3* gene was only significantly increased at 14 dpi in Psa-inoculated plants (becoming 3.0-fold higher than mock-inoculated controls) and remaining elevated until the end of the experimental period. Contrastingly, no significant alterations were observed in the expression of this gene in Pfm-inoculated *A. chinensis* plants (Fig. 7). In *A. arguta*, *Pto3* overexpression occurred at 2 dpi, being 3.3-fold in Psa- and 1.8-fold in Pfm-inoculated plants, gradually decreasing until the end of the experimental period.

4. Discussion

4.1. Bacterial progression is more restricted in *A. arguta*

Limited bacterial progression within plant tissues is regarded as a tolerance trait. However, until now very few long-term disease assessments under the same controlled environmental conditions have been performed to compare Psa- and Pfm-inoculated *A. chinensis* and *A. arguta* plants, hindering the full comprehension of bacterial infection and plant tolerance mechanisms (Wurms *et al*., 2017a). Datson *et al*. (2015) reported that in *A. arguta* plants stab-inoculated with a Psa strain, the endophytic bacterial population was lower and more restricted to the site near the inoculation zone when compared with *A. chinensis*, even four weeks after inoculation. Moreover, in a previous short-term study, we observed that bacterial density of not only Psa but also Pfm inside plant tissues was lower in *A. arguta* than in *A. chinensis* up to 5 days post-inoculation (Nunes da Silva *et al*., 2019). In the present work, the evolution of foliar symptoms (Fig. 1 and 2) seemed to accompany the increase of Psa endophytic population (Fig. 3) throughout the experimental period, with a rapid and intense bacterial multiplication in *A. chinensis* tissues (especially after inoculation with Psa), whereas *A. arguta* tissues had lower bacterial density and symptom severity. Together, these results confirm the higher susceptibility of *A. chinensis* probably because bacteria can easily progress and reproduce inside its vascular system, whereas in *A. arguta* bacterial movement and reproduction are more restricted (Wang *et al*., 2020a). It is interesting to note that in the present work foliar symptoms began to appear as soon 1 dpi, whereas in other studies symptoms only appear after the first 5 dpi (McAtee *et al*., 2018). We hypothesize that the inoculation method selected in the current work (i.e., plant dipping in inoculum) favoured the accumulation of bacterial droplets in plant leaves, propelling the entrance of bacteria into plant tissue and the appearance of disease symptoms shortly after infection. Psa population in plant tissues were always higher than Pfm's, thus demonstrating the less pathogenic character of the second bacterial strain, even when inoculated into the more susceptible kiwifruit species. Looking only at stems mean lesion length and not to bacterial density in

plant tissues *per se*, Wurms *et al*. (2017a) compared *A. chinensis* var. *deliciosa* 'Hayward' plants inoculated with Psa or Pfm, and observed that Psa infection induced more severe symptoms, with the appearance of dark-brown necrotic tissues and water-soaked appearance near the site of inoculation. The present work confirms these findings, as in both plant species leaf symptoms were less severe following Pfm infection, with light- brown necrotic areas appearing after Psa inoculation and almost no necrotic tissues visible after Pfm inoculation. Our results attest the higher pathogenicity of Psa strains belonging to biovar 3, as compared to Pfm, as previously suggested (Hoyte *et al*., 2015).

4.2. Primary and secondary metabolism is less impacted in *A. arguta* than in *A. chinensis*

Plant infection by bacterial pathogens frequently leads to loss of chloroplast functions and, consequently, to tissue chlorosis or necrosis, impairing plant fitness and propelling the disease (Lu and Yao, 2018). Transcripts related to photosynthesis were reported to be repressed in susceptible *Actinidia chinensis* cultivars, but highly expressed in the more tolerant *A. eriantha* species after Psa infection (Wang *et al*., 2017a). Here, decreased total chlorophyll concentration was observed in *A. chinensis* after infection with Psa and Pfm, whereas in *A. arguta* inoculated with either bacterial strain no significant alterations in total chlorophyll concentration were recorded over the experimental period (Fig. 4). Loss of these photosynthetic pigments in *A. chinensis* is probably related to the higher prevalence of tissue necrosis observed (Fig. 2 and 3), thus demonstrating the more tolerant character of *A. arguta*. Increased polyphenols concentration was observed in *A. chinensis* 14 dpi with Psa and Pfm, probably as part of the defence mechanisms employed by the infected plants (Fig. 5). Contrastingly, no significant alterations were observed in soluble polyphenols in *A. arguta*, which is in line with what was observed for total chlorophylls and MDA concentrations, demonstrating that inoculation did not induce severe alterations in plant metabolism. Lignin concentration increased 7 dpi in *A. chinensis* Pfm-inoculated plants and 14 dpi in Psa-inoculated ones, whereas in *A. arguta* it was significantly higher in Psa- inoculated plants in all time-points analysed. So far, the role of lignin accumulation in Psa- and Pfm-infected kiwifruit plants has not been properly explored, but we hypothesize that increased lignin concentration in Psa-inoculated plants may be one of the defence mechanisms employed by *A. arguta* to restrain pathogen penetration and/or migration within plant tissues, possibly contributing to its higher tolerance to Psa.

LOX1 and SAM are involved in JA and ET biosynthesis pathways. Whereas *LOX1* converts *a*-linolenic acid into 13-hydroperoxy-octadecatrienoic acid in the JA pathway, *SAM* encodes S-adenosylmethionine synthetase, a precursor of ET biosynthesis (Kolomiets *et al*.,

2000). Although SAM is the precursor of not only ET but also polyamines, due to its key regulatory role during the first step of ET biosynthesis it is frequently used as a reporter for ET metabolism (Zhao *et al*., 2017). Genes involved in ET biosynthesis, such as *AP2*/*ERF*, *EIN2* and *SAM*, were found to be upregulated just 2 dpi in *A. chinensis* plants inoculated with Psa (Wurms *et al*., 2017a; Wurms *et al*., 2017b, Nunes da Silva *et al*., 2019). *LOX1* increased activity was also previously reported in *A. chinensis* and *A. arguta* Psa- and Pfm-inoculated plants, and is regarded as a strategy used by the pathogen to antagonize plant defence mechanisms (Cellini *et al*., 2014; Nunes da Silva *et al*., 2019). In fact, several studies have confirmed that *Actinidia* defence responses against Psa are mainly regulated by SA-mediated pathways, whereas the ET and JA pathways act synergistically between each other, but antagonistically to SA, leading to increased plant susceptibility (Petriccione *et al*., 2013; Reglinski *et al*., 2013; Cellini *et al*., 2014; Petriccione *et al*., 2014). In the current work, within each species, a similar trend in *LOX1* and *SAM* expression was observed, with little variation between Psa- and Pfm-inoculated plants (Fig. 7). However, it is interesting to note that these genes involved in JA and ET pathways were overexpressed (compared to mock-inoculated controls) shortly after infection and decreased thereafter in *A. arguta*, whereas in *A. chinensis* their transcriptional levels remained near the basal threshold (1-fold) during the first stages of the disease, significantly increasing until the end of the experimental period. Due to their reported antagonistic effect on kiwifruit defence mechanisms, we hypothesize that *LOX1* and *SAM* were upregulated in the latter stages of the disease in *A. chinensis* as result of impaired defence ability due to elevated bacterial density inside plant tissues, but were suppressed in *A. arguta* as part of its coping mechanisms against Psa and Pfm. The fact that *A. arguta* can repress the occurrence of severe impairments to both primary and secondary metabolism from an early stage of the disease can partly explain its increased tolerance to Psa and Pfm.

4.3. Plant antioxidant system is activated earlier in *A. arguta* than in *A. chinensis*

Increased ROS activity in plant tissues during stress conditions induces lipid peroxidation of cell membranes and organelles, thus leading to the formation of MDA. As such, this metabolite is often used to assess the degree of plant oxidative stress and has been shown to increase following chlorophyll loss in genotypes susceptible to several environmental stresses (Sevengor *et al*., 2011; Taheri and Kakooee, 2017). Indeed, here we found that lipid peroxidation occurred in Psa- and Pfm-inoculated *A. chinensis* plants at 7 dpi, which seems to be in line with the increase of bacterial density inside plant tissues and the decrease of total chlorophylls (Fig. 3 and 4). This demonstrates that inoculation negatively

affected *A. chinensis* cellular homeostasis, leading to increased lipid peroxidation. On the contrary, *A. arguta* plants showed lower MDA values, regardless of the bacterial inoculum, without significant changes over the experimental period. This is a reflection of the lower bacterial colonization observed in this plant species, as well as the lower extent of leaf symptoms and impairments of primary and secondary metabolism, corroborating the higher tolerance of this plant species do Psa and Pfm.

To counteract lipid peroxidation and other oxidative stress-related impairments, plant responses against Psa include the expression of several genes related to the antioxidant system (Petriccione *et al*., 2014; Wurms *et al*., 2017a; Wang *et al*., 2018a; Nunes da Silva *et al*., 2019). In a previous short-term evaluation, *APX* and *CAT* transcriptional levels were found to be little affected in both *A. chinensis* and *A. arguta* during the first 5 days after Psa and Pfm infection, whereas *SOD* overexpression was observed at 5 dpi in *A. chinensis* (Nunes da Silva *et al*., 2019). Similar results were observed in two-years-old pot-cultivated *A. chinensis* var. *deliciosa* 'Hayward' plants inoculated with Psa (Petriccione *et al*., 2015). In the current work, in *A. chinensis SOD* and *APX* regulation seemed to accompany the development of bacterial density (independently of the bacterial strain) and MDA content in plant tissues, significantly increasing when compared with mock-inoculated controls throughout the experimental period (Fig. 6). Contrastingly, *CAT* upregulation preceded the moments of more intensive bacterial increase and MDA accumulation, probably as a coping strategy against the pathogens. It seems that the activation of plant antioxidant mechanism occurs in a more precocious stage after infection in *A. arguta* and is not dependent on the bacterial density inside plant tissues nor on the extent of MDA accumulation, as *A. arguta* showed lower endophytic bacterial population and MDA concentrations, but still activated its antioxidant system to a higher extent comparing with *A. chinensis*.

4.4. *A. arguta* seems to identify and respond to Psa- and Pfm-infection from an earlier stage after plant infection

As part of their defence mechanisms, plants can perceive MAMPs, such as flagellin, through PRRs (Clay *et al*., 2009). In tomato plants, the resistance protein Pto interacts with *P. syringae* pv. *tomato* effector AvrPto inside plant cells, activating a cascade of defence-related mechanisms (Mucyn *et al*., 2006). In plants lacking this protein, AvrPto seems to inhibit pathogen recognition and enhance bacterial virulence (Hauck *et al*., 2003). Genes involved in this process, such as *FLS2* and *NBS-LRR* genes, were found to be upregulated in *A. chinensis* plants 2 dpi with Psa (Wurms *et al*., 2017b; Wang *et al*., 2018b; Wang *et al*., 2020b). In the present work *Pto3* relative fold of expression was increased already at 2 dpi in *A. arguta*, but only at 14 dpi in *A. chinensis* Psa-inoculated plants (Fig. 6). It seems that in

A. chinensis Pto3 expression in Psa-inoculated plants accompanies the increase of endophytic bacterial density, whereas in *A. arguta* it precedes the period of higher bacterial multiplication. Pathogen recognition in the early stages of infection in *A. arguta* plants may explain the earlier activation of the antioxidant system and repression of ET and JA pathways, conferring increased tolerance against Psa and Pfm. Notwithstanding, pathogen recognition mechanisms are highly dependent not only on plant species but also on the type of pathogen. Perhaps the lack of alterations in *Pto3* relative expression in Pfm-inoculated *A. chinensis* plants is due to the activation of other PRR, such as *FLS2* and *CC-NBS-LRR*, supporting the evidence that this class of genes underwent adaptive evolution in response to the corresponding evolution of pathogen avirulence genes (Dangl and Jones, 2001). In fact, genome sequencing revealed a large number of differences between alleles associated with the *avrE1* effector gene between Psa biovar 3 and Pfm (Chapman *et al*., 2012). The expression of *Pto3* shortly after *A. arguta* infection with Psa may have allowed the prompt recognition of the pathogen and underpin the higher tolerance of this species. These results also highlight that there is probably a vast repertoire of pathogen recognition genes mediating *Actinidia* and Psa/Pfm interaction yet to be known.

5. Conclusion

The identification and characterisation of tolerance mechanisms against Psa within *Actinidia* germplasm are of extreme importance for the identification of kiwifruit genotypes tolerant to the pathogen. The present work confirmed the greater tolerance of *A. arguta* var. *arguta* to Psa and Pfm infection, compared to *A. chinensis* var. *deliciosa*, since the first had lower bacterial density, higher total chlorophyll concentration and lower MDA concentration throughout the 21 days of the experimental period. Moreover, it showed that the higher tolerance of *A. arguta* to Psa and Pfm seems to be related to early pathogen recognition, with gene *Pto3* being upregulated from an early moment after plant infection, leading to the activation of plant antioxidant system (namely regarding *SOD*, *APX* and *CAT* transcriptional levels) and to the suppression of genes related with the ET and JA pathways shortly after infection. The present study analyses a relevant number and variety of parameters related to the dynamics of kiwifruit plants' response to and Psa and Pfm, contributing to a better understanding of the underlying processes behind the differential tolerance against these pathogens. As future works, it would be interesting to perform a broader transcriptomic analysis of *A. chinensis* and *A. arguta* plants inoculated with both Psa and Pfm, as well as the analysis of metabolomic changes that may fully explain the higher tolerance of *A. arguta* to KBC.

CHAPTER 3

Unravelling plant tolerance mechanisms

CHAPTER 3 - Sub-chapter 3.1

Defence-related pathways, phytohormones and primary metabolism are key players in the distinct tolerance of *Actinidia chinensis* and *A. arguta* to *Pseudomonas syringae* pv. *actinidiae*

Defence-related pathways, phytohormones and primary metabolism are key players in the distinct tolerance of *Actinidia chinensis* and *A. arguta* to *Pseudomonas syringae* pv. *actinidiae*

Abstract

Actinidia arguta is more tolerant than *A. chinensis* to *Pseudomonas syringae* pv. *actinidiae* (Psa), and we hypothesised that plant-defence strategies linked to transcriptome regulation, phytohormones, and other metabolic readjustments, might underpin this differential response. Here, both plant species were inoculated with Psa, and 48 hours post-inoculation, whole-transcriptome, phytohormones and primary metabolites were evaluated. *A. chinensis* and *A. arguta* transcriptomes shared 9 330 genes, with 380 of them being differentially expressed after inoculation. Eighty-nine differentially expressed genes (DEGs) related with e.g., pathogen recognition, plant immunity, and defence regulation, were identified among the two species. Thirty-four DEGs related to abscisic (ABA), jasmonic (JA) and salicylic acid (SA), and 58 DEGs involved in primary metabolism (e.g., glycolysis, tricarboxylic acid and ammonia assimilation cycles) were also identified. Psa density was 10-fold higher in *A. chinensis*, accompanied by significant increases in glutamine (1.3-fold), ornithine (1.5-fold), JA (3.2-fold) and SA (2.1-fold). *A. arguta* showed lower bacterial colonization, decreased abscisic acid (ABA) (0.7-fold) and no changes in primary metabolites. Results suggest that *A. chinensis*' higher susceptibility to Psa is due to an inefficient activation of plant defence mechanisms, with the involvement of ABA, JA and SA, leading to impairments in primary metabolism, including the ammonia assimilation cycle.

1. Introduction

The kiwifruit bacterial canker (KBC), caused by *Pseudomonas syringae* pv. *actinidiae* (Psa), affects plant yield and requires strict orchard management routines, leading to important economic losses (Froud *et al*., 2017). Until now, no curative methods have been developed for KBC, and the most common control strategies consist of preventive measures that limit inoculum load and spread. These strategies mainly rely on copper-based formulations or broad-effect elicitors, which are frequently inefficient during the advanced stages of infection or show distinct efficiency depending on the plant genotype (Reglinski *et al*., 2013; Cameron and Sarojini, 2014; Cellini *et al*., 2014). All species of the genus *Actinidia* can be infected by Psa, but there seems to be considerable variation in their tolerance to the infection. For example, it has been recently demonstrated that species such as *A. arguta* and *A. eriantha* are more tolerant to Psa infection than *A. chinensis* (Song *et al*., 2019; Nunes da Silva *et al*., 2020), but the metabolic and transcriptomic features underpinning plant tolerance to Psa are not yet understood.

The first line of plant defences against pathogenic bacteria is activated after the recognition of specific pathogen-associated molecular patterns (PAMP) by plant cell pattern recognition receptors (PRRs) (i.e., PAMP-triggered immunity, PTI). Genes encoding PPRs, e.g., flagellin (*FLS*) and nucleotide-binding leucine-rich repeat (*NB-LRR*), were found to be induced shortly after Psa infection (Clay *et al*., 2009; Wurms *et al*., 2017a; Michelotti *et al*., 2018; Wang *et al*., 2018a). After recognition of bacterial effectors, a second line of plant defence mechanisms is activated (i.e., effector-triggered immunity, ETI). PTI and ETI can consequently trigger a hypersensitive response (HR) at the infection site, further leading to changes in structural defences and induction of systemic acquired resistance (SAR). These processes may involve strengthening of plant cell walls through the deposition of lignin, impairments in phytohormone regulation, and overexpression of several defence-related genes (Petriccione *et al*., 2015; Wurms *et al*., 2017a; Wurms *et al*., 2017b; Michelotti *et al*., 2018; Li *et al*., 2020; Nunes da Silva *et al*., 2020). Recent studies have revealed that Psa Rpm1 effectors trigger immune responses through the gene *Rpa1*, which encodes a plant NB-LRR protein with an N-terminal coiled-coil domain (Yoon and Rikkerink, 2020). However, the downstream defence mechanisms seemed to be differently activated depending on the kiwifruit genotype. For instance, the expression of the *Pto3* gene, which also interacts with pathogen virulence effectors and activates plant defences, was upregulated sooner in *A. arguta*, as compared with *A. chinensis* (Nunes da Silva *et al*., 2020). Comparative transcriptome analysis also revealed a higher number of differentially expressed genes (DEGs) involved in early disease resistance and rapid response to the pathogen in the tolerant species *A. eriantha*, when compared to *A. chinensis*. Genes encoding PPRs and PTI, such as *RPS2* and *Pti*, and genes involved in the salicylic acid (SA) signalling pathway, including *NPR1*, *TGA*, and *PR1*, were found to be upregulated in the tolerant *A. eriantha*, suggesting that SA plays a key role in the signalling pathways involved in defence responses against Psa (Song *et al*., 2019).

In fact, phytohormones, such as SA, jasmonic acid (JA), ethylene (ET) and abscisic acid (ABA) play critical roles in plant defence responses against pathogens. The complex crosstalk between phytohormone signalling networks makes them crucial for an adequate defence response (Pieterse *et al*., 2012). Several studies have demonstrated that *Actinidia* defences against Psa are mainly regulated by SA-mediated pathways, whereas JA, ET and ABA have a negative effect on these mechanisms (Cellini *et al*., 2014; Petriccione *et al*., 2013, 2014; Reglinski *et al*., 2013). Infection of *A. chinensis* with Psa increased endogenous SA concentrations to a greater extent than JA (Wurms *et al*., 2017b), and treatment with the SA inducer acibenzolar-S-methyl (ASM) reduced the incidence of plant disease (Cellini *et al*., 2014). In contrast, a significant increase in disease severity was observed after elicitation of the JA and ABA pathways (Reglinski *et al*., 2013; Cellini *et al*., 2014). Nevertheless, the networks underlying phytohormone regulation in genotypes with distinct tolerance to Psa are

still poorly understood (Cellini *et al*., 2016; Wurms *et al*., 2017b). A deeper comprehension of phytohormone regulatory mechanisms could allow the identification of key tolerance features and the development of elicitors that promote plant tolerance against this pathogen.

After infection, Psa can colonize the apoplastic fluid and take advantage of plant metabolites to sustain its metabolic requirements. In *A. chinensis*, several proteins involved in carbohydrate metabolism and energy regulation were differentially expressed following infection with Psa (Petriccione *et al*., 2013; 2014). It was also demonstrated that Psa infection impaired the accumulation of several amino and organic acids, leading to extensive reprogramming of carbon (C) and nitrogen (N) cycling in different metabolic pathways, such as photosynthesis, C fixation, and the tricarboxylic acid (TCA) cycle (Li *et al*., 2020). These authors observed that the levels of several primary metabolites (e.g., arginine, asparagine, glutamine, fumarate, fructose, glutamic acid, pyruvate, proline, valine and succinic acid) were differently affected following Psa infection. Li *et al*. (2020) also demonstrated that the activity of a chitinase involved in plant N cycling increased after Psa infection, suggesting that plant N metabolism might be impaired during this process. So far, there are no comparative studies linking plant metabolic profiling and transcriptome analysis in genotypes with contrasting susceptibility to Psa, limiting the knowledge on how plant metabolism is affected by Psa, and how its reprogramming repercusses on the outcome of the infection.

In this work, it was hypothesized that the differential susceptibility between *A. chinensis* and *A. arguta* is determined at early stages of Psa infection, and is linked to the activation of distinct defence-related pathways, hormonal regulation, and general readjustment of primary metabolic pathways. Thus, this work aimed to understand how these biological processes are affected in *A. chinensis* (more susceptible) and *A. arguta* (more tolerant) after Psa infection through: i) determination of Psa endophytic colonization; ii) analysis of phytohormone composition (JA, SA and ABA); iii) primary metabolite profiling (amino acids, organic acids, polyamines and sugars), and iv) whole-transcriptome sequencing.

2. Materials and Methods

2.1. Plant inoculation and sampling

Micropropagated *A. chinensis* 'Hayward' and *A. arguta* 'Ken's Red' plants (with a single shoot, 5 to 6 cm height, and 5 to 10 leaves) were purchased from QualityPlant - Investigação e Produção em Biotecnologia Vegetal, Lda. (Castelo Branco, Portugal). Plants were maintained in a modified full-strength Murashige and Skoog (MS) agarized (0.7%) medium in a climate chamber (Aralab Fitoclima 10 000EH, Aralab, Rio de Mouro, Portugal) as described elsewhere (Nunes da Silva *et al*., 2020). On the day of plant inoculation, a fresh

inoculum with 1-2x10^7 colony-forming units (CFU) mL^{-1} of a virulent Psa strain (CFBP 7286, isolated in Italy) was prepared in sterile Ringer's solution (NaCl 0.72%, $CaCl_2$ 0.017% and KCl 0.037%, pH 7.4). Nine plants were inoculated with Psa inoculum, and nine plants were inoculated with Ringer's solution alone (mock-inoculated controls), by dipping plant shoots in each solution for 15 sec. Forty-eight hours post-inoculation (hpi) plants were removed from the culture medium and the tip (*ca*. 0.5 cm length) of every leaf was aseptically removed and placed in a sterile container for the determination of Psa endophytic population (colony-forming units, CFU). The remaining shoot tissues were flash-frozen in liquid nitrogen, macerated with mortar and pestle and stored at -80 °C for phytohormone analysis, primary metabolite profiling and whole-transcriptome sequencing. Each biological replicate was obtained by pooling three plants randomly selected from the same treatment, and three independent biological replicates were analysed per treatment.

2.2. Psa endophytic population in shoot tissues

Leaf tips were surface sterilized, macerated in Ringer's solution, and used for CFU determination as previously described by Cellini *et al*. (2014). Briefly, samples were surface sterilized by washing in 70% ethanol for 1 min, followed by a 1-min treatment with 1% (v/v) sodium hypochlorite, after which they were rinsed twice in sterile water for 1 min. After maceration in 10 mL Ringer's solution, samples were sequentially diluted ten-fold up to 10^{-4}, and three replicates of 100 µL from each dilution were plated on nutrient sucrose agar (NSA) medium. After plate incubation at 27 °C for 48 hours in the dark, the number of colonies in each plate was counted and Psa endophytic population estimated taking into consideration the fresh weight (FW) of each sample.

2.3. Phytohormone quantification

JA, SA and ABA were quantified following an adapted protocol from de Ollas *et al*. (2013). To lyophilized shoot tissues (*ca*. 50 mg FW) were added 100 ng of $ABAd_6$, 100 ng of SAd_6, 100 ng of di-hydro-JA and 2 mL of distilled water. After vigorous stirring with glass beads for 10 min, samples were centrifuged for 10 min at 12 000 g and 4 °C, and the supernatant was recovered to a new centrifuge tube. The pH of the extract was adjusted to 3.0 with 80% (v/v) acetic acid. Afterwards, 2 mL of diethyl ether were added to each sample, vigorously mixed, and the upper layer evaporated in a centrifuge concentrator (SpeedVac, Jouan, Saint Herblain, France). Samples were resuspended in 1 mL of 10% (v/v) methanol, sonicated for 10 min, filtrated through a 0.2 µm polytetrafluoroethylene membrane filter, and injected into an HPLC system (Waters Alliance 2695, Waters Corporation, Milford, MA, USA).

Phytohormone separation was conducted on a C18 column (Kromasil 100, 5 µm particle size, 100 mm, 2.1 mm, Scharlab, Barcelona, Spain) employing a linear gradient of methanol and ultrapure water supplemented with 0.1% (v/v) acetic acid at a flow rate of 300 mL min^{-1}. Phytohormone quantification was performed in a Quattro LC triple quadrupole mass spectrometer (Micromass, Manchester, United Kingdom) connected online to the output of the column through an orthogonal Z-spray electrospray ion source, after external calibration against authentic standards using Mass Lynx v4.1 software (Waters Corporation, Milford, MA, USA).

2.4. GC-TOF-MS primary metabolite profiling

Primary metabolites were extracted and derivatized following a well-established methanol/chloroform extraction protocol as described in Lisec *et al*. (2006). Metabolites were extracted from 100 mg of plant shoot tissues (FW) by adding 1 400 µL of 100% methanol containing ribitol (0.2 mg mL^{-1} in water) as internal standard (IS). After incubation for 15 min at 950 rpm and 70 °C, samples were centrifuged for 10 min at 11 000 g and 25 °C, after which the supernatant was transferred to a glass vial where 750 µL of chloroform and 1 500 µL of distilled water were added. The resulting mixture was vortex-mixed for 15 sec and centrifuged for 15 min at 2 200 g and 25 °C. A total of 150 µL of the upper phase (polar phase) of each sample were evaporated to dryness using a vacuum concentrator (Vacufuge Plus, Eppendorf, Germany) for 3 hours at 30 °C. Primary metabolites were derivatized and analysed using gas chromatography time of flight mass spectrometry (GC-TOF-MS), as previously described by Lisec *et al*. (2006). Biological variations were controlled by analysing quality control (QC) standards using fatty acid methyl esters internal standard markers and a QC standard solution of 41 pure reference compounds (i.e., the most detected and abundant metabolites) throughout the analysis. Files obtained after GC-TOF-MS analysis (in .cdf format) were subsequently evaluated using the Automated Mass Spectral Deconvolution and Identification System software (AMDIS v 2.71; National Institute of Standards and Technology NIST, Boulder, CO, United States). Primary metabolites were annotated using the TagFinder software (Luedemann *et al.*, 2008) and a reference library of ambient mass spectra and retention indices from the Golm Metabolome Database (http://gmd.mpimp-golm.mpg.de/) (Kopka *et al.*, 2005; Schauer *et al.*, 2005). The relative abundance of primary metabolite levels was normalized taking into consideration the IS (ribitol) and the FW of the samples, and their fold-change in Psa-inoculated plants was determined relatively to mock-inoculated ones.

2.5. Whole transcriptome sequencing

Total RNA was extracted from shoot tissues using the RNeasy Plant Mini Kit (QIAGEN, Hilden, Germany), and genomic DNA was removed from each sample using the TURBO DNA-free Kit (Invitrogen, California, USA), using standard manufacturer's instructions. RNA quality was ensured through gel electrophoresis (1% agarose in TAE) and RNA integrity number (RIN, > 8), after which it was submitted to transcriptome sequencing at STAB VIDA, Lda. (Caparica, Portugal). Whole-transcriptome sequencing (RNA-Seq) was performed to a total of 12 RNA libraries, corresponding to the three biological replicates of mock-inoculated and Psa-inoculated *A. chinensis* and *A. arguta* plants. Library construction of cDNA molecules was carried out using the Kapa Stranded mRNA Library Preparation Kit, and the generated DNA fragments were sequenced in the Illumina Hiseq 4 000 platform, using 150 bp paired-end sequencing reads (Illumina, California, USA). The analysis of the generated sequence raw data was carried out using CLC Genomics Workbench version 12.0.1 (Qiagen, Hilden, Germany). High quality data was ensured by trimming the obtained raw sequences through the removal of sequence regions outside the limit threshold regarding their: quality (0.01 error probability), ambiguity (2 nucleotides) and length (minimum of 15 nucleotides per read). The resulting sequencing reads were *de novo* assembled using Trinity (Broad Institute, Massachusetts, USA) with default settings for pair-end Illumina reads and a custom script to get the longest isoform of each assembled transcript.

2.6. GO enrichment and differential gene expression analysis

Contigs were aligned using BLASTX against the Swiss-Prot database and annotated with Blast2GO 5.0 (BioBam Bioinformatics, Valencia, Spain) using an E-value threshold of 10^{-3}, and mapped against the *de novo* assembled transcriptome if: i) at least 80% of the alignment matched the reference sequence before mapping, and ii) the identity percentage between the aligned region of the read and the reference was higher than 80%. After mapping, gene expression was calculated and normalized using the Reads Per kb per Million reads (RPKM) method, calculated taking into consideration the total number of reads from a particular gene, the length (kb) of that gene, and the number of total mapped reads of the transcriptome (in millions) (Mortazavi *et al*., 2008). Differential expression was assessed using a generalized linear model approach based on the multi-factorial EdgeR method (Robinson *et al*., 2010). Differentially expressed genes (DEGs) were filtered according to their fold change (≥ 2 or ≤ -2) and false discovery rate (FDR) *p*-value < 0.05 (van Iterson *et al*., 2010; Raza *et al*., 2012). All DEGs were mapped in the Gene Ontology (GO) database (http://www.geneontology.org), and total gene numbers were calculated for every term recovered from each sub-ontology (biological process, molecular function and cellular

component). Within *A. chinensis* and *A. arguta* transcriptome, differential expression analysis was performed specifically searching for genes related to plant defences, phytohormone regulation and primary metabolism.

2.7. Data and statistical analysis

Statistically significant differences between means concerning Psa endophytic population, phytohormone concentrations and primary metabolite levels were evaluated through analysis of variance (ANOVA) followed by Fisher's LSD test ($p < 0.05$) using GraphPad Prism version 6.0 (GraphPad Software, Inc., California, United States). Heatmap representation of relative gene expression was produced in Multiple Experiment Viewer version 4.9.0 (Dana-Farber Cancer Institute, Boston, USA). False-colour imaging of primary metabolite data was performed in R software (R Core Team 2019) using the "gplots" package (Warnes *et al*., 2020).

3. Results

3.1. Psa endophytic population in shoot tissues

Forty-height hours after inoculation, the density of Psa endophytic population in *A. chinensis* shoot tissues was 27.8 ± 8.0 x 10^4 CFU g^{-1}, i.e., 10.3-fold higher than in *A. arguta* (with only 2.7 ± 0.3 x 10^4 CFU g^{-1}) (Fig. 1).

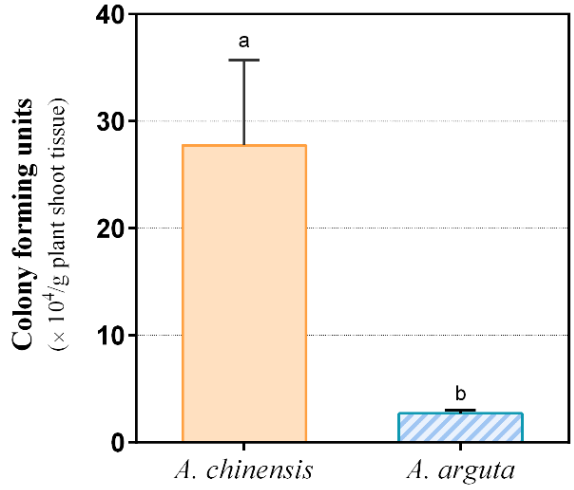

Figure 1 - Colony-forming units (x 10^4 per gram of fresh plant tissue) in *A. chinensis* and *A. arguta* shoot tissues, 48 hours post-inoculation with *P. syringae* pv. *actinidiae*. Data are presented as means ± standard error of the mean of three independent replicates. Different letters indicate significant differences calculated using One-way ANOVA ($p < 0.05$).

3.2. Phytohormone composition

In *A. chinensis*, Psa inoculation led to a significant increase of the absolute concentrations of SA and JA in plant shoots (2.0- and 3.2-fold, respectively), whereas no alteration regarding these phytohormones was observed in *A. arguta* (when compared with mock-inoculated plants) (Fig. 2). Contrastingly, Psa infection led to a significant decrease of the absolute concentration of ABA in *A. arguta*, from 169 ± 3 ng g^{-1} to 53 ± 20 ng g^{-1} (i.e., 0.7-fold), while no changes occurred in *A. chinensis*.

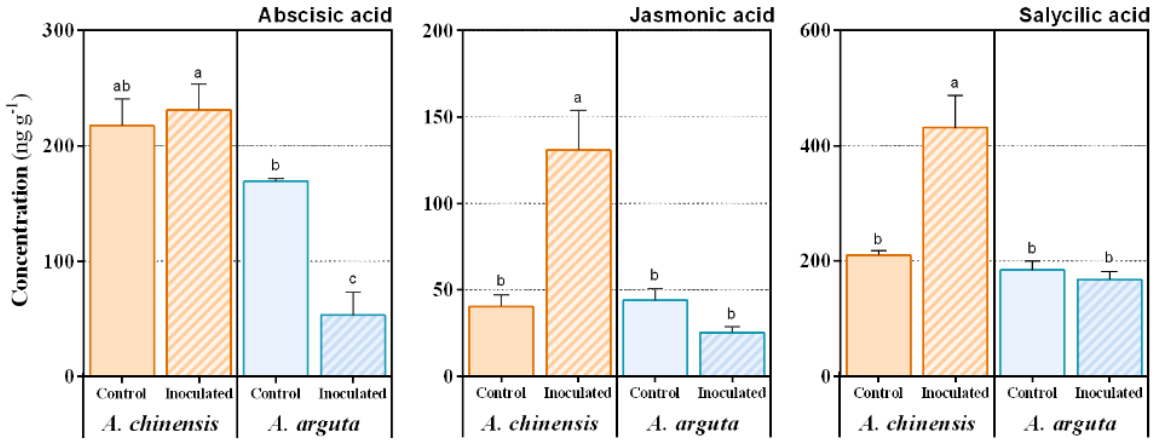

Figure 2 - Abscisic acid, jasmonic acid and salicylic acid concentrations in *A. chinensis* and *A. arguta* shoot tissues, 48 hours post mock-inoculation (Control) or inoculation with *P. syringae* pv. *actinidiae* (Inoculated). Data are presented as means ± standard error of the mean of three independent replicates. Different letters indicate significant differences calculated using Two-way ANOVA ($p < 0.05$).

3.3. Primary metabolism

A total of 32 primary metabolites were identified in plant shoot tissues, namely: i) amino acids and derivatives: alanine, asparagine, aspartate, cystine, glutamine, glycine, isoleucine, ornithine, proline, putrescine, pyroglutamate, serine, threonine and valine; ii) organic acids: 2-oxo-glutarate, fumarate, glycerate, malate, succinate and threonate; iii) sugars: fructose, fucose, galactinol, glucose, *myo*-inositol, raffinose, rhamnose, sucrose and trehalose; and iv) nicotinate, phosphoric acid and urea. Primary metabolite profiling revealed that Psa infection significantly increased the levels of glutamine and ornithine (1.3-fold and 1.5-fold, respectively) in *A. chinensis*, whereas in *A. arguta* no significant differences were found (Fig. 3, Supplementary Material 1). The accumulation of the remaining metabolites identified was not statistically different between mock- and Psa-inoculated plants. However, a general trend for their increase in Psa-infected *A. chinensis* plants was observed, namely concerning, i) amino acids: alanine, asparagine, aspartate, cystine, glycine, isoleucine, proline, putrescine, serine, threonine and valine (from 1.5- up to 2.3-fold); ii) organic acids: succinate, threonate and glycerate (from 1.5- up to 2.0-fold); and iii) sugars: fructose, galactinol and trehalose (up to 1.8-fold).

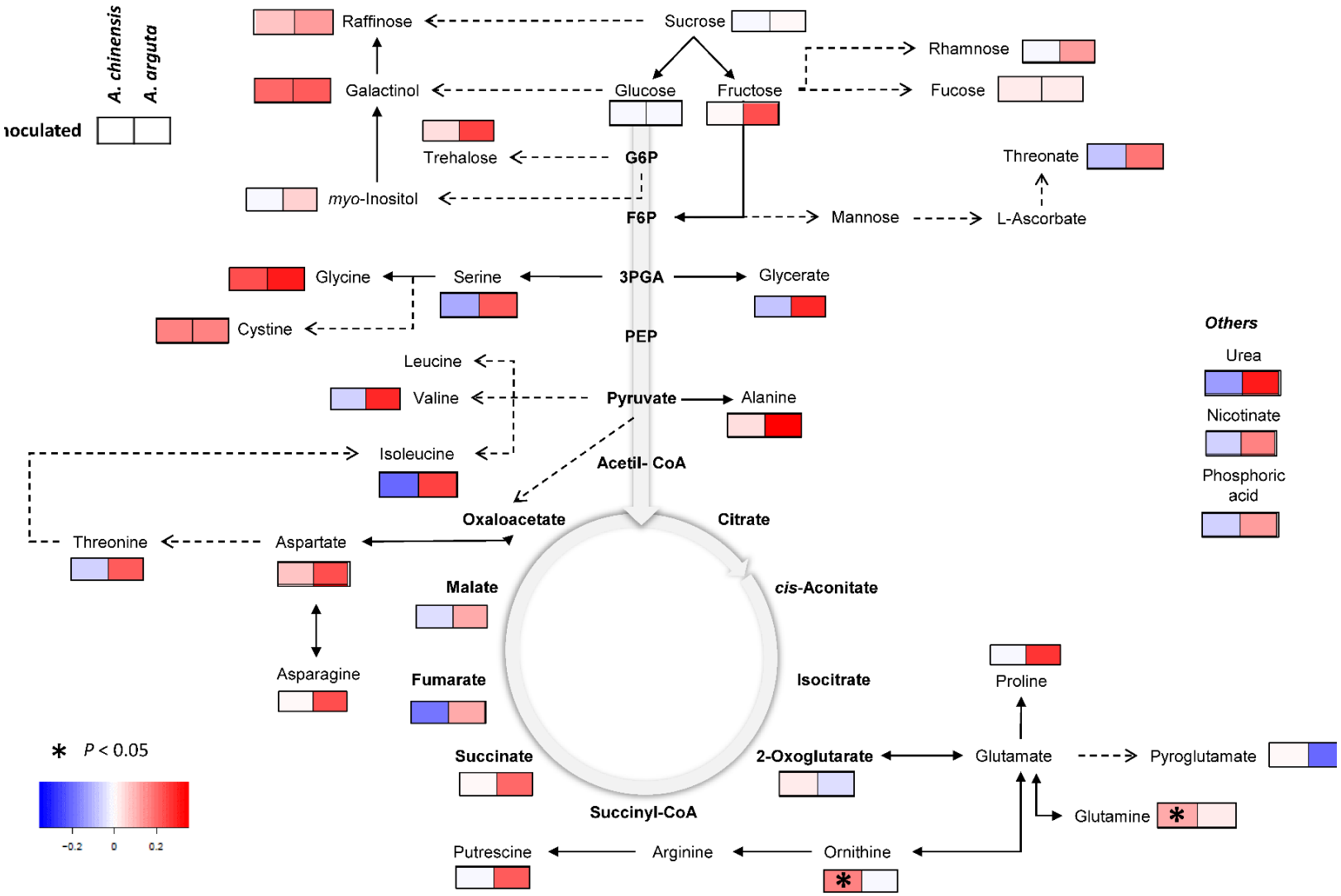

Figure 3 - Metabolic pathway reflecting changes in the levels of primary metabolites in *A. chinensis* and *A. arguta* shoot tissues, 48 hours post-inoculation with *P. syringae* pv. *actinidiae*, in relation to mock-inoculated plants. Relative values were normalized to the internal standard (ribitol) and the fresh weight of samples. The black asterisks indicate significant differences calculated using One-way ANOVA ($p < 0.05$). False-colour imaging was performed on Log_{10}-transformed GC-TOF-MS data.

3.4. Functional classification of differentially expressed genes

The assembly of *A. chinensis* transcriptome revealed a total of 145 122 contigs, of which 44 204 had at least 1 hit against Swiss-Prot, and 25 123 Blast2GO annotations with assigned Gene Ontology (GO) terms (Fig. 4). For *A. arguta*, a total of 112 850 contigs were retrieved, of which 36 956 showed at least 1 hit against Swiss-Prot, and 31 763 had Blast2GO annotation. *A. chinensis* and *A. arguta* had in common 9 330 identified genes, out of 12 315 and 13 256, respectively, and 380 of them were differentially expressed in both plant species after inoculation with Psa (out of 1 514 and 730, respectively) (Fig. 4).

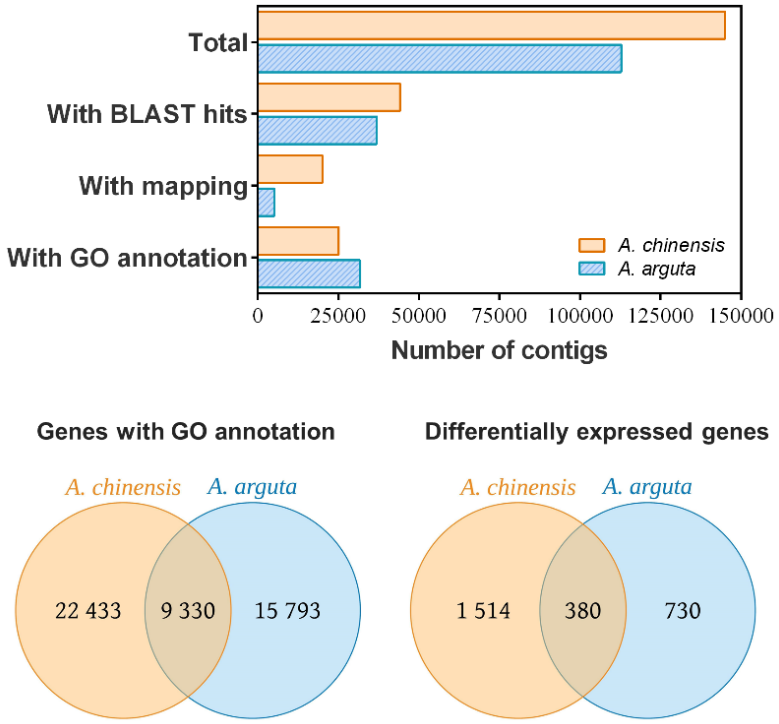

Figure 4 - Total number of contigs and number of contigs with BLAST hits, mapping and GO annotation detected following *de novo* transcriptome assembly of *Actinidia chinensis* and *A. arguta*, number of singular and common genes with GO annotation, and differentially expressed genes 48 hours post-inoculation with *Pseudomonas syringae* pv. *actinidiae*.

To understand the functional activity of the DEGs found in *A. arguta* and *A. chinensis* transcriptome, GO enrichment analysis was performed to identify differently represented GOs (i.e., GOs with the higher number of DEGs). For this, within each plant species, DEGs were categorized according to their sub-ontology (biological process, molecular process or cellular component) and functional group. Within each functional group, the number of up- or downregulated genes was retrieved (Fig. 5, coloured bars) as well as their relative

abundance within all up- and downregulated genes from that sub-ontology (Fig. 5, grey bars). According to this analysis, in both *A. chinensis* and *A. arguta* the biological functions with the higher number of DEGs were associated with regulatory, metabolic and other biological processes (e.g., photoperiodism), response to abiotic stimulus, and plant growth and development (Fig. 5, pink bars). The cellular components with the higher number of DEGs were plastids, other cellular and subcellular components (e.g., cell projections), membranes, macromolecules or macromolecular complexes and cytoplasm (Fig. 5, blue bars). The molecular functions more affected by Psa infection were related to binding, catalytic and transporter activities (Fig. 5, green bars).

3.5. Differential gene expression

To identify specific genes associated with plant defences, hormone regulation and primary metabolism, the FPKM value of each differentially-expressed transcript with homology to GO annotated genes related to these biological functions was investigated (Supplementary Material 2).

3.5.1. Plant defence

Analysis of *A. chinensis* and *A. arguta* transcriptome revealed a total of 89 DEGs with GO annotations related with i) pathogen recognition (*TGA1* and *TGA2*); ii) PPRs (*FLS2* and *RLP30*); iii) PTI and ETI (*BIG5*, *CERK1*, *GFS12*, *PSL5*, *PTI5* and *PTI6*); iv) general defence response (*EIN2*, *EIN3*, *FOX1*, *GLOX*, *M2K2*, *PDR1*, *PLDDELTA*, *HSP70-1*, *NRPE1*, *PIE1*, *PRT6*, *SOBIR1*, *UBA2C* and *SN2*); v) defence response to bacterium (*ABCG14*, *AGD5*, *LECRK42*, *CSP41B*, *UPF3*, *PLDBETA1* and *UPF1*), oomycetes (*MORC7*), insects (*LIP2*) and virus (*DCL4*, *RDR1*, *AGO1*, *AGO4*, *AGO5* and *NIK1*); vi) general disease resistance (*LECRK91*, *LRK10L-2.6*, *LECRKS4*, *RAP2-2* and *EDM2*); vii) disease resistance (R) proteins (*N*, *RFL1*, *TAO1*, *R1B-17*, *RGA3*, *RPM1*, *RPP13*, *RPP13L* and *RGA1*); viii) HR and SAR (*HSR4*, *PLP2*, *SHM1* and *DIR1*); ix) innate immunity (*AGO2*, *RPN1A*, *UGGT*, *ROS1*, *At1g74360*, *CES101*, *PRP19A* and *TPR1*); x) pathogen-induced ROS scavenging (*At4g20830*, *PER1*, *PER3*, *PER4*, *PER27*, *PER43*, *PER44*, *PER52* and *RBOHA*), xi) pathogen-induced lipoxygenase (*LOX1.1*, *LOX1.5* and *LOX2.1*) and cellulose pathways (*CESA3* and *CESA8*); and xii) defence regulation (*BON2*, *FAAH*, *TGA21*, *SRFR1*, *CBP60A*, *CDC48A*, *LSD1*, *PUB13*, *PUB24* and *NTL9*). Among these, 29 genes were upregulated both in *A. chinensis* and *A. arguta* (*AGO1, AGO2, AGO5, CDC48A, CESA3, DCL4, EIN2, EIN3, FLS2, GFS12, LECRK91, LRK10L-2.6, MORC7, N, PDR1, PER1, PER4, PLDBETA1, PLDDELTA, PLP2, PSL5, RDR1, RFL1, RPM1, RPN1A, RPP13, TAO1, UGGT* and *UPF1*).

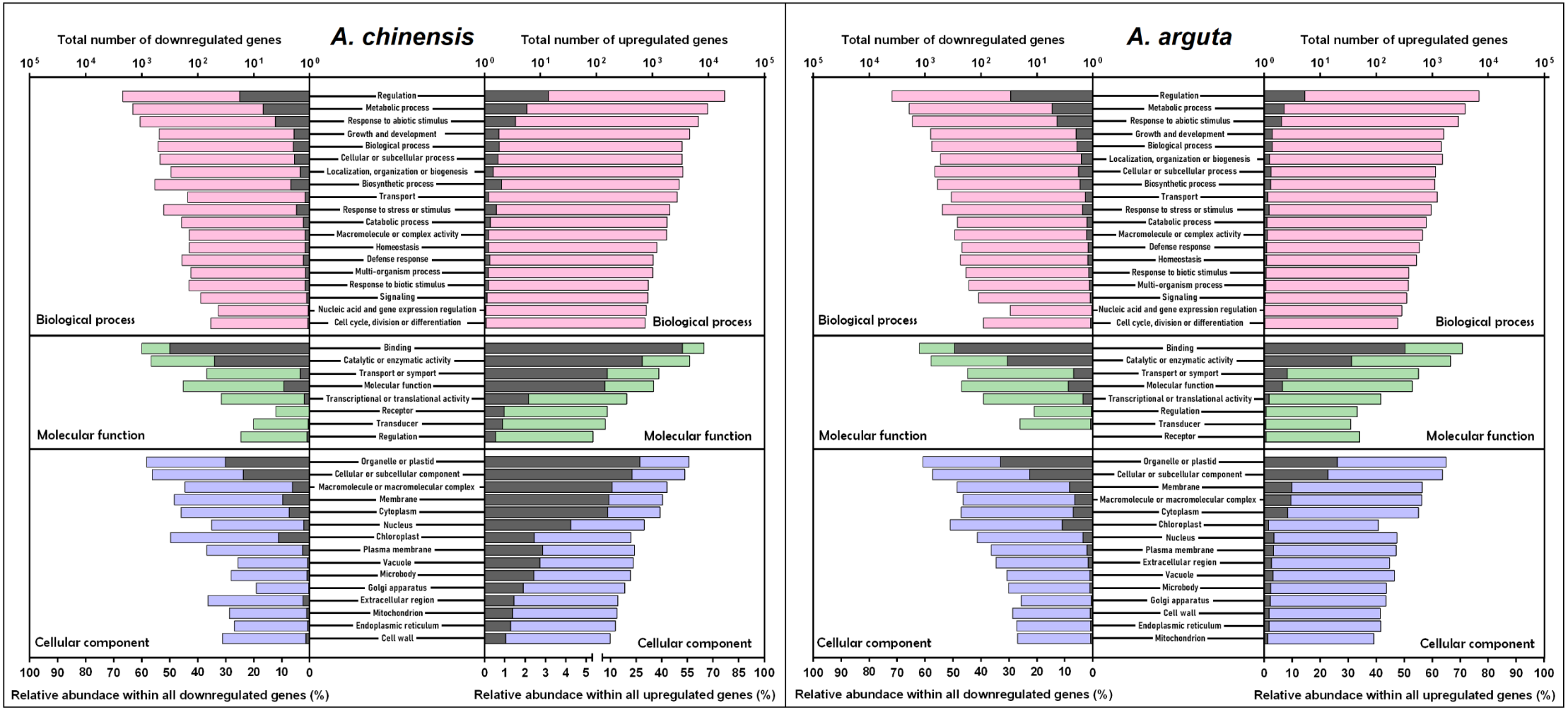

Figure 5 - Gene Ontology (GO) classification and differential expression of genes identified in *A. chinensis* and *A. arguta*, 48 hours post-inoculation with *P. syringae* pv. *actinidiae*, as compared with mock-inoculated plants. Within each GO type (biological process, molecular function or cellular component), processes are classified from the most to the less differentially represented. Coloured bars show the total number of genes differentially regulated (downregulated: left; upregulated: right), whereas the grey bars represent their relative abundance within all down- or upregulated genes from that GO type.

Also, several genes were only differently regulated in one of the plant species. Thirty-three genes were significantly upregulated following Psa infection only in *A. chinensis* (*ABCG14, AGD5, AGO4, At1g74360, BON2, CBP60A, CERK1, CES101, CESA8, FAAH, HSP70-1, HSR4, LECRK42, LECRKS4, LOX1.1, M2K2, NIK1, NTL9, PIE1, PRP19A, PRT6, PTI5, PUB13, R1B-17, RAP2-2, RGA3, RLP30, ROS1, SHM1, SOBIR1, TGA1, UBA2C* and *UPF3*), whereas 4 were downregulated (*CSP41B, LOX2.1, LSD1* and *PER44*).

Genes differently regulated in *A. arguta*, either with no changes or with opposite behaviour in *A. chinensis*, were regarded as potential candidates for increased tolerance to Psa (Fig. 6). These include: i) 18 genes only significantly upregulated in *A. arguta* (*At4g20830, BIG5, DIR1, EDM2, GLOX, NRPE1, PER3, PER27, PER52, PUB24, RBOHA, RGA1, RPP13L, SN2, SRFR1, TGA2, TGA21* and *TPR1*); ii) two genes only significantly downregulated in *A. arguta* (*PTI6* and *PER43*); iii) two genes significantly upregulated in *A. arguta*, but downregulated in *A. chinensis* (*LOX1.5* and *FOX1*); and iv) *LIP2*, which was upregulated in *A. chinensis,* but downregulated in *A. arguta*.

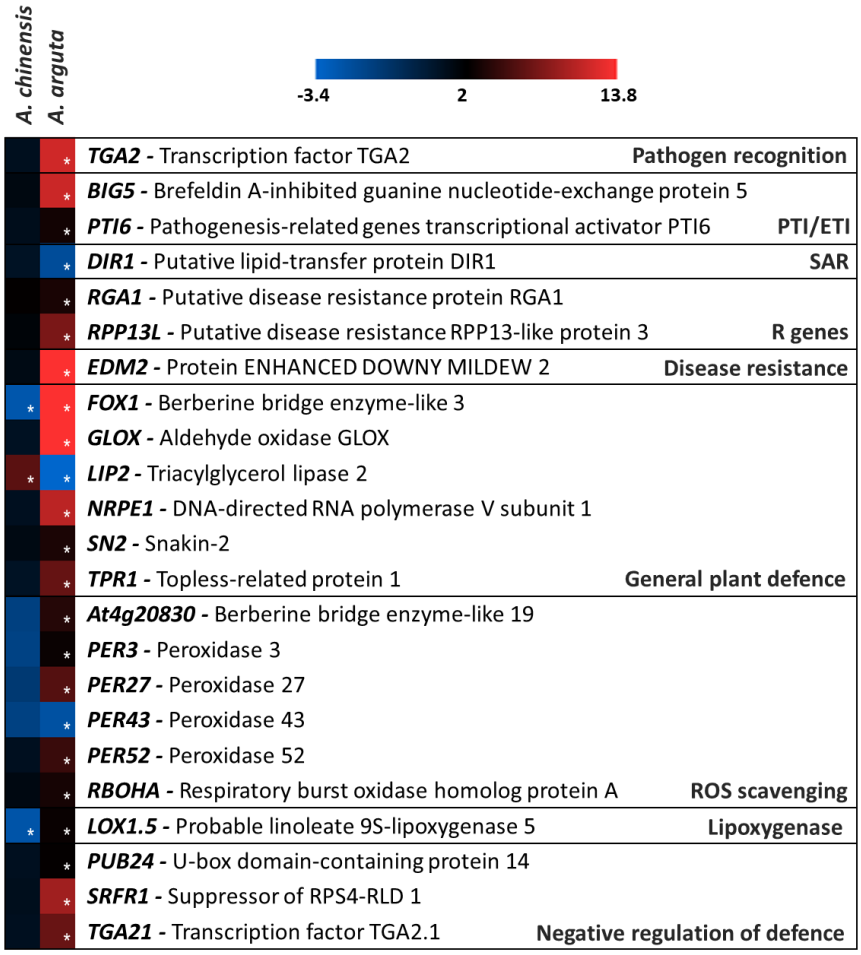

Figure 6 - Heatmap of the fold of expression of statistically significant differentially expressed genes related to plant defence in *A. chinensis* and *A. arguta* plants, 48 hours post-inoculation with *P. syringae* pv. *actinidiae* (Psa, relatively to mock-inoculated plants). White asterisks indicate significant differences between Psa-inoculated and mock-inoculated plants, calculated using false discovery rate (p-value < 0.05). In blue: no alteration or downregulation of gene expression; in black and red: upregulation of gene expression.

3.5.2. Hormonal regulation

A total of 34 DEGs involved in the ABA, JA and SA pathways were identified among the two plant species (Fig. 7, Supplementary Material 2). From these, 16 DEGs were associated with ABA biosynthesis, catabolism, reception, transport, and ABA-mediated defences and signalling (Fig. 7). In *A. chinensis*, several DEGs participating in: i) ABA transport (*ABCG25* and *ABCG31*), ii) ABA-mediated defences (KEG) and, iii) ABA-mediated signalling (*ABCC5*, *ANN4*, *IP5P2*, *KPNB1*, *MIF1*, *ASPG2* and *HAT22*) were upregulated. On the contrary, genes *NCED1* (ABA biosynthetic process) and *CYP707A1*(ABA catabolic process) were downregulated. In *A. arguta*, DEGs related to ABA biosynthetic processes were also downregulated (*NCED1* and *ZEP*), and the ones involved with ABA catabolic processes (*CYP707A1* and *CYP707A3*) and ABA receptors (*PYL4* and *PYL5*) were significantly upregulated. Concerning JA, 8 DEGs involved in JA biosynthesis and JA-mediated defences and signalling were identified within *A. chinensis* and *A. arguta* transcriptomes (Fig. 7). Among these, 5 were only upregulated in *A. chinensis* (*PTR6*, *COI1*, *LRR-RLK*, *UBP13* and *RGS1*), *PLA1* was only upregulated in *A. arguta*, and *SYD* and *UBP12* were upregulated in both plant species. Regarding SA, 10 DEGs related to its biosynthesis, catabolic processes and mediated defences were found both in *A. chinensis* and *A. arguta* (Fig. 7). Gene *SABP2* (SA biosynthetic process) was significantly downregulated in *A. arguta*, whereas no change was observed in *A. chinensis*. Among genes related to SA catabolic processes, *At1g06620* was upregulated in both plant species, whereas *DLO2* was only upregulated in *A. chinensis* and *DLO1* in *A. arguta*. A higher number of genes involved in SA-mediated plant defences were significantly upregulated in *A. chinensis* (*CALS12*, *ACA11*, *ACA4*, *ALD1*, *SIZ1* and *MKP1*), as compared with *A. arguta* (in which only *CALS12* was upregulated).

3.5.3. Primary metabolism

The expression of several genes related to the primary metabolites previously identified through GC-TOF-MS was also significantly affected by Psa infection, particularly in *A. chinensis* (Fig. 8, Supplementary Material 2). This species had a higher number of upregulated genes involved in: i) sucrose metabolism and transport (*SUS2*, *CINV1*, *INVB*, *SUT* and *SUT2*); ii) acetyl coenzyme A catabolism, biosynthesis and metabolism (*ACC1*, *AAT1*, *LPD1*, *ACLA-1*, *ACLB-1* and *ACLB-2*); iii) L-serine biosynthesis and L-serine/glycine interconversion (*PGDH1*, *PGDH3*, *PSAT1*, *SHM1*, *SHM6* and *SHM7*); iv) the aspartate-family pathway (*AK2*, *MSL1.19*, *THA1* and *ALS1*), v) the TCA cycle (*ACO1*, *ACO2*, *ME1*, *MODA*, *MAOM* , *ALMT12*, *PPC16* and *PPCC*); and vi) the ammonia assimilation cycle (*DIT1*, *ogdh*, *CARB*, *GAD1*, *GAD4*, *GLSN* and *GLT1*). In *A. arguta*, only genes *SUS2*, *ACC1*, *ACO2*, *ME1* and *GLT1*, *GLU1* and *GLN1* were significantly upregulated, whereas *ASN1* and *ALM13* were downregulated.

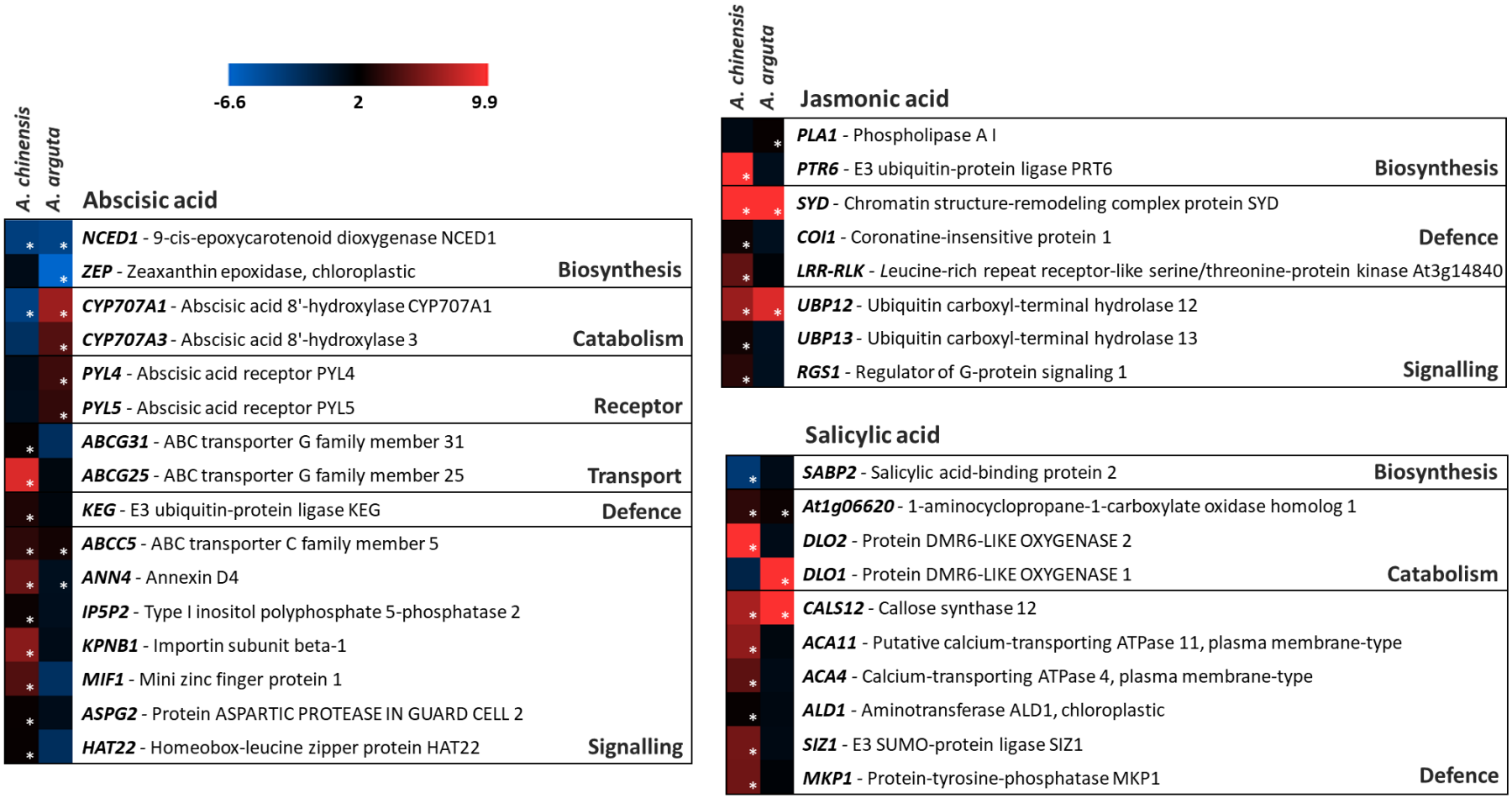

Figure 7 - Heatmap of the fold of expression of statistically significant differentially expressed genes related with the abscisic acid, jasmonic acid and salicylic acid pathways identified in *A. chinensis* and *A. arguta* plants, 48 hours post-inoculation with *P. syringae* pv. *actinidiae* (Psa, relatively to mock-inoculated plants). White asterisks indicate significant differences between Psa-inoculated and mock-inoculated plants, calculated using false discovery rate (p-value < 0.05). In blue: no alteration or downregulation of gene expression; in black and red: upregulation of gene expression.

DEGs involved in *myo*-inositol, galactinol and raffinose metabolism were mostly downregulated in both plant species (*MIOX1*, *GOLS2* and *GOLS4* in *A. chinensis*, and *IPS1*, *GOLS2*, *RFS2* and *STS1* in *A. arguta*) (Fig. 8). Similarly, DEGs involved in glucose metabolism were generally downregulated in both *A. chinensis* and *A. arguta* (*FBA*, *FBA1* and *FBA2* in the first species, and *FBA* and *FBA2* in the latter). Oppositely, DEGs involved in the downstream steps of glycolysis were generally upregulated (*G6PD6*, *PGI1*, *GAPC*, *GAPC2*, *GAPCP2*, *PGAM-I*, *OsI_37456* and *PPT2* in *A. chinensis*, and *GAPC*, *GAPC2*, *GAPCP2* and *OsI_37456* in *A. arguta*).

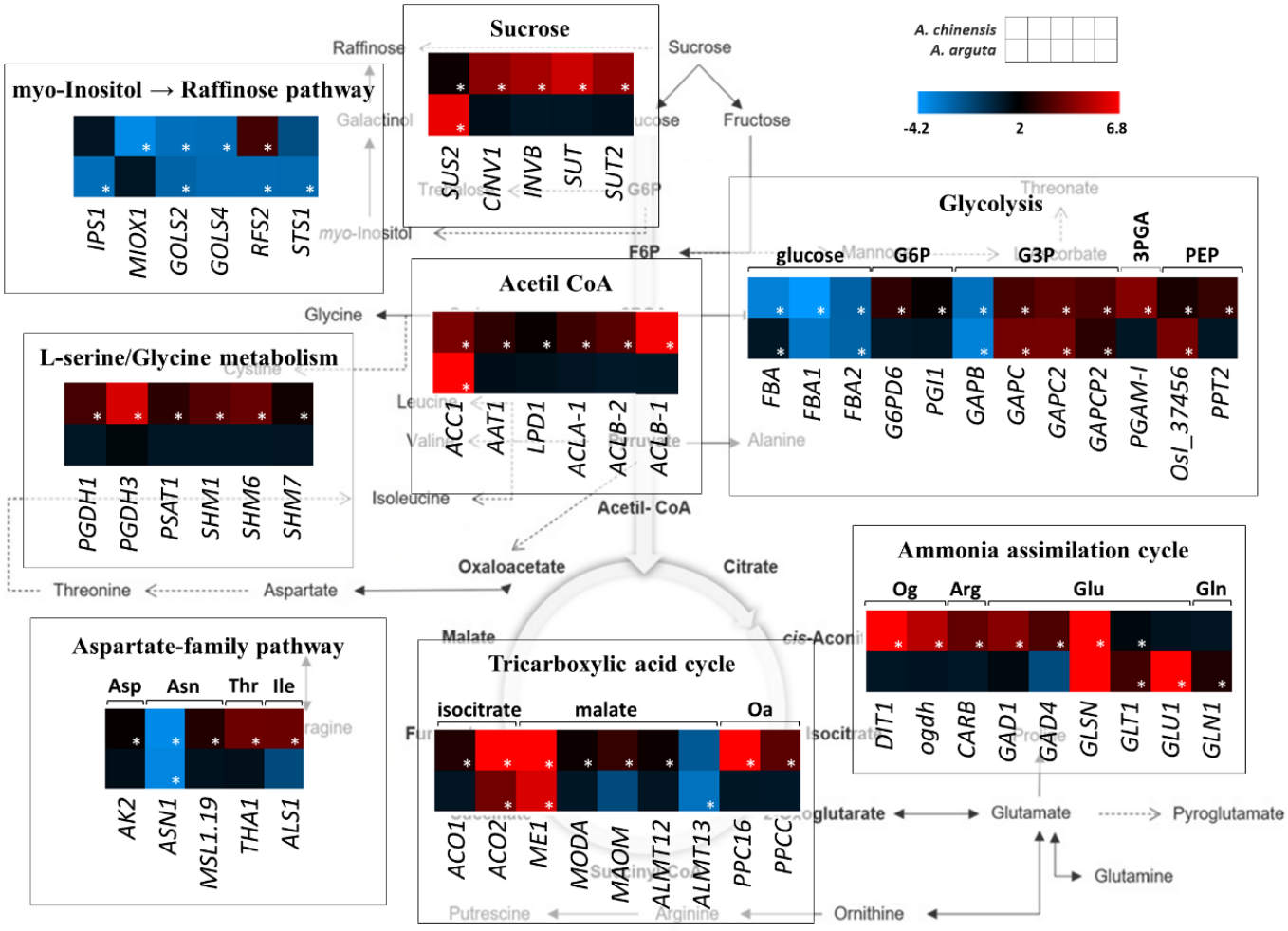

Figure 8 - Heatmap of the fold of expression of statistically significant differentially expressed genes related to primary metabolism identified in *A. chinensis* and *A. arguta* plants, 48 hours post-inoculation with *P. syringae* pv. *actinidiae* (Psa, relatively to mock-inoculated plants). White asterisks indicate significant differences between Psa-inoculated and mock-inoculated plants, calculated using false discovery rate (p-value < 0.05). In blue: no alteration or downregulation of gene expression; in black and red: upregulation of gene expression. Abbreviations: Acetyl-CoA - acetyl coenzyme A; G6P - glucose 6-phosphate; glyceraldehyde 3-phosphate; 3PGA - 3-phosphoglyceric acid; PEP - phosphoenolpyruvic acid; Asp - aspartic acid; Asn - asparagine; Thr - threonine; Ile - isoleucine; Og - oxoglutarate; Arg - arginine; Glu - glutamic acid; Gln - glutamine.

4. Discussion

4.1. Psa infection differently regulates defence-related pathways in *A. chinensis* and *A. arguta*

Several studies aiming at understanding the crosstalk between Psa and *Actinidia* spp. have demonstrated that the expression of numerous plant genes encoding different defence-related pathways is induced in the first hours after infection, including: i) pathogen recognition, e.g. *CC-NBS-LRR*, *FLS2* and *pto3*; ii) PTI and ETI, e.g. *Pti1*, *Pti4* and *CERK1*; iii) disease resistance, e.g. *RPM1*, *RPS2*, *RPP13* and *RIN4;* iv) general plant defences, e.g. *EIN2*, *PR1*, *PR8*, *PR5* and *TLP1*; v) ROS scavenging, e.g. *APX*, *CAT*, *CXXS1* and *SOD*; and vi) signalling, e.g. *WRKY25* and *WRKY29* (Cellini *et al*., 2014; Wurms *et al*., 2017a; Wurms *et al*., 2017b; Wang *et al*., 2018a; Tahir *et al*., 2019; Nunes da Silva *et al*., 2020; Sun *et al*., 2020). In the present work, Psa endophytic population was significantly higher in *A. chinensis* than in *A. arguta* (Fig. 1), corroborating recent findings that attest the higher tolerance of the latter species (Nunes da Silva *et al*., 2020). To unravel the molecular mechanisms underpinning the contrasting susceptibility of *A. chinensis* and *A. arguta* to Psa, whole-transcriptome sequencing was performed. Transcriptome analysis revealed the differential expression of 89 genes related with: pathogen recognition, PPRs, PTI and ETI, general plant defence and defence response to pests and pathogens, disease resistance, HR, SAR, innate immunity, pathogen-induced ROS scavenging, lipoxygenase and cellulose pathways, and defence regulation (Supplementary Material 2). In agreement with previous reports, an upregulation of the genes *FLS2*, *RPM1*, and *RPP13* after infection of both *A. chinensis* and *A. arguta*, and of gene *CERK1* in *A. chinensis* were observed in the present study. Further, several plant genes previously described for other pathosystems were also differently regulated in *A. chinensis* and *A. arguta*. These include *GFS12* and *PSL5*, previously implicated in PTI and ETI activation in *Arabidopsis thaliana* (Lu *et al*., 2009; Teh *et al*., 2015), *PLDDELTA* and *PLDBETA1*, which encode phospholipases involved in basal defence and non-host resistance against bacterial and fungal pathogens (Pinosa *et al*., 2013; Zhao *et al*., 2013), *AGO1*, *AGO5*, *DCL4* and *RDR1*, related to antiviral RNA silencing (Qu *et al*., 2008), and several R-proteins (*N*, *RFL1*, *TAO1*, *RPM1*, *RPP13*), which contribute to disease resistance induced by e.g. type III effectors from *Pseudomonas syringae* spp. (Eitas *et al*., 2008).

To better understand the contrasting susceptibility of the plant genotypes used in this study, genes only differently regulated in the tolerant *A. arguta* or with opposite regulation between the two species were investigated (Fig. 6). These include genes related with: i) pathogen recognition (*TGA2*); ii) PTI and ETI (*BIG5* and *PTI6*); iii) SAR (*DIR1*); iv) R-genes (*RGA1*, *RPP13L*); v) disease resistance (*EDM2*); vi) general plant defence (*FOX1*, *GLOX*,

LIP2, *NRPE1* and *SN2*); vii) innate immunity (*TPR1*); viii) pathogen-induced ROS scavenging (*At4g20830*, *PER3*, *PER27*, *PER43*, *PER52* and *RBOHA*), ix) pathogen-induced lipoxygenase activity (*LOX1.5*) and x) negative regulation of plant defences (*PUB24*, *SRFR1*and *TGA21*). In *A. thaliana*, *TGA2* is required to induce SAR through the regulation of pathogenesis-related genes expression, whereas *EDM2* is essential for disease resistance against the pathogen *Hyaloperonospora arabidopsidis* (Johnson *et al*., 2003; Eulgem *et al*., 2007). Previous studies have also shown that general plant defence mechanisms are controlled by *FOX1*, which encodes an important oxidoreductase involved in *A. thaliana* defences against *P. syringae* (Rajniak *et al*., 2015), and *GLOX*, which confers disease resistance against the grapevine powdery mildew (Guan *et al*., 2010). In addition, *SN2* encodes an antimicrobial peptide that has shown high antimicrobial activity against both Gram-positive and Gram-negative bacteria in potato (Berrocal-Lobo *et al*., 2002), suggesting that the upregulation of this gene in *A. arguta* might contribute to the lower Psa colonization observed. In *A. chinensis* only the expression of *PER1*, *PER4* and *PER44*, responsible for the removal of H_2O_2 in response to environmental stresses such pathogen attack (Yoshioka *et al*., 2001), were significantly affected by Psa infection, whereas in *A. arguta* a higher number of genes involved in ROS scavenging in response to pathogen infection were observed. These included *RBOHA*, related to a rapid and transient phase I oxidative burst induced by pathogen infection, and four different peroxidases (*PER3*, *PER27*, *PER43*, *PER52*). This demonstrates that the antioxidant system plays an active role in plant responses to Psa shortly after infection, which is in agreement with previous studies reporting an increase in peroxidase 4 activity and the upregulation of other antioxidant enzyme-encoding genes, such as *SOD*, *APX* and *CAT*, at early stages of Psa infection (Petriccione *et al*., 2014, 2015; Nunes da Silva *et al*., 2019, 2020). However, the mechanisms involved in ROS scavenging seemed to be differently regulated in susceptible and tolerant genotypes, with *A. arguta* showing a more complex antioxidant response, as already hypothesized (Nunes da Silva *et al*., 2020). Upregulation of *FAAH,* a gene involved in the negative regulation of defence responses to bacteria, is known to enhance *A. thaliana* susceptibility to *P. syringae* pv*. tomato* (Kang *et al*., 2008). In the current study, *FAAH* and other genes with similar functions (*BON2*, *CBP60A*, *CDC48A* and *PUB13*), were also upregulated in *A. chinensis*, which may have contributed to its higher susceptibility to Psa infection. Altogether, these results provide novel genomic-based tools which may allow elucidating the mechanisms involved in plant responses to Psa and propel the development of tolerant genotypes through e.g., targeted breeding.

4.2. The ABA pathway is downregulated in *A. arguta*, whereas the JA and SA pathways are upregulated in *A. chinensis*

Here, Psa inoculation led to increased concentrations of JA and SA in *A. chinensis*, but not in *A. arguta* (Fig. 2). Accordingly, transcriptome analysis of *A. chinensis* revealed the upregulation of several genes related with: i) JA-mediated defences (*SYD*, *COI1* and *LRR-RLK*); ii) JA-mediated signalling (*UBP12*, *UBP13* and *RGS1*); iii) SA catabolism (*At1g06620* and *DLO2*); and iv) SA-mediated defences (*CALS12*, *ACA11*, *ACA4*, *ALD1*, *SIZ1* and *MKP1*) (Fig. 7, Supplementary Material 2). Similar findings were obtained by Wurms *et al*. (2017b), with *A. chinensis* showing increased endogenous SA and JA concentration following Psa infection. Previous studies have also demonstrated that *Actinidia* spp. defence responses against Psa are mainly regulated by SA-mediated pathways, whereas the JA-mediated ones negatively affect plant tolerance to the pathogen (Cellini *et al.,* 2014; Collina *et al.,* 2016; de Jong *et al.,* 2019). It has been demonstrated that elicitation of the JA pathway increased disease incidence, most likely due to the suppression of the SA pathway and to the promotion of the stomatal opening, thus facilitating Psa colonization (Bektas and Eulgem 2015; Michelotti *et al.,* 2018). In this study, Psa infection led to increased concentration of both JA and SA, as well as to the upregulation of several genes related to the regulation of these pathways, in *A. chinensis*, but not in the more tolerant *A. arguta*. This demonstrates that phytohormones other than SA may also be key players in plant tolerance to Psa. Previous works have shown that exogenous ABA application to *A. chinensis* increases the extent of Psa-induced disease symptoms (Cellini *et al*., 2014), and in *Nicotiana tabacum* cell cultures ABA downregulates the expression of a β-1,3-glucanase (Rezzonico *et al*., 1998). This protein is involved in carbon utilization, cell-wall organization, and pathogen defence, and was shown to be upregulated upon Psa infection in *A. chinensis* (Petriccione *et al*., 2014). In this study, a lower ABA concentration was observed following Psa infection in the tolerant *A. arguta*, whereas in the susceptible *A. chinensis* no changes in the concentration of this hormone were observed (Fig. 2). Concordantly, in *A. arguta* genes *NCED1* and *ZEP*, related with ABA-biosynthesis (Xiong *et al*., 2002; Ji *et al*., 2014), were downregulated, whereas *CYP707A1* and *CYP707A3*, related to ABA catabolism (Santiago *et al*., 2009) were upregulated (Fig. 7, Supplementary Material 2). ABA is a key regulator of stomatal closure, which acts as a mechanical barrier against several plant pathogens, and has potential implications for the JA (synergism) and SA (antagonism) pathways during infection with Psa (Melotto *et al*., 2006, Cellini *et al*., 2014). Therefore, the downregulation of the ABA pathway in *A. arguta* shortly following infection could be a coping mechanism to regulate plant responses to Psa, and might have a central role in its higher tolerance to the pathogen.

4.3. Psa infection impairs plant primary metabolism, particularly the ammonia-assimilation cycle

It has been demonstrated that Psa infection significantly increased the levels of several amino and organic acids (e.g., alanine, arginine, asparagine, glutamic acid, pyroglutamic acid and 2-oxo-glutarate) in *A. chinensis* tissues, leading to extensive C and N reprogramming in various metabolic pathways (Li *et al*., 2020). In the present study, Psa infection led to a significant increase of ornithine and glutamine levels in the susceptible *A. chinensis*, but not in *A. arguta* (Fig. 3). In agreement with these findings, several genes related to the ammonia-assimilation cycle, which involves not only ornithine and glutamine, but also arginine and glutamic acid (e.g., *DIT1*, *ogdh*, *CARB*, *GAD1*, *GAD4* and *GLT1*), were significantly upregulated following Psa infection, presenting a more dramatic increase in *A. chinensis* (Fig. 8, Supplementary Material 2). A similar result was observed for genes related to the TCA cycle (*ACO1*, *MODA*, *MAOM*, *ALMT13*, *PPC16* and *PPCC*). A general upregulation of genes involved in L-serine biosynthesis and L-serine/glycine interconversion (*PGDH1*, *PGDH3*, *PSAT1*, *SHM1*, *SHM6* and *SHM7*), and aspartate-family pathway (*AK2*, *MSL1.19*, *THA1* and *ALS1*) was also observed in *A. chinensis*, but not in *A. arguta*. Although carbohydrates generally act as signalling molecules and provide energy to support the demanding plant defence mechanisms, it has been proposed that accumulation of sugars might propel Psa colonization in *A. chinensis* (Li *et al*., 2020). Here, the expression of several genes related to sucrose metabolism and transport (*SUS2*, *CINV1*, *INVB*, *SUT* and *SUT2*) were upregulated in *A. chinensis*, whereas genes involved in *myo*-inositol, galactinol and raffinose metabolism were downregulated in both plant species (*MIOX1*, *GOLS2* and *GOLS4* in *A. chinensis*, and *IPS1*, *GOLS2*, *RFS2* and *STS1* in *A. arguta*). Moreover, Psa infection also led to a downregulation of glucose-related genes in both plant species, but genes involved in the downstream steps of glycolysis (particularly pertaining glucose 6-phosphate, glyceraldehyde 3-phosphate, 3-phosphoglyceric acid and phosphoenolpyruvic acid) were mainly upregulated. Similarly, lower levels of *myo*-inositol, sucrose, glucose, galactose, sorbose, idose, psicose and mannose in *A. chinensis* following Psa infection have been reported (Li *et al*., 2020). In addition, a gene encoding a putative beta-galactosidase (*BGAL*) linked to carbohydrate metabolism, was upregulated in moderately tolerant genotypes, but downregulated in highly tolerant ones (Tahir *et al*., 2019). Overall, these results indicate that Psa infection impairs plant primary metabolism to a different extent depending on the degree of plant susceptibility. Furthermore, data suggests that the lower impact of Psa in *A. arguta*'s primary metabolism might not only result from the lower degree of bacterial colonization, but also constitute an important copping mechanism against the pathogen by restricting its access to plant metabolic resources, such as nitrogen and sugars.

5. Conclusion

To the best of our knowledge, this is the first study that performed a comparative analysis of plant transcriptome, phytohormone and metabolic profiling in genotypes with contrasting susceptibility to Psa. Here, in the more susceptible *A. chinensis*, higher bacterial colonization was observed, accompanied by increased concentrations of the phytohormones JA and SA, and higher levels of the amino acids glutamine and ornithine. Contrarily, in *A. arguta*, Psa endophytic population was lower and led to a significant decrease in ABA concentration, no alterations in primary metabolite profiling, and the upregulation of specific genes involved in pathogen recognition, PTI and ETI, disease resistance, SAR, ROS scavenging and defence regulation, which might underpin the higher tolerance of this plant species to Psa. Moreover, several DEGs involved in sugar metabolism, N cycling and the TCA cycle were identified, demonstrating the negative effect of Psa in plant primary metabolism, particularly in the susceptible *A. chinensis*. Taken together, these results provide novel insights on plant regulatory mechanisms against Psa infection, contributing to unravel the higher tolerance of some plant species, such as *A. arguta*, against this pathogen.

Supplementary Material

SM1 - GC-TOF-MS primary metabolite profiling of *Actinidia chinensis* and *A. arguta* shoot tissues, 48 hours post-inoculation with *Pseudomonas syringae pv. actinidiae* or with water (mock-inoculated control plants). Relative values are normalized to the internal standard (ribitol) and fresh weight of the samples. Data are presented as means ± standard error of the mean of three independent measurements. Values in bold-type indicate significant differences calculated using One-way ANOVA ($p < 0.05$) with respect to mock-inoculated control.

Metabolite	*Actinidia chinensis*		*Actinidia arguta*	
	Control	Inoculated	Control	Inoculated
Alanine	1.00 ± 0.065	1.13 ± 0.15	1.00 ± 0.12	2.25 ± 0.48
Asparagine	1.00 ± 0.18	1.01 ± 0.13	1.00 ± 0.23	1.75 ± 1.01
Aspartate	1.00 ± 0.074	1.22 ± 0.065	1.00 ± 0.050	1.74 ± 0.54
Cystine	1.00 ± 0.15	1.46 ± 0.13	1.00 ± 0.13	1.45 ± 0.39
Glutamine	1.00 ± 0.015	**1.32 ± 0.10**	1.00 ± 0.059	1.06 ± 0.0059
Glycine	1.00 ± 0.066	1.75 ± 0.32	1.00 ± 0.13	2.01 ± 0.61
Isoleucine	1.00 ± 0.32	0.63 ± 0.063	1.00 ± 0.072	1.82 ± 0.31
Ornithine	1.00 ± 0.010	**1.46 ± 0.13**	1.00 ± 0.068	0.98 ± 1.12
Proline	1.00 ± 0.083	0.99 ± 0.13	1.00 ± 0.017	1.88 ± 0.62
Putrescine	1.00 ± 0.059	1.00 ± 0.082	1.00 ± 0.14	1.69 ± 0.74
Pyroglutamate	1.00 ± 0.047	1.03 ± 0.065	1.00 ± 0.061	0.63 ± 0.18
Serine	1.00 ± 0.086	0.76 ± 0.069	1.00 ± 0.13	1.67 ± 0.65
Threonine	1.00 ± 0.11	0.86 ± 0.053	1.00 ± 0.046	1.67 ± 0.58
Valine	1.00 ± 0.19	0.88 ± 0.020	1.00 ± 0.024	1.93 ± 0.34
2-oxo-Glutarate	1.00 ± 0.17	1.08 ± 0.12	1.00 ± 0.068	0.89 ± 0.090
Fumarate	1.00 ± 0.15	0.65 ± 0.0072	1.00 ± 0.063	1.31 ± 0.39
Malate	1.00 ± 0.17	0.90 ± 0.043	1.00 ± 0.20	1.28 ± 0.32
Succinate	1.00 ± 0.060	1.03 ± 0.072	1.00 ± 0.13	1.61 ± 0.45
Threonate	1.00 ± 0.16	0.82 ± 0.16	1.00 ± 0.13	1.54 ± 0.47
Glycerate	1.00 ± 0.12	0.82 ± 0.084	1.00 ± 0.059	1.99 ± 0.70
Fructose	1.00 ± 0.081	1.02 ± 0.12	1.00 ± 0.23	1.75 ± 0.68
Fucose	1.00 ± 0.19	1.08 ± 0.089	1.00 ± 0.024	1.06 ± 0.12
Galactinol	1.00 ± 0.052	1.58 ± 0.37	1.00 ± 0.28	1.67 ± 0.62
Glucose	1.00 ± 0.19	0.96 ± 0.15	1.00 ± 0.25	1.00 ± 0.058
myo-Inositol	1.00 ± 0.030	0.97 ± 0.068	1.00 ± 0.13	1.15 ± 0.12
Raffinose	1.00 ± 0.11	1.21 ± 0.36	1.00 ± 0.23	1.35 ± 0.35
Rhamnose	1.00 ± 0.15	0.98 ± 0.14	1.00 ± 0.090	1.36 ± 0.42
Sucrose	1.00 ± 0.068	0.97 ± 0.047	1.00 ± 0.031	1.01 ± 0.061
Trehalose	1.00 ± 0.026	1.09 ± 0.073	1.00 ± 0.15	1.81 ± 0.66
Nicotinate	1.00 ± 0.097	0.86 ± 0.043	1.00 ± 0.033	1.50 ± 0.34
Phosphoric acid	1.00 ± 0.090	0.87 ± 0.12	1.00 ± 0.079	1.34 ± 0.23
Urea	1.00 ± 0.47	0.74 ± 0.17	1.00 ± 0.49	2.06 ± 0.49

SM2 - Fold of expression of differentially expressed transcripts with homology to GO annotated genes encoding biological functions related with plant defence, primary metabolism and hormonal regulation in *Actinidia chinensis* and *A. arguta* shoot tissues, 48 hours post-inoculation with *Pseudomonas syringae* pv. *actinidiae* (relatively to mock-inoculated plants). For each fold of expression, the *p*-value is provided, and statistically significant values between mock- and Psa-inoculated plants are marked in bold.

Gene	Encoded protein	GO Biological Function	*A. chinensis*		*A. arguta*	
			Fold	*p*-value	Fold	*p*-value
Plant-pathogen interaction and defence						
TGA1	Transcription factor TGA1	Pathogen recognition	**7.31**	**0.0084**	1.01	0.9916
TGA2	Transcription factor TGA2		1.20	0.8536	**7.78**	**0.0024**
FLS2	LRR receptor-like serine/threonine-protein kinase FLS2	Pattern-recognition receptor (PPR)	**2.39**	**< 0.0001**	**2.65**	**0.0315**
RLP30	Receptor-like protein 30		**3.29**	**0.0083**	1.09	0.9777
BIG5	Brefeldin A-inhibited guanine nucleotide-exchange protein 5	PAMP-triggered immunity (PTI) and effector-triggered immunity (ETI)	1.56	0.0399	**7.63**	**0.0346**
CERK1	Chitin elicitor receptor kinase 1		**2.49**	**0.0116**	1.14	0.9148
GFS12	Protein GFS12		**4.80**	**0.0322**	**4.42**	**0.0052**
PSL5	Probable glucan 1,3-alpha-glucosidase		**6.38**	**< 0.0001**	**3.55**	**0.0002**
PTI5	Pathogenesis-related genes transcriptional activator PTI5		**2.19**	**0.0366**	1.09	0.9565
PTI6	Pathogenesis-related genes transcriptional activator PTI6		1.04	0.9483	**-2.08**	**0.0047**
EIN2	Ethylene-insensitive protein 2	General plant defence	**7.26**	**0.0004**	**6.59**	**0.0004**
EIN3	Protein ETHYLENE INSENSITIVE 3		**2.40**	**0.0199**	**2.23**	**0.0009**
FOX1	Berberine bridge enzyme-like 3		**-2.58**	**0.0224**	**11.3**	**< 0.0001**
GLOX	Aldehyde oxidase GLOX		1.11	0.9172	**9.33**	**< 0.0001**
M2K2	Mitogen-activated protein kinase kinase 2		**2.16**	**0.0075**	1.67	0.3483
PDR1	Pleiotropic drug resistance protein 1		**2.89**	**0.0304**	**3.97**	**< 0.0001**
PLDDELTA	Phospholipase D delta		**2.81**	**0.0395**	**7.36**	**0.0163**
HSP70-1	Heat shock 70 kDa protein 1		**2.10**	**< 0.0001**	1.04	0.9750
NRPE1	DNA-directed RNA polymerase V subunit 1		1.17	0.5806	**7.23**	**0.0195**
PIE1	Protein PHOTOPERIOD-INDEPENDENT EARLY FLOWERING 1		**4.06**	**0.0067**	1.08	0.9173
PRT6	E3 ubiquitin-protein ligase PRT6		**6.33**	**0.0016**	1.12	0.8533
SOBIR1	Leucine-rich repeat receptor-like serine/threonine/tyrosine-protein kinase SOBIR1		**2.48**	**0.0007**	1.90	0.7029
UBA2C	UBP1-associated protein 2C		**2.20**	**0.0206**	1.17	0.7549
SN2	Snakin-2		1.52	0.2747	**2.77**	**< 0.0001**
ABCG14	ABC transporter G family member 14	Defence response to bacterium	**4.56**	**0.0004**	1.14	0.8946
AGD5	ADP-ribosylation factor GTPase-activating protein AGD5		**2.01**	**0.0402**	1.20	0.7361
LECRK42	L-type lectin-domain containing receptor kinase IV.2		**4.09**	**0.0203**	1.52	0.7070
CSP41B	Chloroplast stem-loop binding protein of 41 kDa b, chloroplastic		**-2.22**	**< 0.0001**	-1.62	0.6029
UPF3	Regulator of nonsense transcripts UPF3		**2.32**	**0.0419**	1.40	0.8824
PLDBETA1	Phospholipase D beta 1		**2.78**	**0.0003**	**2.75**	**0.0090**
UPF1	Regulator of nonsense transcripts 1 homolog		**2.20**	**0.0252**	**4.81**	**< 0.0001**
MORC7	Protein MICRORCHIDIA 7	Defence response to oomycetes	**4.29**	**0.0408**	**3.06**	**0.0034**

LIP2	Triacylglycerol lipase 2	Defence against insects	**4.55**	**0.0018**	**-3.43**	**0.0307**
DCL4	Dicer-like protein 4	Defence response to virus	**3.96**	**0.0011**	**4.71**	**0.0221**
RDR1	RNA-dependent RNA polymerase 1		**2.35**	**0.0067**	**10.1**	**0.0014**
AGO1	Protein argonaute 1		**3.16**	**0.0020**	**2.42**	**0.0006**
AGO4	Protein argonaute 4		**2.23**	**0.0423**	1.37	0.7951
AGO5	Protein argonaute 5		**2.06**	**0.0055**	**2.94**	**0.0262**
NIK1	Protein NSP-INTERACTING KINASE 1		**2.60**	**0.0394**	1.06	0.9867
LECRK91	L-type lectin-domain containing receptor kinase IX.1	Disease resistance	**2.38**	**0.0131**	**2.28**	**0.0121**
LRK10L-2.6	Protein SUPPRESSOR OF NPR1-1 CONSTITUTIVE 4		**3.01**	**0.0111**	**3.54**	**0.0094**
LECRKS4	L-type lectin-domain containing receptor kinase S.4		**3.29**	**0.0239**	1.23	0.8945
RAP2-2	Ethylene-responsive transcription factor RAP2-2		**2.87**	**0.0039**	1.09	0.8984
EDM2	Protein ENHANCED DOWNY MILDEW 2		1.47	0.5364	**13.8**	**0.0076**
N	TMV resistance protein N	Disease resistance (R) protein	**6.95**	**0.0077**	**2.33**	**0.0064**
RFL1	Disease resistance protein RFL1		**5.05**	**0.0007**	**3.13**	**0.0157**
TAO1	Disease resistance protein TAO1		**5.50**	**0.0259**	**2.06**	**0.0145**
R1B-17	Putative late blight resistance protein homolog R1B-17		**2.69**	**0.0324**	1.84	0.6130
RGA3	Putative disease resistance protein RGA3		**3.24**	**0.0359**	1.03	0.9897
RPM1	Disease resistance protein RPM1		**2.72**	**0.0135**	**3.24**	**0.0155**
RPP13	Disease resistance protein RPP13		**2.67**	**0.0025**	**2.45**	**0.0437**
RPP13L	Putative disease resistance RPP13-like protein 3		1.77	0.1203	**5.41**	**0.0376**
RGA1	Putative disease resistance protein RGA1		2.11	0.4436	**2.74**	**0.0109**
HSR4	Protein HYPER-SENSITIVITY-RELATED 4	Hypersensitive response	**2.25**	**0.0179**	1.57	0.5000
PLP2	Patatin-like protein 2		**2.72**	**0.0012**	**3.09**	**< 0.0001**
SHM1	Serine hydroxymethyltransferase 1, mitochondrial		**2.73**	**0.0219**	1.08	0.9527
DIR1	Putative lipid-transfer protein DIR1	Systemic acquired resistance	1.29	0.5326	**2.53**	**0.0180**
AGO2	Protein argonaute 2	Innate immunity	**2.68**	**0.0371**	**3.05**	**< 0.0001**
RPN1A	26S proteasome non-ATPase regulatory subunit 2 homolog A		**4.02**	**0.0004**	**5.17**	**0.0130**
UGGT	UDP-glucose: glycoprotein glucosyltransferase		**5.08**	**0.0005**	**12.7**	**0.0023**
ROS1	DNA glycosylase/AP lyase ROS1		**3.56**	**0.0016**	1.12	0.9751
At1g74360	Probable LRR receptor-like serine/threonine-protein kinase At1g74360		**3.24**	**0.0111**	1.16	0.8747
CES101	G-type lectin S-receptor-like serine/threonine-protein kinase CES101		**2.10**	**0.0259**	1.21	0.9526
PRP19A	Pre-mRNA-processing factor 19 homolog 1		**2.01**	**0.0247**	1.71	0.5914
TPR1	Topless-related protein 1		1.03	0.9594	**4.83**	**0.0037**
4g20830	Berberine bridge enzyme-like 19	ROS scavenging	-1.39	0.5033	**3.06**	**0.0030**
RBOHA	Respiratory burst oxidase homolog protein A		1.55	0.0353	**2.65**	**0.0069**
PER1	Peroxidase 1		**17.0**	**< 0.0001**	**2.31**	**0.0053**
PER27	Peroxidase 27		-1.04	0.9873	**4.38**	**0.0016**
PER3	Peroxidase 3		-1.50	0.8332	**2.31**	**0.0218**
PER4	Peroxidase 4		**2.66**	**0.0003**	**4.19**	**< 0.0001**

PER43	Peroxidase 43		-1.46	0.3765	**-2.30**	**0.0074**
PER44	Peroxidase 44		**-2.45**	**0.0394**	-1.06	0.9441
PER52	Peroxidase 52		1.19	0.7616	**3.60**	**0.0108**
LOX1.1	Linoleate 9S-lipoxygenase 1	Lipoxygenase	**2.86**	**0.0183**	-1.04	0.9837
LOX1.5	Probable linoleate 9S-lipoxygenase 5		**-2.45**	**0.0467**	**2.28**	**< 0.0001**
LOX2.1	Linoleate 13S-lipoxygenase 2-1, chloroplastic		**-2.87**	**< 0.0001**	1.02	0.9932
CESA3	Cellulose synthase A catalytic subunit 3 [UDP-forming]	Cellulose pathway	**3.17**	**0.0031**	**4.02**	**< 0.0001**
CESA8	Cellulose synthase A catalytic subunit 8 [UDP-forming]		**3.41**	**0.0027**	1.01	0.9930
BON2	Protein BONZAI 2	Negative regulation of defence	**2.46**	**0.0440**	1.29	0.7951
FAAH	Fatty acid amide hydrolase		**2.27**	**0.0044**	1.13	0.9609
TGA21	Transcription factor TGA2.1		1.17	0.8536	**4.91**	**0.0024**
SRFR1	Suppressor of RPS4-RLD 1		1.24	0.4377	**6.45**	**0.0236**
CBP60A	Calmodulin-binding protein 60 A		**2.04**	**0.0014**	1.04	0.9777
CDC48A	Cell division control protein 48 homolog A		**2.76**	**0.0036**	2.29	0.3177
LSD1	Protein LSD1		**-2.14**	**0.0068**	-1.05	0.9568
PUB13	U-box domain-containing protein 13		**2.71**	**0.0227**	1.05	0.9514
PUB24	U-box domain-containing protein 14		1.18	0.8954	**2.15**	**0.0392**
NTL9	Protein NTM1-like 9	Positive regulation of defence	**2.16**	**0.0136**	1.39	0.7593
Plant primary metabolism						
IPS1	Inositol-3-phosphate synthase isozyme 1	Myo-inositol biosynthesis	1.18	0.8602	**-2.51**	**< 0.0001**
MIOX1	Inositol oxygenase 1	Myo-inositol degradation	**-3.59**	**0.0002**	1.15	0.9099
GOLS2	Galactinol synthase 2	Galactinol biosynthesis	**-2.59**	**0.0016**	**-2.03**	**0.0129**
GOLS4	Galactinol synthase 4		**-2.44**	**0.0050**	-2.36	0.0758
RFS2	Probable galactinol--sucrose galactosyltransferase 2	Raffinose biosynthesis	**2.59**	**0.0035**	**-2.35**	**0.0002**
STS1	Stachyose synthase	Raffinose catabolism	-1.16	0.6475	**-2.30**	**0.0020**
SUS2	Sucrose synthase 2	Sucrose metabolism	**2.11**	**< 0.0001**	**4.05**	**0.0084**
CINV1	Alkaline/neutral invertase CINV1		**3.21**	**0.0073**	1.46	0.8542
INVB	Probable alkaline/neutral invertase B		**3.44**	**0.0001**	1.08	0.9180
SUT	Sucrose transport protein SUT1	Sucrose transport	**3.77**	**< 0.0001**	1.14	0.8027
SUT2	Sucrose transport protein SUT2		**3.29**	**0.0037**	1.29	0.7743
PGDH1	D-3-phosphoglycerate dehydrogenase 1, chloroplastic	L-serine biosynthesis	**2.60**	**0.0046**	1.05	0.9463
PGDH3	D-3-phosphoglycerate dehydrogenase 3, chloroplastic		**3.87**	**0.0011**	1.73	0.2869
PSAT1	Phosphoserine aminotransferase 1, chloroplastic		**2.38**	**< 0.0001**	1.12	0.8201
SHM1	Serine hydroxy methyltransferase 1, mitochondrial	L-serine/glycine interconversion	**2.73**	**0.0219**	1.08	0.9527
SHM6	Serine hydroxymethyltransferase 6		**2.90**	**0.0068**	1.10	0.9737
SHM7	Serine hydroxymethyltransferase 7		**2.16**	**0.0018**	1.16	0.9465
ACC1	Acetyl-CoA carboxylase 1	Acetyl-coA catabolism	**3.07**	**0.0047**	**6.75**	**< 0.0001**
AAT1	Dihydrolipoyl dehydrogenase 1, chloroplastic		**2.41**	**< 0.0001**	1.45	0.8080

LPD1	Dihydrolipoyl dehydrogenase 1, mitochondrial	Acetyl-coA biosynthesis	**2.08**	**0.0326**	1.32	0.8532
ACLA-1	ATP-citrate synthase alpha chain protein 1	Acetyl-coA metabolism	**2.52**	**< 0.0001**	1.15	0.9237
ACLB-2	ATP-citrate synthase beta chain protein 2		**2.75**	**< 0.0001**	1.02	0.9986
ACLB-1	ATP-citrate synthase beta chain protein 1		**4.12**	**0.0005**	1.06	0.9695
FBA	Fructose-bisphosphate aldolase, cytoplasmic isozyme	Glycolysis and gluconeogenesis	**-3.24**	**< 0.0001**	1.09	0.8940
FBA1	Fructose-bisphosphate aldolase, cytoplasmic isozyme 1		**-4.21**	**0.0326**	**-2.79**	**< 0.0001**
FBA2	Fructose-bisphosphate aldolase 2, chloroplastic		**-1.99**	0.3342	**-2.03**	**< 0.0001**
G6PD6	Glucose-6-phosphate 1-dehydrogenase 6, cytoplasmic	Glucose-6-phosphate catabolism	**2.41**	**0.0315**	1.00	1.0000
PGI1	Glucose-6-phosphate isomerase 1, chloroplastic		**2.08**	**0.0299**	1.13	0.8090
GAPB	Glyceraldehyde-3-phosphate dehydrogenase GAPB, chloroplastic	Glyceraldehyde-3-phosphate catabolism	**-2.62**	**0.0257**	**-3.28**	**0.0016**
GAPC	Glyceraldehyde-3-phosphate dehydrogenase, cytosolic		**2.61**	**< 0.0001**	**3.00**	**< 0.0001**
GAPC2	Glyceraldehyde-3-phosphate dehydrogenase GAPC2, cytosolic		**2.81**	**< 0.0001**	**3.03**	**0.0003**
GAPCP2	Glyceraldehyde-3-phosphate dehydrogenase GAPCP2, chloroplastic		**2.65**	**0.0099**	**2.38**	**0.0497**
PGAM-I	2,3-bisphosphoglycerate-independent phosphoglycerate mutase	3-phosphoglyceric acid biosynthesis	**3.16**	**< 0.0001**	1.11	0.9513
OsI_37456	Pyruvate kinase 2, cytosolic	Phosphoenolpyruvate biosynthesis	**2.22**	**< 0.0001**	**3.03**	**0.0216**
PPT2	Phosphoenolpyruvate/phosphate translocator 2, chloroplastic	Phosphoenolpyruvate transport	**2.46**	**0.0031**	1.13	0.8845
AK2	Aspartokinase 2, chloroplastic	Aspartate-family pathway	**2.07**	**0.0003**	1.44	0.1467
ASN1	Asparagine synthetase [glutamine-hydrolyzing] 1	Asparagine biosynthesis	**-3.67**	**< 0.0001**	**-3.46**	**0.0006**
MSL1.19	Probable isoaspartyl peptidase/L-asparaginase 2	Asparagine catabolism	**2.31**	**0.0228**	1.26	0.6347
THA1	Probable low-specificity L-threonine aldolase 1	Threonine catabolism	**2.95**	**0.0002**	1.38	0.3463
ALS1	Acetolactate synthase 1, chloroplastic	Isoleucine biosynthesis	**2.93**	**0.0002**	-1.03	0.9916
ACO1	Aconitate hydratase 1	Isocitrate biosynthesis	**2.29**	**< 0.0001**	1.19	0.9087
ACO2	Aconitate hydratase 2		**4.33**	**0.0109**	**3.00**	**0.0014**
ME1	NADP-dependent malic enzyme	Malate metabolism	**4.71**	**< 0.0001**	**3.89**	**0.0018**
MODA	NADP-dependent malic enzyme, chloroplastic		**2.11**	**0.0005**	1.11	0.8721
MAOM	NAD-dependent malic enzyme 62 kDa isoform, mitochondrial		**2.46**	**0.0418**	-1.03	0.9761
ALMT12	Aluminum-activated malate transporter 12	Malate transport	-1.62	0.3802	**-2.65**	**0.0029**
ALMT13	Aluminum-activated malate transporter 13		**2.12**	**0.0373**	1.16	0.8974
PPC16	Phosphoenolpyruvate carboxylase, housekeeping isozyme	Oxaloacetate catabolism	**4.26**	**0.0005**	1.12	0.4391
PPCC	Phosphoenolpyruvate carboxylase 2		**2.80**	**0.0003**	1.05	0.9674
DIT1	Dicarboxylate transporter 1, chloroplastic	2-oxoglutarate transport	**4.80**	**0.0008**	1.14	0.9230
ogdh	2-oxoglutarate dehydrogenase, mitochondrial	2-oxoglutarate catabolism	**3.60**	**0.0017**	1.20	0.6886
CARB	Carbamoyl-phosphate synthase large chain, chloroplastic	Arginine biosynthesis	**2.87**	**0.0215**	1.03	0.9925
GAD1	Glutamate decarboxylase 1	Glutamate catabolism	**3.18**	**0.0400**	1.62	0.4476
GAD4	Glutamate decarboxylase 4		**2.67**	**0.0010**	-1.09	0.8974
GLSN	Glutamate synthase [NADH], amyloplastic	Glutamic acid biosynthesis	1.66	0.1580	**2.58**	**0.0473**
GLT1	Glutamate synthase 1 [NADH], chloroplastic		**4.37**	**0.0009**	**4.25**	**0.0229**
GLU1	Ferredoxin-dependent glutamate synthase 1		1.25	0.5994	**6.02**	**< 0.0001**
GLN1	Glutamine synthetase cytosolic isozyme 1-3		1.17	0.6409	**2.28**	**0.0037**

Hormonal regulation						
NCED1	9-cis-epoxycarotenoid dioxygenase NCED1, chloroplastic	Abscisic acid biosynthesis	**-2.09**	**0.0005**	**-2.37**	**0.0143**
ZEP	Zeaxanthin epoxidase, chloroplastic		1.26	0.5613	**-6.61**	**0.0106**
CYP707A1	Abscisic acid 8'-hydroxylase CYP707A1	Abscisic acid catabolism	**-2.21**	**0.0386**	**4.48**	**0.0257**
CYP707A3	Abscisic acid 8'-hydroxylase 3		-1.13	0.8565	**3.33**	**0.0284**
PYL4	Abscisic acid receptor PYL4	Abscisic acid receptor	1.19	0.7539	**2.98**	**0.0003**
PYL5	Abscisic acid receptor PYL5		1.05	0.9386	**2.80**	**0.0009**
ABCG25	ABC transporter G family member 25	Abscisic acid transport	**2.10**	**0.0421**	-1.01	0.9932
ABCG31	ABC transporter G family member 31		**5.49**	**0.0001**	1.56	0.9382
KEG	E3 ubiquitin-protein ligase KEG	Abscisic acid-mediated defences	**2.50**	**0.0184**	**5.95**	**0.0027**
ABCC5	ABC transporter C family member 5	Abscisic acid-mediated signalling	**2.71**	**0.0168**	**2.33**	**0.0357**
ANN4	Annexin D4		**3.65**	**0.0107**	1.02	0.9817
IP5P2	Type I inositol polyphosphate 5-phosphatase 2		**2.19**	**0.0117**	1.06	0.9624
KPNB1	Importin subunit beta-1		**4.17**	**0.0003**	1.27	0.5547
MIF1	Mini zinc finger protein 1		**3.29**	**0.0445**	-1.11	0.9456
ASPG2	Protein ASPARTIC PROTEASE IN GUARD CELL 2		**2.14**	**0.0442**	1.18	0.8600
HAT22	Homeobox-leucine zipper protein HAT22		**2.13**	**0.0212**	-1.00	1.0000
PLA1	Phospholipase A I	Jasmonic acid biosynthesis	1.35	0.1997	**2.13**	**0.0344**
PTR6	E3 ubiquitin-protein ligase PRT6		**6.33**	**0.0016**	1.12	0.8533
SYD	Chromatin structure-remodeling complex protein SYD	Jasmonic acid-mediated defences	**6.33**	**0.0003**	**7.76**	**0.0143**
COI1	Coronatine-insensitive protein 1		**2.25**	**0.0029**	1.04	0.9923
LRR-RLK	Probable leucine-rich repeat receptor-like serine/threonine-protein kinase At3g14840		**3.56**	**0.0024**	1.78	0.5862
UBP12	Ubiquitin carboxyl-terminal hydrolase 12	Jasmonic acid-mediated signalling	**4.44**	**0.0055**	**5.50**	**0.0001**
UBP13	Ubiquitin carboxyl-terminal hydrolase 13		**2.29**	**0.0237**	1.00	0.9983
RGS1	Regulator of G-protein signaling 1		**2.65**	**0.0465**	1.04	0.9755
SABP2	Salicylic acid-binding protein 2	Salicylic acid biosynthesis	**-2.87**	**0.0237**	1.04	0.9942
At1g06620	1-aminocyclopropane-1-carboxylate oxidase homolog 1	Salicylic acid catabolism	**2.55**	**0.0011**	**2.16**	**< 0.0001**
DLO2	Protein DMR6-LIKE OXYGENASE 2		**5.73**	**0.0063**	1.03	0.9879
DLO1	Protein DMR6-LIKE OXYGENASE 1		-1.01	0.9897	**9.92**	**< 0.0001**
CALS12	Callose synthase 12	Salicylic acid-mediated defences	**4.02**	**0.0007**	**8.64**	**0.0012**
ACA11	Putative calcium-transporting ATPase 11, plasma membrane-type		**3.71**	**0.0019**	1.42	**0.7218**
ACA4	Calcium-transporting ATPase 4, plasma membrane-type		**3.12**	**0.0101**	1.10	**0.8883**
ALD1	Aminotransferase ALD1, chloroplastic		**2.10**	**0.0130**	1.29	0.9458
SIZ1	E3 SUMO-protein ligase SIZ1		**3.38**	**0.0027**	1.20	0.7156
MKP1	Protein-tyrosine-phosphatase MKP1		**3.33**	**0.0004**	1.67	0.0015

CHAPTER 3 - Sub-chapter 3.2

Role of methyl jasmonate and salicylic acid in kiwifruit plants further subjected to Psa infection: biochemical and genetic responses

The contents of this chapter have been published as:
Nunes da Silva, M., Vasconcelos, M.W., Pinto, V., Balestra, G.M., Mazzaglia, A., Carvalho, S.M.P. (2021) Role of methyl jasmonate and salicylic acid in kiwifruit plants further subjected to Psa infection: biochemical and genetic responses. *Plant Physiology and Biochemistry*, 162, 258–266. DOI: 10.1016/j.plaphy.2021.02.045.

Role of methyl jasmonate and salicylic acid in kiwifruit plants further subjected to Psa infection: biochemical and genetic responses

Abstract

The use of plant elicitors for controlling *Pseudomonas syringae* pv*. actinidiae* (Psa), the etiological agent of the kiwifruit bacterial canker (KBC), has been analysed in the past and, while the salicylic acid (SA) pathway seems to promote disease tolerance, the jasmonic acid (JA) pathway has a negative effect. However, the metabolic and genomic responses of Psa-infected kiwifruit plants following elicitation of these phytohormone pathways, as compared with non-elicited Psa-inoculated plants, are poorly understood, being the focus of this study. Micropropagated *A. chinensis* 'Hayward' plants were treated with methyl jasmonate (MJ, an elicitor of the JA pathway) or SA, and further inoculated with Psa. Fifteen days post-inoculation, Psa population in MJ-treated plants was increased by 7.4-fold, whereas SA elicitation led to decreased Psa colonization (0.5-fold), as compared with non-elicited inoculated controls. Additionally, elicitation with MJ or SA generally decreased polyphenols and lignin concentrations (by at least 20%) and increased total proteins (by at least 50%). MJ led to upregulation of *SOD*, involved in plant antioxidant system, and reporter genes for JA (*JIH* and *LOX1*) abscisic acid (ABA) (*SnRK*), SA (*ICS1*), and ethylene (*ACAS1*, *ETR1* and *SAM*) pathways. Moreover, it increased ABA concentration (40%) and decreased carotenoids (30%) concentrations. Contrastingly, comparing with non-elicited Psa-inoculated plants, SA application resulted in the downregulation of antioxidant system-related genes (*SOD* and *APX*) and of reporter genes for ethylene (*ETR1*) and JA (*JIH* and *ETR1*). This study contributes to the understanding of potential mechanisms involved in kiwifruit plant defences against Psa, highlighting the role of JA, SA and ABA pathways in plant susceptibility to the pathogen.

1. Introduction

Pseudomonas syringae pv*. actinidiae* (Psa), responsible for the kiwifruit bacterial canker (KBC), affects plant yield, leading to important economic losses and requiring strict orchard management routines (Froud *et al*., 2017). All the currently cultivated *Actinidia chinensis* varieties, including var. *chinensis* (yellow kiwifruit) and var. *deliciosa* (green kiwifruit), are susceptible to Psa, and the pathogen has been reported in all major kiwifruit-producing countries, the reason why it is considered a pandemic microorganism (Scortichini *et al*., 2012).

In Psa infected kiwifruit plants distinct bacterial factors (e.g., production of specific effector proteins) and plant signalling events occur at the same time, ultimately defining the outcome of the infection process (Petriccione *et al*., 2014; Wang *et al*., 2018a; Nunes da Silva *et al*., 2020). Psa inoculation of *A. chinensis*, triggers the expression of numerous

genes encoding different defence-related pathways, namely: i) antioxidant enzymes biosynthesis, such as *SOD*, *APX* and *CAT* (as soon as 1 day post-inoculation (dpi)) (Petriccione *et al*., 2015; Nunes da Silva *et al*., 2019; Nunes da Silva *et al*., 2020); ii) ethylene (ET) biosynthesis, such as *ETR1* and *EIN2* (2 dpi) (Wurms *et al*., 2017a); iii) pathogenesis related-proteins (PR-proteins), in particular, *PR1* (2 dpi) (Wurms *et al*., 2017a); iv) salicylic acid (SA) signalling pathway, such as *ICS1* (6 hours post-infection, hpi) and *PAD4* (2 dpi) (Cellini *et al*., 2014; Wurms *et al*., 2017a); v) pathogen recognition, such as *CC-NBS-LRR* and *FLS2* (2 dpi) (Wurms *et al*., 2017b); and vi) phenylpropanoid pathway, such as *PAL* (1 dpi) (Cellini *et al*., 2014). These findings seem to corroborate other studies that evaluated biochemical changes in kiwifruit plants following Psa infection. For example, Cellini *et al*. (2014) found that Psa infection induced the accumulation of reactive oxygen species (ROS), such as hydrogen peroxide and superoxide. To counteract the noxious effects of these molecules, plants produce a wide variety of antioxidant enzymes, e.g., peroxidases, which were increased both in susceptible and tolerant kiwifruit cultivars after Psa infection, but to a higher extent in the tolerant ones (Miao *et al*., 2005). Also, before infection with Psa soluble proteins concentration in tolerant kiwifruit cultivars were higher than in susceptible ones, and increased in susceptible cultivars and decreased in the tolerant ones after infection (Miao *et al*., 2005). Higher phenolic compounds concentration was also observed in tolerant kiwifruit cultivars, compared with susceptible ones, and were found to accumulate in both resistant and susceptible cultivars after Psa inoculation (Miao *et al*., 2009). Moreover, Psa-infected plants showed a higher accumulation of precursors of polyphenol biosynthesis, such as phenylpropanoids and metabolites of the phenylalanine ammonia-lyase pathways, suggesting that these metabolic pathways may play central roles in *A. chinensis* resistance against the bacterium (Wang *et al*., 2018a). Taken together, these studies provide valuable clues on the activation of kiwifruit plants defence mechanisms against Psa, but the key metabolic and genomic features responsible for the higher tolerance against Psa are far from being fully understood. Therefore, further studies could allow the identification of crucial genotypic and metabolic traits with potential to be used as markers in plant breeding endeavours and/or for developing sustainable plant protection strategies.

Given the fast dispersion ability and devastation potential of Psa, recent studies have focused on the development of environmental-friendly alternatives to the currently used antibiotic- and copper-based products, namely through the use of plant elicitors (Scortichini, 2014; Wurms *et al.*, 2017b). Most elicitor compounds act through phytohormone-mediated signalling pathways, involving a complex cross-talk between SA, ET, abscisic acid (ABA) and jasmonic acid (JA) (Reglinski *et al.*, 2013). In other species, including *Oryza sativa* (rice) and *Tsuga canadensis* (eastern hemlock), elicitors such as SA and methyl jasmonate (MJ, an elicitor of the JA pathway) have been used with some

degree of success for the control of several plant pathogens (Stella de Freitas *et al*., 2019; Rigsby *et al*., 2019). However, in the case of KBC, whereas elicitation of the SA pathway seems to increase plant tolerance to Psa, elicitation of the JA pathway has been shown to have the opposite effect. For instance, it was shown that elicitation of *A. chinensis* seedlings one week before inoculation with Psa significantly decreased Psa incidence when using 1.7 mM of acibenzolar-S-methyl (ASM), a SA analogue, whereas disease index significantly increased in plants treated with 1.1 mM MJ (Reglinski *et al*., 2013). Furthermore, treatment with two SA-antagonistic hormones, ET and MJ (at 10 ppm and 100 µM, respectively), increased disease development within the first two weeks after inoculation, while application of the ET receptor blocker 1-methyl cyclopropane (1-MCP, at 1 ppm), seven and one days before inoculation, tended to decrease disease incidence (Cellini *et al*., 2014). Although these pieces of evidence attest the importance of plant hormones in the development of KBC, little information on the genetic and metabolomic mechanisms triggered by elicitation of the SA and JA pathways in Psa-inoculated plants is available at the moment. In fact, in kiwifruit plants, in particular, limited knowledge is available on how these antagonistic pathways modulate the production of plant primary and secondary metabolites and the expression of defence-related genes and, more importantly, on how we can take advantage of this information to develop more effective and ecological disease control strategies.

The main aims of the present work were to: (i) unravel genetic and biochemical responses induced by Psa inoculation in *A. chinensis*; (ii) understand the impact at a metabolomic and genetic level of MJ and SA application to kiwifruit plants further subjected to Psa infection. For this, *A. chinensis* micropropagated plants were mock-inoculated (mock-inoculated control) or inoculated with Psa, 15 days after mock-elicitation (non-elicited inoculated control), or elicitation with SA (inoculated SA-treated plants) or MJ (inoculated MJ-treated plants) and sampled at 15 dpi for an integrative analysis of: Psa endophytic population, primary and secondary metabolites (total chlorophyll, carotenoids, flavonoids, polyphenols and lignin), total protein, phytohormones (JA, SA and ABA), and gene expression related with plant antioxidant and defence systems and phenylpropanoids, JA, ABA and ET pathways. Finally, we performed a Principal Component Analysis (PCA) on the collective data to look at global patterns in the metabolic and genomic data in relation to the impact of MJ and SA on plant responses to Psa.

2. Materials and Methods

2.1. Plant maintenance and Psa inoculum

Micropropagated *A. chinensis* var. *deliciosa* 'Hayward' plants (with a single shoot, 5 to 6 cm height, and 8 to 12 leaves) were purchased from QualityPlant - Investigação e Produção em Biotecnologia Vegetal, Lda. (Castelo Branco, Portugal). Plants were maintained in a modified full-strength Murashige and Skoog (MS) agarized medium in a climate chamber (Aralab Fitoclima 10 000EH, Aralab, Rio de Mouro, Portugal) as described elsewhere (Nunes da Silva *et al*., 2020). On the day of plant inoculation, a fresh 1-2x10^7 CFU mL^{-1} inoculum of a virulent Psa strain (CFBP7286) was prepared in sterile Ringer's solution.

2.2. Plant elicitation, inoculation and sampling

Solutions of 1 mM of MJ and 2.5 mM of SA (Sigma Aldrich Co Ltd, St. Louis, Missouri, USA) were prepared in 1% ethanol with 0.1% Tween 20 and used for plant elicitation 15 days before Psa inoculation, as described by Reglinski *et al*. (2013) and Cellini *et al*. (2014), respectively. These concentrations were selected based not only on those studies, but also on preliminary trials where we tested a range of MJ and SA concentrations (1 to 25 mM), from which we selected the highest ones where no toxicity symptoms appeared (data not shown). Nine plants were treated with MJ or with SA and 18 plants were treated with 1% ethanol with 0.1% Tween 20 (non-elicited control) by dipping each plant in the respective elicitor solution for 15 sec.

Fifteen days after, nine non-elicited plants and plants elicited with MJ or SA were inoculated with a Psa suspension by submerging each plant for 15 sec in the inoculum. The remaining nine non-elicited plants were inoculated with Ringer's solution alone (NaCl 0.72%, $CaCl_2$ 0.017% and KCl 0.037%, pH 7.4). This resulted in four treatments with three biological replicates (each of them consisting of a pool of three individual plants): non-elicited mock-inoculated controls (niCTR), non-elicited Psa-inoculated controls (iCTR), MJ-elicited Psa-inoculated plants (iMJ), and SA-elicited Psa-inoculated plants (iSA). At 15 dpi, plants were removed from the culturing medium and the degree of disease symptoms was evaluated through the percentage of leaf area presenting necrotic spots (as described in Nunes da Silva *et al.*, 2020). The tip (*ca*. 0.5 cm length) of every leaf of every plant was aseptically removed and placed in a sterile container for the determination of Psa endophytic population and the remaining plant tissues were flash-frozen in liquid nitrogen, macerated with mortar and pestle and stored at -80 °C for biochemical, metabolomic and gene expression analysis.

2.3. Psa endophytic population

Leaf tips, sampled as previously described, were surface sterilised, macerated in Ringer's solution, and used for CFU estimation through an adapted protocol from Cellini *et al*. (2014) previously described (Nunes da Silva *et al*., 2020).

2.4. Total proteins, primary and secondary metabolites

Protein concentration was determined through the Bradford methodology (Bradford, 1976) using the Pierce Coomassie Plus Assay Kit (Thermo Fisher Scientific, Massachusetts, USA). The kit manufacturer's instructions were adapted for standard 1.5 mL cuvettes by adding 33 µL of sample extract to 990 µL of Coomassie Plus Reagent.

Lyophilized plant tissues (*ca*. 50 mg FW) were used for total chlorophyll, carotenoids, total soluble polyphenols, flavonoids and lignin quantification. Total chlorophyll, total soluble polyphenols, and lignin were quantified through spectrophotometric methods through adapted protocols from Sumanta *et al*. (2014), Marinova *et al*. (2005) and Hatfield *et al*. (1999), as previously described by Nunes da Silva *et al*. (2020).

Carotenoids (µg g^{-1} dry weight) were quantified according to Sumanta *et al*. (2014) by recording sample absorbances at 470, 652 and 665 nm:

$$\frac{1000Abs_{470} - 1.63(16.72Abs_{665} - 9.16Abs_{652}) - 104.96(34.09Abs_{652} - 15.28Abs_{665})}{221x\ biomass}$$

For flavonoids quantification, 2 mL of ultrapure water and 150 µL of 5% sodium nitrite were added to 100 µL of sample. After a 5 min incubation period at room temperature, 150 µL of 10% aluminium chloride, 1 mL of 1 M sodium hydroxide and 1.2 mL ultrapure water were gently mixed with each sample. Absorbance was recorded at 510 nm and flavonoids concentration was determined considering a catechin standard curve (Zhishen *et al*., 1999).

2.5. Phytohormones

JA, SA and ABA were quantified following an adapted protocol from de Ollas *et al*. (2013). To lyophilized shoot tissues (*ca*. 50 mg FW) were added 100 ng of $ABAd_6$, 100 ng of SAd_6, 100 ng of di-hydro-JA and 2 mL of distilled water. After vigorous stirring with glass beads for 10 min, samples were centrifuged for 10 min at 12 000 g and 4 °C, and the supernatant was recovered to a new centrifuge tube. The pH of the extract was adjusted to 3.0 with 80% (v/v) acetic acid. Afterwards, 2 mL of diethyl ether were added to each sample, vigorously mixed, and the upper layer evaporated in a centrifuge concentrator (SpeedVac, Jouan, Saint Herblain, France). Samples were resuspended in 1 mL of 10% (v/v) methanol,

sonicated for 10 min, filtrated through a 0.2 µm polytetrafluoroethylene membrane filter, and injected into an HPLC system (Waters Alliance 2695, Waters Corporation, Milford, MA, USA). Phytohormone separation was conducted on a C18 column (Kromasil 100, 5 µm particle size, 100 mm, 2.1 mm, Scharlab, Barcelona, Spain) employing a linear gradient of methanol and ultrapure water supplemented with 0.1% (v/v) acetic acid at a flow rate of 300 mL min^{-1}. Phytohormone quantification was performed in a Quattro LC triple quadrupole mass spectrometer (Micromass, Manchester, United Kingdom) connected online to the output of the column through an orthogonal Z-spray electrospray ion source, after external calibration against authentic standards using Mass Lynx v4.1 software (Waters Corporation, Milford, MA, USA).

2.6. Gene expression

Plant RNA was extracted following an adapted protocol from Cellini *et al*. (2014) and single-stranded cDNA was synthesized using iScript cDNA Synthesis Kit (Bio-Rad, California, United States of America), as described by Nunes da Silva *et al*. (2020). Primers for *LOX1* (lipoxygenase 1, accession number: DQ497792), *CHS* (chalcone synthase, KF157394), *DFR* (dihydroflavonol 4-reductase, KF157393), *SnRK* (sucrose non-fermenting kinase, JX067541), *ACAS1* (1-aminocyclopropane-1-carboxylate synthase 1, AB007449), *ETR1* (ethylene receptor 1, EU170628) and *SAM* (S-adenosylmethionine synthetase, U17240) were designed using Primer3, whereas primer sequences for *APX* (ascorbate peroxidase), *CAT* (catalase), *SOD* (superoxide dismutase), *JIH* (jasmonoyl-isoleucine-12-hydrolase), *ICS1* (isochorismate synthase 1), *PAL* (phenylalanine ammonia-lyase) and *PR8* (pathogenesis-related protein 8) were obtained from other published studies (Cellini *et al*., 2014; Petriccione *et al., 2*015; Wurms *et al*., 2017b) (Table 1). Reverse transcription quantitative real-time polymerase chain reactions (RT-qPCR) were carried out on a StepOne Real-Time PCR System (Applied Biosystems, California, USA) and the comparative CT method (ΔΔCT, Livak and Schmittgen, 2001) was used for relative gene expression quantification using actin (*ACT*) and protein phosphatase 2A (*PP2A*) as housekeeping genes and non-elicited mock-inoculated plants (niCTR) as reference samples (Nunes da Silva *et al*., 2020). For relative gene expression analysis, the minimum fold change with physiological significance was considered to be two (Vaerman *et al*., 2004), and for each of the three biological replicates and target gene, two technical replicates were analysed.

Table 1 - Primer sequences and annealing temperature (T_{ann}) of housekeeping and target genes used for RT-qPCR analysis.

Gene		Primer sequence (5′-3′)		T_{ann} (ºC)	Reference
		Forward	Reverse		
Housekeeping genes					
ACT	Actin	CCAAGGCCAACAGAGAGAAG	GACGGAGGATAGCATGAGGA	56.0	Ledger *et al*., 2010
PP2A	Protein phosphatase 2A	GCAGCACATAATTCCACAGG	TTTCTGAGCCCATAACAGGAG	55.2	Nardozza *et al*., 2013
Antioxidant system					
APX	Ascorbate peroxidase	GGAGCCGATCAAGGAACAGT	AACGGAATATCAGGGCCTCC	57.8	Petriccione *et al*., 2015
CAT	Catalase	GCTTGGACCCAACTATCTGC	TTGACCTCCTCATCCCTGTG	56.9	Petriccione *et al*., 2015
SOD	Superoxide dismutase	CACAAGAAGCACCACCAGAC	TCTGCAATTTGACGACGGTG	57.8	Petriccione *et al*., 2015
Phenylpropanoids					
CHS	Chalcone synthase	ACGCCTCATGATGTACCAAC	TGGGTCAGCCCCAACTATAA	55.8	This study
DFR	Dihydroflavonol 4-reductase	TGCCAAAAAGATGACTGGCT	TCGTCTAGGTGCACGAATTG	56.7	This study
PAL	Phenylalanine ammonia-lyase	CGGAGCAACACAACCAAGA	CCTGACATAGTGCGACTACATAG	55.2	Cellini *et al*., 2014
Jasmonic *acid*					
JIH	Jasmonoyl-isoleucine-12-hydrolase	CGGCTCTGATCTGGTTTTTC	CCTCATGCTCTCACTCAACG	55.8	Wurms *et al*., 2017b
LOX1	Lipoxygenase 1	GTTAGAGGGGTGGTGACTCT	CTTTAGCACTGCTTGGTTGC	53.5	This study
Abscisic acid					
ICS1	Isochorismate synthase 1	AGGCGAGGCTTCTAATTG	ACAGCAAACTCACTCTCTC	47.8	Cellini *et al*., 2014
SnRK	Sucrose non-fermenting kinase	GATTCTCTTCGCAACCGAGT	GGGGTTTTGAACCCATTCCT	56.7	This study
Ethylene					
ACAS1	1-aminocyclopropane-1-carboxylate synthase 1	AGCCACTCCACTGAAGTTTG	AAACTAGCCCGAAACTCGAC	54.5	This study
ETR1	Ethylene receptor 1	ATCTAGCAAGGAGGGAAGCA	AACCATCAGACGTTGCTCAG	54.8	This study
SAM	S-adenosylmethionine synthetase	GAATAGTACTTGCCCCTGGC	TACAAATCGACCAGAGGGGT	55.1	This study
Defence					
PR8	Pathogenesis-related protein 8	TTTGGATGGAATTGACTTTGACA	TTCTTGCCACGACTGCTATA	55.5	Cellini *et al*., 2014

2.7. Data analysis

Differences between treatments were tested through analysis of variance (ANOVA) and mean separation was done using Student's T-test ($p < 0.05$) in GraphPad Prism v6.0 (GraphPad Software, Inc., California, USA). To establish the relationship among the different variables analysed, principal component analysis (PCA) was performed in IBM SPSS Statistics v24.0 (IBM Corporation, New York, USA). For PCA, data set included 24 continuous variables (corresponding to CFU, total chlorophyll, carotenoids, proteins, flavonoids, polyphenols, lignin, abscisic acid, jasmonic acid, salicylic acid and 14 target genes), which resulted in a matrix containing 288 averaged measurements (corresponding to four treatments with three samples each). Averaged data was mean centred and weighed with the inverse of the standard deviation before applying the PCA to guarantee that all variables had the same weight in influencing the model.

3. Results

3.1. Foliar disease symptoms and Psa endophytic population

At 15 dpi, foliar symptoms were mild (less than 5% of leaf area affected with light brown necrotic spots) and they did not differ between plant treatments (data not shown). In contrast, the density of leaf Psa endophytic population was distinct amongst them: non-elicited Psa-inoculated plants (iCTR) had a leaf endophytic bacterial population of 2.11 ± 0.44 x 10^7 CFU g^{-1} of plant tissue, whereas MJ-elicited plants (iMJ) had a 7.4-fold significantly higher Psa colonization, and SA-elicited plants (iSA) had only 0.92 ± 0.35 x 10^7 CFU g^{-1} (Fig. 1). Although no significant differences were observed between iCTR and iSA plants, Psa colonization in iSA represented only 46 % of the bacterial density observed in iCTR, and only 6% of the value registered in iMJ.

3.2. Photosynthetic pigments and proteins

Plant inoculation significantly decreased total chlorophylls, regardless of the elicitation treatment previously applied (Fig. 2A). Non-elicited mock-inoculated plants (niCTR) presented on average 5.13 ± 0.42 ng g^{-1} total chlorophylls, which decreased by *ca*. 40% after inoculation in all treatments.

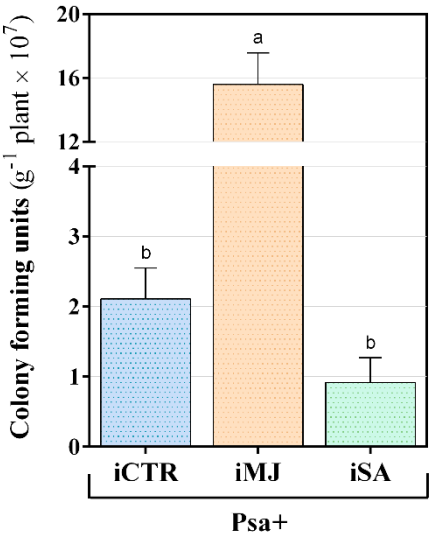

Figure 1 - Colony-forming Units (x 10^7 per gram of fresh plant tissue) 15 days post-inoculation with *Pseudomonas syringae* pv. *actinidiae* (Psa) of kiwifruit plants previously submitted to: no-elicitation (iCTR), elicitation with 1.0 mM methyl jasmonate (iMJ) or with 2.5 mM salicylic acid (iSA). Values represent the mean ± standard error of the mean, and different letters indicate statistically different means at $p < 0.05$.

Plant inoculation *per se* had no significant effect on carotenoids, but when combined with MJ elicitation it significantly decreased carotenoids concentration by 30% (attaining 0.36 ± 0.04 ng g^{-1}), whereas SA elicitation had no significant effect (Fig. 2B). Also, whereas plant inoculation with no elicitation (iCTR) did not alter total protein concentration (comparing with niCTR plants), iMJ and iSA showed significantly higher total protein concentration (Fig. 2C). The magnitude of this effect was more pronounced in iMJ: protein concentration increased from 19.7 ± 2.01 mg g^{-1} in niCTR and 30.9 ± 2.03 mg g^{-1} in iSA to 48.1 ± 5.61 mg g^{-1} in MJ-treated plants (i.e., 244 and 156%, respectively).

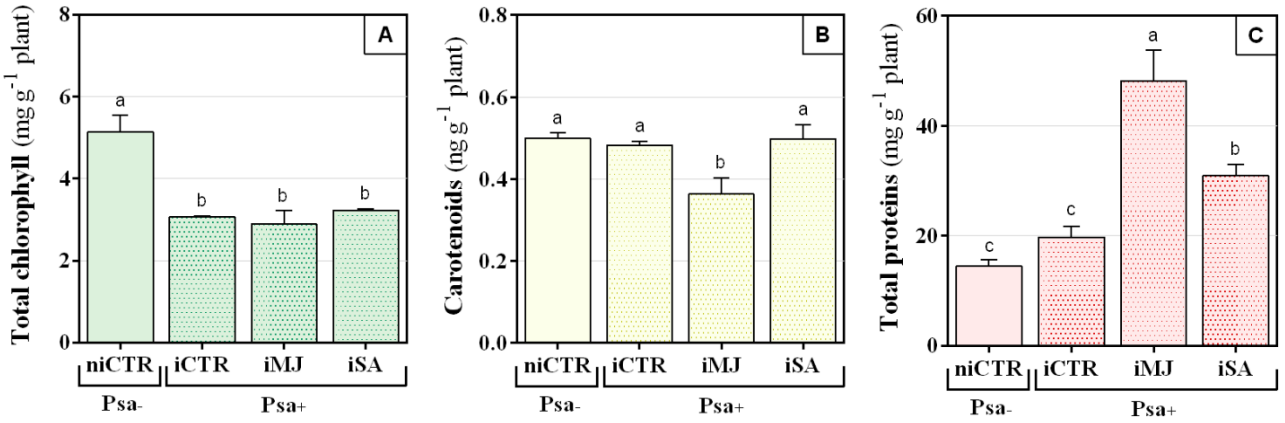

Figure 2 - Total chlorophyll (A), carotenoids (B) and total protein (C) concentrations in mock-inoculated non-elicited plants (niCTR), and in plants previously submitted to: no-elicitation (iCTR), elicitation with 1.0 mM methyl jasmonate (iMJ) or with 2.5 mM salicylic acid (iSA), 15 days post-inoculation with *P. syringae* pv. *actinidiae* (Psa). Values represent the mean ± standard error of the mean, and different letters indicate statistically different means at $p < 0.05$.

3.3. Secondary metabolites

Significant alterations were found in two metabolites related to the phenylpropanoid pathway (soluble polyphenols and lignin). Whereas no significant alterations were observed in flavonoids concentration (Fig. 3A), Psa inoculation in non-elicited plants (iCTR) significantly increased soluble polyphenols by 140%, reaching 28.9 ± 0.6 μg g^{-1}, comparing with niCTR plants (Fig. 3B). In addition, comparing with iCTR plants, which presented 1.9 ± 0.2 μg g^{-1} plant tissue, lignin concentration was significantly decreased by 30% and 40% in iMJ and iSA, respectively (Fig. 3C).

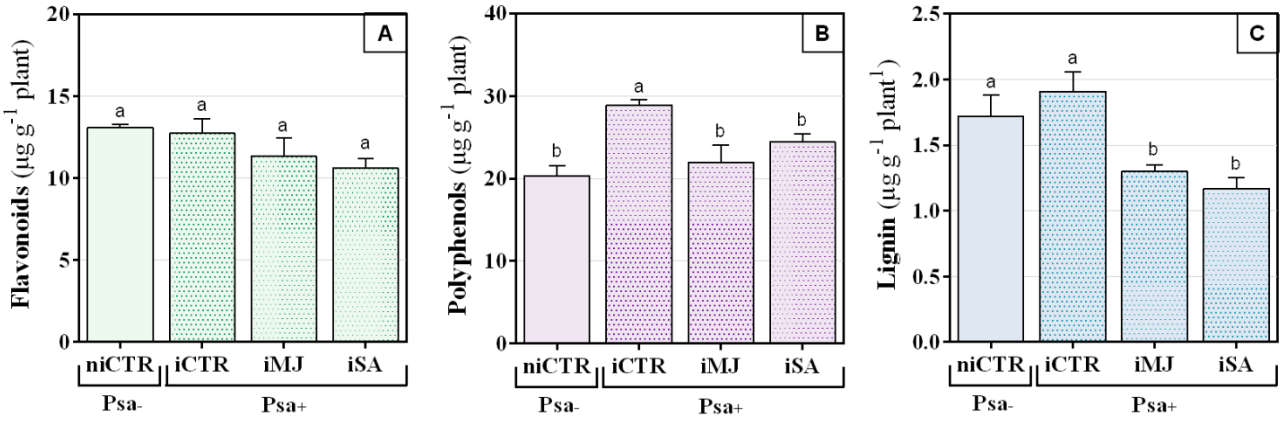

Figure 3 - Flavonoids (A), total polyphenols (B) and lignin (C) concentrations in mock-inoculated non-elicited plants (niCTR), and in plants previously submitted to: no-elicitation (iCTR), elicitation with 1.0 mM methyl jasmonate (iMJ) or with 2.5 mM salicylic acid (iSA), 15 days post-inoculation with *P. syringae* pv. *actinidiae* (Psa). Values represent the mean ± standard error of the mean, and different letters indicate statistically different means at $p < 0.05$.

3.4. Phytohormones

Plant inoculation in the absence of elicitation (iCTR) significantly reduced ABA concentration in plant tissues (Fig. 4A), which decreased from 173 ± 12 ng g^{-1} (niCTR) to 110 ± 10 ng g^{-1} (iCTR), i.e., by 40%. Comparing with iCTR, inoculation of MJ-elicited plants significantly increased ABA concentration in plant tissues by 140%, reaching 261 ± 68 ng g^{-1}, whereas SA significantly decreased ABA concentration by 30%, attaining 127.5 ± 5.1 ng g^{-1}. Jasmonic acid (JA) and SA concentrations varied very little between niCTR and iCTR plants, which had on average 0.95 mg g^{-1} JA and 0.19 mg g^{-1} SA. Inoculation of SA-treated plants did not induce significant changes in JA concentration in plant tissues (Fig. 4B) and inoculation of MJ-treated plants had no significant impact on SA concentration (Fig. 4C). However, comparing with iCTR plants, MJ application significantly increased JA concentration to 3.60 ± 0.49 mg g^{-1}, i.e., by 33-fold, and SA treatment induced a significant increment of 41-fold in SA concentration in plant tissues, which reached 29.2 ± 2.8 mg g^{-1}.

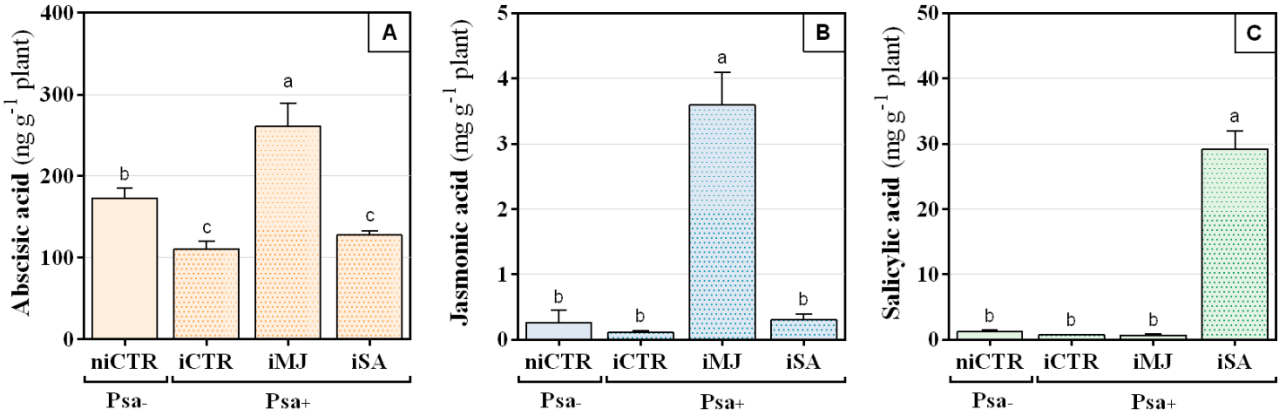

Figure 4 - Abscisic (A), jasmonic (B) and salicylic (C) acid concentrations in mock-inoculated non-elicited plants (niCTR), and in plants previously submitted to: no-elicitation (iCTR), elicitation with 1.0 mM methyl jasmonate (iMJ) or with 2.5 mM salicylic acid (iSA), 15 days post-inoculation with *P. syringae* pv. *actinidiae* (Psa). Values represent the mean ± standard error of the mean, and different letters indicate statistically different means at $p < 0.05$.

3.5. Gene expression

Concerning the relative expression of antioxidant system-related genes, plant inoculation with Psa without elicitor application (iCTR) significantly increased *SOD* and *APX* expression by 2.9- and 4.6-fold, respectively, but not affecting *CAT* regulation (Table 2). Comparing with iCTR, MJ treatment increased *SOD* expression by 1.5-fold, whereas SA treatment reduced *SOD* and *APX* expression by 0.7- and 0.8-fold, respectively. Among genes related to the phenylpropanoid pathway, plant inoculation without elicitation (iCTR) significantly increased *DFR* relative expression by 4.8-fold. The relative expression of this gene was found to be significantly reduced by 0.9-fold in iMJ, and significantly increased by 2.1-fold in iSA. Contrastingly, inoculation of MJ-elicited plants led to a significant downregulation of *PAL* by 0.6-fold, and elicitation with SA of *CHS* by 0.8-fold, in comparison with iCTR plants (Table 2). Moreover, whereas *JIH* relative expression significantly increased by 1.9-fold following Psa inoculation in non-elicited plants (iCTR), *LOX1*, *SnRK* and *ICS1* genes relative expression was not significantly affected by Psa inoculation alone. However, when compared with non-elicited inoculated plants (iCTR), iMJ showed significant overexpression of these genes, by 4.0-, 4.7-, 4.4- and 2.5-fold, respectively. Contrarily, SA treatment significantly decreased *JIH* transcriptional levels by 0.6-fold. Concerning genes related to the ET pathway, Psa inoculation alone (iCTR) induced a 2.2-fold upregulation of *ETR1*, whereas in iSA this gene was downregulated by 0.7-fold, compared with the first ones. Moreover, in iMJ there was an overexpression of *ACAS1*, *ETR1* and *SAM* (by 6.2-, 3.2- and 3.1-fold, respectively). A similar trend was

observed in the expression of *PR8*, a pathogenesis-related protein-encoding gene, with iMJ showing a 4.6-fold increase in its relative fold of expression, compared with iCTR.

Table 2 - Relative fold of expression of target genes in non-elicited (iCTR), MJ-elicited (1.0 mM methyl jasmonate, iMJ) or SA-elicited (2.5 mM salicylic acid, iSA) *A. chinensis* plants, analysed 15 days post-inoculation with *P. syringae* pv. *actinidiae* (Psa), as compared with non-elicited mock-inoculated plants (niCTR). Values represent the mean of three biological replicates ± standard error of the mean, and different letters represent statistically different means at $p < 0.05$ (comparison in rows). A one-fold change of expression represents no relative change in gene expression, as compared with niCTR. Biologically significant differences between mock- and Psa-inoculated plants are marked in bold.

Gene	Psa +			*p* value
	iCTR	MJ	SA	
Antioxidant system				
SOD	**2.9 ± 0.2^{b}**	**4.3 ± 0.5^{a}**	0.7 ± 0.2^{c}	**0.0011**
APX	**4.6 ± 0.5^{a}**	**4.9 ± 0.8^{a}**	1.1 ± 0.1^{b}	**0.0037**
CAT	0.8 ± 0.1^{a}	1.0 ± 0.1^{a}	0.9 ± 0.3^{a}	0.6055
Phenylpropanoids				
CHS	1.6 ± 0.3^{a}	0.9 ± 0.1^{ab}	0.4 ± 0.2^{b}	**0.0257**
DFR	**4.8 ± 0.5^{b}**	**0.4 ± 0.2^{c}**	**10.1 ± 0.5^{a}**	**< 0.0001**
PAL	1.7 ± 0.2^{a}	0.7 ± 0.1^{b}	1.8 ± 0.1^{a}	**0.0026**
Jasmonic acid				
JIH	1.9 ± 0.2^{b}	**7.7 ± 0.7^{a}**	0.7 ± 0.4^{b}	**0.0001**
LOX1	0.8 ± 0.1^{b}	**3.8 ± 1.0^{a}**	0.9 ± 0.5^{b}	**0.0257**
Abscisic acid				
ICS1	0.7 ± 0.1^{b}	**3.0 ± 0.4^{a}**	**0.3 ± 0.2^{b}**	**0.0009**
SnRK	0.7 ± 0.1^{b}	1.7 ± 0.2^{a}	0.5 ± 0.1^{b}	**0.0003**
Ethylene				
ACAS1	0.6 ± 0.2^{b}	**3.4 ± 0.6^{a}**	0.9 ± 0.4^{b}	**0.0045**
ETR1	**2.2 ± 0.6^{b}**	**6.8 ± 0.1^{a}**	0.7 ± 0.4^{c}	**< 0.0001**
SAM	0.7 ± 0.2^{b}	**2.1 ± 0.1^{a}**	0.7 ± 0.4^{b}	**0.0122**
Defence				
PR8	0.7 ± 0.1^{b}	**3.3 ± 0.1^{a}**	0.5 ± 0.1^{b}	**< 0.0001**

3.6. Principal component analysis (PCA)

The PCA between non-elicited mock- (niCTR) and Psa-inoculated plants (iCTR) explained 76% of the total variance in the data (Fig. 5A). The loading plot of PC1 vs. PC2 showed a high correlation between plant inoculation with several factors including density of Psa endophytic population (CFU), polyphenols, *SOD* and *APX* (antioxidant system), *DFR* (phenylpropanoids pathway) and *ETR1* (ET pathway), while being negatively correlated with factors such as total chlorophyll, ABA, *ACAS1* and *SAM* (ET pathway), *SnRK* (ABA pathway) and *PR8* (defence).

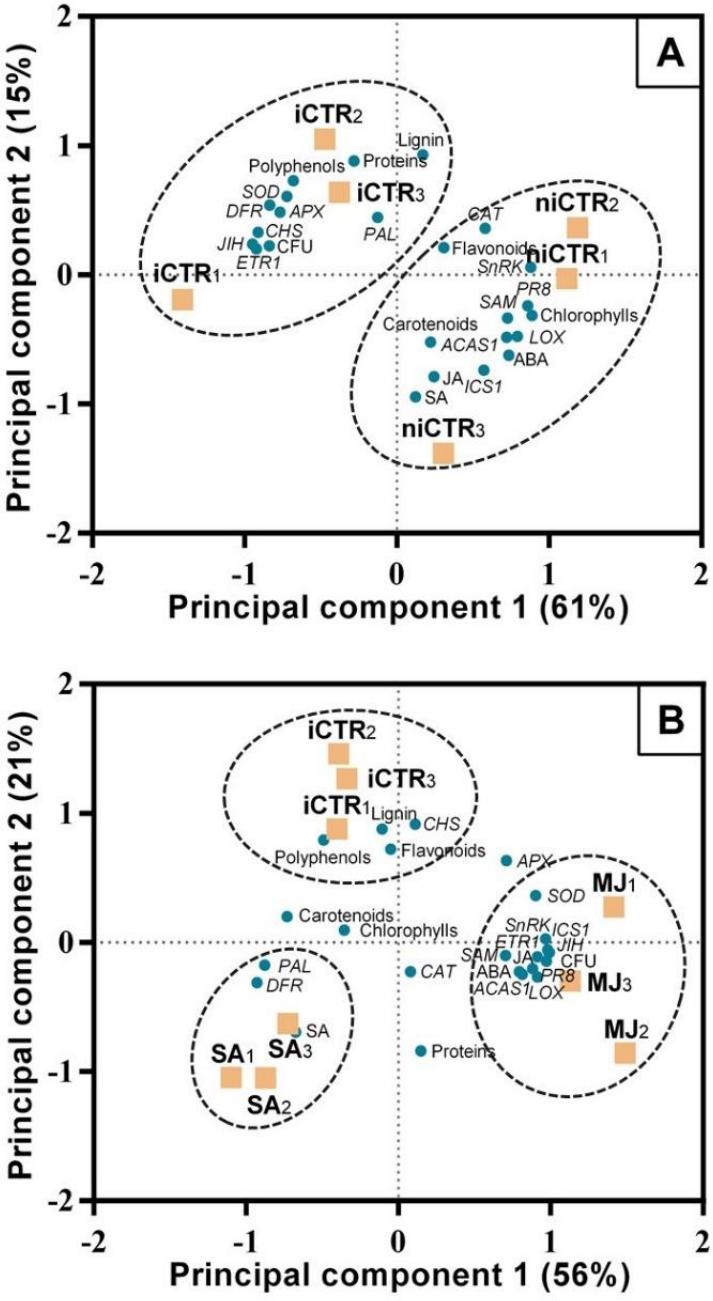

Figure 5 - Principal component analyses between: (A) non-elicited mock-inoculated plants (niCTR) and non-elicited Psa-inoculated plants (iCTR); and between (B) non-elicited (iCTR), methyl jasmonate-elicited (iMJ) or salicylic acid-elicited (iSA) Psa-inoculated plants. The correlation matrixes comprise all variables analysed (colony-forming units (CFU), total chlorophylls, carotenoids, proteins, flavonoids, total polyphenols, lignin, jasmonic acid (JA), salicylic acid (SA), abscisic acid (ABA), and genes superoxide dismutase (*SOD*), ascorbate peroxidase (*APX*), catalase (*CAT*), chalcone synthase (*CHS*), dihydroflavonol 4-reductase (*DFR*), phenylalanine ammonia-lyase (*PAL*), jasmonoyl-isoleucine-12-hydrolase (*JIH*), lipoxygenase 1 (*LOX1*), isochorismate synthase 1 (*ICS1*), sucrose non-fermenting kinase (*SnRK*), 1-aminocyclopropane-1-carboxylate synthase 1 (*ACAS1*), ethylene receptor 1 (*ETR1*), S-adenosylmethionine synthetase (*SAM*) and pathogenesis-related protein 8 (*PR8*)) and loadings factors, which correspond to the four treatments employed (niCTR, iCTR, iMJ and iSA). Ellipses were drawn for helping visualizing treatment characterization.

On the other hand, PCA between non-elicited (iCTR), MJ-elicited (iMJ) or SA-elicited (iSA) Psa-inoculated plants, which explained 77% of the total variance in the data, showed a high correlation between iMJ and enhanced levels of Psa endophytic population, proteins, JA, ABA, gene *PR8* and genes related with the biosynthesis of ET (*ACAS1*, *ETR1* and *SAM*), ABA (*SnRK*), SA (*ICS1*) and JA (*JIH* and *LOX1*). Contrarily, iSA positively correlated with high values of SA and *DFR* gene, while showing a negative correlation with Psa endophytic population. Both iMJ and iSA were negatively correlated with polyphenols, flavonoids and lignin and with *CHS* gene (phenylpropanoids pathway).

4. Discussion

4.1. Biochemical and genetic alterations induced by Psa infection

Secondary metabolites seem to be of great importance in *Actinidia* defences against Psa. Miao *et al*. (2009) observed that tolerant kiwifruit cultivars had significantly higher phenolic compounds concentration than susceptible cultivars, and that it increased in both resistant and susceptible cultivars after Psa infection. More recently, increased concentrations of soluble phenolic compounds and lignin were observed in *A. chinensis* and *A. arguta* following Psa inoculation (Nunes da Silva *et al*., 2020). In line with these previous reports, in the present work, Psa inoculation (without elicitation) significantly increased soluble polyphenols, probably as a strategy employed by infected plants to counteract the pathogen, as previously hypothesised (Nunes da Silva *et al*., 2020) (Fig. 3). Contrarily, Psa inoculation had a negative effect on ABA concentration and on the expression of gene *SnRK*, related to plant responses to ABA (Fig. 5). ABA, ROS, SA and MJ are known to regulate stomatal functions, e.g., size and density, which have been correlated with increased susceptibility to Psa (Miao *et al*., 2005). However, following plant infection ABA seems to have a deleterious effect on plant immunity (Yasuda *et al*., 2008), and exogenous application of ABA also increased disease development on several *A. chinensis* genotypes (Cellini *et al*., 2014). This occurs because ABA can modify plant cellular metabolic homeostasis, namely regarding water availability within the apoplast, facilitating bacterial growth and impairing signalling networks that orchestrate plant defences (Ton *et al*., 2009). We hypothesise that, in the present work, lower ABA concentrations in Psa-infected plants could be a strategy to regulate stomatal activity as a way to impair bacterial entrance and proliferation and maintain plant cellular functions (Reglinski *et al*., 2013).

The phenylpropanoid pathway plays a key role in plant defence responses, participating in the synthesis of a wide variety of phenolic compounds, e.g., phenolic acids, lignins, flavonoids and stilbenes (Dixon *et al*., 2002). In this work, genes related to phenylpropanoids biosynthesis, such as *PAL*, were upregulated in non-elicited Psa-infected plants. This is in accordance with Wang *et al*. (2017a), who found that the expression of as many as 64 genes related to the phenylpropanoid biosynthesis pathway, including *PAL*, were upregulated after *A. chinensis* inoculation with Psa. Moreover, *PAL* expression was significantly increased in ASM-treated Psa-inoculated plants (Cellini *et al*., 2014; Wurms *et al*., 2017b), probably because SA positively regulates phenylpropanoid biosynthesis and vice-versa (Chen *et al*., 2016). *JIH*, a gene commonly used as a negative marker of the JA pathway, is thought to allow plants to modulate SA-mediated responses according to their needs (Woldemariam *et al*., 2012). Therefore, our observations on the overexpression of this gene in non-elicited inoculated plants may demonstrate a strategy to attenuate the increase of JA pathway-related events induced by Psa infection.

4.2. Kiwifruit plant responses to Psa infection after elicitation with MJ or SA

In the present work, MJ application drastically increased bacterial count in plant tissues (Fig. 1). Contrarily, plant treatment with SA followed by Psa inoculation decreased bacterial density in plant tissues, corroborating the evidences that SA elicitation increases kiwifruit plant tolerance to this pathogen (Cellini *et al*., 2014). Accordingly, PCA revealed that iMJ and iSA had contrasting behaviours concerning Psa endophytic population in plant tissues (CFU), with iMJ positively correlating with high bacterial density (Fig. 5B). Similarly, Cellini *et al*. (2014) reported a higher disease index in *A. chinensis* plants infected with Psa after treatment with 100 µM MJ, probably because this compound counteracts SA-mediated defence related pathways.

The activation of plant defences upon pathogen recognition, the withdrawal of nutrients and the induction of tissue necrosis by the pathogen increases plant demand for assimilates, subsequently leading to the down-regulation of plant source metabolism, namely photosynthesis (Lu *et al*., 2018). Decreased photosynthesis has been observed in other incompatible plant-pathogen interactions, such as in *Arabidopsis thaliana* plants infected with *P. syringae* pv. *tomato*, in which downregulation of transcripts associated with chlorophyll, carotenoid and xanthophyll biosynthesis was observed (Truman *et al*., 2006). This may explain the decrease in total chlorophyll observed in this study after plant inoculation with Psa, regardless of the elicitor treatment applied (Fig. 2A), pinpointing that the extent of impairments to these metabolites are not directly correlated with bacterial density inside plant tissues.

Total protein significantly increased after Psa inoculation of elicited plants, especially with MJ treatment (Fig. 2C). Elevated protein and enzymatic concentrations in iMJ are most likely due to the elevated bacterial density observed in plant tissues and to the activation of several defence-related pathways as an attempt to respond to the bacterial infection. Contrastingly, higher protein in iSA is probably related to its beneficial role in enhancing plants antioxidant system, as induction of NADPH oxidase and glutathione peroxidase activities was observed as soon as 72 h after treatment with ASM in *A. chinensis* (Cellini *et al*., 2016). Altogether, the results demonstrate the potential of elicitors of the SA pathway in enhancing kiwifruit plants defence mechanisms, previously to plant infection. Regarding plant secondary metabolites, MJ and SA treatment followed by Psa inoculation significantly decreased lignin concentration in plant tissues; however, cell wall constituents, including lignin and cellulose, have been found to increase after MJ and SA treatment in tissues of several plant species (Napoleão *et al*., 2017). Therefore, the alterations observed in this work may result from a synergic effect between Psa and the elicitors tested and may involve the reallocation of metabolic resources to other defensive pathways. It was recently shown that during *Actinidia* defence against Psa and its closely related but less virulent strain *P. syringae* pv. *actinidifoliorum* (Pfm) the SA pathway is predominant over the JA pathway (Wurms *et al*., 2017a). These authors showed that SA concentration increased to a greater extent than JA, and that, concomitantly, JA-isoleucine remained unchanged, thus demonstrating the antagonism between JA and SA. In the present work plant treatment with MJ or SA induced endogenous JA and SA concentrations, respectively, which remained elevated even after 30 days of elicitation (Fig. 4). Moreover, iSA significantly decreased ABA concentration in plant tissues, whereas iMJ showed increased ABA levels. We hypothesise that increased ABA-mediated stomatal opening and the suppression of SA-mediated defences in MJ-elicited plants may be the key factors contributing to the higher Psa colonization observed with this treatment.

Concerning gene expression analysis, in the present work *SOD* and *APX* genes were upregulated in iMJ, probably due to the high bacterial density observed in plant tissues (Table 2). Genes related with phenylpropanoids biosynthesis, such as *PAL*, were also upregulated in iSA, thus supporting the evidence that the SA pathway positively regulates phenylpropanoid biosynthesis and vice-versa (Chen *et al*., 2016). *SnRK*, involved in plant responses to ABA, was overexpressed in iMJ. A similar trend was observed in *ICS1* regulation, which was more upregulated in iMJ than in iCTR or iSA. Previous works have demonstrated that exposure of healthy kiwifruit plants to Psa-infected neighbour plants increased the transcriptional levels of *ICS1*, probably due to alterations in plant respiratory metabolism (Cellini *et al*., 2016). Altogether, these results corroborate the positive feedback that MJ has in the ABA pathway, as previously discussed. It is interesting to note that elicitation with JA, but not with SA, also increased the expression of *ICS1*, related to

SA biosynthesis (Gao *et al*., 2015). We hypothesise that, as plants were exogenously supplied with SA, its biosynthetic pathway decreased, leading to lower transcription of *ICS1*. On the other hand, it has been shown that in *Arabidopsis thaliana* ABA can suppress SA biosynthesis by inhibiting ICS (Yasuda *et al*., 2008). Therefore, it is also possible that iMJ increased ABA concentration, negatively affecting ICS, leading to increased *ICS1* expression to counteract this negative feedback. *JIH1*, which encodes an enzyme that degrades the active metabolite JA-isoleucine in the JA pathway, and *LOX1*, involved in the first step of the JA pathway, were highly upregulated in iJA, which seems to be in accordance with previous studies (Wurms *et al*., 2017b, Cellini *et al*., 2014). Similarly, genes related to ET biosynthesis, as *ETR1*, *SAM* and *ACAS1*, were upregulated in iJA. ET and JA can act synergistically or antagonistically during exposure to both biotic and abiotic stresses (Lorenzo *et al*., 2003); however, in the case of KBC, genes involved in ET biosynthesis, such as *ERF2* (ET response factor 2), have shown to be upregulated upon Psa infection (Wurms *et al*., 2017a), demonstrating that a synergistic effect occurs between ET and the JA in the *Actinidia*-Psa pathosystem. PR proteins are synthesised after pathogen attack as part of plants' systemic acquired resistance, and PR8, in particular, was already shown increase after exogenous treatment with MJ and SA just 1 dpi and until 15 dpi with Psa in *A. chinensis* (Zhang *et al*., 2010a; Cellini *et al*., 2014). In the current work, this gene was upregulated in iMJ, which could partially explain the high increase in total protein in these plants. Although total protein also increased in iSA, no significant alterations in *PR8* transcriptional levels were observed. Therefore, further PR proteins other than *PR8*, such as *PR1*, or other classes of proteins, such as heat shock proteins, could have contributed to this increase in total protein (Petriccione *et al*, 2013; Petriccione *et al*., 2014).

Accordingly, PCA demonstrated that both iMJ and iSA had a positive correlation with total proteins, but negatively correlated with total polyphenols, flavonoids and lignin. Moreover, iSA positively correlated with the expression of genes related to phenylpropanoids, and SA concentration in plant tissues, whereas iMJ showed a positive correlation with JA, ABA and ET pathways, clearly demonstrating that each compound activates distinct pathways inside plant tissues, which ultimately regulates the outcome of Psa colonization. A similar trend was observed by Michelotti *et al*. (2018), which observed that ASM treatment of *A. chinensis* plants without Psa infection was able to modulate 974 differentially expressed genes, of which 70 were further modulated by Psa-inoculation, suggesting that plant molecular responses to Psa is highly influenced by phytohormone regulatory mechanisms. These pieces of evidence should be taken into consideration and further explored to fully understand how kiwifruit plants respond to chemical elicitation and Psa infection, and how these molecular and metabolic mechanisms could be explored to increase plant tolerance to the disease.

5. Conclusion

Inoculation of kiwifruit plants with Psa had a negative effect on ABA concentration in plant tissues, which may be a coping strategy employed by infected plants to regulate stomatal activity as a way to impair bacterial entrance and proliferation. On the contrary, genes involved in phenylpropanoids biosynthesis and the JA pathway were upregulated in non-elicited Psa-infected plants, possibly to counteract increased JA pathway-related events induced by the bacteria.

Plants elicited with MJ prior to Psa inoculation had enhanced levels of Psa endophytic population in plant tissues, whereas SA application had the lowest. MJ treatment showed a positive correlation with JA, ABA and ET pathways, and negative correlation with the phenylpropanoids pathway. In contrast SA positively correlated with the phenylpropanoids and SA pathways. This demonstrates that each compound induces distinct metabolic resources involved in plant defensive pathways during Psa colonization, which ultimately regulates the extent of the infection. Also, given the important role of ABA in the regulation of stomata and other phytohormones, the positive correlation observed between MJ and ABA, known to negatively regulate the SA pathway, may contribute to the higher Psa endophytic population observed with MJ elicitation. Unravelling the role of host phytohormone balance in response to Psa infection could allow the selection of more promising elicitors that, by modulating these regulatory networks, increase plant tolerance to the pathogen.

CHAPTER 4

Developing novel control strategies

CHAPTER 4 - Sub-chapter 4.1

Nitrogen source impacts mineral accumulation and gene expression in young kiwifruit plants

Nitrogen source impacts mineral accumulation and gene expression in young kiwifruit plants

Abstract

Nitrogen (N) source may impact plant growth and development, but the processes underlying plant responses to nitrate and ammonium are still poorly understood. Here, *Actinidia chinensis* var. *deliciosa* 'Hayward' was grown hydroponically in three nutrient solutions differing in the source of N (214 µM of NO_3^-, 214 µM NH_4^+ or a mix with 107 µM NO_3^- and 107 µM NH_4^+). After 21 days, plants were analysed for: i) biometric parameters, ii) photosynthetic and secondary metabolites, iii) total protein and N concentrations, iv) mineral composition, and v) expression of genes related to oxidative stress (*SOD*, *APX*, *CAT, TLP1*), secondary metabolism (*F3H*, *LOX1*, *PAL, SAM*, *ICS1*, *JIH*) and N and mineral metabolism (*GLU1*, *GDH1, GAD1*, *MOT1*, *FER1*). Shoot and root length and fresh weight were not affected by the N source, but total chlorophyll and total carotenoids were significantly higher in plants grown with NO_3^-, compared with the other N sources (up to 1.7- and 2.5-fold, respectively). Soluble polyphenolics were also significantly higher in the roots of plants grown with NO_3^- (4.8-fold). In contrast, total protein and N concentrations were significantly lower in shoots and roots of NO_3^--supplied plants (by up to 0.2- and 0.7-fold, respectively). In general, NO_3^- and Mix led to the highest concentrations of P, K, Mg, Ca, Zn and Mn in plant tissues. Concordantly, gene expression analysis revealed the overexpression of *TLP1*, *GLU1*, *GAD1*, *MOT1* and *FER1* in NO_3^--supplied plants, demonstrating the activation of N and mineral uptake and remobilization in these plants. These results provide a novel insight into the biochemical and molecular processes triggered in kiwifruit plants when grown under different sources of N, revealing that the accumulation of several minerals is promoted by NO_3^- supplementation, either by itself or in a 1:1 combination with NH_4^+ (Mix).

1. Introduction

Nitrogen (N) is an essential macronutrient that constitutes up to 5% of total dry matter in plants, and it is an integral constituent of nucleic acids, proteins, enzymes, chlorophyll, and secondary metabolites, being a decisive factor for plant growth (Hawkesford *et al*., 2012). When under insufficient N levels, plants show impaired development and chlorosis (Pacheco *et al*., 2008; Gupta *et al*., 2013; Na *et al*., 2014; Tsabarducas *et al*., 2017). To avoid N limitations, *Actinidia chinensis* vines may require up to 450 kg ha^{-1} of N, making this element the major nutrient applied as a fertilizer to this crop (Buwalda *et al*., 1990). Nitrogen can be supplied in the form of nitrate (NO_3^-), ammonium (NH_4^+), or a combination of both, but its uptake and metabolism is very distinct. In plant tissues, NO_3^- is reduced by nitrate reductase generating NO_2^-, which is further reduced to NH_4^+. This last form can be directly assimilated

by glutamine synthetase to form glutamine, or be oxidized to NO_2^- and subsequently to NO_3^- by the nitrification pathway. While several plant species (e.g., quinoa and rapeseed) favour N uptake in the form of NO_3^- (Kammann *et al*., 2015; Hachiya *et al*., 2017), others (e.g., rice and tomato) benefit from NH_4^+, resulting in increased plant fitness (Horchani *et al*., 2010; Cao *et al*., 2018).

Although NH_4^+ is an important intermediate in many metabolic reactions, high concentrations of NH_4^+ in the soil or nutrient solution may lead to decreased net photosynthesis (Britto and Kronzucker, 2002). Photosynthetic rates of *Pinus radiata* seedlings decreased under higher NH_4^+:NO_3^- ratios, suggesting that when N uptake increased with the higher NH_4^+ supplies, Rubisco activity decreased (Bown *et al*., 2010). Contrarily to what occurs with photosynthesis, NH_4^+-supplied plants frequently show higher amino-acid and protein synthesis when compared to NO_3^- (Horchani *et al*., 2010; Borgognone *et al*., 2013). This occurs because NH_4^+ assimilation and metabolism are less time- and energy-consuming than NO_3^-, being rapidly incorporated into organic compounds, and also to avoid potentially toxic concentrations of free NH_4^+ in the xylem sap (Borgognone *et al*., 2013). Horchani *et al*. (2010), for example, demonstrated that root protein concentration in tomato plants increased when supplied with increasing NH_4^+ concentrations (from 2.5 to 10 mM), whereas leaf protein concentration was only increased when NH_4^+ concentrations were higher than 7.5 mM. On the contrary, under NO_3^- nutrition, protein concentration remained unchanged both in roots and leaves, independently of the dose applied (Horchani *et al*., 2010). Different N sources may also impact the synthesis of secondary metabolites, namely the phenolic compounds, which play important roles in plant growth regulation and response against oxidative stress (Kulbat, 2016). This partly occurs due to an apparent competition between protein and phenolics synthesis in plant tissues (Ibrahim *et al*., 2011; Qadir *et al*., 2017). In fact, total phenolic compounds were found to increase under limiting N fertilization (in the form of ammonium nitrate and urea) in *Lactuca sativa* and *Labisia Pumila*, possibly because low N fertilization impairs protein production, thus increasing the availability of phenylalanine for the production of these secondary metabolites (Ibrahim *et al*., 2011; Qadir *et al*., 2017). Also, under supra-optimal N supply, kiwifruit plants had lower phenolic content and total antioxidant capacity, with negative implications for disease tolerance and fruit shelf-life (Morton, 2013; Stefaniak *et al*., 2019).

Several studies have also shown that the form of N that is supplied to plants affects macronutrient availability (Bown *et al*., 2010; Hoopen *et al*., 2010; Na *et al*., 2014; Pedersen *et al*., 2019). For example, high NH_4^+ supply decreased the uptake of calcium (Ca), which can impair pericarp formation and affect fruit shelf-life (Mills *et al*., 2007; Pacheco *et al*., 2008), and also of potassium (K) and magnesium (Mg), with potential repercussions to plant secondary growth (Hoopen *et al*., 2010). This antagonistic effect results from the acidification of the rooting medium caused by NH_4^+, and from the competition between these cations for

assimilation and transport sites. Contrarily, NH_4^+ has been demonstrated to increase the uptake of other minerals including phosphorous (P), possibly because it induces higher solubility of Ca-phosphates, thus increasing the root assimilation of phosphate ions (Pedersen *et al*., 2019). Other nutrients such as manganese (Mn), zinc (Zn), boron (B) and iron (Fe) may also be impacted by the source of N nutrition (Broadley *et al*., 2012). For example, the concentration of Mn, Zn, B and Fe in *Solanum lycopersicum* and of Mn, Zn and Fe in *Olea europaea*, linearly increased with increasing NH_4^+ supply, but not with NO_3^- (Borgognone *et al*., 2013, Tsabarducas *et al*., 2017). Contrastingly to these pieces of evidence, strong antagonistic effects between Mn and Zn shoot concentrations and NH_4^+ were observed in *Triticum aestivum* and *T. durum* (Wang and Below, 1998). These impairments in mineral accumulation may have a negative impact in plant root to shoot biomass allocation, as under nutrient limitation biomass allocation to roots tends to be greater, thus increasing root to shoot ratio (Agren and Franklin, 2003). Garbin and Dillenburg (2008) reported that N deficiency symptoms, including increased root to shoot ratio and decreased chlorophyll concentration, were induced in *Araucaria angustifolia* when NO_3^- was provided alone as N source. Root to shoot ratio also increased in *O. europaea* supplemented with NO_3^- (Tsabarducas *et al*., 2017).

Nutrient imbalances can lead to the generation of reactive oxygen species (ROS), which may impair plant cellular homeostasis (Gill and Tuteja, 2010). To avoid oxidative damage, plants synthesize antioxidant enzymes directly involved in ROS detoxification, such as superoxide dismutase (SOD), catalase (CAT), ascorbate peroxidase (APX) and glutathione reductase (GR) (Sharma *et al*., 2012). Increasing N supply has led to higher CAT activity in *Oryza sativa* and *Coffea arabica*, APX in *Coffea arabica* and *Psidium guajava* and GR in *Brassica oleracea* (Huang *et al*., 2004; Łata, 2014; Reis *et al*., 2015; Lima *et al*., 2018). In kiwifruits orchards, it has been suggested that in soils with lower N concentration (30 mg kg^{-1}, as compared with 50-80 mg kg^{-1} soil) the antioxidant system shifts towards enzymatic defences to maintain non-enzymatic antioxidants at a steady level, leading to lower antioxidant capacity (Stefaniak *et al*., 2020).

Knowledge on how plants regulate their morphological and physiological processes under different N-source supplies, as well as their relationship with metabolic pathways and nutrient balance, is of utmost importance to promote plant fitness and increase nutrient use efficiency. Some of these processes have been previously studied, but they mostly focused on one or two levels of integration. Thus, this study aimed to perform a more comprehensive analysis of the effects of the N source at different levels of plant processes, allowing a better knowledge integration. To this end, in this study, *A. chinensis* var. *deliciosa* ‘Hayward’ plants were grown under three distinct N sources (NO_3^-, NH_4^+ or 1:1 Mix), and evaluated for a broad range of responses including: i) biometric parameters (plant height, fresh weight and shoot to root ratio), ii) metabolites related with photosynthesis (total chlorophylls) and secondary

metabolism (carotenoids, total soluble polyphenolics, flavonoids and lignin), iii) total protein concentration, iv) macro (N, P, K, Mg, Ca) and micronutrient (Bo, Zn, Mn and Fe) composition, and v) expression of genes related with oxidative stress (*SOD*, *APX*, *CAT* and *TLP1*), secondary metabolism (*F3H*, *LOX1*, *PAL*, *SAM*, *ICS1* and *JIH*) and N and mineral metabolism (*GLU1*, *GDH1*, *GAD1*, *MOT1* and *FER1*).

2. Material and methods

2.1. Plant maintenance

Micropropagated plants of *A. chinensis* var. *deliciosa* 'Hayward' were obtained from QualityPlant - Investigação e Produção em Biotecnologia Vegetal, Lda. (Castelo Branco, Portugal). Plants were transferred to Murashige and Skoog rooting medium with 0.7% agar, complemented with 20 g L^{-1} of sucrose and 0.3 mg L^{-1} of indole-3-butyric acid (adjusted to a pH 5.7 with KOH) (Bourrain, 2018), where they were maintained for one month in a climate chamber (Aralab Fitoclima 10 000EHF, Aralab, Rio de Mouro, Portugal) with a 16 h light photoperiod at 22 °C, providing 325 µmol s^{-1} m^{-2} of photosynthetic photon flux density, and 8 h dark at 19 °C.

Thereafter, plants were transferred to a hydroponic solution (1.2 mM KNO_3; 0.8 mM $Ca(NO_3)_2$; 0.2 mM $MgSO_4$; 0.3 mM; $NH_4H_2PO_4$; 25 mM $CaCl_2$; 25 mM H_3BO_3; 0.5 mM $MnSO_4$; 2 mM; $ZnSO_4$; 0.5 mM $CuSO_4$; 0.5 mM MoO_3; 0.1 mM $NiSO_4$), being kept under the same environmental settings. After seven days of acclimation to the hydroponic conditions, plants were distributed among three distinct hydroponic solutions with the same N concentration, differing only in the type of its source: 214 µM NO_3^-, 214 µM NH_4^+ or a mixture of both (Mix - 107 µM NO_3^- + 107 µM ppm NH_4^+), as in Gupta *et al*. (2017). The choice of using hydroponic conditions (rather than soil or substrate) was made to allow complete control of the root zone and nutrient supply. For each N treatment, five biological replicates were used.

2.2. Plant sampling and biometric analysis

Twenty-one days after transferring to the hydroponic system with different N sources, plants were removed from the solution, carefully washed with deionized water and dissected into shoots and roots. The biometric analysis was performed by measuring shoot and root length and fresh weight, which were used to calculate shoot to root ratios. Afterwards, each plant tissue (shoot or root) was individually flash-frozen in liquid nitrogen, ground with a mortar and pestle, and stored at -80 °C for further analysis.

2.3. Quantification of photosynthetic pigments and secondary metabolites

One hundred milligrams of freeze-dried sample were extracted with 1 mL of methanol at 80% (v/v). Samples were placed in an ultrasonic bath for 20 min, after which they were centrifuged at 15 000 g for 15 min. The resulting supernatant from shoots was used for the quantification of total chlorophylls and carotenoids. Supernatants from shoots and roots were used total soluble polyphenolics and flavonoids, while the sedimented biomass from shoots and roots was used for lignin quantification. Total chlorophyll, total soluble polyphenols, and lignin were quantified through spectrophotometric methods using adapted protocols from Sumanta *et al*. (2014), Marinova *et al*. (2005) and Fukushima and Hatfield (1999), as previously described by Nunes da Silva *et al*. (2020). Carotenoids (μg g^{-1} dry weight) were quantified as in Sumanta *et al*. (2014) by measuring sample absorbances at 470, 652 and 665 nm in a nanophotometer (Implen GmbH, München, Germany), and using the following formula:

$$\frac{1000Abs_{470} - 1.63(16.72Abs_{665} - 9.16Abs_{652}) - 104.96(34.09Abs_{652} - 15.28Abs_{665})}{221x\ biomass}$$

For flavonoids quantification, 2 mL of ultrapure water and 150 μL of 5% sodium nitrite were added to 100 μL of sample. After a 5 min incubation period at room temperature, 150 μL of 10% aluminium chloride, 1 mL of 1 M sodium hydroxide and 1.2 mL ultrapure water were added to each sample. Absorbance was recorded at 510 nm, and flavonoids concentration was determined through a catechin standard curve (Zhishen *et al*., 1999).

2.4. Total protein, nitrogen and mineral analysis

Total N was quantified after sample combustion in an oxygen-rich high-temperature environment using a Leco N analyser (Model FP-528, Leco Corporation, St. Joseph, USA) (Valente *et al*., 2019). Protein content was calculated considering an N-to-protein conversion factor of 5.5 (Mariotti *et al*., 2008). Mineral composition (phosphorous- P, potassium - K, magnesium - Mg, calcium - Ca, boron - B, zinc - Zn, manganese - Mn, and iron - Fe) was evaluated as described by Santos *et al*. (2015). Briefly, one hundred mg of dried plant tissue (root and shoot) were mixed with 5 mL of 65% HNO_3 and 1 mL of H_2O_2 in a Teflon reaction vessel and heated in a SpeedwaveTM MWS-3+ (Berghof, Germany) microwave system. Digestion procedure was conducted in five steps, consisting of different temperature and time sets: 130 °C for 10 min, 160 °C for 15 min, 170 °C for 12 min, 100 °C for 7 min, and 100 °C for 3 min. After digestion, the resulting solutions were diluted with ultrapure water until a final sample volume of 20 mL. Mineral concentration determination was performed using inductively coupled plasma optical emission spectrometry (ICP-OES Optima 7000 DV, PerkinElmer, USA) with radial configuration.

2.5. Gene expression

Total RNA was extracted from shoot and root tissues according to an adapted protocol from Cellini *et al*. (2014), and single-stranded cDNA was synthesized using iScript cDNA Synthesis Kit (Bio-Rad, California, USA), as described by Nunes da Silva *et al*. (2020). Fifteen genes (Table 1) were selected to be used as reporter genes for: i) plant response to stress (superoxide dismutase - *SOD*; ascorbate peroxidase - *APX*; catalase - *CAT* and thaumatin-like protein 1 - *TLP1*); ii) secondary metabolism (flavanone 3-hydroxylase - *F3H*; lipoxygenase 1 - *LOX1,* phenylalanine ammonia-lyase - *PAL*; S-adenosylmethionine synthetase - *SAM*; isochorismate synthase 1 - *ICS1* and jasmonoyl-isoleucine-12-hydrolase - *JIH*); and iii) N and mineral metabolism (glutamate synthase 1 - *GLU1*; glutamate dehydrogenase 1 - *GDH1*; glutamate decarboxylase 1 - *GAD1*; molybdate transporter 1 - *MOT1* and ferritin 1 - *FER1*).

Primers for *F3H* (accession number: FJ542819), *GLU1* (AT5G04140), *GDH1* (AT5G18170), *GAD1* (AT5G17330), *FER1* (AT5G01600) and *MOT1* (AT2G25680) were designed using Primer3 for an expected PCR product of 100-200 bp and primer annealing temperatures between 56 and 58 °C, whereas primer sequences for *APX*, *CAT*, *SOD, JIH*, *ICS1*, *PAL*, *PR8, LOX1, TLP1* and *SAM* were obtained from other published studies (Cellini *et al*., 2014; Petriccione *et al., 2*015; Wurms *et al*., 2017; Nunes da Silva *et al*., 2019) (Table 1). Reverse transcription quantitative real-time polymerase chain reactions (RT-qPCR) were performed on a StepOne Real-Time PCR System (Applied Biosystems, California, USA) and the comparative CT method (ΔCT) (Schmittgen *et al*., 2000) was used for the relative quantification of gene expression values, with the housekeeping genes actin (*ACT*) and protein phosphatase 2A (*PP2A*) as control transcript (Petriccione *et al*., 2015). For relative gene expression analysis, the minimum fold change with physiological significance was considered to be two (Vaerman *et al*., 2004). For all target genes, three randomly-selected biological replicates and two technical replicates were analysed.

2.6. Statistical analysis

Data were analysed with GraphPad Prism version 6.0 (GraphPad Software, Inc., California, USA) with significant differences between treatments being determined by analysis of variance (One-Way ANOVA) followed by Fisher's LSD test ($p < 0.05$). Heatmap representation of relative gene expression was produced in Multiple Experiment Viewer version 4.9.0 (Dana-Farber Cancer Institute, Boston, USA).

Table 1 - Primer sequences and annealing temperature (T_{ann}) of housekeeping and target genes used for RT-qPCR analysis.

Gene		Primer sequence (5′-3′)		T_{ann} (ºC)	Reference
		Forward	Reverse		
Housekeeping genes					
ACT	Actin	CCAAGGCCAACAGAGAGAAG	GACGGAGGATAGCATGAGGA	56.0	Ledger *et al*., 2010
PP2A	Protein phosphatase 2A	GCAGCACATAATTCCACAGG	TTTCTGAGCCCATAACAGGAG	55.2	Nardozza *et al*., 2013
Response to stress					
SOD	Superoxide dismutase	CACAAGAAGCACCACCAGAC	TCTGCAATTTGACGACGGTG	57.8	Petriccione *et al*., 2015
APX	Ascorbate peroxidase	GGAGCCGATCAAGGAACAGT	AACGGAATATCAGGGCCTCC	57.8	
CAT	Catalase	GCTTGGACCCAACTATCTGC	TTGACCTCCTCATCCCTGTG	56.9	
TLP1	Thaumatin-like protein 1	CAACCCCCTAACACACTAGC	ATTTCCGGAGTTGCAACAGT	54.6	Nunes da Silva *et al*., 2019
Secondary metabolism					
F3H	Flavanone 3-hydroxylase	TTTGCCGTAAGATCGTGGAG	CCTGAAGATGACTGGACACG	56.8	This study
LOX1	Lipoxygenase 1	GTTAGAGGGGTGGTGACTCT	CTTTAGCACTGCTTGGTTGC	53.5	Nunes da Silva *et al*., 2019
PAL	Phenylalanine ammonia-lyase	CGGAGCAACACAACCAAGA	CCTGACATAGTGCGACTACATAG	55.2	Cellini *et al*., 2014
SAMs	S-adenosylmethionine synthetase	GAATAGTACTTGCCCCTGGC	TACAAATCGACCAGAGGGGT	55.1	Nunes da Silva *et al*., 2019
ICS1	Isochorismate synthase 1	AGGCGAGGCTTCTAATTG	ACAGCAAACTCACTCTCTC	47.8	Cellini *et al*., 2014
JIH	Jasmonoyl-isoleucine-12-hydrolase	CGGCTCTGATCTGGTTTTTC	CCTCATGCTCTCACTCAACG	55.8	Wurms *et al*., 2017b
N and mineral metabolism					
GLU1	Glutamate synthase 1	TTCAGGGGCTAAGGCAGTTG	CACCACTCATACCAGCAGCA	57.8	This study
GDH1	Glutamate dehydrogenase 1	TGATGGCACTTTGGCTTCTT	ACCGTACGGGATATTGGCTA	56.4	
GAD1	Glutamate decarboxylase 1	GGAAGCGGCGTATCAGATCA	TCTGAAGTTCGGTGGTGACG	59.0	
MOT1	Molybdate transporter 1	ATGGAGCTGGTGGTTTAGCC	ATAGTAGCAATGCCCCGAGC	57.5	
FER1	Ferritin 1	CTGCTTCTCCGTCGGTTTCT	TTCGAAAGGCTGGAACACGA	59.1	

3. Results

3.1 Plant growth, photosynthetic pigments and secondary metabolites

Shoot and root length did not vary significantly between N treatments, with plants ranging between 6.9 to 7.9 cm of shoot height and 13.4 to 14.8 cm of root length (Fig. 1A). Accordingly, shoot and root biomass were also statistically similar among treatments (Fig. 1B). This resulted in similar shoot to root ratios, which were also not significantly affected by the N treatment (Fig. 1C).

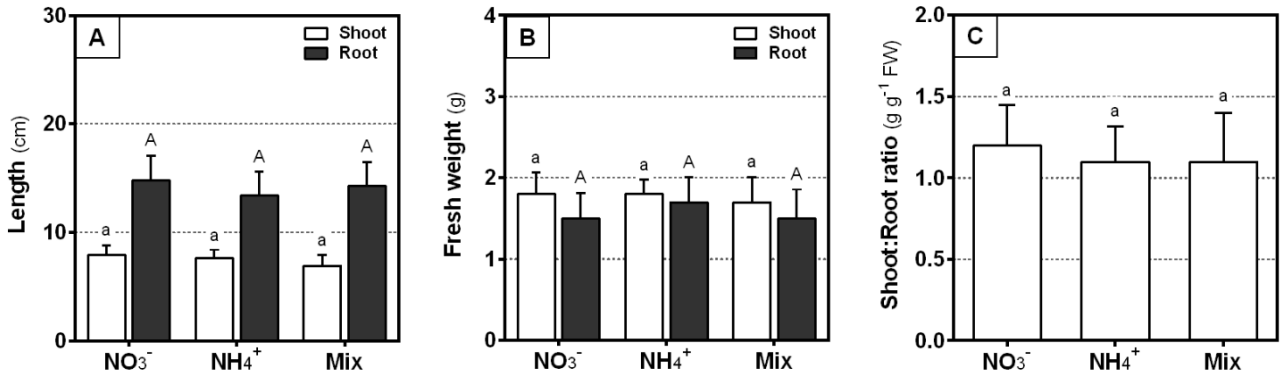

Figure 1 - Shoot and root length (A), fresh weight (B) and shoot to root ratio (C) of *A. chinensis* var. *deliciosa* 'Hayward' plants grown with 214 μM NO_3^-, 214 μM NH_4^+ or 107 μM NO_3^- + 107 μM NH_4^+ (Mix) for 21 days. Each value represents the mean of five biological replicates and vertical bars the standard error of the mean. Within each plant tissue, bars showing different letters are statistically different at $p < 0.05$.

Unlike the plant growth parameters, the source of N had a significant effect on leaf photosynthetic pigments. Plants grown with NO_3^- as the N source showed a significantly higher total chlorophyll concentration as compared to NH_4^+ or Mix (by 1.7- and 1.4-fold respectively) (Fig. 2A). Similarly, carotenoids concentration was also significantly higher in NO_3^--supplied plants than in NH_4^+ and Mix (by 2.5- and 1.5-fold, respectively) (Fig. 2B).

Total soluble polyphenolics concentration in plant roots were also significantly influenced by the source of N, being *ca*. 4.8-fold higher with NO_3^- (reaching 5.4 mg g^{-1}, compared with only *ca*. 1.1 mg g^{-1} in the other N treatments), whereas in shoots no significant differences were observed among N sources (Fig. 3A). Flavonoids were not significantly affected by the N source and were consistently higher in shoots than in roots (Fig. 3B). Lignin concentration was also not influenced by the source of supplied N, being generally higher in roots than in shoots (Fig. 3C).

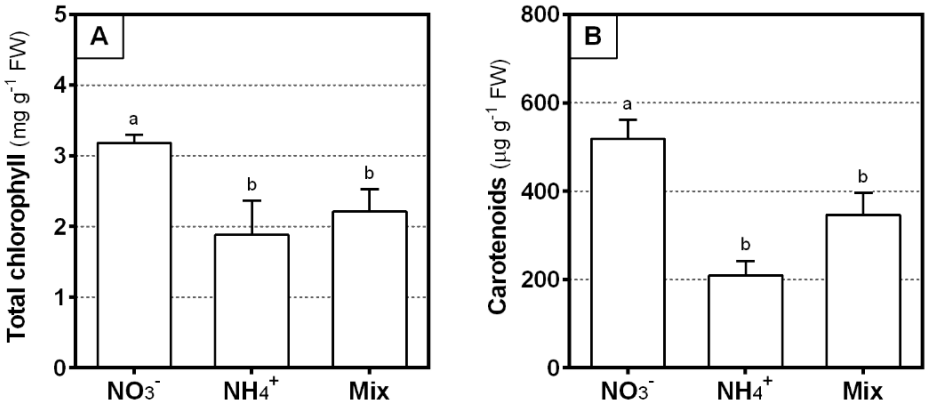

Figure 2 - Total chlorophyll (A) and carotenoids (B) concentrations in shoots of *A. chinensis* var. *deliciosa* 'Hayward' plants grown with 214 µM NO_3^-, 214 µM NH_4^+ or 107 µM NO_3^- + 107 µM NH_4^+ (Mix) for 21 days. Each value represents the mean of five biological replicates and vertical bars the standard error of the mean. Bars showing different letters are statistically different at $p < 0.05$.

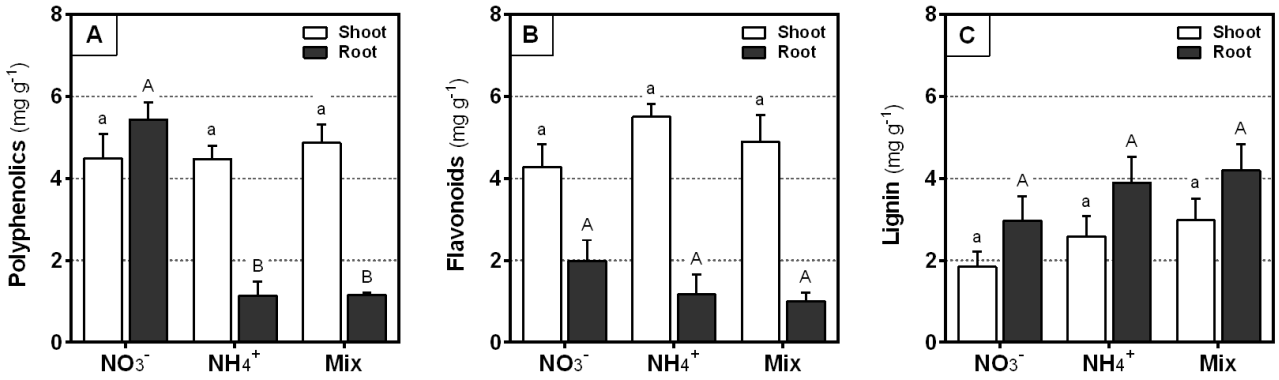

Figure 3 - Total soluble polyphenolics (A), flavonoids (B) and lignin (C) concentrations in shoots and roots of *A. chinensis* var. *deliciosa* 'Hayward' plants grown with 214 µM NO_3^-, 214 µM NH_4^+ or 107 µM NO_3^- + 107 µM NH_4^+ (Mix) for 21 days. Each value represents the mean of five biological replicates and vertical bars the standard error of the mean. Within each plant tissue, bars showing different letters are statistically different at $p < 0.05$.

3.2 Total protein, nitrogen and mineral concentration

Although total protein did not differ between shoots and roots of the same N treatment, plants grown with NO_3^- showed the lowest concentrations of total protein in both plant tissues, when compared with the other N sources (up to 0.2-fold lower) (Fig. 4A). Similarly, N concentration in shoots and roots was also significantly lower in NO_3^--supplied plants, than in NH_4^+ or Mix-supplied ones (resulting in up to 0.4-fold lower N concentration in shoots and 0.7-fold in roots) (Fig. 4B).

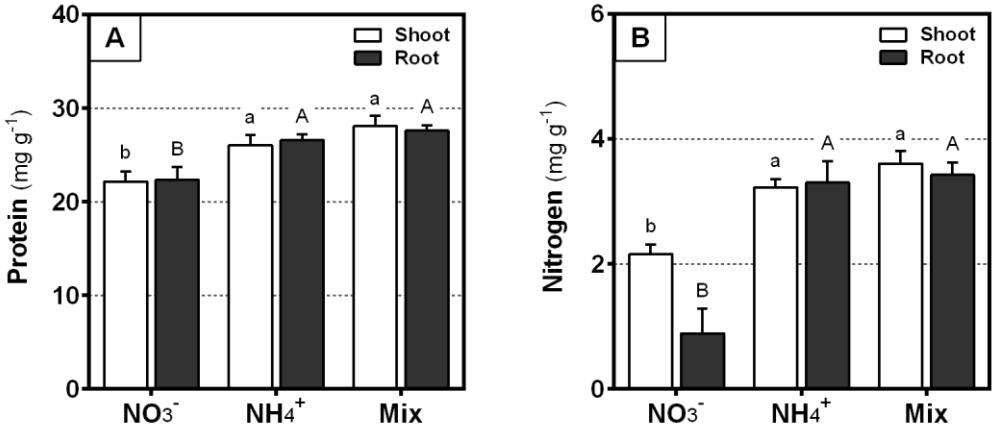

Figure 4 - Total protein (A) and total nitrogen (B) concentrations in shoots and roots of *A. chinensis* var. *deliciosa* 'Hayward' plants grown with 214 μM NO_3^-, 214 μM NH_4^+ or 107 μM NO_3^- + 107 μM NH_4^+ (Mix) for 21 days. Each value represents the mean of five biological replicates and vertical bars the standard error of the mean. Within each plant tissue, bars showing different letters are statistically different at $p < 0.05$.

Shoot and root mineral concentration was significantly influenced by the source of N supplied, with plants grown with NO_3^- and Mix generally showing higher concentrations of most of the minerals under study (Table 2). NO_3^- resulted in enhanced P, K, Mg and Ca concentrations in plant shoots and, along with Mix, in enhanced Mg, Ca and Mn in the roots. Mix supply also resulted in significantly higher concentrations of P, K, B, Zn and Fe in roots, whereas NH_4^+ only favoured the accumulation of B and Fe in roots.

3.3. Gene expression analysis

Concerning the relative expression of genes related to plant responses to stress, the most pronounced effect of the source of N was observed in *TLP1*, which was upregulated (by 2.7-fold) in the roots of NO_3^--supplied plants (Fig. 5). Regarding the genes involved in plant secondary metabolism, the only significant effect was observed in *SAM* expression, which was upregulated (by 2.7-fold) in shoots of NH_4^+-supplied plants. Amongst genes related with N and mineral metabolism, in NO_3^--supplied plants *GLU1*, *GAD1*, *FER1* and *MOT1* were upregulated in shoots (by 2.7-, 3.6-, 2.5- and 4.5-fold, respectively), and *GAD1* and *FER1* in roots (by 4.0- and 2.2-fold, respectively). *SOD*, *APX, CAT*, *F3H*, *LOX1*, *PAL*, *ICS1*, *JIH* and *GDH1* remained within their basal threshold of expression (from 0.5- to 2-fold), both in plant shoots and roots, and were not significantly affected by the N source).

Table 2 - Shoot and root mineral concentration in *A. chinensis* var. *deliciosa* 'Hayward' plants grown with 214 μM NO_3^-, 214 μM NH_4^+ or 107 μM NO_3^- + 107 μM NH_4^+ (Mix) for 21 days. Values represent the mean of five biological replicates ± standard error of the mean. Within each row and plant tissue, different letters represent statistically different means at $p < 0.05$.

	Mineral (mg g^{-1})	NO_3^-	NH_4^+	Mix	*p-value*
Shoot	**P**	3.36 ± 0.27 [a]	1.79 ± 0.30 [b]	1.94 ± 0.24 [b]	**0.0016**
	K	26.44 ± 0.75 [a]	20.50 ± 1.07 [b]	17.34 ± 3.30 [b]	**0.0387**
	Mg	2.17 ± 0.41 [a]	1.29 ± 0.19 [b]	0.81 ± 0.06 [b]	**0.0076**
	Ca	12.31 ± 1.97 [a]	4.51 ± 1.00 [b]	6.49 ± 1.74 [b]	**0.0107**
	B	0.017 ± 0.001 [b]	0.030 ± 0.001 [a]	0.010 ± 0.003 [c]	**< 0.0001**
	Zn	0.024 ± 0.004	0.014 ± 0.004	0.028 ± 0.004	0.0672
	Mn	0.11 ± 0.02	0.09 ± 0.01	0.10 ± 0.02	0.4435
	Fe	0.12 ± 0.02 [b]	0.30 ± 0.02 [a]	0.20 ± 0.03 [b]	**0.0011**
Root	**P**	5.43 ± 1.02 [b]	6.06 ± 0.23 [b]	8.81 ± 0.58 [a]	**0.0080**
	K	53.63 ± 2.38 [b]	48.06 ± 0.65 [b]	64.74 ± 5.77 [a]	**0.0162**
	Mg	5.34 ± 0.57 [a]	2.56 ± 0.37 [b]	5.76 ± 0.58 [a]	**0.0010**
	Ca	8.33 ± 0.62 [a]	3.37 ± 1.03 [b]	9.79 ± 0.88 [a]	**0.0002**
	B	0.011 ± 0.001 [b]	0.008 ± 0.001 [b]	0.016 ± 0.001 [a]	**0.0002**
	Zn	0.35 ± 0.04 [b]	0.21 ± 0.01[b]	0.58 ± 0.07 [b]	**0.0002**
	Mn	0.59 ± 0.01 [a]	0.34 ± 0.03 [b]	0.42 ± 0.04 [b]	**< 0.0001**
	Fe	2.99 ± 0.05 [b]	4.11 ± 0.48 [b]	8.09 ± 0.71 [a]	**< 0.0001**

4. Discussion

4.1 NH_4^+ reduced total chlorophyll, carotenoids and polyphenolics

In the present work, plant growth was not affected by the source of N supply (Fig. 1). Nonetheless, total chlorophyll and carotenoids concentrations were lower in plants grown with NH_4^+ and Mix, as compared with NO_3^- (Fig. 2). Previous studies have shown that kiwifruit plants supplied with NH_4Cl or NH_4NO_3 were smaller and had lower leaf area, as compared to NO_3^-, possibly due to lower ascorbic acid concentrations that lead to stunted growth (Rinallo and Modi, 2002). On the other hand, this phenomenon may also result from NO_3^- acting as a signalling molecule in roots, which promotes the auxin pathway and propels plant growth (Mounier *et al.,* 2014).

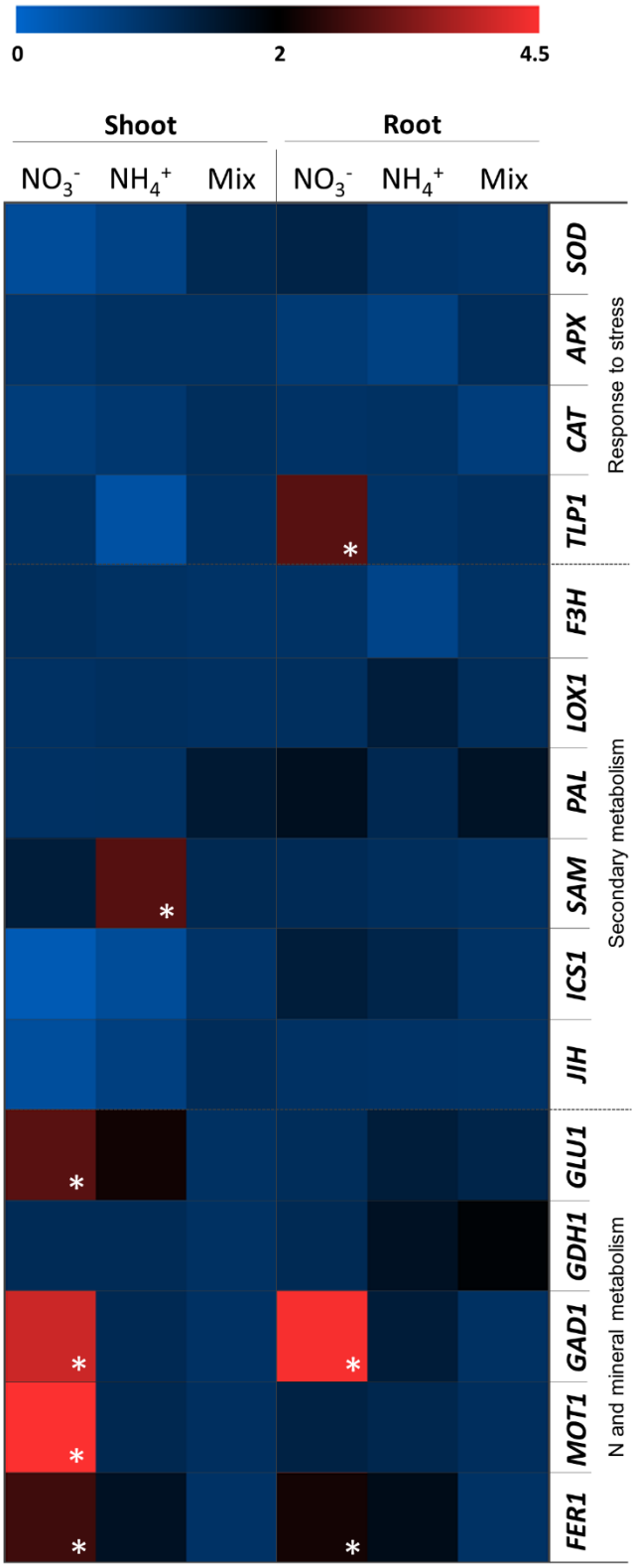

Figure 5 - Heatmap of the relative fold of expression of genes *SOD*, *APX*, *CAT*, *TLP1*, *F3H*, *LOX1*, *PAL*, *SAM*, *ICS1*, *JIH*, *GLU1*, *GDH1, GAD1, MOT1* and *FER1* in shoots and roots of *A. chinensis* var. *deliciosa* 'Hayward' plants grown with 214 μM NO_3^-, 214 μM NH_4^+ or 107 μM NO_3^- + 107 μM NH_4^+ (Mix) for 21 days. Asterisks indicate significant differences between the expression of each target and housekeeping genes (actin - *ACT* and protein phosphatase 2A - *PP2A*), at $p < 0.05$. In blue: no alteration or downregulation of gene expression; in black/red: upregulation of gene expression.

Besides, NH_4^+ may have a detrimental effect on plant growth by inhibiting photosynthesis due to the higher demand for carbon skeletons to detoxify excess NH_3 in plants supplied with NH_4^+ as sole N source (Britto and Kronzucker, 2002). Higher photosynthetic rates were observed in kiwifruit plants supplied with 25% NH_4^+:75% NO_3^- when compared with 75% NH_4^+: 25% NO_3^- (Tabatabaei *et al*., 2006), probably due to changes in the activity of photosynthesis-related enzymes such as phosphoenolpyruvate and ribulose 1,5-bisphosphate (Raab and Terry, 1994). This phenomenon possibly explains the higher concentrations of total chlorophylls in NO_3^--supplied plants observed in the present work. We hypothesise that a longer duration of the experimental period would possibly result in significant differences in terms of plant growth.

Although many studies have attempted to explain the metabolic networks involved in plant N metabolism, the exact mechanisms involved and the factors controlling these processes are still controversial. In this work, roots of NO_3^--supplied plants showed a higher concentration of soluble polyphenolics (Fig. 3A), which is probably due to the lower N concentration observed in these plants (Fig. 4B). Accordingly, Ibrahim *et al*. (2011) and Qadir *et al*. (2017) showed that total polyphenols were higher under limiting N fertilization, possibly because low N fertilization increases the availability of phenylalanine for the production of polyphenols at the expense of protein biosynthesis (Ibrahim *et al*., 2011; Qadir *et al*., 2017). Concerning the effect of N supply on flavonoids content, some studies demonstrated a negative correlation between these parameters in lettuce and *Arabidopsis* plants (Becker *et al*., 2015; Lea *et al*., 2016; Munene *et al*., 2017). It has also been found that in *Populus* spp. lignin decreases with higher N supply, possibly because more carbon is partitioned into cellulose required for plant growth (Novaes *et al*., 2009). Lignification was also strongly increased in and around the xylem vessels of nitrogen-deficient *Nicotiana* plants, but in *Populus trichocarpa* lignin concentration was unaffected by the N supply (Euring *et al*., 2012), which is in accordance with the findings from the present study. This suggests that the outcome of the N source on plant secondary metabolism, including flavonoids and lignin, is highly influenced by the plant species. The higher protein concentrations observed in NH_4^+- and Mix-supplied plants of the present study probably result from the active N transport between and within plant tissues, as these treatments also resulted in higher N concentration in shoots and roots. Previous works in other plant species reported an increase in amino-acid and protein synthesis with NH_4^+ supply, as compared with NO_3^- (Horchani *et al*., 2010; Borgognone *et al*., 2013). This occurs because NH_4^+ has a less time- and energy-consuming metabolism than NO_3^-, and is quickly transported from roots to shoots as amino acids, proteins and other organic N compounds to e.g., avoid toxic concentrations of free NH_4^+ in the xylem sap (Borgognone *et al*., 2013). Our results demonstrate that these processes occur in a similar manner in kiwifruit plants, also suggesting a relationship between plant

polyphenolics, total N and total protein in the responses of this plant species to different sources of N.

4.2 NO_3^- and Mix increased the concentration of several minerals in plant tissues

Along with N, P and K are also important in plant growth and metabolism, e.g., as components of macromolecular structures (Hawkesford *et al*., 2012). In the present work, higher P and K concentrations were observed in the shoots of NO_3^- and roots of Mix-supplied plants (Table 2), which may result from the co-transportation of NO_3^- and P and K, as well as to competition with NH_4^+ (Zhang *et al*., 2010a). In fact, several studies have reported deficient K uptake in response to NH_4^+ supplementation as the sole N source, mostly because NH_4^+ and K^+ have similar charges and hydrated diameters, resulting in competition for the same transportation sites (Na *et al*., 2014). Mg and Ca concentrations were also higher in plants grown with NO_3^- (in both shoots and roots) and Mix (only in roots), as compared with NH_4^+. These results are in agreement with previous observations in *O. europaea,* S*. lycopersicum*, *Acer pseudoplatanus*, and *Calamagrostis villosa*, in which Ca and Mg concentrations decreased when N was exclusively provided as NH_4^+ in the nutrient solution (Gloser and Gloser, 2000, Borgognone *et al*., 2013, Tsabarducas *et al*., 2017). Boron and Fe were significantly higher in shoots of NH_4^+-supplied plants and roots of plants supplied with Mix source of N. Similar findings were reported in *S. lycopersicum* and *O. europaea*, in which B and Fe linearly increased with increasing NH_4^+ concentrations, but not with NO_3^- (Borgognone *et al*., 2013, Tsabarducas *et al*., 2017). Taken together, data shows that when kiwifruit plants are supplied with NO_3^- (either as the sole N source or as a 1:1 Mix), there is a generally positive effect on the accumulation of P, K, Mg, Ca and Mn in plant tissues, with Zn accumulation also being promoted in by a Mix N supply.

4.3. The N source influenced the regulation of plant genetic resources

The reporter genes for plant antioxidant system *SOD*, *APX* and *CAT* were not significantly impacted by the source of N supply (Fig. 5), suggesting that although plants responded differently according to the source of N, they were not under significant oxidative stress. Nevertheless, increased expression of gene *TLP1* was observed in the roots of NO_3^--supplied plants, probably as part of plants' osmotolerance mechanisms. Thaumatin-like proteins, e.g., osmotin, have been linked with osmoregulation in plants, which is often affected by NO_3^- due to increased assimilation of several minerals and water uptake (Deak and Malamy, 2005; Guo *et al., 2*007).

SAM is the key enzyme involved in the biosynthesis of S-adenosylmethionine, which is involved in plant development, response to abiotic or biotic stress, and metabolism, and has been linked to modulating plant polyamine metabolism, promoting nutrient balance and plant homeostasis (Gong *et al*., 2014). Here, *SAM* transcriptional levels were significantly higher in shoots of NH_4^+-supplied plants, probably because these plants were attempting to cope with the decreased levels of several minerals, such as P, K, Mg, Ca and Mn, which were consistently lower in these tissues. Also, in the current work, *GLU1* and *GAD1*, involved in N assimilation and metabolism, respectively, were upregulated in NO_3^--supplied plants. This is in line with a previous work in potato plants that showed that *GLU1* was upregulated by increasing concentrations of NO_3^-, whereas NH_4^+ did not affect the expression of this gene (Zebarth *et al*., 2012). On the other hand, the substitution of KNO_3 for reduced forms of nitrogen (NH_4Cl, NH_4NO_3, glutamate or glutamine) did not affect *GAD1* transcriptional levels, but led to increased upregulation of *GAD2* and proteins in leaves, increasing total GAD specific activity in these structures (Kinnersley and Turano, 2000). Our results suggest that kiwifruit plants supplied with NO_3^- responded with the upregulation of *GLU1* and *GAD1* to counteract the lower total protein and N concentrations observed with this treatment. Similarly, *MOT1* and *FER1* transcriptional levels were also higher in NO_3^--supplied plants. *MOT1* plays an important role in Mo uptake, but also in N metabolism through the activation of nitrate reductase (Tomatsu *et al*., 2007; Ide *et al*., 2011). Thus, our results suggest that NO_3^--supplied plants were trying to cope with the lower N concentrations observed in their tissues by activating this enzyme. *FER1* gene, which encodes a protein-iron complex, ferritin, primarily acting as an iron storage molecule (Bournier *et al*., 2013), was upregulated in NO_3^--supplied plants, most likely to promote Fe accumulation in plant tissues (as this N source resulted in the lower Fe concentrations).

5. Conclusion

Although the importance of N in plant growth and development has been well documented, knowledge on how plants under different N sources regulate their morphological, physiological and molecular processes, and the relationship with nutrient balance, is still far from being understood. In the current work, the N source (NO_3^-, NH_4^+ or 1:1 Mix) did not affect plant growth, but NO_3^- led to higher total chlorophyll and carotenoids concentration. Contrastingly, NO_3^--supplied plants had lower protein and N concentrations in shoots and roots. Nevertheless, N supply in the form of NO_3^- or Mix induced the highest concentrations of several macro- and micro-nutrients in plant tissues (P, K, Mg, Ca, Zn and Mn), which was accompanied by the differential expression of genes related to osmoregulation and N and mineral metabolism. Compared with NH_4^+ alone, these results

demonstrate an overall positive effect of NO_3^- (either as the sole N source or provided as a 1:1 Mix) in plants' physiological and mineral status, supporting its potential to integrate N fertilization regimens that improve plant fitness and nutrient use efficiency.

Supplementary Material

SM 1 - Relative fold of expression of genes *SOD* (superoxide dismutase), *APX* (ascorbate peroxidase), *CAT* (catalase), *TLP1* (thaumatin-like protein 1), *F3H* (flavanone 3-hydroxylase), *LOX1* (lipoxygenase 1), *PAL* (phenylalanine ammonia-lyase), *SAM* (S-adenosylmethionine synthetase), *ICS1* (isochorismate synthase 1), *JIH* (jasmonoyl-isoleucine-12-hydrolase), *GLU1* (glutamate synthase 1), *GDH1* (glutamate dehydrogenase 1), *GAD1* (glutamate decarboxylase 1), *FER1* (ferritin 1), and *MOT1* (molybdate transporter 1) in shoots and roots of *A. chinensis* var. *deliciosa* 'Hayward' plants grown with 214 μM NO_3^-, 214 μM NH_4^+ or 107 μM NO_3^- + 107 μM NH_4^+ (Mix) for 21 days. Values represent the mean of three biological replicates ± standard error of the mean and, within each plant tissue and gene, different letters represent significant differences at $p < 0.05$. Biologically significant alterations in gene expression (as compared with housekeeping genes actin - *ACT* and protein phosphatase 2A - *PP2A*) are marked in bold.

	Shoot			**Root**		
	NO_3^-	**NH_4^+**	**Mix**	**NO_3^-**	**NH_4^+**	**Mix**
SOD	0.49 ± 0.06 ^{a}	0.68 ± 0.19 ^{a}	1.19 ± 0.17 ^{a}	1.30 ± 0.23 ^{a}	1.01 ± 0.09 ^{a}	0.97 ± 0.24 ^{a}
APX	0.92 ± 0.04 ^{a}	1.04 ± 0.25 ^{a}	1.03 ± 0.21 ^{a}	0.86 ± 0.06 ^{b}	0.72 ± 0.05 ^{b}	1.11 ± 0.13 ^{a}
CAT	0.79 ± 0.03 ^{a}	0.91 ± 0.08 ^{a}	1.09 ± 0.13 ^{a}	1.01 ± 0.10 ^{a}	1.03 ± 0.17 ^{a}	0.79 ± 0.19 ^{a}
TLP1	1.04 ± 0.22 ^{a}	0.40 ± 0.07 ^{a}	1.05 ± 0.26 ^{a}	**2.71 ± 0.78 ^{a}**	1.00 ± 0.33 ^{b}	1.07 ± 0.30 ^{b}
F3H	1.10 ± 0.12 ^{a}	1.04 ± 0.18 ^{a}	1.00 ± 0.06 ^{a}	1.02 ± 0.13 ^{a}	0.66 ± 0.20 ^{a}	1.01 ± 0.16 ^{a}
LOX1	1.02 ± 0.17 ^{a}	1.07 ± 0.27 ^{a}	1.05 ± 0.25 ^{a}	1.07 ± 0.24 ^{a}	1.42 ± 0.28 ^{a}	1.11 ± 0.40 ^{a}
PAL	1.02 ± 0.17 ^{a}	1.03 ± 0.18 ^{a}	1.50 ± 0.30 ^{a}	1.70 ± 0.39 ^{a}	1.20 ± 0.58 ^{a}	1.63 ± 0.35 ^{a}
SAM	1.42 ± 0.34 ^{ab}	**2.69 ± 0.74 ^{a}**	1.20 ± 0.27 ^{b}	1.16 ± 0.47 ^{a}	1.10 ± 0.34 ^{a}	1.03 ± 0.21 ^{a}
ICS1	0.23 ± 0.03 ^{a}	0.51 ± 0.11 ^{a}	0.98 ± 0.27 ^{a}	1.43 ± 0.29 ^{a}	1.28 ± 0.23 ^{a}	1.01 ± 0.13 ^{a}
JIH	0.47 ± 0.12 ^{a}	0.75 ± 0.14 ^{a}	1.13 ± 0.21 ^{a}	1.02 ± 0.15 ^{a}	1.01 ± 0.08 ^{a}	1.00 ± 0.05 ^{a}
GLU1	**2.71 ± 0.68 ^{a}**	**2.14 ± 0.57 ^{a}**	1.04 ± 0.23 ^{b}	1.12 ± 0.36 ^{a}	1.42 ± 0.29 ^{a}	1.27 ± 0.64 ^{a}
GDH1	1.15 ± 0.46 ^{a}	1.15 ± 0.37 ^{a}	1.03 ± 0.20 ^{a}	1.17 ± 0.47 ^{a}	1.65 ± 0.38 ^{a}	1.94 ± 0.45 ^{a}
GAD1	**3.62 ± 0.95 ^{a}**	1.18 ± 0.40 ^{b}	1.02 ± 0.17 ^{b}	**3.97 ± 1.21 ^{a}**	1.44 ± 0.63 ^{b}	1.04 ± 0.23 ^{b}
MOT1	**4.53 ± 1.20 ^{a}**	1.21 ± 0.55 ^{b}	1.06 ± 0.29 ^{b}	1.33 ± 0.67 ^{a}	1.23 ± 0.43 ^{a}	1.09 ± 0.35 ^{a}
FER1	**2.50 ± 0.62 ^{a}**	1.65 ± 0.31 ^{ab}	1.01 ± 0.12 ^{b}	**2.17 ± 0.58 ^{a}**	1.76 ± 0.27 ^{ab}	1.01 ± 0.14 ^{b}

CHAPTER 4 - Sub-chapter 4.2

Influence of the nitrogen source on the tolerance of kiwifruit plants to *Pseudomonas syringae* pv*. actinidiae*

Influence of the nitrogen source on the tolerance of kiwifruit plants to *Pseudomonas syringae* pv. *actinidiae*

Abstract

The type of nitrogen (N) source has consequences on plant nutritional status, which may affect the plant´s predisposition for pathogen infection. The lack of knowledge on how kiwifruit plants (*Actinidia* spp.) respond to infection by *Pseudomonas syringae* pv. *actinidiae* (Psa) when grown under different N sources, hinders the efficacy to optimize N supply in integrated approaches to mitigate the disease. Here, *A. chinensis* var. *deliciosa* plants were grown for 21 days in a nutrient solution differing only in the type of N source: 214 µM of NO_3^-, 214 µM NH_4^+ or a mixture of both (107 µM NO_3^- + 107 µM NH_4^+ - Mix), after which plants were inoculated with Psa. Fourteen days post-inoculation, plant growth was not affected by Psa infection, but plants grown with NO_3^- or Mix had higher shoot and root fresh weight, as compared with NH_4^+, accompanied by an increase in P, K, Mg, Ca and Mn concentration in plant tissues. Supplementation with NO_3^- led to lower Psa endophytic population in plant tissues, whereas NH_4^+ led to the highest infection rate (by 33-fold). NH_4^+ also resulted in: loss of photosynthetic capacity (by 0.3-fold), upregulation of *PR1*, involved in plant defence, and of *LOX1*, *SAM* and *PAL*, related with the jasmonic acid (JA), ethylene (ET) and phenylpropanoids pathways, respectively. Results suggest that with NH_4^+ Psa colonization is favoured by the higher N concentrations in plant tissues, accompanied by the upregulation of genes involved in the JA and ET pathways, known to antagonize plant defences. With NO_3^-, plant tolerance to the pathogen increases, most likely due to lower N accumulation and improved overall mineral nutrition. Therefore, the N source affects plant metabolic allocation strategies, leading to distinct outcomes in Psa infection, and should be taken into consideration for the successful management of the disease.

1. Introduction

Pseudomonas syringae pv. *actinidiae* (Psa) is the pathogen responsible for the kiwifruit bacterial canker (KBC), for which no curative methods have been developed yet. Currently used strategies consist of preventive measures, mostly based on cupric formulations, that often show low efficacy in latter stages of disease development, or environmental risks (Vanneste *et al*., 2011; Cameron and Sarojni, 2014). Several orchard management techniques, such as fertilization, have been shown to influence Psa incidence and epidemiology by impacting plant vegetative and reproductive performance (Vanneste *et al*., 2011; Mauri *et al*., 2016; Donati *et al*., 2020). However, the role of specific minerals and nutrients on the outcome of the disease has been scarcely addressed (Holmes, 2012; Gupta *et al*., 2015; Mowat *et al*., 2015; Mauri *et al*., 2016).

Albeit being the most important nutrient for plant growth, the role of nitrogen (N) on disease tolerance has been found non-conclusive, probably due to differences amongst different studies in the type of pathogen, plant species, source of N supply or application regimen (Hoffland *et al*., 2000; Huber *et al*., 2012a; Gupta *et al*., 2017). The main forms of N assimilated by plants are nitrate (NO_3^-) and ammonium (NH_4^+), but plant species have different adaptabilities to absorb and utilize these two N sources (Horchani *et al*., 2010; Kammann, *et al., 2*015; Hachiya *et al*., 2017; Cao *et al*., 2018). The assimilation mechanisms of these two ionic forms of N are distinct because, while NH_4^+ may be promptly assimilated into amino acids and other organic compounds after absorption, the use of NO_3^- by plants requires the presence of the enzymes nitrate reductase (for NO_3^- reduction to nitrite) and nitrite reductase (for the reduction of nitrite to NH_4^+). Thus, NO_3^- assimilation is a more demanding process in terms of time and energy (Haynes and Goh, 1978). In a previous study, we have found that the N source (supplied as 214 µM NO_3^-, 214 µM NH_4^+ or a 1:1 Mix for 21 days) affects the concentration of photosynthetic pigments, total N, total protein and minerals in healthy *A. chinensis* plants. In particular, NO_3^- supply led to higher total chlorophyll and carotenoids, lower total protein and total N, while favouring the accumulation of several macro- and micronutrients in plant tissues (Nunes da Silva *et al*., unpublished data). These differential responses may have downstream implications in plant responses to environmental stresses, such as bacterial pathogens.

Pathogenic invasions can also alter plant nutrient composition, since the pathogen itself needs and utilizes these nutrients, thus rendering the host more susceptible due to decreased nutrient availability. Mineral nutrients are involved in plant resistance against pathogens by being enzymatic co-factors in several metabolic pathways, modulating phytohormone regulation and the expression of defence-related genes (Dordas, 2008; Gupta *et al*., 2017). NO_3^- has been correlated with both constitutive and induced resistance traits by enhancing nitric oxide (NO) and salicylic acid (SA) accumulation, which is implicated in the effector-triggered immunity (ETI) by manipulating plant hypersensitive responses (HR) (Dietrich *et al*., 2004; Gupta *et al*., 2013). On the contrary, NH_4^+ seems to favour a metabolic reprogramming of HR-defences towards the production of sugars and 4-aminobutyric acid (Gupta *et al*., 2013). Studies on the effect of N supply on plant tolerance to pathogenic agents tend to report that higher N concentration increases susceptibility to obligate parasites and increases tolerance to facultative parasites (Dordas, 2008; Gupta *et al*., 2017). For example, with increasing concentrations of N, Howard *et al*. (1994) noted an increase of disease severity caused by *Puccinia graminis* on wheat, while Chase (1989) observed a decrease of disease severity caused by *Xanthomonas blight* in *Syngonium podophyllum* plants. Nevertheless, most studies fail to take into consideration the effect of the source of N supplied, which also may affect the outcome of infection (Huber *et al*., 2012a). In tomato plants, increased susceptibility to *P. syringae* pv. *tomato* and *Oidium lycopersicum* was

observed with higher N concentrations (provided as NO_3^-), although no effect on susceptibility to *Fusarium oxysporum* f.sp. *lycopersici* was observed (Hoffland *et al*., 2000). Contrastingly, high NO_3^- rates increased tobacco plant´s resistance to *P. syringae* pv. *phaseolicola* by promoting HR and cell death, as compared with NH_4^+ (Gupta *et al*., 2013). On the other hand, higher NH_4^+ rates increased disease symptoms caused by *Rhizoctonia solani* in sugar beets and *F. oxysporum* f.sp. *lycopersici* in tomato plants (Afanasiev and Carlson, 1942; Borrero *et al*., 2012).

Regarding kiwifruit plants, there is limited information on how N nutrition affects the plants' ability to tolerate Psa infection. High N fertilization is generally discouraged in kiwifruit orchards, as it seems to increase plant susceptibility to Psa, probably by increasing plant vigour and sprouting of new shoots (Costa *et al., 2*013; Donati *et al*., 2014; Mauri *et al*., 2016). The few reports that attempted to explore the role of different sources of N in *A. chinensis* responses to Psa utilized different supplementation and disease measurement methodologies, and provided limited information on plant physiological responses to the pathogen under those N conditions (Mowat *et al.,* 2015; Mauri *et al*., 2016). Mowat *et al*. (2015) reported that higher NO_3^- rates positively influenced *A. chinensis* var. *deliciosa* responses against Psa, whereas high NH_4^+ showed higher disease incidence and severity (cane collapse), 25 days post-inoculation (dpi). Mauri *et al*. (2016) did not observe significant differences in Psa endophytic populations between the N sources used (NH_4NO_3 or $(NH_4)_2SO_4$), although plants supplied with NH_4NO_3 showed generally higher disease incidence than a standard NPK fertilization (16N-8P-32K), 1 month after inoculation. Also, it is not clear whether Psa infection alters the balance of leaf nutrients when plants are grown under different sources of N (Mills *et al*., 2007; Holmes, 2012). As such, in the present work, we hypothesise that NO_3^- nutrition increases *A. chinensis* var. *deliciosa* 'Hayward' tolerance to Psa infection through its direct involvement in: i) plant growth; ii) photosynthetic capacity; iii) total protein, N and mineral accumulation; and iv) expression of genes related with plant response to stress, secondary metabolism and N metabolism.

2. Material and methods

2.1. Plant maintenance

Micropropagated plants of *A. chinensis* var. *deliciosa* 'Hayward' were obtained from QualityPlant - Investigação e Produção em Biotecnologia Vegetal, Lda (Castelo Branco, Portugal) and kept in a climate chamber (Aralab Fitoclima 10 000EHF, Aralab, Rio de Mouro, Portugal) with a 16 h light photoperiod at 22 °C, providing 325 µmol $s^{-1}m^{-2}$ of photosynthetic photon flux density, 8 h dark at 19 °C, and relative humidity of 75% throughout day and night

periods. Plants were transferred to Murashige and Skoog rooting medium with 0.7% agar, complemented with 20 g L^{-1} of sucrose and 0.3 mg L^{-1} of indole-3-butyric acid (adjusted to a pH 5.7 with KOH) (Bourrain, 2018), where they were kept for one month. Thereafter, plants were transferred to a hydroponic solution with optimal nutrient solution (1.2 mM KNO_3; 0.8 mM $Ca(NO_3)_2$; 0.2 mM $MgSO_4$; 0.3 mM; $NH_4H_2PO_4$; 25 mM $CaCl_2$; 25 mM H_3BO_3; 0.5 mM $MnSO_4$; 2 mM; $ZnSO_4$; 0.5 mM $CuSO_4$; 0.5 mM MoO_3; 0.1 mM $NiSO_4$) and seven days later to a hydroponic system with three distinct hydroponic solutions, differing only in the type of N supply: 214 µM NO_3^-, 214 µM NH_4^+ or a mixture of both (Mix - 107 µM NO_3^- + 107 µM ppm NH_4^+), as in Gupta *et al*. (2017). For each N condition, 12 biological replicates were used.

2.2. Inoculum preparation and plant inoculation

For artificial bacterial inoculation, Psa biovar 3 strain CFBP7286 was grown in Luria Bertani medium (LB) at 27 °C with shaking (75 rpm) for 16 h. On the day of inoculation, bacterial colonies were resuspended in sterile Ringer's solution and a 1-2x10^7 CFU mL^{-1} inoculum was prepared by measuring inoculum absorbance at 600 nm in a nanophotometer (Implen GmbH, Munich, Germany). Twenty-one days post transfer to each N solution, plants were inoculated with Psa or with Ringer's solution (mock-inoculated control plants), by dipping a sterile swab on the respective solution and rubbing the abaxial surface of each plant leaf three times. For each type of N solution and inoculum, six biological replicates were prepared.

2.3. SPAD scoring, sampling and biometric analysis

On the day of inoculation (day 0) and 3, 7, 10 and 14 days post-inoculation (dpi), leaf chlorophyll was measured non-destructively with a SPAD meter (502-Plus Chlorophyll Meter, Minolta corporation, Ltd., Osaka, Japan). For each plant, three readings of three independent leaves were recorded.

At the end of the assay, plants were removed from the hydroponics solution, carefully washed with deionized water and dissected into shoots and roots. The biometric analysis was performed by measuring shoot height, root length and shoot and root fresh weight (FW), which were used to extrapolate root to shoot ratios. After biometric analysis, a longitudinal half of each plant leaf was used for the determination of Psa endophytic population, and the remaining plant tissue was flash-frozen in liquid N and stored at -80 °C for subsequent metabolic, nutritional and gene expression analysis.

2.4. Determination of Psa endophytic population

Leaf samples (collected as described above) were surface sterilised, macerated in Ringer's solution, and used for CFU estimation through an adapted protocol from Cellini *et al*. (2014). Psa endophytic population was estimated taking into consideration CFU counting and tissue FW, as previously described by Nunes da Silva *et al*. (2020).

2.5. Total N, protein and mineral concentrations

Total N was quantified after sample combustion in an oxygen-rich high-temperature environment using a Leco N analyser (Model FP-528, Leco Corporation, St. Joseph, USA) (Valente *et al*., 2019). Protein content was calculated considering an N-to-protein conversion factor of 5.5 (Mariotti *et al*., 2008). Mineral composition (phosphorous- P, potassium - K, magnesium - Mg, calcium - Ca, boron - B, zinc - Zn, manganese - Mn, and iron - Fe) was evaluated as described by Santos *et al*. (2015). Briefly, 100 mg of dried plant tissue (root and shoot) were mixed with 5 mL of 65% HNO_3 and 1 mL of H_2O_2 in a Teflon reaction vessel and heated in a SpeedwaveTM MWS-3+ (Berghof, Germany) microwave system. Digestion procedure was conducted in five steps, consisting of different temperature and time sets: 130 °C for 10 min, 160 °C for 15 min, 170 °C for 12 min, 100 °C for 7 min, and 100 °C for 3 min. After digestion, the resulting solutions were diluted with ultrapure water until a final sample volume of 20 mL. Mineral quantification was performed using inductively coupled plasma optical emission spectrometry (ICP-OES Optima 7000 DV, PerkinElmer, USA) with radial configuration.

2.6. Gene expression

From the six biological replicates of each treatment, three were randomly selected for gene expression analysis. Total RNA was extracted following an adapted protocol from Cellini *et al*. (2014) and single-stranded cDNA was synthesized using iScript cDNA Synthesis Kit (Bio-Rad, California, USA), as described by Nunes da Silva *et al*. (2020). Eleven genes were selected to be used as reporters for: i) plant defence and response to stress (*SOD* - superoxide dismutase, *APX* - ascorbate peroxidase, *CAT* - catalase, *TLP1* - thaumatin-like protein 1, and *PR1* - pathogenesis-related protein 1); ii) secondary metabolism (*LOX1* - lipoxygenase 1, *PAL* - phenylalanine ammonia-lyase, and *SAM* - S-adenosylmethionine synthetase -); and iii) N metabolism (*GLU1* - glutamate synthase 1, *GDH1* - glutamate dehydrogenase 1, and *GAD1* - glutamate decarboxylase).

Table 1 - Primer sequences and annealing temperature (T_{ann}) of housekeeping and target genes used for RT-qPCR analysis.

Gene		Primer sequence (5′-3′)		T_{ann}	Reference
		Forward	Reverse	(ºC)	
Housekeeping genes					
ACT	Actin	CCAAGGCCAACAGAGAGAAG	GACGGAGGATAGCATGAGGA	56.0	Ledger *et al*., 2010
PP2A	Protein phosphatase 2A	GCAGCACATAATTCCACAGG	TTTCTGAGCCCATAACAGGAG	55.2	Nardozza *et al*., 2013
Response to stress					
APX	Ascorbate peroxidase	GGAGCCGATCAAGGAACAGT	AACGGAATATCAGGGCCTCC	57.8	Petriccione *et al*., 2015
CAT	Catalase	GCTTGGACCCAACTATCTGC	TTGACCTCCTCATCCCTGTG	56.9	
SOD	Superoxide dismutase	CACAAGAAGCACCACCAGAC	TCTGCAATTTGACGACGGTG	57.8	
PR1	Pathogenesis-related protein 1	GCCCCCGGTAAGGTTTGT	CGAACCAAGACCCACTATTGC	58.1	Cellini *et al*., 2014
TLP1	Thaumatin-like protein 1	CAACCCCCTAACACACTAGC	ATTTCCGGAGTTGCAACAGT	54.6	Nunes da Silva *et al*., 2019
Secondary metabolism					
LOX1	Lipoxygenase 1	GTTAGAGGGGTGGTGACTCT	CTTTAGCACTGCTTGGTTGC	53.5	Nunes da Silva *et al*., 2019
SAM	S-adenosylmethionine synthetase	GAATAGTACTTGCCCCTGGC	TACAAATCGACCAGAGGGGT	55.1	
PAL	Phenylalanine ammonia-lyase	CGGAGCAACACAACCAAGA	CCTGACATAGTGCGACTACATAG	55.2	Cellini *et al*., 2014
N metabolism					
GLU1	Glutamate synthase 1	TTCAGGGGCTAAGGCAGTTG	CACCACTCATACCAGCAGCA	57.8	This study
GDH1	Glutamate dehydrogenase 1	TGATGGCACTTTGGCTTCTT	ACCGTACGGGATATTGGCTA	56.4	
GAD1	Glutamate decarboxylase 1	GGAAGCGGCGTATCAGATCA	TCTGAAGTTCGGTGGTGACG	59.0	

Primers for *GLU1* (accession number: AT5G04140), *GDH1* (AT5G18170) and *GAD1* (AT5G17330) were designed using Primer3 for an expected PCR product of 100-200 bp and primer annealing temperatures between 56 and 58 ℃, whereas primer sequences for *APX*, *CAT*, *SOD, PAL*, *PR1, LOX1, TLP1* and *SAM* were obtained from published studies (Cellini *et al*., 2014; Petriccione *et al., 2*015; Nunes da Silva *et al*., 2019) (Table 1). Reverse transcription quantitative real-time polymerase chain reactions (RT-qPCR) were performed on a StepOne Real-Time PCR System (Applied Biosystems, California, USA) and the comparative CT method (ΔΔCT, Livak and Schmittgen, 2001) was used for relative gene expression quantification using actin (*ACT*) and protein phosphatase 2A (*PP2A*) as housekeeping genes and mock-inoculated control plants as reference samples (Nunes da Silva *et al*., 2020). For relative gene expression analysis, the minimum fold change with physiological significance was considered to be two (Vaerman *et al*., 2004). For each of the three biological replicates and target gene, two technical replicates were analysed.

2.7. Statistical analysis

Data were analysed with GraphPad Prism version 6.0 (GraphPad Software, Inc., California, USA) with significant differences between treatments being determined by analysis of variance (ANOVA) followed by Fisher's LSD test ($p < 0.05$). Heatmap representation of relative gene expression was produced in Multiple Experiment Viewer version 4.9.0 (Dana-Farber Cancer Institute, Boston, USA).

3. Results

3.1. Plant growth and SPAD scoring

Regarding plant height, root length (Fig. 1A) and root and shoot fresh-weight (Fig. 1B), no significant differences were observed between mock- and Psa-inoculated plants. Roots of NO_3^--supplied plants were significantly longer than those from NH_4^+ (by *ca*. 2.2-fold), with Mix showing intermediate values. NO_3^- and Mix-treated plants had significantly higher shoot FW than NH_4^+ (up to 2-fold), with NO_3^- also showing significantly higher root FW as compared with NH_4^+. This resulted in significantly higher root to shoot ratios in plants grown with Mix, as compared to NO_3^- (by up to 2.3-fold in controls and 1.8-fold in Psa-inoculated plants), with NH_4^+ showing an intermediate performance (Fig. 2).

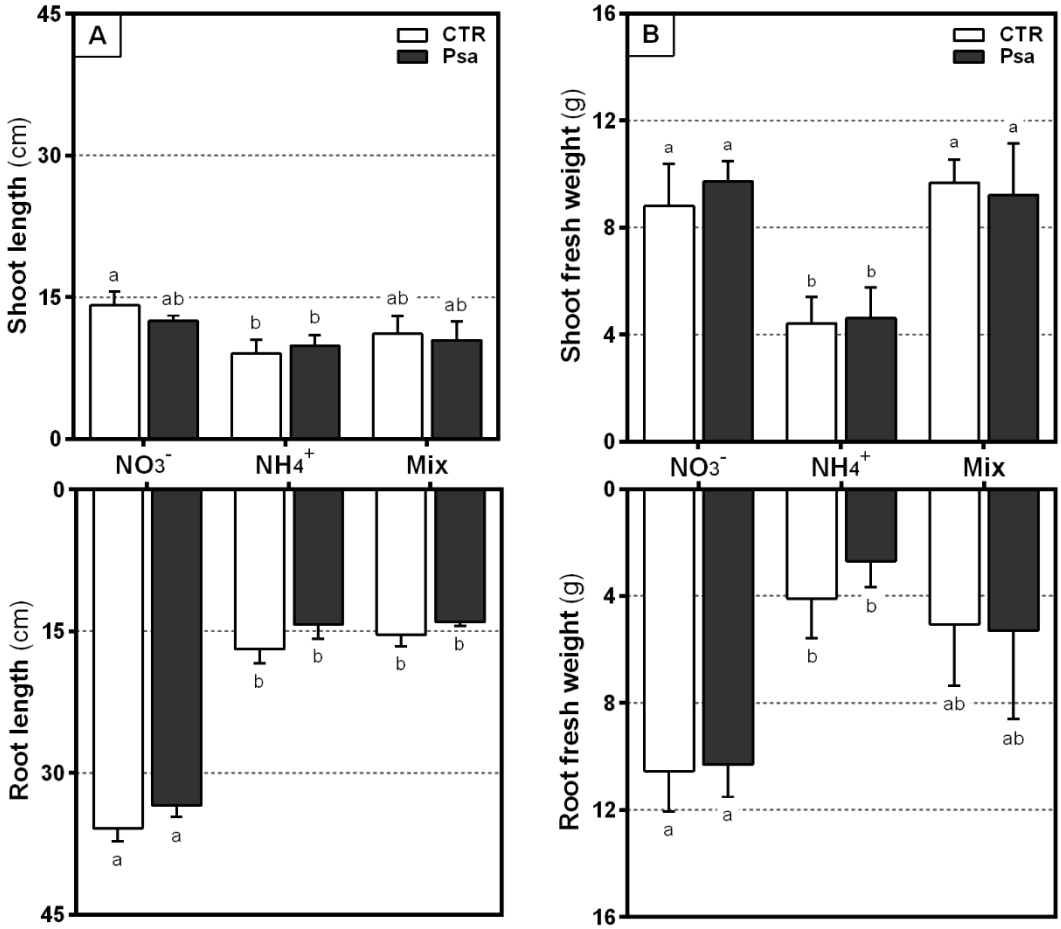

Figure 1 - Shoot and root length (cm) (A), and fresh weight (g) (B) of *A. chinensis* var. *deliciosa* 'Hayward' plants grown with three different nitrogen treatments [214 μM NO_3^-, 214 μM NH_4^+ or 107 μM NO_3^- + 107 μM NH_4^+ (Mix)] for a total of 35 days. At day 21, plants were inoculated with saline solution (mock-inoculated control, CTR) or with *P. syringae* pv. *actinidiae* (Psa). Each value represents the mean of six biological replicates and vertical bars represent the standard error of the mean. Bars showing different letters are statistically different at $p < 0.05$.

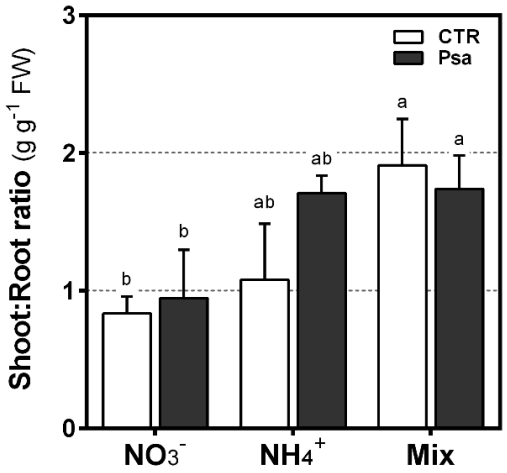

Figure 2 - Shoot to root ratio of *A. chinensis* var. *deliciosa* 'Hayward' plants grown with three different nitrogen treatments [214 μM NO_3^-, 214 μM NH_4^+ or 107 μM NO_3^- + 107 μM NH_4^+ (Mix)] for a total of 35 days. At day 21, plants were inoculated with saline solution (mock-inoculated control, CTR) or with *P. syringae* pv. *actinidiae* (Psa). Each value represents the mean of six biological replicates and vertical bars represent the standard error of the mean. Bars showing different letters are statistically different at $p < 0.05$.

Psa inoculation led to a significant decrease in SPAD values in plants grown with NH_4^+ from as early as 3 dpi, leading to a 0.3-fold decrease at 14 dpi (from 48.5 ± 1.6 in control plants to 34.2 ± 2.0 in Psa-inoculated ones) (Fig. 3).

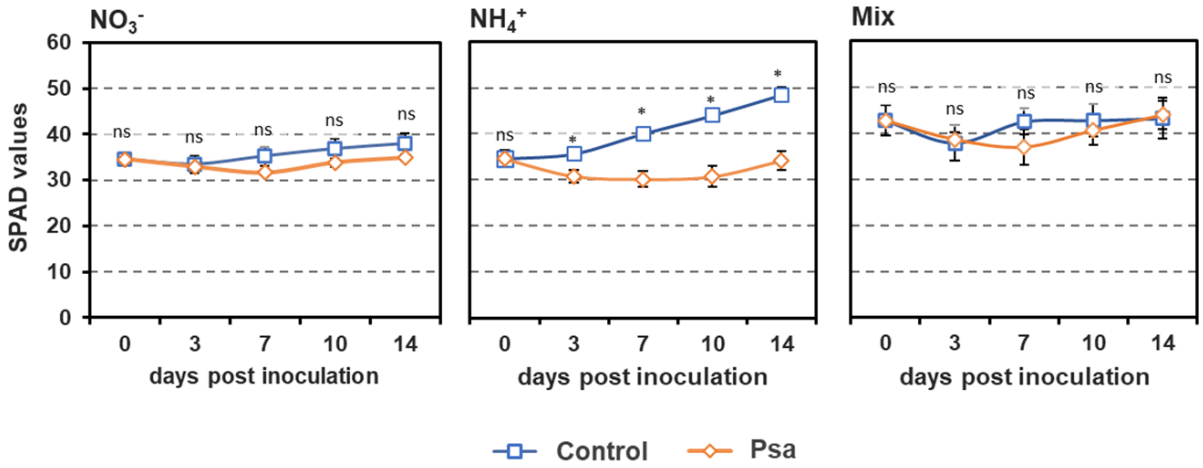

Figure 3 - SPAD values of *A. chinensis* var. *deliciosa* 'Hayward' plants grown with three different nitrogen treatments [214 µM NO_3^-, 214 µM NH_4^+ or 107 µM NO_3^- + 107 µM NH_4^+ (Mix)] for a total of 35 days. At day 21, plants were inoculated with saline solution (mock-inoculated control) or with *P. syringae* pv. *actinidiae* (Psa). Each symbol represents the mean of six biological replicates and vertical bars represent the standard error of the mean. Within each time-point, asterisks represent statistically different means at $p < 0.05$ ("ns" indicates no significant differences).

3.2. Psa endophytic population in plant tissues

Plants maintained with NO_3^- presented the lowest Psa endophytic population, with only 7.1 ± 0.4 × 10^{10} CFU g^{-1} (Fig. 4). Plants grown with NH_4^+ had a 33-fold higher Psa endophytic population, as compared with NO_3^- treated plants. Although there was no significant difference between Mix and NO_3^- treatments regarding Psa density in plant tissues, a tendency for a lower degree of colonization was observed in plants maintained with NO_3^- as sole N source (by 0.8-fold).

3.3. Total protein, total N and mineral concentration

Total protein concentration did not change significantly with Psa inoculation in NO_3^- and Mix-supplied plants, as compared with mock-inoculated ones (Fig. 5A). Contrarily, under NH_4^+ supplementation total protein significantly increased by 1.1-fold in shoots of Psa-inoculated plants, which showed 20.1 ± 0.9 mg g^{-1} protein, as compared with mock-inoculated controls. Roots of mock-inoculated NH_4^+-supplied plants showed the highest protein concentrations (up to 25.9 ± 1.5 mg g^{-1}), whereas roots of mock-inoculated NO_3^--treated plants resulted in the lowest (10.0 ± 0.3 mg g^{-1}).

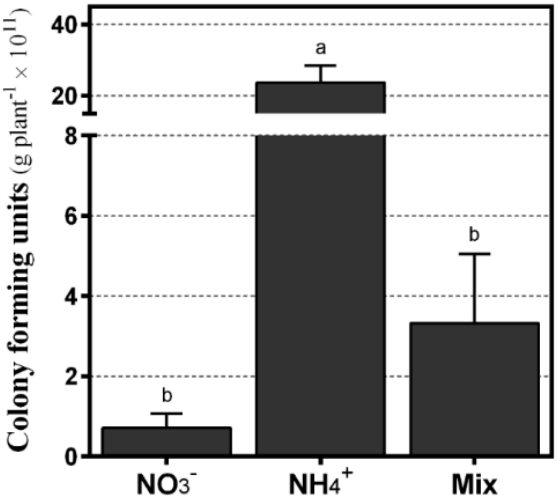

Figure 4 - Colony-forming units (x 10^{11} per gram of plant tissue) in *A. chinensis* var. *deliciosa* 'Hayward' plants grown with three different nitrogen (N) treatments [214 μM NO_3^-, 214 μM NH_4^+ or 107 μM NO_3^- + 107 μM NH_4^+ (Mix)] for a total of 35 days. At day 21, plants were inoculated with *P. syringae* pv. *actinidiae* (Psa). Each value represents the mean of six biological replicates and vertical bars represent the standard error of the mean. Bars showing different letters are statistically different at $p < 0.05$.

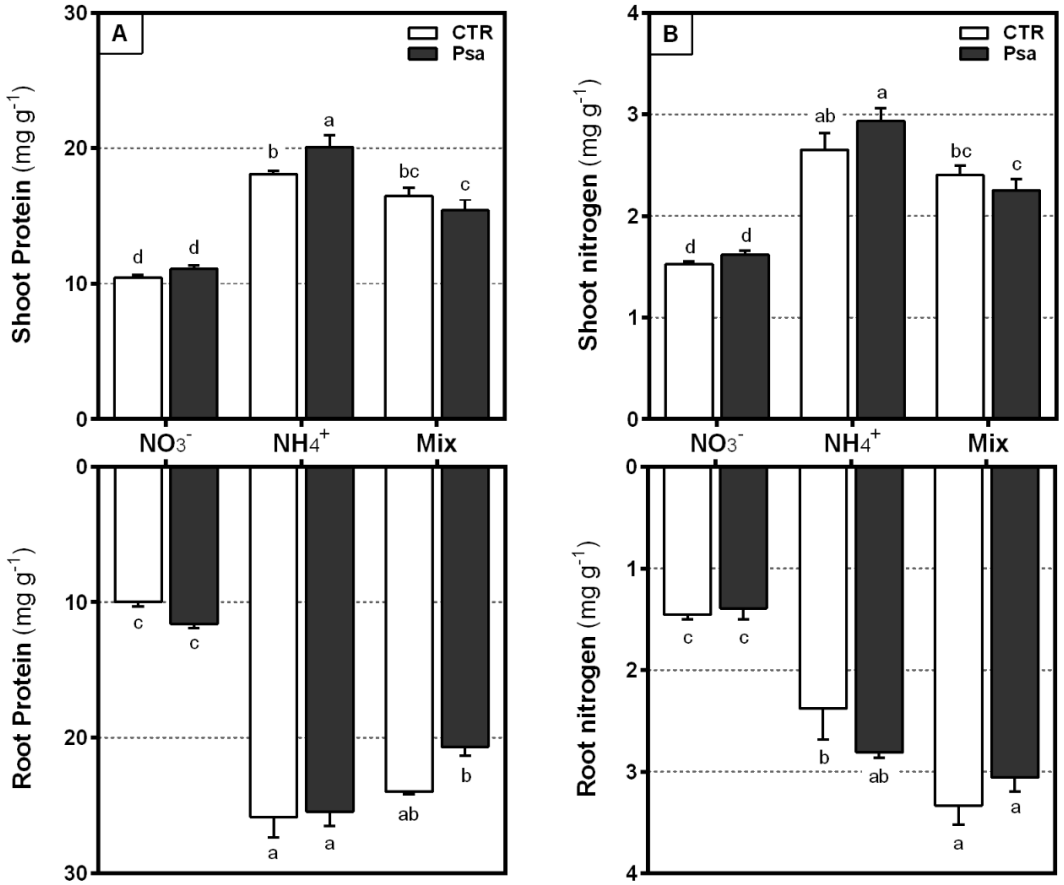

Figure 5 - Total protein (A) and nitrogen (B) concentrations in shoots and roots of *A. chinensis* var. *deliciosa* 'Hayward' plants grown with three different nitrogen treatments [214 μM NO_3^-, 214 μM NH_4^+ or 107 μM NO_3^- + 107 μM NH_4^+ (Mix)] for a total of 35 days. At day 21, plants were inoculated with saline solution (mock-inoculated control, CTR) or with *Pseudomonas syringae* pv. *actinidiae* (Psa). Each value represents the mean of six biological replicates and vertical bars represent the standard error of the mean. Bars showing different letters are statistically different at $p < 0.05$.

Concerning total N concentration, within the same N treatment, Psa inoculation did not induce significant alterations in this parameter. However, Psa-inoculated plants supplemented with NH_4^+ showed significantly higher total N concentrations than with Mix (by 1.3-fold), reaching 2.9 ± 0.1 mg g^{-1} at 14 dpi (Fig. 5B). Moreover, significantly lower N concentrations were observed in roots and shoots of NO_3^--supplied plants, compared with NH_4^+ and Mix (up to 0.4-fold in shoots and 0.6-fold in roots).

Comparing with mock-inoculated plants, Psa inoculation significantly increased P shoot concentrations in plants under NH_4^+ and Mix supply (by 1.4-fold and 1.6-fold, respectively) but not with NO_3^- (Table 2). A similar trend was observed in K concentration, which was significantly higher in Psa- than in mock-inoculated plants in: shoots and roots of plants supplemented with NH_4^+ (by 1.8- and 1.4-fold, respectively), and in shoots of Mix-supplied plants (by 1.5-fold). Roots and shoots of NH_4^+ treated plants generally presented significantly lower Mg concentrations, as compared to NO_3^- supplementation (up to 2.3-fold in both structures) and Mix (up to 2.6-fold in roots). Nevertheless, Mg concentration significantly increased by 1.3-fold with Psa inoculation in shoots of NH_4^+-supplemented plants (comparing with mock-inoculated plants). Ca concentration did not vary significantly with Psa infection, although lower values of this mineral were generally recorded in plants maintained with NH_4^+ (up to 0.8-fold), as compared to the other N treatments. B concentration in shoots was significantly decreased by 0.2-fold in Psa-inoculated plants under Mix supply. In mock-inoculated plants, Zn concentration in roots was significantly higher with NH_4^+ supply than with NO_3^- or Mix, but significantly decreased by 0.5-fold with Psa inoculation. Contrarily, Psa inoculation under NH_4^+ supply resulted in higher Fe concentrations, by 1.5-fold in roots and 1.8-fold in shoots, comparing with control plants of the same N treatment.

3.4. Gene expression

Psa infection induced the upregulation of *PR1* gene in shoots and roots of NH_4^+-supplied plants (by 2.0- and 3.5-fold, respectively), as compared with mock-inoculated control plants (Fig. 6). A similar trend was observed for gene *LOX1*, which was upregulated after Psa inoculation of plants under NH_4^+ supply by 3.2- and 2.1-fold in shoots and roots (respectively). Psa infection also led to an upregulation of *SAM* and *PAL* genes in shoots of NH_4^+ and Mix-supplied plants (by at least 3.3-fold). Plant inoculation with Psa under NH_4^+ and Mix-supply increased the transcriptional levels of *GLU1* and *GDH1* in shoots (up to 4.9-fold), whereas *GAD1* was significantly upregulated by 2.8-fold in shoots of NO_3^--supplied plants (as compared with mock-inoculated plants). *SOD*, *CAT*, *APX* and *TLP1* did not suffer significant alterations in their expression levels due to infection, either in shoots or in roots, and were generally not affected by the N source.

Table 2 - Shoot and root mineral concentration in *A. chinensis* var. *deliciosa* 'Hayward' plants grown with three different nitrogen (N) treatments [214 μM NO_3^-, 214 μM NH_4^+ or 107 μM NO_3^- + 107 μM NH_4^+ (Mix)] for a total of 35 days. At day 21, plants were inoculated with saline solution (mock-inoculated control) or with *P. syringae* pv. *actinidiae* (Psa). Values represent the mean of six biological replicates ± standard error of the mean. Within each row, different letters represent statistically different means at $p < 0.05$.

	Mineral (mg g^{-1})	Control			Psa			*p* value		
		NO_3^-	NH_4^+	Mix	NO_3^-	NH_4^+	Mix	N treatment	Inoculum	Interaction
Root	**P**	2.62 ± 0.15 ^{a}	1.73 ± 0.16 ^{bc}	1.45 ± 0.12 ^{c}	2.82 ± 0.15 ^{a}	2.41 ± 0.26 ^{a}	2.34 ± 0.25 ^{ab}	**0.0005**	**0.0007**	0.2119
	K	25.80 ± 1.81 ^{a}	9.79 ± 0.49 ^{c}	9.79 ± 0.36 ^{c}	27.98 ± 0.48 ^{a}	17.36 ± 1.73 ^{b}	14.48 ± 0.39 ^{b}	**< 0.0001**	**< 0.0001**	0.0515
	Mg	2.17 ± 0.07^{a}	0.92 ± 0.08 ^{c}	1.15 ± 0.10 ^{bc}	2.17 ± 0.12 ^{a}	1.22 ± 0.03 ^{b}	1.26 ± 0.08 ^{b}	**< 0.0001**	0.0647	0.2378
	Ca	11.84 ± 0.59 ^{a}	2.81 ± 0.16 ^{c}	4.06 ± 0.52 ^{bc}	12.19 ± 1.12 ^{a}	3.73 ± 0.49 ^{bc}	5.35 ± 0.89 ^{b}	**< 0.0001**	0.1511	0.8076
	B	0.022 ± 0.002 ^{ab}	0.026 ± 0.001 ^{a}	0.020 ± 0.003 ^{ab}	0.019 ± 0.001 ^{bc}	0.023 ± 0.003 ^{a}	0.016 ± 0.001 ^{c}	**0.0043**	**0.0227**	0.9502
	Zn	0.024 ± 0.001 ^{a}	0.008 ± 0.002 ^{b}	0.009 ± 0.003 ^{b}	0.024 ± 0.003 ^{a}	0.015 ± 0.004 ^{b}	0.015 ± 0.003 ^{b}	**0.0003**	0.0756	0.4584
	Mn	0.094 ± 0.006 ^{a}	0.046 ± 0.004 ^{c}	0.065 ± 0.006 ^{b}	0.093 ± 0.010 ^{a}	0.062 ± 0.003 ^{bc}	0.068 ± 0.005 ^{b}	**< 0.0001**	0.2808	0.3817
	Fe	0.187 ± 0.005 ^{a}	0.133 ± 0.008 ^{b}	0.164 ± 0.025 ^{ab}	0.173 ± 0.023 ^{ab}	0.201 ± 0.007 ^{a}	0.163 ± 0.007 ^{ab}	0.5310	0.1683	**0.0197**
Shoot	**P**	6.38 ± 0.20 ^{a}	4.40 ± 0.35 ^{b}	6.20 ± 0.26 ^{a}	6.14 ± 0.43 ^{a}	5.56 ± 0.76 ^{ab}	6.85 ± 0.35 ^{a}	**0.0043**	0.1721	0.2576
	K	55.35 ± 0.98 ^{a}	28.58 ± 1.07 ^{c}	54.78 ± 1.36 ^{a}	55.65 ± 2.21 ^{a}	38.90 ± 2.15 ^{b}	56.24 ± 2.79 ^{a}	**< 0.0001**	**0.0099**	**0.0105**
	Mg	4.42 ± 0.46 ^{a}	2.11 ± 0.17 ^{b}	3.93 ± 0.48 ^{a}	3.31 ± 0.22 ^{a}	1.43 ± 0.33 ^{b}	3.73 ± 0.20 ^{a}	**< 0.0001**	**0.0355**	0.4967
	Ca	9.51 ± 0.36 ^{b}	2.64 ± 0.35 ^{c}	11.75 ± 1.09 ^{a}	9.25 ± 0.93 ^{b}	2.82 ± 0.55 ^{c}	10.05 ± 0.86 ^{ab}	**< 0.0001**	0.3448	0.4705
	B	0.008 ± 0.001 ^{a}	0.006 ± 0.001 ^{a}	0.010 ± 0.002 ^{a}	0.008 ± 0.001 ^{a}	0.008 ± 0.002 ^{a}	0.009 ± 0.001 ^{a}	0.2567	0.5673	0.6059
	Zn	0.108 ± 0.007 ^{c}	0.536 ± 0.055 ^{a}	0.113 ± 0.009 ^{c}	0.123 ± 0.020 ^{c}	0.256 ± 0.066 ^{b}	0.148 ± 0.025 ^{bc}	**< 0.0001**	**0.0382**	**0.0011**
	Mn	0.329 ± 0.041 ^{b}	0.267 ± 0.013 ^{b}	0.355 ± 0.057 ^{ab}	0.437 ± 0.036 ^{a}	0.256 ± 0.026 ^{b}	0.330 ± 0.047 ^{ab}	**0.0061**	0.4489	0.1521
	Fe	3.06 ± 0.17 ^{bc}	2.76 ± 0.26 ^{c}	3.03 ± 0.30 ^{bc}	4.19 ± 0.54 ^{abc}	4.94 ± 0.93 ^{a}	4.37 ± 0.58 ^{ab}	0.9094	**0.0025**	0.5823

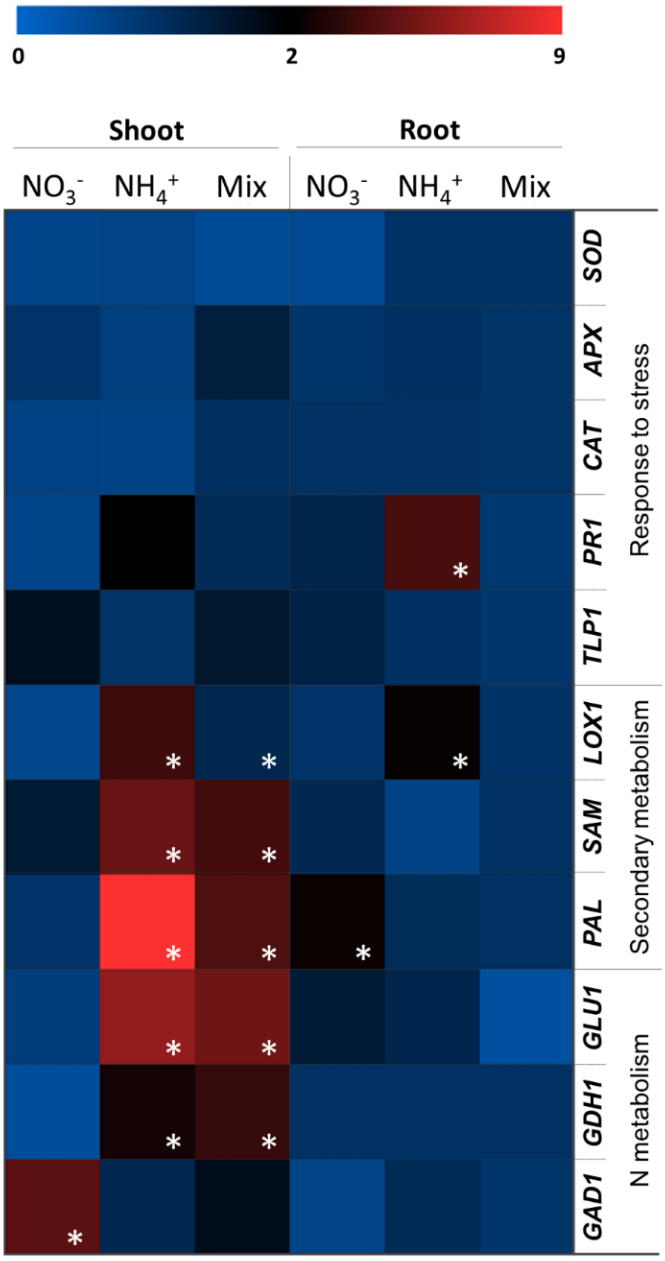

Figure 6 - Heatmap of the relative fold of expression of genes *SOD*, *APX*, *CAT*, *PR1*, *TLP1*, *LOX1*, *PAL*, *SAM*, *GLU1, GDH1* and *GAD1* in shoots and roots of *A. chinensis* var. *deliciosa* 'Hayward' plants grown with three different nitrogen treatments [214 μM NO_3^-, 214 μM NH_4^+ or 107 μM NO_3^- + 107 μM NH_4^+ (Mix)] for a total of 35 days. At day 21, plants were inoculated with saline solution (mock-inoculated control) or with *P. syringae* pv. *actinidiae* (Psa). Asterisks indicate significant differences between Psa-inoculated and mock-inoculated plants, at $p < 0.05$. In blue: no alteration or downregulation of gene expression; in black/red: upregulation of gene expression.

4. Discussion

4.1. Nitrate increased plant tolerance to Psa, preventing the impairment of photosynthetic and metabolic functions

In the present study, Psa did not significantly impair plant growth parameters, regardless of the N source (Fig. 1 and 2). This is unexpected, since most pathogens, including *Pseudomonas* spp., commonly secrete effector proteins that suppress plant immune responses and lead to overall changes in plant growth and architecture (Ditommaso and Watson, 1995; Calonnec *et al*., 2012). For example, *P. syringae* pv. *tomato* possesses a particular type III effector that induces dwarfism in *Arabidopsis thaliana*, *Nicotiana tabacum* and S. *lycopersicum* plants, impairing plant development (Lastdrager *et al*., 2014; Nardozza *et al*, 2015). In this work, a longer experimental period could have allowed a higher bacterial colonization, thus resulting in impaired plant growth and observation of significative structural changes.

In general, plants grown with NO_3^- and Mix had significantly higher FW than NH_4^+. However, due to the higher root growth of plants supplied with NO_3^-, these plants had significantly lower shoot to root ratios than Mix (by *ca*. 0.5-fold in both mock- and Psa-inoculated plants) (Fig. 1 and 2). Plants supplemented with NH_4^+ had the lowest FW (up to 0.5-fold in shoots and 0.6-fold in roots). It has been suggested that supplementation of kiwifruit plants with ammonium chloride or ammonium nitrate reduces plant growth, as compared to NO_3^- supplementation, possibly due to lower ascorbic acid, which is involved in cell division and expansion and photosynthesis (Rinallo and Modi, 2002). This could explain why NH_4^+-supplied plants from the present study generally were smaller.

One of the most characteristic symptoms caused by Psa infection is the development of chlorotic spots in plant leaves, which could lead to impairments in chloroplast functioning and photosynthesis (Berger *et al*., 2007; Petriccione *et al*., 2013). In the present work, the lower SPAD values observed in NH_4^+-supplied plants (Fig. 3) is probably due to the damage caused by the higher Psa colonization (Fig. 4). The lowest endophytic Psa colonization was observed in NO_3^- and Mix-supplied plants, which did not show significant impairments in plant photosynthetic capacity after inoculation. This corroborates that the form of N supply can affect disease development and plant resistance, with different outcomes depending on the plant species (Mur *et al*., 2016). The results observed in the present work are in line with a preliminary report by Mowat *et al*. (2012), that observed higher survival rates when Psa-inoculated *A. chinensis* var. *deliciosa* 'Hayward' plants were supplied with NO_3^-, and a detrimental effect on survival rate when with high NH_4^+. Supply with NO_3^- has been associated with higher resistance of tobacco to *P. syringae* pv. p*haseolicola*, whereas NH_4^+ had the opposite effect, probably because NO_3^- increases HR-mediated plant resistance

through NO and SA generation (Gupta *et al*., 2013). These authors also suggest that NH_4^+ can compromise resistance by promoting the reprogramming of plant HR-defence towards the production of sugar and 4-aminobutyric acid (Gupta *et al*., 2013).

Proteins related to plant protection, including pathogenesis-related (PR) proteins, and the ones involved in oxidative stress, were reported to increase in kiwifruit plants following Psa infection (Petriccione *et al., 2*013 and 2014). In the present work, increased protein content in Psa-inoculated plants only occurred with NH_4^+ supply (Fig. 5), which could be due to the more drastic activation of plant metabolic and defence signalling pathways to restrain the higher Psa colonization observed in this treatment. These plants may require a more rapid assimilation of NH_4^+ into organic compounds as part of their defence system, resulting in higher total protein contents (Atanasova, 2008; Horchani *et al*., 2010). This hypothesis is corroborated by the fact that, here, Psa-inoculation under NH_4^+-supply induced the expression of *PR1* gene, which encodes a PR-protein (Fig. 6). In previous studies, *PR1* was correlated with salicylic acid-mediated responses of kiwifruit plants against Psa (Cellini *et al*., 2014), being overexpressed in plant tissues following infection (Beatrice *et al*., 2017). Moreover, *LOX1*, *SAM* and *PAL* were upregulated in shoots of plants showing the highest levels of Psa colonization (the ones under NH_4^+ and Mix supply). These genes are involved in the JA, ET and phenylpropanoids pathways, respectively, which were shown to be upregulated in susceptible kiwifruit cultivars, especially in later phases of the disease when Psa density inside plant tissues is high (Cellini *et al*., 2014; Nunes da Silva *et al*., 2019; Nunes da Silva *et al*., 2020). Concomitantly, the higher bacterial colonization observed with NH_4^+ and Mix supplies may also result from the activation of JA- and ET-related pathways, which negatively affect *A. chinensis* tolerance to Psa (Reglinski *et al*., 2013; Cellini *et al*., 2014).

4.2. Nitrogen and mineral composition were affected by the N source, with potential implications to plant responses against Psa infection

The lower total N concentration observed in shoots and roots of NO_3^--supplied plants (Fig. 5) (regardless of Psa inoculation), is most likely due to its slower and more time and energy costly assimilation, as compared with NH_4^+, which is more easily absorbed and assimilated (Haynes and Goh, 1978). High levels of N in NH_4^+-treated plants could underpin the higher Psa colonization observed in this treatment, suggesting that this bacterium thrives better with higher N levels, as previously hypothesized (Li *et al*., 2020). Similarly, in tomato plants, increasing concentrations of foliar N has been correlated with a more intense colonization of *P. syringae* pv. *tomato* (Hoffland *et al*., 2000). Here, following Psa inoculation, *GLU1* and *GADH1*, involved in N assimilation and metabolism, respectively, were upregulated in NH_4^+ and Mix-supplied plants, but not in NO_3^- (Fig. 6). This suggests that, with

NH_4^+ and Mix, plants were actively investing not only in N assimilation, but also in N remobilization between plant tissues. This could explain why these treatments showed higher N concentrations in both shoots and roots, comparing with NO_3^-. On the other hand, *GAD1*, involved in N metabolism, was upregulated in plants under NO_3^- supply, but not in the other treatments, possibly contributing to the lower levels of total N and, by extent, to the lower bacterial colonization.

Without Psa infection, NO_3^- supply generally led to higher concentrations of P, K, Mg, Ca, Mn and Fe, as compared with the other treatments (Table 2). Similar results in other plant species were observed by other authors, with lower levels of mineral accumulation in plants supplied with NH_4^+, comparing with NO_3^- (Lu *et al*., 2005; Na *et al*., 2014; Tsabarducas *et al*., 2017). The lower accumulation of these minerals in plants supplied with NH_4^+ may result from competition events with other cations (Haynes and Goh, 1978; Ashraf and Sultana, 2000; Tsabarducas *et al*., 2017). Infection of plants maintained under NH_4^+ and Mix led to a general increase in P, K, Mg and Fe concentration in plant tissues. Phosphorous and K are involved in a vast array of metabolic processes, e.g., energy transfer, and are a component of several organic molecules like proteins or ribonucleic acids (Hawkesford *et al*., 2012; Huber *et al*., 2012b), whereas Mg and Fe have been linked with plants resistance against several environmental stresses, partly due to their roles as co-factors of important molecules (Tripathi *et al*., 2015 and references therein). It was recently demonstrated that Psa infection impairs several amino and organic acids, leading to extensive reprogramming of carbon (C) and nitrogen (N) cycling in diverse metabolic pathways, such as photosynthesis, C fixation, and the tricarboxylic acid cycle (Li *et al*., 2020). We hypothesize that in NH_4^+-supplied plants the increased concentrations of P, K, Mg and Fe results from a higher metabolic demand to cope with the elevated bacterial infection observed with this N source (Fig. 3). On the other hand, results also suggest that supplying NO_3^- as N source leads to a general improvement of plant mineral status, with potential beneficial implications for plant tolerance in cases of subsequent Psa infection.

5. Conclusion

The role of N in plant defence against pathogenic agents, particularly concerning kiwifruit plants infected with Psa, is still not fully understood, limiting the possibilities to integrate N nutrition in novel approaches to control KBC. In the current work, kiwifruit plants growth was not affected by Psa infection, but it was generally favoured when plants were supplied with NO_3^- and Mix. The higher levels of total N in NH_4^+ and Mix-supplied plants may have provided a more favourable environment for bacterial growth, thus leading to the increased Psa colonization observed with these treatments. Moreover, with NH_4^+, Psa infection increased

the concentrations of P, K, Mg and Fe in plant tissues, suggesting a higher metabolic demand in these plants to cope with the infection. Overall, results show that N supply as NO_3^- has advantages against NH_4^+ in increasing plant tolerance to Psa. This probably occurs through the decrease of N concentration in plant tissues, a macronutrient that favours pathogen growth, and the improvement of plant mineral status (particularly of P, K, Mg, Ca and Mn, implicated in several defence-related pathways). This study provides innovative knowledge on how N sources modulate plant defence mechanisms against Psa, which could allow the development of N fertilization regimens that ensure both nutrient use efficiency and increased plant tolerance to Psa.

Supplementary Material

SM1 - Relative fold of expression of genes *SOD* (superoxide dismutase), *APX* (ascorbate peroxidase), *CAT* (catalase), *PR1* (pathogenesis-related protein 1), *TLP1* (thaumatin-like protein 1), *LOX1* (lipoxygenase 1), *PAL* (phenylalanine ammonia-lyase), SAM (s-adenosylmethionine synthetase 1), *GLU1* (glutamate synthase 1) and *GDH1* (glutamate dehydrogenase) and *GAD1* (glutamate decarboxylase) in shoots and roots of *A. chinensis* var. *deliciosa* 'Hayward' plants grown with three different nitrogen treatments [214 μM NO_3^-, 214 μM NH_4^+ or 107 μM NO_3^- + 107 μM NH_4^+ (Mix)] for a total of 35 days. At day 21, plants were inoculated with saline solution (mock-inoculated control) or with *P. syringae* pv. *actinidiae* (Psa).. Values represent the mean of three biological replicates ± standard error of the mean and, within each plant tissue and gene, different letters represent significant differences at $p < 0.05$. Biologically significant alterations in gene expression in Psa-infected plants (as compared with mock-inoculated ones) are marked in bold.

	Shoot			**Root**		
	NO_3^-	**NH_4^+**	**Mix**	**NO_3^-**	**NH_4^+**	**Mix**
SOD	0.6 ± 0.1 ^{a}	0.7 ± 0.2 ^{a}	0.5 ± 0.1 ^{a}	0.6 ± 0.1 ^{a}	1.0 ± 0.1 ^{a}	1.0 ± 0.1 ^{a}
APX	1.0 ± 0.1 ^{a}	0.8 ± 0.1 ^{a}	1.4 ± 0.3 ^{a}	1.0 ± 0.2 ^{a}	1.0 ± 0.2 ^{a}	1.0 ± 0.1 ^{a}
CAT	0.7 ± 0.2 ^{a}	0.7 ± 0.1 ^{a}	1.1 ± 0.1 ^{a}	1.0 ± 0.2 ^{a}	1.0 ± 0.1 ^{a}	1.0 ± 0.1 ^{a}
PR1	0.7 ± 0.3 ^{b}	**2.0 ± 0.4 ^{a}**	1.2 ± 0.3 ^{ab}	1.3 ± 0.2 ^{b}	**3.5 ± 0.6 ^{a}**	0.9 ± 0.4 ^{b}
TLP1	1.0 ± 0.2 ^{a}	1.7 ± 0.3 ^{a}	1.5 ± 0.3 ^{a}	1.0 ± 0.3 ^{a}	1.3 ± 0.5 ^{a}	0.9 ± 0.3 ^{a}
LOX1	0.6 ± 0.2 ^{b}	**3.2 ± 0.3 ^{a}**	1.2 ± 0.2 ^{b}	1.0 ± 0.2 ^{b}	**2.1 ± 0.4 ^{a}**	1.0 ± 0.1 ^{b}
PAL	1.0 ± 0.4 ^{c}	**9.0 ± 1.6 ^{a}**	**3.6 ± 0.7 ^{b}**	2.3 ± 1.0 ^{a}	1.1 ± 0.4 ^{a}	1.0 ± 0.2 ^{a}
SAM	1.5 ± 0.4 ^{b}	**4.1 ± 0.3 ^{a}**	**3.3 ± 0.4 ^{a}**	1.2 ± 0.4 ^{a}	0.7 ± 0.5 ^{b}	1.0 ± 0.2 ^{b}
GLU1	0.8 ± 0.4 ^{b}	**4.9 ± 0.5 ^{a}**	**4.2 ± 1.0 ^{a}**	1.5 ± 0.4 ^{a}	1.2 ± 0.3 ^{ab}	0.4 ± 0.3 ^{b}
GDH1	0.5 ± 0.2 ^{b}	**2.4 ± 0.4 ^{a}**	**3.1 ± 0.6 ^{a}**	1.0 ± 0.2 ^{a}	1.0 ± 0.2 ^{a}	1.0 ± 0.2 ^{a}
GAD1	**2.8 ± 0.5 ^{a}**	1.2 ± 0.6 ^{b}	1.7 ± 0.5 ^{b}	0.7 ± 0.2 ^{a}	1.2 ± 0.5 ^{a}	1.0 ± 0.3 ^{a}

CHAPTER 4 - Sub-chapter 4.3

Cumin essential oil reduces *Actinidia chinensis* infection by *Pseudomonas syringae* pv. *actinidiae*

Cumin essential oil reduces *Actinidia chinensis* infection by *Pseudomonas syringae* pv. *actinidiae*

Abstract

Pseudomonas syringae pv. *actinidiae* (Psa), has become the main threat for kiwifruit (*Actinidia* spp.) production, being present in almost all top kiwifruit producing countries. Its closely-related pathovar *P. syringae pv. actinidifoliorum* (Pfm) is also able to infect kiwifruit plants, having a more restricted dispersion and a lower virulence degree. As current chemical control strategies against these pathogens are mainly focused on antibiotic- and copper-based compounds, which pose several environmental challenges, plant essential oils (PEOs) have been receiving attention as environmentally friendly substitutes. In this work, six PEOs (anise, basil, cardamom, cumin, fennel and laurel) were chemically characterised by gas chromatography-mass spectrometry (GC-MS), and their antimicrobial activity was evaluated against two Psa (1F and 7286) and two Pfm (18804 and 19441) strains. Cumin was generally the most effective PEO in inhibiting bacterial growth, inducing the highest inhibition halos from concentrations as low as 5%. On the contrary, anise was the least effective in inhibiting growth, inducing the narrowest inhibition halos even at 90%. GC-MS analysis revealed that cumin EO was mostly composed of cuminaldehyde (41.9%), β-cymene (16.3%) and 3-carene (12.0%), whereas in anise the most abundant compounds were anethole (87.7%), longifolene (3.71%) and estragole (2.6%). Intraspecific and interspecific differences in bacteria sensitiveness to distinct PEOs was observed. For example, Pfm18804 was the least sensitive to anise and cardamom, whereas Pfm19441 was the most sensitive. As cumin revealed the most interesting antibacterial activity in the *in vitro* trials, its potential was also evaluated *in planta* against a highly virulent Psa strain (7286). Foliar spray with 0.1% cumin EO 15 days before plant inoculation significantly decreased Psa endophytic population in plant tissues by 73% (15 days post-inoculation). These results indicate that PEOs, particularly from cumin, have great potential to be used in integrated pest management strategies against Psa and Pfm. Nevertheless, potential limitations regarding intraspecific and interspecific differences in bacterial sensitiveness to PEOs should be further explored to improve the effectiveness of these compounds against distinct kiwifruit pathogens.

1. Introduction

Kiwifruit bacterial canker (KBC), caused by *Pseudomonas syringae* pv. *actinidiae* (Psa), severely affects plant growth and productivity, leading to important economic losses and requiring strict orchard management practices (Froud *et al., 2*017). Psa is considered a pandemic microorganism, since the disease has been reported in all major kiwifruit-producing countries, being able to infect almost all *Actinidia* spp. (Scortichini *et al., 2*012). In contrast, the genetically close bacterial strain *P. syringae* pv. *actinidifoliorum* (Pfm), is less virulent to kiwifruit plants, not causing important economic and production losses, but

inducing the appearance of necrotic spots in infected plants (Cunty *et al., 2*014; Nunes da Silva *et al., 2*020). These pathogens must be properly managed for optimal crop performance and yield, and different products aiming at reducing bacterial inoculum have been tested. The most commonly used are formulated with antibiotics (e.g., streptomycin) or heavy metals (mainly copper), which have limited effectiveness in successfully controlling the disease, also posing ecological threats due to phytotoxicity, microbial resistance or environmental persistence (Han *et al., 2*004; Pietrzak and McPhail, 2004). Recent studies have focused on the development of alternatives to these products, such as plant elicitors (Scortichini, 2014; Wurms *et al., 2*017b), and, to a lesser extent, plant essential oil (PEOs).

PEOs are complex compounds that have been extensively studied for their antimicrobial activity against viruses, fungi and bacteria of agronomic importance (Mattarelli *et al., 2*017). PEOs are composed of up to 60 different chemicals, including organic and amino acids, carbohydrates, phenols and aromatic compounds, although the main components of each PEO can reach up to 90% of their composition (Song *et al., 2*016; Vavala *et al., 2*016; Mattarelli *et al., 2*017). PEOs antibacterial activity is based on their attachment to the pathogen's cell surface, followed by alterations in membrane permeability, disruption of its integrity, loss of intracellular contents and, consequently, death of the microorganism. In addition, PEOs also impair the microorganism's motility and quorum sensing mechanisms (Pucci *et al., 2*018; Lovato *et al., 2*019). The antibacterial, bactericidal or bacteriostatic activity of several PEOs and plant extracts against Psa has been under scrutiny over the last decade, but most studies only evaluated their antimicrobial activity in *in vitro* conditions (Monchiero *et al., 2*015; Vavala *et al., 2*016; Song *et al., 2*016; Mattarelli *et al., 2*017; Pucci *et al., 2*018; Lovato *et al., 2*019). For example, EOs from e.g., *Mentha suaveolens*, *Rosmarinus officinalis* and *Melaleuca alternifolia* showed antibacterial activity against Psa to a higher extent than those of *Salvia officinalis* and *Laurus nobili,* with *M. suaveolens* and *M. alternifolia* also having a bactericidal effect (Vavala *et al., 2*016). The authors also assessed potential synergisms between different PEOs, reporting that exposure of Psa to *R. officinalis* and *M. alternifolia* EOs in combination with *M. suaveolens* EO significantly increased their efficacy, as compared with their individual application (Vavala *et al., 2*016). Essential oils from *C. zeylanicum* also displayed antibacterial activity, but the ones from *Lavandula angustifolia*, *Mentha piperita*, *Rosmarinus officinalis* and *Piper nigrum* had no inhibitory effect against Psa (Pucci *et al., 2*018).

Despite the promising *in vitro* evidence on the antimicrobial potential of some PEOs, so far, very few works explored their ability to suppress bacterial pathogens, including Psa, *in planta*. For example, treatment of cumin seeds with PEOs from cumin, basil and geranium before planting (at 4% concentration) resulted in reduced root rot caused by *Fusarium* spp. (Hashem *et al*., 2010). Origanum EO (at 0.0025-0.0100%) and clove EO (at 0.0020-0.0100%) significantly decreased disease symptoms caused by *Botrytis cinerea* and

Ralstonia solanacearum, respectively, in potted tomato seedlings (Soylu *et al*., 2010; Hee Lee *et al*., 2012). In another greenhouse trial, PEOs from *Cymbopogon citratus* and *O. Basilicum* applied as a soil drench (50 mL/plant) significantly reduced disease severity of *Phytophthora* diseases on pepper, cucumber and melon plants, as compared with non-treated controls (Amini *et al*., 2016). The only available study at present dealing with Psa-infected kiwifruit plants demonstrated that treatment with *Satureja* spp. and *Thymus* spp. EOs led to a lower number of diseased leaves and/or lower leaf area affected by disease symptoms (Monchiero *et al., 2*015).

To understand PEOs' mode of action, it is important to assess their chemical composition; however, so far, few studies focusing on Psa have provided the chemical composition of the PEOs or plant extracts tested, hindering the understanding of their mode of action and the anticipation of their antimicrobial potential. Chemical analysis of PEOs with antibacterial activity against Psa revealed the most abundant compounds were piperitenone oxide (*Mentha suaveolens*), borneole (*Rosmarinus officinalis*), caryophyllene (*Salvia officinalis*), camphene and cynnamil acetate (*Laurus nobili*), or terpinene-4-ol (*Melaleuca alternifolia*) (Vavala *et al., 2*016). Individual compounds as cinnamaldehyde, eugenol, estragole and methyl-eugenol, extracted from *Pimenta* spp. or *Cinnamomum cassia*, were demonstrated to have inhibitory activity against Psa, although their efficacy was distinct between different Psa strains, with estragole being generally more effective (Song *et al., 2*016). Although single compound studies may be useful, they frequently fall short in explaining the antimicrobial potential of a given PEO, as they may have synergistic or antagonistic effects with other compounds. For example, eugenol, estragole and methyl-eugenol had high inhibitory activity against Psa, but extracts of *P. racemosa* and *P. dioica*, rich in these compounds, were as effective as *C. cassia*, in which they were not detected (Song *et al., 2*016). Mattarelli *et al*. (2017) observed that thymol content was higher in *Monarda didyma* (ranging from 59.4 to 64.3% of the total composition) than in its closely related species *M. fistulosa* (38.0 to 42.4%), but the antimicrobial activity against Psa was similar between both PEOs, presumably due to the presence of carvacrol in *M. fistulosa* (*ca*. 3.9%). Recent studies attested for the high inhibitory activity of carvacrol against Psa, especially when combined with phages (Ni *et al., 2*020). Thus, the use of PEOs and their constituents, either in combination or alone, could benefit the efforts for the control of KBC by integrating currently used orchard management routines or even substituting environmentally noxious compounds. However, the little knowledge available on PEOs activity and chemical composition against Psa and the inexistent knowledge on their potential application regarding Pfm greatly hinders these efforts. Moreover, even though many PEOs have been tested, the identification of others with potential against these pathogens, e.g., anise, could provide novel tools for their control.

We hypothesise that EOs from the same plant species could have distinct performances between different studies, mainly due to variations in their chemical composition and bacterial intra- and interspecific sensitiveness. Thus, the aims of this work were to: i) assess the chemical composition of PEOs from six common spices and herbs (anise - *Pimpinella anisum*, basil - *Ocimum basilicum*, cardamom - *Elettaria cardamomum*, cumin - *Cuminum cyminum*, fennel - *Foeniculum vulgare* and laurel - *Laurus nobilis*); ii) evaluate their antibacterial activity against two Psa and two Pfm strains; iii) compare the sensitiveness of different Psa and Pfm strains to each PEO; and iv) validate the potential of the most promising PEO from the *in vitro* trials against the highly virulent Psa 7286 *in planta*.

2. Materials and methods

2.1. PEOs chemical characterization

Essential oils were acquired from H. Reynaud & Fils (Montbrun Les Bains, France) and chemically analysed by gas chromatography-mass spectrometry (GC-MS). Each PEO was diluted in 10% ethanol (GC grade, Sigma-Aldrich, Missouri, USA). GC-MS analysis was performed using a gas Chromatographer with an autoinjector (Varian CP-3800, Agilent, California, USA) equipped with an ion-trap mass detector (Varian Saturn 4000) and a workstation software (Varian, version 6.9.1). Chromatographic separation was achieved using a capillary column VF-5ms (30 m x 0.25 mm x 0.25 mm) (Agilent, California, USA) and high purity helium C-60 (Gasin, Portugal) as carrier gas at a constant flow of 1.0 mL min^{-1}, in splitless injection mode. An initial oven temperature of 40 °C was held for 1 min, then increasing 5 °C min^{-1} to 250 °C (5 min) followed by an increase of 5 °C min^{-1} up to 300 °C (0 min). Other analytical specifications have been previously described (Barros *et al., 2*012). Non-targeted compound identification was performed using pure and combined standards with NIST/EPA/NIH Mass Spectral Library version 2.2 (National Institute of Standards and Technology, Maryland, USA).

2.2. Preparation of PEO emulsions

Due to the low water solubility of the PEOs, a 90% stock emulsion (90% essential oil, 8% sterile distilled water, and 2% Tween 20, Merck, Darmstadt, Germany) was prepared from each PEO. Emulsions of 1, 5, 10, 25, 50 and 75% (v/v) were prepared by successively diluting the stock emulsion of each PEO in sterile distilled water. To ensure that the Tween 20 had no interference in the results, equivalent dilutions without PEOs (with only sterile

distilled water) were also prepared and tested. All the emulsions were shaken for 30 sec before application to ensure a homogeneous mixture.

2.3. Bacterial strains, culturing media and antibacterial activity

Two Psa strains (CFBP7286, isolated in Italy, and 1F, isolated in France) and two Pfm strains (CFBP18804, isolated in New Zealand and CFBP19441, isolated in Australia) were maintained in nutrient agar with 5% sucrose (NSA) at 27 °C in the dark. For inoculum preparation, a single bacterial colony of each strain was grown overnight in liquid Luria-Bertani (LB) medium, at 27 °C and 75 rpm.

The antibacterial activity of the six PEOs was tested on NSA plates using the paper disk diffusion test (Vincent *et al., 1*944). After inoculum streaking into separate plates (OD_{600} = 0,1; ≈ 1.5 x 10^8 cells mL^{-1}), 10 µL of each PEO or corresponding Tween 20 dilution solution were placed in blank antimicrobial susceptibility disks (Thermo Fisher Scientific, Massachusetts, USA) positioned in the middle of each plate. Inhibition of bacterial growth was evaluated after plate incubation at 27 °C for 48h in the dark through the measurement of the diameter of the inhibition zone. Each solution was tested in biological triplicates, with three technical replicates per treatment.

2.4. *In planta* validation of cumin EO antimicrobial activity against Psa

Micropropagated *A. chinensis* var. *deliciosa* 'Tomuri' plants (with a single shoot, 5 to 6 cm height, and 5 to 10 leaves) were purchased from QualityPlant - Investigação e Produção em Biotecnologia Vegetal, Lda. (Castelo Branco, Portugal). Plants were maintained in a modified full-strength Murashige and Skoog (MS) agarized medium in a climate chamber (Aralab Fitoclima 10 000EH, Aralab, Rio de Mouro, Portugal) as described elsewhere (Nunes da Silva *et al*., 2020). Fifteen days before Psa inoculation, 18 plants were treated with 0.1% of cumin EO (prepared through the dilution of the stock solution previously described), by dipping plant shoots in the solution for 15 sec. An additional set of 18 plants were treated with 2% Tween 20 alone (negative control). PEO concentration for plant treatment was determined by previous tests which showed toxicity symptoms with higher concentrations (data not shown).

On the day of plant inoculation, a fresh 1-2x10^7 CFU mL^{-1} inoculum of a virulent Psa strain (CFBP7286) was prepared in sterile Ringer's solution. Nine plants previously treated with cumin EO and nine plants treated with 2% Tween 20 (negative-controls), were inoculated by plant dipping in the inoculum for 15 sec. The remaining plants (nine from each

PEO treatment) were mock-inoculated using the same procedure using a sterile Ringer's solution (mock-inoculated controls). At 15 days post-inoculation (dpi), Psa-inoculated plants were removed from the culturing medium, homogenized in Ringer's solution and used for the determination of Psa endophytic population as described by Nunes da Silva *et al*. (2020). Each biological replicate was obtained by randomly pooling three plants from each experimental condition.

2.5. Statistical analysis

Data were analysed with GraphPad Prism version 6.0 (GraphPad Software, Inc., California, USA) with significant differences between treatments being determined by analysis of variance (ANOVA) followed by Fisher's LSD test ($p < 0.05$).

3. Results

Chemical characterization by GC-MS revealed that PEOs from cardamom and anise were the most complex, with 28 and 26 identified compounds, respectively, whereas basil (with 20 compounds), cumin (21) and laurel (21) were the least (Supplementary Material 1). Anise EO was mostly composed of anethole (87.65%), basil of estragole (93.0%), cardamom of β-himachalene (75.9%), cumin of cuminaldehyde (41.9%), fennel of eucalyptol (68.6%), and laurel of anethole (77.4%) (Table 1). All PEOs had three compounds in common (estragole, p-cymene and terpinen-4-ol), but several others were present only in one of the PEOs. For example, 3-chromanol, aromandrene, chrysanthenol, L-α-terpineol and phellandral were only quantified in cumin EO. Compared with other PEOs, anise had the highest relative abundance of anethole (87.65%) and 2-benzimidazolemethanol (1.22%), estragole (93.0%) was more abundant in basil EO, whereas α-himachalene (75.9%), D-limonene (7.3%), linalyl acetate (3.7%), trans-4-thujanol (0.1%) were most abundant in cardamon EO. Cumin showed the highest concentrations of cuminaldehyde (41.93%), β-cymene (16.33%), 3-carene (12.04%), guanidineacetic acid (1.46%), β-terpinene (1.32%) and epicubebol (0.18%). The relative abundance of eucalyptol (68.6%), β-himachalene (17.1%), lynalyl acetate (1.83%), bornyl acetate (1.7%), terpinen-4-ol (1.0%), γ-terpinene (1.0%), p-cymene (0.9%), methyleugenol (0.2%) and cis-4-thujanol (0.2%) was higher in fennel EO, whereas fenchone (9.0%), terpinolene (1.5%) and camphor (0.2%) were more abundant in laurel EO.

Table 1 - Quantitative and qualitative composition (% w/w) of the Top 5 compounds contributing to the chemical composition of essential oils from anise, basil, cardamom, cumin, fennel and laurel. Abbreviations: R. Ab. - Relative Abundance.

Anise		Basil		Cardamom		Cumin		Fennel		Laurel	
Compound	R. Ab. (%)	Compound	R. Ab. (%)	Compound	R. Ab. (%)	Compound	R. Ab. (%)	Compound	R. Ab. (%)	Compound	R. Ab. (%)
Anethole	87.6	Estragole	93.0	β-himachalene	75.9	Cuminaldehyde	41.9	Eucalyptol	68.6	Anethole	77.4
Longifolene	3.7	Eucalyptol	3.2	D-Limonene	7.2	β-Cymene	16.3	β-himachalene	17.1	Fenchone	9.0
Estragole	2.6	Anethole	1.7	Linalyl acetate	3.7	3-carene	12.0	D-Limonene	2.8	Estragole	6.6
Thunbergol	1.4	Bornyl acetate	0.5	2-Dimethylaminoaniline	2.3	3-Chromanol	11.1	Linalyl acetate	1.8	D-Limonene	1.8
2-Benzimidazolemethanol	1.2	Linalyl acetate	0.3	3-carene	2.2	Chrysanthenol	8.1	Bornyl acetate	1.7	Terpinolene	1.5

In general, the antimicrobial activity of the PEOs increased with increasing concentrations (Fig. 1), with almost all showing a coefficient of correlation (R^2) of at least 0.67 and up to 0.99 (data not shown). The only exception was observed for Psa7286 exposed to anise, in which the R^2 of the linearity between the concentrations and inhibition halos was only 0.50 (data not shown).

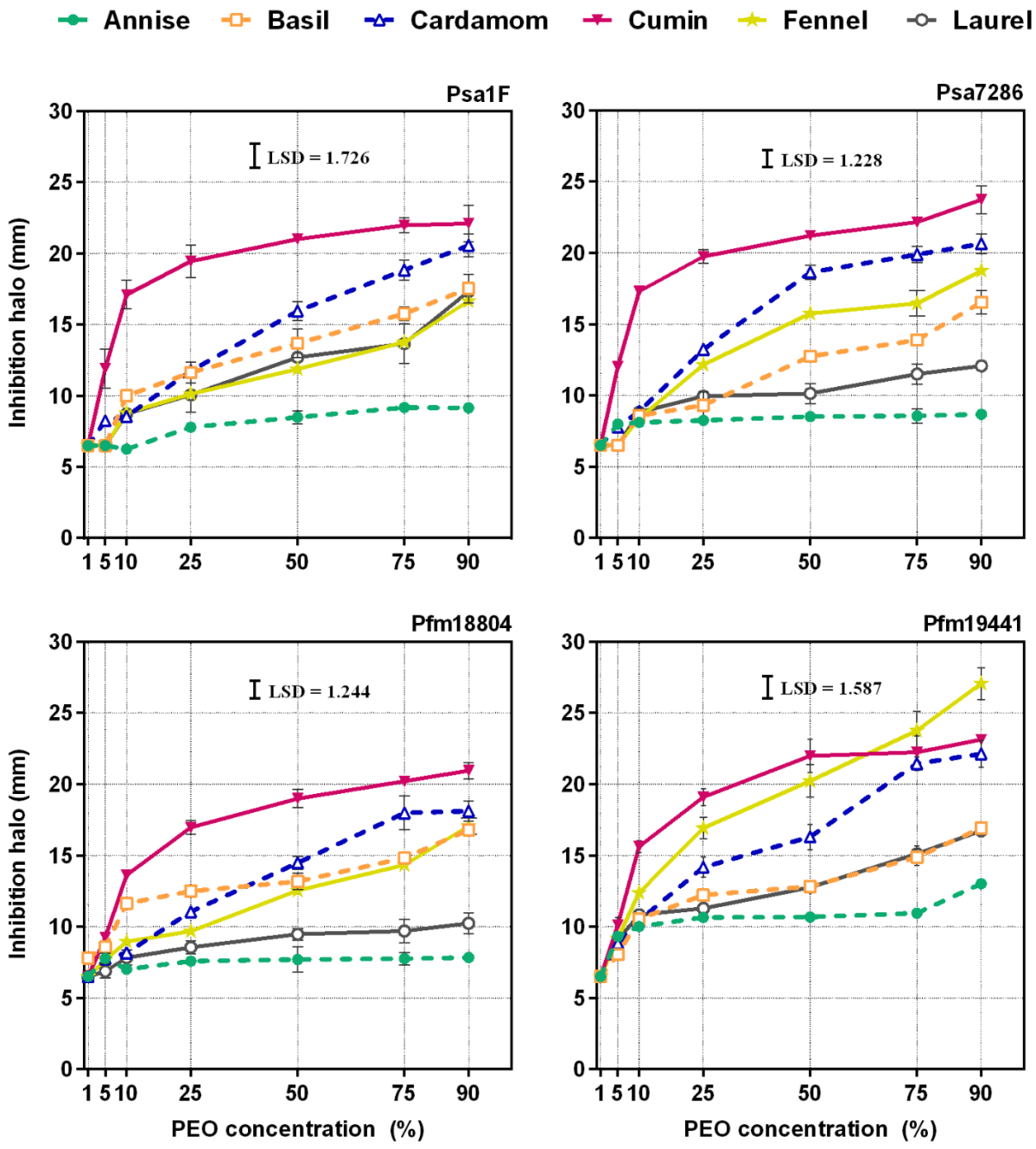

Figure 1 - Diameter of the inhibition halo of *Pseudomonas syringae* pv. *actinidiae* (Psa, strains 1F and 7286) and *P. syringae* pv. *actinidifoliorum* (Pfm, strains 18804 and 19441) cultures exposed to 1, 5, 10, 25, 50, 75 and 90% of anise, basil, cardamom, cumin, fennel and laurel essential oils for 48h. Each value represents the mean of three biological replicates and vertical lines the standard error of the mean. For each panel, the Least Significant Difference (LSD) value is provided ($p < 0.05$).

In fact, anise was the least effective PEO, showing the smallest inhibition halos even at 90% (from 8.7 ± 0.4 cm for Psa7286 up to 13.0 ± 0.2 cm for Pfm19441). In general, cumin was the most effective PEO, inducing wider inhibition halos (of at least 9.2 ± 0.6 cm at 5% and up to 23.7 ± 1.0 at 90%) in all bacterial strains. The only exceptions were observed for Pfm19441, in which at 75 and 90% fennel inhibited bacterial growth at a higher extent than cumin (with significantly wider inhibition halos of 27.1 ± 1.1 cm at 90%). Basil, cardamon and laurel had an intermediate performance, with maximum inhibition halos of: 8.6 ± 0.2, 8.8 ± 0.4 and 9.1 ± 0.2 cm at 5%, and 17.5 ± 1.0, 22.1 ± 0.9 and 17.3 ± 0.3 cm at 90%, respectively.

Moreover, bacterial strains showed intra- and interspecific sensitiveness to the PEOs. At 90% PEO concentration, Psa1F was the least sensitive strain to fennel and the most sensitive to laurel, Psa7286 was the most sensitive to cumin and the least sensitive to basil, Pfm18804 was the least sensitive to anise, cardamom, cumin and laurel and Pfm19441 was the most sensitive to anise, basil, cardamom and fennel.

Plant treatment with cumin EO decreased plant tissue colonization by Psa by 73%, with control plants having 16.7 ± 2.1 CFU g^{-1} shoot tissue and treated plants only 4.5 ± 1.9 CFU g^{-1} plant tissue at 15 dpi (Fig. 2).

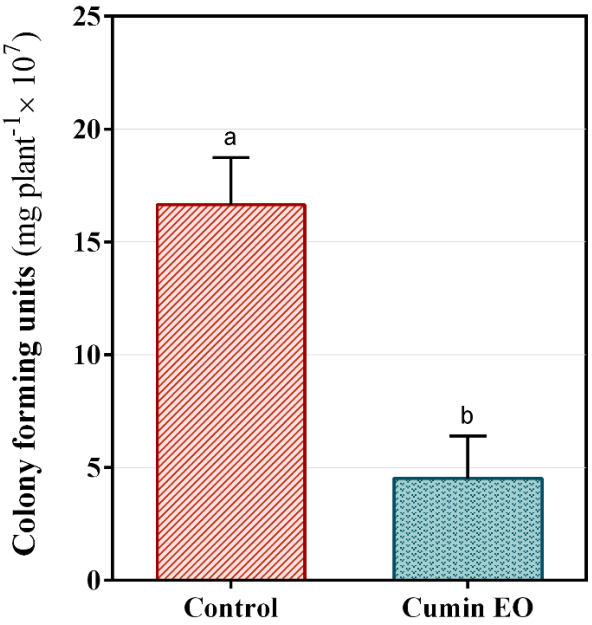

Figure 2 - Colony-forming units (x 10^7 per gram of plant tissue) in *A. chinensis* var. *deliciosa* 'Tomuri' plants, 30 days after foliar treatment with 0.1% of cumin essential oil (EO), and 15 days post-inoculation with *Pseudomonas syringae* pv. *actinidiae* strain 7286. Each value represents the mean of three biological replicates and vertical bars the standard error of the mean. Different letters represent statistically different values at $p < 0.05$.

4. Discussion

All PEOs tested in the present work showed antibacterial activity against Psa and Pfm, but cumin was generally more effective, inducing the widest inhibition halos at lower concentrations. Nevertheless, Psa and Pfm strains showed different sensitiveness to the different PEOs: Psa1F was the least sensitive strain to fennel and the most sensitive to laurel, whereas Psa7286 was the most sensitive to cumin and the least sensitive to basil. For Pfm, Pfm18804 was the least sensitive to anise and cardamon EOs, whereas Pfm19441 was the most sensitive to those EOs. Song *et al*. (2016) observed that Psa KBE9 was less inhibited by *C. cassia* and *C. sativa* extracts than YCS3 and SYS1, but was more sensitive to eugenol (Song *et al., 2*016). This work supports the evidence that Psa sensitiveness to PEOs varies among different strains, also demonstrating for the first time the inhibitory potential of PEOs against Pfm. These results suggest that rather than selecting a single type of essential oil to inhibit bacterial growth, a more efficient approach could be the selection of the most appropriate PEO to each specific pathogen or a mixture of PEOs that target several pathogens at the same time. However, exposure of Psa to *R. officinalis* and *M. alternifolia* EOs in combination with *M. suaveolens* EO significantly decreased their antimicrobial activity, compared with their application alone (Vavala *et al., 2*016.). As such, further studies on the sensitivity of Psa and Pfm strains to single or multiple PEOs should be pursued for the full assessment of their efficacy and anticipation of potential shortcomings in their use. Our results corroborate previous findings on the ability of basil, cumin, fennel and laurel to inhibit Psa growth (Valvala *et al., 2*016; Pucci *et al., 2*018), demonstrating the antimicrobial potential of anise and cardamom against Psa for the first time. Interestingly, cardamom EO has been previously assessed for its antibacterial and bactericidal activity against Psa, but it did not show inhibitory ability (Pucci *et al., 2*018). The contrasting results may be explained by the use of PEOs obtained from different plant chemotypes and through distinct procedures, supporting our initial hypothesis on the importance of the chemical characterization of the utilized compounds.

Although the antibacterial potential of cumin has been addressed in previous publications (Pucci *et al., 2*018), its activity against Psa *in planta* was never demonstrated before. Here, the application of 0.1% of cumin EO 15 days before *A. chinensis* var. *deliciosa* 'Tomuri' infection with the highly virulent Psa strain 7286, significantly reduced bacterial colonization by 73% (at 15 dpi). We hypothesise that the higher antimicrobial activity of cumin EO observed in the present work results not only from the higher concentration of cuminaldehyde, but also of β-cymene, 3-carene, guanidineacetic acid, β-terpinene and epicubebol. In fact, as anise and laurel were both mostly composed of anethole but showed very distinct inhibition abilities, it is clear that the antimicrobial potential of a given PEO results not only from the most abundant compounds, but from synergistic or antagonistic relationships between them. Similar observations were reported by Mattarelli *et al*. (2017), in which thymol content was higher in

Monarda didyma than in the closely related *M. fistulosa*, but the antimicrobial activity against Psa was similar between both PEOs, probably due to the presence of carvacrol in the latter species. Moreover, estragole was demonstrated to have strong inhibitory activity against Psa (Song *et al., 2*016). However, in the present work basil had the highest relative abundance of estragole (93.0%), but cumin, which only presented 0.5% of this compound in its composition, had a better antimicrobial performance.

5. Conclusion

In the last decades, PEOs have been under attention due to their interesting antimicrobial activity and natural sources, but few studies have demonstrated their potential *in planta* against pathogens of agronomical importance, including Psa. Cumin EO could become a useful tool in Psa management, as it demonstrated high antimicrobial activity *in vitro* against different Psa and Pfm strains, also reducing the colonization of the highly virulent Psa 7286 in the susceptible *A. chinensis*. Nevertheless, we advise caution when selecting single compounds based on their higher concentration in PEOs composition, as their antimicrobial activity most likely results from an interaction with the other constituents from that PEO. Moreover, as different bacterial strains showed distinct degrees of sensitivity to the PEOs tested here, care should be taken when applying these compounds, as their efficiency may vary between plants infected by distinct bacterial strains. Nevertheless, PEOs seem to have great potential as an environmental-friendly approach to control KBC, reason why additional researches on this topic should be dully pursued, particularly concerning potential shortcoming in plant productivity and/or fruit quality.

Supplementary Material

SM1 - Quantitative and qualitative composition (% w/w) of anise, basil, cardamom, cumin, fennel and laurel essential oils.

Compound	Anise	Basil	Cardamom	Cumin	Fennel	Laurel
1,11-Undecanediol			0.16			
1-Nonanol			0.30			
2-Benzimidazolemethanol	1.22	0.16			0.09	0.60
2-Dimethylaminoaniline			2.32			
2-Methyl-2-bornene			0.09			
3-carene		0.03	2.18	12.04	1.45	0.69
3-Chromanol				11.10		
4-Terpinenyl acetate			0.14			
4-Thujen-2-α-yl acetate					0.05	
Anethole	87.65	1.73	0.18	0.12		77.36
Aromandrene				0.39		
Benzene, 4-ethenyl-1,2-dimethyl-					0.03	0.04
Bicyclogermacrene			0.13			
Bornyl acetate	0.01	0.49	0.24	1.10	1.66	
Camphor	0.02	0.19				0.23
Caryophyllene				0.11		0.07
Chrysanthenol				8.07		
cis-4-thujanol			0.15		0.17	
cis-α-Bergamotene		0.22				
Cuminaldehyde				41.93		0.08
Cuparene	0.39					
D-Limonene		0.02	7.25	0.35	2.83	1.83
Epicubebol		0.04		0.18		
Estragole	2.63	93.04	0.45	0.47	0.44	6.60
Eucalyptol		3.18	0.13	2.97	68.63	
Fenchene			0.58	0.32	0.55	
Fenchone		0.10			0.03	9.00
Fenchyl acetate		0.11				0.03
Germacrene B			0.13			
Guaiol acetate		0.11				
Guanidineacetic acid	0.17	0.09		1.46		0.22
Isogeraniol			0.12			
Isolongifolene, 4,5,9,10-dehydro-	0.05					
Linalyl acetate	0.11	0.32	3.68	0.30		
Longifolene	3.71					
Lynalyl acetate					1.83	0.02
Linalyl formate			0.40		0.14	
L-α-Terpineol				0.12		
m-Cymenene	0.13					

Methyleugenol		0.03			0.20	
Myristicin	0.06					
Nerol acetate			1.11			
p-Cymene	0.49	0.01	0.06	0.30	0.89	0.25
Phellandral				0.60		
Spathunol		0.00				
Terpinen-4-ol	0.02	0.02	0.58	0.43	1.04	0.04
Terpinolene					0.32	1.47
Thunbergol	1.44					
Thymol	0.01					
trans-4-Thujanol			0.07		0.03	
trans-Valerenyl acetate	0.03					
α-Copaene	0.10					0.10
α-himachalene	0.32		75.92			
β-Calacorene	0.09					
β-Curcumene	0.09					
β-Cymene			1.17	16.33	1.18	1.09
β-Elemene			0.31			
β-himachalene	0.36				17.13	0.07
β-Isocumene			1.22			
β-Longipinene	0.19					
β-Terpinene				1.32	0.30	
γ-Cadinene		0.09				
γ-Dehydro-ar-himachalene	0.12					
γ-Himalachene	0.54					
γ-Muurolene			0.39			
γ-Terpinene			0.18		1.00	0.17
δ-Elemene			0.37			
σ-Elemene	0.06					

CHAPTER 5

General Discussion

1. Evaluation of plant genotypic susceptibility to Psa

Field observations generally point out to the higher susceptibility of *A. chinensis* var. *chinensis* (yellow kiwifruit) and *A. chinensis* var. *deliciosa* (green kiwifruit) to Psa, as compared with *A. arguta* (kiwi berry). Nevertheless, this differential susceptibility was never demonstrated under comparable environmental settings, i.e., with plants at the same stage of development being artificially inoculated and grown at the same conditions. Moreover, due to the lower frequency of orchard infections by Pfm and the lower extent of disease symptoms, it is generally acknowledged that this bacterium is less pathogenic to *Actinidia* spp. than Psa, but the reasons for its lower virulence and plant responses to this strain are not yet known.

In the present work, both a short-term and a longer-term disease evaluation (**Chap. 2.1** and **2.2**) revealed a more rapid Psa colonization and higher extent of disease symptoms in *A. chinensis*, as compared with *A. arguta*. This is in line with the observations that *A. chinensis* orchards frequently show a higher extent of disease symptoms and higher removal rates due to infection, as compared with *A. arguta* (Datson *et al*., 2015; Nardozza *et al*., 2015; Wang *et al*., 2020a). In a preliminary work, Datson *et al*. (2015) observed limited Psa progression within *A. arguta* tissues, with the bacterial endophytic population being lower and more restricted to the site near the inoculation zone than in *A. chinensis*. Our results corroborate these previous findings, demonstrating not only the higher tolerance degree of *A. arguta*, as compared with *A. chinensis*, but also the lower virulence of Pfm. In agreement with our observation of a higher Psa colonization throughout the experimental period, a previous work by Wurms *et al*. (2017a) reported more pronounced symptoms following Psa inoculation, with Pfm only leading to woodier, less water-soaked appearance. Taken together, these results corroborate field observations pointing to the higher pathogenicity of Psa, as compared with Pfm (Vanneste *et al*., 2014).

After infection with Psa and Pfm, we also observed an increase in MDA and a decrease in total chlorophyll concentrations in *A. chinensis*, whereas in *A. arguta* no alterations were observed (**Chap. 2.2**). It seems that, in *A. arguta*, plant infection does not lead to oxidative stress nor loss of these photosynthetic pigments, further demonstrating the tolerant character of this species. Psa infection also had a distinct impact on plant primary metabolism depending on the plant species, with *A. chinensis* being generally more affected (**Chap. 3.1**). In this species, Psa led to a significant increase in ornithine and glutamine concentrations in plant tissues, accompanied by the upregulation of several genes related to the ammonia assimilation and the TCA cycle. We also observed a general upregulation of genes involved in amino acids and organic acids metabolism in *A. chinensis*, but not in *A. arguta*. (**Chap. 3.1**). Concordantly, Li *et al*. (2020) demonstrated that in *A. chinensis* Psa-infection increases the content of amino acids and organic acids in plant tissues, leading to an extensive C and N reprogramming in various

metabolic pathways, impairing photosynthesis, C fixation, and the TCA cycle. It is generally acknowledged that glutamate metabolism into ornithine and arginine, together with proline and polyamines, represents a key mechanism of N metabolization in plant tissues, leading to the production of other intermediates related to plant defence, such as NO and GABA (Roberts, 2007). Therefore, we hypothesized that the changes observed in *A. chinensis* may result from the utilization of plant N resources by Psa, which ultimately unbalances the ammonia assimilation and the TCA cycle (Tavernier *et al., 2*007; Rico and Preston, 2008). Additionally, the expression of several genes involved in glucose, *myo*-inositol, galactinol and raffinose metabolism were generally downregulated in both *A. chinensis* and *A. arguta*. In contrast, genes involved in the downstream steps of glycolysis were generally upregulated. Also, genes related to sucrose metabolism and transport were upregulated in *A. chinensis*, but not in *A. arguta*. Similarly, Li *et al*. (2020) reported lower content of e.g., *myo*-inositol, glucose and galactose in *A. chinensis* following Psa infection. Although carbohydrates generally act as signalling molecules and provide energy to support the demanding defence mechanisms, it seems that high concentration of sugars propels Psa colonization in *A. chinensis* (Li *et al*., 2020). In addition, a gene encoding a putative beta-galactosidase (*BGAL*), related to carbohydrate metabolism, was found to be upregulated in moderately tolerant genotypes, but downregulated in highly tolerant ones (Tahir *et al*., 2019). Taken together, these data indicate that Psa infection promotes N and carbohydrate metabolism in *A. chinensis*, possibly to take advantage of the plant's nutritional resources to meet its own metabolic needs (Petriccione *et al*., 2014). The lower degree of impairments to *A. arguta*'s primary metabolism may be an important coping mechanism against Psa, by restricting its access to growth-promoting metabolites, such as N and sugars, thus impairing its colonization rate.

2. Unravelling plant tolerance mechanisms

When plant PRRs, e.g., flagellin and NB-LRR proteins, recognize specific PAMPs characteristic to each pathogen, PTI is activated (Michelotti *et al., 2*018; Wang *et al*., 2018a; Wang *et al*., 2020b). These mechanisms can further lead to ETI, which is activated after recognition of bacterial effectors by plant R-proteins. PTI and ETI can subsequently develop into HR and SAR, involving e.g., strengthening of the cell wall through the deposition of lignin and increased enzymatic activity (Petriccione *et al*., 2014; Wurms *et al*., 2017a; Michelotti *et al*., 2018; Wang *et al*., 2018a; Nunes da Silva *et al*., 2020; Tahir *et al*., 2020). However, how these pathways are activated in susceptible and tolerant genotypes is still not fully understood.

Through whole transcriptome sequencing (**Chap. 3.1**) we identified a total of 89 DEGs related with: pathogen recognition, PPRs, PTI and ETI, general plant defence, defence response to pests and pathogens, disease resistance, HR, SAR, innate immunity, pathogen-

induced ROS scavenging, lipoxygenase activity and cellulose pathway, and defence regulation. Several of these genes have been previously correlated with plant defences in other pathosystems, but not in *Actinidia*/Psa. These include, for example: i) *GFS12* and *PSL5* (involved in PTI and ETI); ii) *PLDDELTA* and *PLDBETA1* (basal defence and nonhost resistance against pathogens); iii) *AGO1*, *AGO5*, *DCL4* and *RDR1* (antiviral RNA silencing); and iv) *N*, *RFL1*, *RPM1* and *RPP13* (disease resistance induced by bacterial effectors) (Eitas *et al*., 2008; Qu *et al*., 2008; Pinosa *et al*., 2013; Zhao *et al*., 2013; Teh *et al*., 2015). In addition, we observed that Psa inoculation in *A. arguta* (tolerant species) led to the overexpression of specific genes involved in pathogen recognition (*TGA2*), PTI and ETI (*BIG5* and *PTI6*), SAR (*DIR1*), disease resistance (*EDM2*), general plant defence (*FOX1*, *GLOX*, *LIP2*, *NRPE1* and *SN2*), innate immunity (*TPR1*), ROS scavenging (*At4g20830*, *PER3*, *PER27*, *PER43*, *PER52* and *RBOHA*), pathogen-induced lipoxygenase activity (*LOX1.5*) and negative regulation of plant defences (*PUB24*, *SRFR1*and *TGA21*). A higher number of genes related to negative regulation of defence responses were upregulated in *A. chinensis* (*BON2*, *FAAH*, *CBP60A*, *CDC48A* and *PUB13*), which may contribute to its higher susceptibility to Psa (Kang *et al*., 2008). We anticipate that these genes may be good candidates as biomarkers for screening Psa tolerance/susceptibility, with potential in the development of more tolerant kiwifruit genotypes through plant breeding. Moreover, it seems that different *Actinidia* spp. genotypes have distinct responses to Psa concerning several defence-related pathways, such as: i) pathogen recognition; ii) ROS scavenging; iii) phenylpropanoids; and iv) phytohormone regulation.

2.1. Pathogen recognition

Genes related with PTI and ETI, such as *FLS2*, *CC-NBS-LRR, CERK1*, *Pti1, Pti4*, *RPP13*, *RPM1* and *RPS2*, have been found to be upregulated in *A. chinensis* 2 dpi with Psa (Wurms *et al*., 2017b; Wang *et al*., 2018b; Song *et al*., 2019; Wang *et al*., 2020b). In the present work, RT-qPCR analysis of gene *Pto3*, involved in pathogen recognition, revealed its overexpression as soon as 2 dpi with Psa in *A. arguta*, whereas in *A. chinensis Pto3* upregulation only occurred 14 dpi (**Chap. 2.2**). In *A. chinensis* the expression of *Pto3* accompanied the increase of Psa endophytic population inside plant tissues, whereas in *A. arguta* it preceded the period of higher bacterial colonization. Besides, RNA-Seq analysis (**Chap. 3.1**) demonstrated that several other genes related with pathogen recognition, PTI and ETI were upregulated shortly after infection with Psa: *FLS2, GFS12* and *PSL5* genes both in *A. chinensis* and *A. arguta*, *TGA1*, *CERK1* and *PTI5* in *A. chinensis*, and *TGA2*, *BIG5* and *PTI6* in *A. arguta*. It seems that Psa recognition by *A. chinensis* and *A. arguta* involves a species-dependent gene activation, which may lead to a more tailored and effective defence response in *A. arguta*, as previously hypothesized (Nunes da Silva *et al*., 2020).

2.2. ROS scavenging

Previous works have shown that in A. *chinensis*, Psa infection promotes ROS generation, such as O^{2-} and H_2O_2, which may lead to e.g., lipid peroxidation, cellular imbalances and cell death (Sharma *et al*., 2012; Cellini *et al*., 2014). In the present work, lipid peroxidation was observed 7 dpi with Psa in *A. chinensis*, and seemed to follow the increase of bacterial density inside plant tissues and the decrease of total chlorophyll (**Chap. 2.1**). This demonstrates that inoculation negatively affected *A. chinensis* cellular homeostasis, whereas in *A. arguta* it did not, further confirming its tolerant trait.

To counteract the noxious effects of ROS, kiwifruit plants produce several antioxidant enzymes. Through RT-qPCR analysis, we observed that the expression of *SOD*, *APX* and *CAT* genes occurred at different stages following infection depending on the plant species (**Chap. 2.1 and 2.2**). These genes were generally upregulated to a higher extent in *A. chinensis*, and tended to increase throughout the development of the disease, whereas in *A. arguta*, the expression of *SOD*, *APX* and *CAT* highly increased in the first stages of infection, decreasing thereafter. RNA-Seq analysis (**Chap. 3.1**) also revealed the involvement of other genes related to ROS scavenging, which were distinct between *A. chinensis* and *A. arguta*. In *A. arguta*, we identified six genes involved in ROS scavenging in response to pathogen infection, including *RBOHA* (related with a rapid and transient phase I oxidative burst induced by pathogen infection), and four different peroxidases (*PER3*, *PER27*, *PER43*, *PER52*, responsible for the removal of H_2O_2 in response to environmental stresses such pathogen attack) (Yoshioka *et al*., 2001). In *A. chinensis*, however, only the expression of *PER1*, *PER4* and *PER44* were significantly affected by Psa infection. Previous studies have reported an increase in peroxidase 4 activity and the upregulation of other antioxidant enzyme-encoding genes, such as *SOD*, *APX* and *CAT*, shortly after Psa infection of *A. chinensis* (Petriccione *et al*., 2014, 2015; Nunes da Silva *et al*., 2019, 2020). Taken together, data demonstrates that the antioxidant system plays an active role during the early stages of infection. Nevertheless, it seems that these mechanisms are differently regulated between susceptible and tolerant genotypes, with *A. arguta* possibly employing a more effective antioxidant response shortly after infection, thus preventing Psa-induced lipid peroxidation (**Chap. 2.2**).

2.3. Phenylpropanoids

Although few studies have explored the role of secondary metabolites in *Actinidia* spp. responses to Psa, phenylpropanoids seem to be of great importance in this pathosystem. In the present work, soluble polyphenols and lignin were found to increase in specific moments following Psa inoculation in *A. chinensis*, with lignin levels being consistently higher in Psa-infected *A. arguta* than in mock-inoculated plants (**Chap. 2.2 and 3.2**). Also, targeted gene expression analysis showed that *DFR*, involved in flavonoid metabolism, was upregulated in Psa-infected *A. chinensis* plants (**Chap. 3.2**). Wang *et al*. (2018a) observed that infection of *A. chinensis* with Psa impaired multiple pathways involved in the metabolism of: terpenes (e.g., carotenoids), phenols (e.g., phenylpropanoids, flavonoids, and phenylalanine), and alkaloids. Besides, tolerant genotypes seem to have constitutively higher concentrations of phenolic compounds, which also increase more drastically than in susceptible genotypes following Psa infection (Miao *et al*., 2009). Taken together, these results indicate that both *A. chinensis* and *A. arguta* can activate the phenylpropanoids pathway as a coping mechanism against Psa infection, although in a distinct manner. In *A. arguta*, lignin accumulation may play a key role in restricting bacterial density in plant tissues (Lee *et al*., 2020), thus contributing to its higher tolerance against the pathogen.

2.4. Phytohormone regulation

Plant responses against pathogens are mediated by complex phytohormone-mediated networks in which SA, JA, ET and ABA counteract and interact with each other, modulating defence responses according to the type of pathogen and host plant (Pieterse *et al*., 2012). In the present work, we observed that with Psa infection: i) JA and SA concentrations increased 2 dpi in *A. chinensis*, but not in *A. arguta*; ii) ABA concentration decreased as soon as 2 dpi in *A. arguta* and only at 15 dpi in *A. chinensis*; and iii) elicitation of the JA pathway in *A. chinensis* increased ABA concentration and disease susceptibility, whereas elicitation with SA did not (**Chap. 3.1 and 3.2**). Our findings corroborate previous works reporting that during Psa infection SA and JA concentrations increase in *A. chinensis* (Wurms *et al*., 2017a). RNA-Seq analysis (**Chap. 3.1**) showed that the increased concentrations of JA and SA in *A. chinensis* were accompanied by the upregulation of several genes related to these pathways, namely: JA-mediated defences (*SYD*, *COI1* and *LRR-RLK*), JA-mediated signalling (*UBP12*, *UBP13* and *RGS1*), SA catabolism (*At1g06620* and *DLO2*) and SA-mediated defences (*CALS12*, *ACA11*, *ACA4*, *ALD1*, *SIZ1* and *MKP1*). In *A. arguta*, in which no changes were observed in JA and SA concentrations, only *CALS12* was upregulated following infection. Several studies have demonstrated that *Actinidia* spp. defence responses against Psa are mainly regulated by SA-mediated pathways, whereas the ABA, ET and JA pathways antagonise plant defences

(Reglinski *et al*., 2013; Cellini *et al*., 2014; Song *et al*., 2019). Although it is generally acknowledged that the JA and SA pathways are mutually antagonistic, it seems that both are triggered shortly after infection with Psa in *A. chinensis*, potently impairing general plant metabolism and defence responses and underpinning its higher susceptibility. We also observed that exogenous application of MJ, an elicitor of the JA pathway, drastically increased Psa endophytic population and ABA concentration in *A. chinensis*, as compared with non-elicited and SA-elicited plants (**Chap. 3.2**). Although ABA is a key player in plant defence responses against several pathogens, Cellini *et al*. (2014) demonstrated that exogenous ABA application increased the extent of Psa infection in *A. chinensis*, possibly because it interferes with SA-mediated defence pathways. Our results demonstrate a positive feedback between the JA and ABA pathways during Psa infection, and corroborates previous findings on ABA's negative regulatory effects on plant defences against this pathogen (Song *et al*., 2019). Moreover, here, ABA concentration decreased 2 dpi after infection in *A. arguta* (**Chap. 3.1**), whereas in *A. chinensis* this was only observed at 15 dpi (**Chap. 3.2**), possibly due to a delayed regulation of ABA metabolism in the later species upon infection. Concordantly, in *A. arguta* genes *NCED1* and *ZEP*, related with ABA-biosynthesis (Xiong *et al*., 2002; Ji *et al*., 2014) were downregulated, whereas *CYP707A1* and *CYP707A3* related to ABA catabolism (Santiago *et al*., 2009) were upregulated shortly after infection (**Chap. 3.1**). Contrastingly, in *A. chinensis* Psa infection led to the upregulation of several genes involved in ABA transport, ABA-mediated defences and ABA-mediated signalling (*ANN4*, *IP5P2*, *KPNB1*, *MIF1*, *ASPG2* and *HAT22*). Overall, results indicate that the downregulation of ABA-mediated pathways could underpin the more effective defence responses against Psa in *A. arguta*, most likely through the promotion of SA-mediated pathways resulting from the negative feedback between these hormonal networks.

3. Developing novel control strategies

So far, no effective methods have been developed for controlling Psa infection and dispersion, and current strategies are largely based on removing infected plants and applying cupric formulations during specific stages of plant development. However, these strategies are frequently ineffective in successfully controlling endophytic Psa populations, or pose ecological risks (Han *et al*., 2004; Pietrzak and McPhail, 2004). As such, recent studies have focused on the development of alternatives to these products, namely through the use of plant elicitors (Reglinski *et al*., 2013; Cellini *et al*., 2014; Scortichini, 2014, Wurms *et al.*, 2017b), but the potential of other strategies against Psa has been overlooked, namely the role of plant fertilization and PEOs application.

3.1. Nitrate fertilization

Nitrogen (N), an essential macronutrient, is the major nutrient applied as a fertilizer to most crop species, as is the case of kiwifruit plants (Mowat *et al*., 2015). Nitrogen can be supplied in the form of nitrate (NO_3^-), ammonium (NH_4^+), or a combination of both, but its uptake and metabolism are very distinct, depending not only on its source, but also on the plant species (Horchani *et al*., 2010; Kammann *et al., 2*015; Hachiya *et al*., 2017; Cao *et al*., 2018). As transcriptome analysis showed that plant infection with Psa leads to several impairments in the ammonia assimilation cycle (**Chap. 3.1**), we hypothesized that the manipulation of N source in kiwifruit plants might allow to tailor defence responses and increase plant tolerance against the pathogen. However, the role of N nutrition in plant responses against Psa is currently poorly understood. High N fertilization is generally discouraged in kiwifruit orchards, as it seems to increase plant susceptibility to Psa, probably by increasing plant vigour and sprouting of new shoots (Costa *et al., 2*013; Donati *et al*., 2014). Moreover, the few reports that attempted to explore the impact of the type of N source in *A. chinensis* susceptibility to Psa used distinct testing methodologies and showed inconclusive results (Mowat *et al.*, 2015; Mauri *et al*., 2016). As such, in a first trial, we explored how NO_3^- and NH_4^+ impacted healthy *A. chinensis* growth, biochemical and mineral composition (**Chap. 4.1**), after which we evaluated how plants responded to Psa infection when grown under different N sources (214 µM of NO_3^-, 214 µM NH_4^+ or a Mix with 107 µM NO_3^- and 107 µM NH_4^+) (**Chap. 4.2**).

Plant growth and fresh weight were not affected by the N source (NO_3^-, NH_4^+ and 1:1 Mix) at 21 dpi (**Chap. 4.1**), but a lower total chlorophyll concentration was observed in plants grown exclusively with NH_4^+ as N source, probably due to the competition for carbon skeletons between NH_4^+ metabolism and photosynthesis (Winter *et al*., 1982; Tabatabaei *et al*., 2006). Roots of NO_3^--supplied plants showed higher concentration of polyphenols, which probably correlates to the lower N concentration observed in these plants that may allow an increased availability of phenylalanine (due to restrictions in protein production) for the production of secondary metabolites (Ibrahim *et al*., 2011; Qadir *et al*., 2017). On the other hand, the higher protein concentrations observed in NH_4^+- and Mix-supplied plants of the present study may result from the active transport of N between and within plant tissues. These treatments also led to higher N concentration in shoots and roots. Contrarily to N, the concentration of P, K, Ca, Mg, Zn and Mn was higher in NO_3^--treated plants, possibly due to a synergic effect in cation uptake (Zhang *et al*., 2010b; Borgognone *et al*., 2013; Na *et al*., 2014; Tsabarducas *et al*., 2017). Concordantly, targeted gene analysis revealed that plants supplied with NO_3^- were more actively increasing N metabolism, by inducing the upregulation of *GLU1* and *GAD1*. This response is likely to counteract the lower total protein and N concentrations observed with this treatment. *FER1* and *MOT1*, involved mineral uptake and storage, were also upregulated in NO_3^--supplied plants. Overall, these results demonstrate that NO_3^- leads to lower accumulation of total N in

plant tissues, but generally improves plant mineral metabolism. As such, it could provide an adaptative advantage in cases of Psa infection.

Although we did not observe differences regarding biometric parameters in plants supplied with NO_3^-, NH_4^+ or Mix for 21 days (**Chap. 4.1**), after 36 days plants grown with NO_3^- and Mix supplementation generally presented higher length, biomass, and shoot to root ratios, as compared with NH_4^+ (**Chap. 4.2**). This is most likely due to impairments induced by NH_4^+ in cell division, expansion and photosynthesis (Rinallo and Modi, 2002). Nevertheless, plant growth parameters were not affected by Psa infection. The lowest endophytic Psa colonization was observed in NO_3^--supplied plants, which is in agreement with preliminary reports by Mowat *et al*. (2015), and may result from the induction by NO_3^- of HR-mediated resistance (Gupta *et al*., 2013). On the other hand, we found that plants grown with NH_4^+ showed higher Psa endophytic population, higher total protein content and overexpression of gene *PR1*, which encodes a PR-protein involved in plant defences (Cellini *et al*., 2014). This demonstrates that NH_4^+-supplied plants might be trying to cope with Psa colonization, promoted by the higher concentration of N in plant tissues, through increased defence-related proteins. In addition, *LOX1* (related to the JA pathway) and *SAM* (ET pathway) were upregulated in Psa-inoculated plants under NH_4^+ and Mix supply. We hypothesize that NH_4^+ has a detrimental effect on *A. chinensis* defence-related mechanisms by: i) increasing N accumulation in plant tissues, favouring pathogen growth and multiplication, and ii) promoting the JA and ET-related pathways, which antagonize kiwifruit plants defences against Psa, as previously discussed. Our results demonstrate that the adoption of tailored N fertilization regimens based on NO_3^- as the source of N (avoiding fertilizers with NH_4^+) may be a useful tool for an integrated Psa management.

3.2. PEOs application

Several studies have shown that PEOs impair bacterial membrane permeability, leading to loss of motility, leakage of intracellular contents and death of the microorganism (Mattarelli *et al., 2*017; Pucci *et al., 2*018; Lovato *et al., 2*019). However, the potential of PEOs to inhibit Psa colonization has been mostly evaluated in *in vitro* conditions and their chemical composition is rarely provided. So far, the only study with Psa-infected kiwifruit plants demonstrated that plant treatment with EOs from *Satureja* spp. and *Thymus* spp. led to a lower number of diseased leaves and/or lower leaf area affected by disease symptoms (Monchiero *et al., 2*015). Thus, additional studies on this subject are needed to better evaluate the potential of PEOs in mitigating Psa infection, propelling their use as environmentally friendly alternatives to the currently used phytosanitary products, but also looking at potential limitations to promote a knowledge-based regulation of their eventual utilization.

In this work, all PEOs tested (anise, basil, cardamom, cumin, laurel and fennel) had *in vitro* antibacterial activity against distinct Psa (1F and 7286) and Pfm strains (18804 and 19441), with cumin being generally more effective (inducing the widest inhibition halos at lower concentrations) (**Chap. 4.3**). However, Psa and Pfm strains showed different sensitiveness to the PEOs tested. Psa1F was the least sensitive strain to fennel and the most sensitive to laurel, whereas Psa7286 was the most sensitive to cumin and the least sensitive to basil. In the case of Pfm, the strain 18804 was the least sensitive to anise and cardamon, whereas 19441 was the most sensitive to these PEOs. These results are in accordance with a previous work reporting that *C. cassia* and *C. sativa* extracts and eugenol had different antibacterial activity depending on the Psa strains (Song *et al*., 2016), also demonstrating a similar behaviour among Pfm strains. As cumin EO had the highest antibacterial activity in the *in vitro* trials, its potential was also evaluated *in planta* against the highly virulent Psa strain 7286. Foliar application of 0.1% of cumin EO 15 days before *A. chinensis* infection with Psa, significantly reduced bacterial colonization by 73% (at 15 dpi). We hypothesise that the higher antimicrobial activity of cumin EO observed in the present work results from its particular chemical composition, rich in e.g., cuminaldehyde, β-cymene and 3-carene. Thus, we attest to the potential of cumin EO in the development of more effective and environmental-friendly approaches to control Psa. Moreover, we advise caution when selecting single compounds based on their higher concentration in PEOs composition (e.g., cuminaldehyde), and when applying PEOs to orchards affected by different bacterial strains. Further studies, particularly concerning the impact of PEOs in plant metabolism and defence regulation, could greatly support their use as environmentally friendly alternatives to the currently used copper-based formulations.

Conclusions and Future Prospects

The overall goal of this thesis was to explore plant tolerance mechanisms against Psa and Pfm, and to identify novel control strategies for a more efficient and sustainable management of kiwifruit bacterial canker. Here, the differential susceptibility of *A. chinensis* and *A. arguta* was confirmed under laboratory conditions for the first time, and analysed through an integrated approach involving conventional and high throughput methodologies, allowing to unravel several pathways that contribute to the higher tolerance of *A. arguta*. Psa rapidly colonized *A. chinensis* tissues following infection, inducing lipid peroxidation and loss of photosynthetic pigments, and inducing N and carbohydrate metabolism, probably to exploit the plant's nutritional resources for its metabolic requirements. On the other hand, *A. arguta*'s higher tolerance seems to result from a faster recognition of the pathogen, a more complex antioxidant response in earlier stages of infection, tissue reinforcement with lignin, and the downregulation of ABA-mediated pathways. Moreover, a total of 20 genes involved in plant response to pathogen infection were only identified in *A. arguta*. These genes have the potential to contribute to unravelling Psa tolerance mechanisms and developing more tolerant kiwifruit genotypes through e.g., gene-targeted plant breeding. We also demonstrate that Psa is more virulent to kiwifruits plants than Pfm, by colonizing plant tissues more rapidly and inducing higher symptom severity, corroborating previous empirical field evidence from other groups.

We also demonstrated that plant fertilization and foliar treatment with PEOs may be useful tools to mitigate Psa infection in *A. chinensis*. N supply using 214 µM NO_3^- (rather than 214 µM NH_4^+ or a 1:1 mix of these two sources), decreased Psa colonization in *A. chinensis*, leading to a general improvement of plant mineral metabolism, which could benefit plant defence mechanisms during infection. Contrastingly, NH_4^+ had a detrimental effect on *A. chinensis* defence-related mechanisms by increasing N accumulation in plant tissues, thus favouring pathogen growth and multiplication, and by promoting the JA and ET-related pathways, which negatively affect kiwifruit plants´ defences against Psa. Besides, the application of cumin EO 15 days before before Psa inoculation decreased its tissue colonization, possibly due to its particular chemical composition, rich in e.g., cuminaldehyde, β-cymene and 3-carene. The present study provides innovative and extensive knowledge on the regulatory pathways triggered by Psa infection in *Actinidia* spp., and demonstrates the relevance of the N source and use PEOs for a more sustainable disease management. However, further studies are needed to fully unravel *Actinidia* spp. tolerance mechanisms to Psa and to validate the field efficacy of the mitigation tools identified in the present work. For example, the full assessment of plant genotypic variability to Psa would benefit from additional studies with a higher number of species

and cultivars, particularly including the more susceptible *A. chinensis* var. *chinensis*. Moreover, from the high amount of transcriptomic data collected during the development of the work described in Chapter 3.1, only a subset of genes related to plant defences, hormonal regulation and primary metabolism was selected. It would be interesting to further explore this data looking for other important pathways, particularly the ones negatively affected by Psa infection, such as plant photosynthesis and secondary metabolism. This could allow elucidating how Psa affects these metabolic pathways in plant species with distinct susceptibilities. It would also be important to correlate the genomic-based data with a broader analysis of plant metabolome, as gene expression is frequently subjected to post-translational modifications that do not result in the anticipated metabolic outcomes.

Finally, although the use of micropropagated plants provides several advantages regarding their laboratorial handling, it would be important to validate the findings described in this thesis in field conditions. This is particularly important regarding the use of NO_3^- and PEOs, as field plants will certainly require higher doses or application frequency, which should be optimized to achieve their full potential against Psa. In addition, other nutrients and minerals should also be explored for improved fertilization-based Psa management. Calcium, for example, would be a good candidate to pursue this research, as its accumulation is generally reduced in fruits of Psa-infected plants (with negative implication for fruit quality and shelf-life).

Reference List

Abelleira, A., Ares, A., Aguín, O., Mansilla, P., López, M.C. (2015). Distribution, detection protocols and characterization of *Pseudomonas syringae* pv*. actinidiae* from kiwifruit in Galicia (northwest Spain). *Acta Horticulturae* **1095**, 49-56.

Afanasiev, M.M., Carlson, W.E. (1943). The relation of phosphorus and nitrogen ratio to the amount of seedling diseases of sugar beets. *The American Society of Sugar Beet Technologist* **1942**, 407-411.

Aguín, O., Ares, A., Abelleira, A., Mansilla, P. (2015). Survival of *Pseudomonas syringae* pv*. actinidiae* in leaf-litter of *Actinidia deliciosa* in Galicia (northwest Spain). *Acta Horticulturae* **1095**, 111-116.

Al-Saddik, H., Simon, J., Cointault, F. (2017). Development of spectral disease indices for 'flavescence dorée' grapevine disease identification. Sensors **17**(12), 2772. DOI: 10.3390/s17122772.

Al-Saddik, H., Simon, J., Cointault, F. (2019). Assessment of the optimal spectral bands for designing a sensor for vineyard disease detection: the case of 'flavescence dorée'. *Precision Agriculture* **20**, 398-422.

Amini, J., Farhang, V., Javadi, T., Nazemi, J. (2016). Antifungal effect of plant essential oils on controlling *Phytophthora* species. *The Plant Pathology Journal* **32**, 16-24.

Andolfi, A., Ferrante, P., Petriccione, M., Cimmino, A., Evidente, A., Scortichini, M. (2014). Production of phytotoxic metabolites by *Pseudomonas syringae* pv*. actinidiae*, the causal agent of bacterial canker of kiwifruit. *Journal of Plant Pathology* **96**, 169-175.

Antoniacci, L., Bugiani, R., Rossi, R., Calzolari, A., Alessandrini, A., Gozzi, R., Spinelli, F., Cellini, A., Mauri, S., Donati, I. (2019). Validation of New Zealand Psa forecasting model in Emilia Romagna Region, Italy. *Acta Horticulturae* **1243**, 71-78.

Antunes, M.D. 2008. Kiwi: da produção à comercialização, Universidade do Algarve, 208 p. ISBN: 978-972-9341-71-7.

Asakura, I., Hoshino, Y. (2018). Interspecific hybridization using miyama matatabi (*Actinidia kolomikta*), a Japanese indigenous wild kiwifruit relative. *The Horticulture Journal* **87**(4), 481-489.

Ashourloo, D., Mobasheri, M., Huete, A. (2014). Developing two spectral disease indices for detection of wheat leaf rust (*Pucciniatriticina*). *Remote Sensing* **6**, 4723-4740.

Ashraf, M., Sultana, R. (2000). Combination effect of NaCl salinity and nitrogen form on mineral composition of sunflower plants. *Biologia Plantarum* **43**(4), 615-619.

Ashrafzadeh, S., Leung, D. (2019). *In vitro* breeding - shortcut to *Pseudomonas syringae* pv*. actinidiae* (Psa) tolerant kiwifruit. *Archives of Phytopathology and Plant Protection* **52**, 501-506.

Atanasova, E. (2008). Effect of nitrogen sources on the nitrogenous forms and accumulation of amino acid in head cabbage. *Plant, Soil and Environment* **54**(2), 66-71.

Atkinson, R., Sharma, N., Hallett, I., Johnston, S., Schröder, R. (2009). *Actinidia eriantha*: a parental species for breeding kiwifruit with novel peelability and health attributes. *New Zealand Journal of Forestry Science* **39**, 207-216.

Baccelli, I., Mauch-Mani, B. (2016). Beta-aminobutyric acid priming of plant defence: the role of ABA and other hormones. *Plant Molecular Biology* **91**, 703-711.

Balestra, G. (2007). Biocontrol of bacterial pathogens of kiwifruit plants. *Acta Horticulturae* **753**, 635-638.

Balestra, G., Renzi, M., Mazzaglia, A. (2010). First report of bacterial canker of *Actinidia deliciosa* caused by *Pseudomonas syringae pv. actinidiae* in Portugal. *New Disease Reports* **22**, 10.

Balestra, G.M., Buriani, G., Cellini, A., Donati, I., Mazzaglia, A., Spinelli, F. (2018). First report of *Pseudomonas syringae* pv*. actinidiae* on kiwifruit pollen from Argentina. *Plant Disease* **102**, 237-237.

Balestra, G.M., Mazzaglia, A., Quattrucci, A., Renzi, M., Rossetti, A. (2009a). Current status of bacterial canker spread on kiwifruit in Italy. *Australasian Plant Disease* Notes **4**, 34-36.

Balestra, G.M., Mazzaglia, A., Quattrucci, A., Renzi, M., Rossetti, A. (2009b). Occurrence of *Pseudomonas syringae* pv*. actinidiae* in Jin Tao kiwi plants in Italy. *Phytopathologia Mediterranea* **48**, 299-301.

Barros, E.P., Moreira, N., Pereira, G.E., Leite, S.G., Rezende, C.M., Pinho, P.G. (2012). Development and validation of automatic HS-SPME with a gas chromatography-ion trap/mass spectrometry method for analysis of volatiles in wines. *Talanta* **101**, 177-86.

Beatrice, C., Linthorst, J., Cinzia, F., Luca, R. (2017). Enhancement of *PR1* and *PR5* gene expressions by chitosan treatment in kiwifruit plants inoculated with *Pseudomonas syringae* pv*. actinidiae*. *European Journal of Plant Pathology* **148**, 163-179.

Beatson, R.A., Datson, P.M., Ferguson, A.R., Montefiori, M. (2014). Use of kiwifruit germplasm resources for genetic improvement. *Acta Horticulturae* **1048**, 25-34.

Becker, C., Urlić, B., Jukić Špika, M., Kläring, H., Krumbein, A., Baldermann, S., *et al*. (2015). Nitrogen limited red and green leaf lettuce accumulate flavonoid glycosides, caffeic acid derivatives, and sucrose while losing chlorophylls, B-carotene and xanthophylls. *PLoS ONE* **10**: e0142867. DOI: 10.1371/journal.pone.0142867.

Bektas, Y., Eulgem, T. (2015). Synthetic plant defence elicitors. *Frontiers in Plant Science* **5**, 804. DOI: 10.3389/fpls.2014.00804.

Beresford, R., Tyson, J., Henshall, W. (2017). Development and validation of an Infection risk model for bacterial canker of kiwifruit, using a multiplication and dispersal concept for forecasting bacterial diseases. *Phytopathology* **107**, 184-191.

Berger, S., Sinha, A.K., Roitsch, T. (2007). Plant physiology meets phytopathology: plant primary metabolism and plant-pathogen interactions. *Journal of Experimental Botany* **58**, 4019-4026. DOI: 10.1093/jxb/erm298.

Bergsträsser, S., Fanourakis, D., Schmittgen, S., Cendrero-Mateo, M.P., Jansen, M., Scharr, H., Rascher, U. (2015). HyperART: non-invasive quantification of leaf traits using hyperspectral absorption-reflectance-transmittance imaging. *Plant Methods* **11**, 1. DOI: 10.1186/s13007-015-0043-0.

Berrocal-Lobo, M., Segura, A., Moreno, M., López, G., García-Olmedo, F., Molina, A. (2002). Snakin-2, an antimicrobial peptide from potato whose gene is locally induced by wounding and responds to pathogen infection. *Plant Physiology* **128**, 951-961.

Black, M., Casonato, S., Bent, S. (2015). Opportunities for environmental modification to control *Pseudomonas syringae* pv*. actinidiae* in kiwifruit. *Acta Horticulturae* **1105**, 253-260.

Borgognone, D., Colla, G., Rouphael, Y., Cardarelli, M., Rea, E., Schwarz, D. (2013). Effect of nitrogen form and nutrient solution pH on growth and mineral composition of self-grafted and grafted tomatoes. *Scientia Horticulturae* **149**, 61-69.

Borrelli, V., Brambilla, V., Rogowsky, P., Marocco, A., Lanubile, A. (2018). The enhancement of plant disease resistance using CRISPR/Cas9 technology. *Frontiers in Plant Science* **9**, 1245. DOI: 10.3389/fpls.2018.01245.

Borrero, C., Trillas, M.I., Delgado, A., Aviles, M. (2012). Effect of ammonium/nitrate ratio in nutrient solution on control of *Fusarium* wilt of tomato by *Trichoderma asperellum* T34. *Plant Pathology* **61**, 132-139.

Boulent, J., Foucher, S., Théau, J., St-Charles, P. (2019). Convolutional neural networks for the automatic identification of plant diseases. *Frontiers in Plant Science* **10**, 941.

Bournier, M., Tissot, N., Mari, S., Boucherez, J., Lacombe, E., Briat, J. F., Gaymard, F. (2013). *Arabidopsis ferritin 1* (*AtFer1*) gene regulation by the phosphate starvation response 1 (*AtPHR1*) transcription factor reveals a direct molecular link between iron and phosphate homeostasis. *Journal of Biological Chemistry* **288**(31), 22670-22680.

Bourrain, L. (2018). *In vitro* propagation of *Actinidia melanandra* Franch. and *Actinidia rubricaulis* Dunn. from shoot tip explants. *New Zealand Journal of Crop and Horticultural Science* **46**, 162-173.

Bown, H.E., Watt, M.S., Clinton, P.W., Mason, E.G. (2010). Influence of ammonium and nitrate supply on growth, dry matter partitioning, N uptake and photosynthetic capacity of *Pinus radiata* seedlings. *Trees* **24**, 1097-1107.

Bradford, M.M. (1976). A rapid and sensitive method for the quantitation of microgram quantities of protein utilizing the principle of protein-dye binding. *Analytical Biochemistry* **72**, 248-254.

Britto, D., Kronzucker, H. (2002). NH_4 toxicity in higher plants: A critical review. *Journal of Plant Physiology* **159**, 567-584.

Broadley, M., Brown, P., Cakmak, I., Rengel, Z., Zhao, F. (2012). Function of nutrients: micronutrients, In: Marschner, P. (Ed.), *Marschner's Mineral Nutrition of Higher Plants* Ed 3. Academic Press, Massachusetts, USA, pp. 135-189.

Brunetti, A., Pucci, N., Modesti, V., Lumia, V., Latini, A., Loreti, S., Pilotti, M. (2020). *In vitro* and *in planta* screening of compounds for the control of *Pseudomonas syringae* pv*. actinidiae* in *Actinidia chinensis* var. *chinensis*. *European Journal of Plant Pathology* **158**, 829-848.

Bulman, Z., Le, P., Hudson, A., Savka, M. (2011). A novel property of propolis (bee glue): Anti-pathogenic activity by inhibition of N-acyl-homoserine lactone mediated signaling in bacteria. *Journal of Ethnopharmacology* **138**, 788-797.

Buwalda, J., Wilson, G., Smith, G., Littler, R. (1990). The development and effects of nitrogen deficiency in field-grown kiwifruit (*Actinidia deliciosa*) vines. *Plant and Soil* **129**, 173-182.

Cacioppo, O., Marcon, M., Tacconi, G. (2015). Pedoclimatic web monitoring system for *Pseudomonas syringae* pv*. actinidiae* (Psa) and orchard management. *Acta Horticulturae* **1095**, 129-134.

Callaway, E. (2018). EU law deals blow to CRISPR crops. Nature News, 560. Available at: https://media.nature.com/original/magazine-assets/d41586-018-05814-6/d41586-018-05814-6.pdf [Last accessed in 16 January 2021].

Calonnec, A., Burie, J.-B., Langlais, M., Guyader, S., Saint-Jean, S., Sache, I., Tivoli, B. (2012). Impacts of plant growth and architecture on pathogen processes and their consequences for epidemic behavior. *European Journal of Plant Pathology* **135**(3), 479-497.

Cameron, A., De Zoysa, G., Sarojini, V. (2014). Antimicrobial peptides against *Pseudomonas syringae* pv*. actinidiae* and *Erwinia amylovora*: chemical synthesis, secondary structure, efficacy, and mechanistic investigations. *Biopolymers* **102**, 88-96.

Cameron, A., Sarojini, V. (2014). *Pseudomonas syringae* pv*. actinidiae*: chemical control, resistance mechanisms and possible alternatives. *Plant Pathology* **63**, 1-11.

Camó, C., Bonaterra, A., Badosa, E., Baró, A., Feliu, L. (2019). Antimicrobial peptide KSL-W and analogues: Promising agents to control plant diseases. *Peptides* **112**, 85-95.

Cao, P., Lu, C., Yu, Z. (2018). Historical nitrogen fertilizer use in agricultural ecosystems of the contiguous United States during 1850-2015: application rate, timing, and fertilizer types. *Earth System Science Data* **10**, 969-984.

Cellini, A., Biondi, E., Buriani, G., Farneti, B., Rodriguez-Estrada, M.T., Braschi, I., Savioli, S., Blasioli, S., Rocchi, L., Biasioli, F., Costa, G., Spinelli, F. (2016). Characterization of volatile organic compounds emitted by kiwifruit plants infected with *Pseudomonas syringae* pv*. actinidiae* and their effects on host defences. *Trees* **30**, 795-806.

Cellini, A., Donati, I., Fiorentini, L., Vandelle, E., Polverari, A., Venturi, V., Buriani, G., Vanneste, J.L., Spinelli, F. (2020). N-acyl homoserine lactones and lux solos regulate social behaviour and virulence of *Pseudomonas syringae* pv*. actinidiae*. *Microbial Ecology* **79**(2), 383-396.

Cellini, A., Fiorentini, L., Buriani, G., Yu, J., Donati, I., Cornish, D.A., Novak, B., Costa, G., Vanneste, J.L., Spinelli, F. (2014). Elicitors of the salicylic acid pathway reduce incidence of bacterial canker of kiwifruit caused by *Pseudomonas syringae* pv. *actinidae*. *Annals of Applied Biology* **165**, 441-453.

Cellini, A., Fiorentini, L., Dharmaraj, K., Vanneste, J.L., Cristescu, S.M., Harren, F.J.M., Costa, G., Spinelli, F. (2012). Evidences of ethylene as a virulence factor for *Pseudomonas syringae* pv*. actinidiae* and field measures to limit the kiwifruit plant bacterial canker. In Proceedings of the IXth International Conference on the Plant Hormone Ethylene, 19-23 March 2012, Rotorua, New Zealand.

Cesco, S., Tolotti, A., Nadalini, S., Rizzi, S., Valentinuzzi, F., Mimmo, T., Porfido, C., Allegretta, I., Giovannini, O., Perazzolli, M., Cipriani, G., Terzano, R., Pertot, I., Pii, Y. (2020). *Plasmopara viticola* infection affects mineral elements allocation and distribution in *Vitis vinifera* leaves. *Scientific Reports* **10**, 18759. DOI: 10.1038/s41598-020-75990-x.

Chapman, J., Taylor, R., Weir, B., Romberg, M., Vanneste, J., Luck, J, Alexander, B. (2012). Phylogenetic relationships among global populations of *Pseudomonas syringae pv. actinidiae*. *Phytopathology* **102**(11), 1034-1044.

Chase, A.R. (1989). Effect of nitrogen and potassium fertilizer rates on severity of *Xanthomonas* blight of *Syngonium podophyllum*. Plant Disease **73**, 972-975.

Chen, J., Wen, P., Kong, W., Pan, Q., Zhan, J., Li, J., Wan, S., Huang, W. (2006). Effect of salicylic acid on phenylpropanoids and phenylalanine ammonia-lyase in harvested grape berries. *Postharvest Biology and Technology* **40**, 64-72.

Cheng, H.-Y., Li, Y., Wan, S., Zhang, J., Pang, Q., Li, G, Jing, J. (1995). Pathogenic identification of kiwifruit bacterial canker in Anhui. *Journal of Anhui Agricultural University* **22**, 219-223.

Cheng, L., Nie, X., Jiang, C., Li, S. (2019). The combined use of the antagonistic yeast *Hanseniaspora uvarum* with β-aminobutyric acid for the management of postharvest diseases of kiwifruit. *Biological Control* **137**, 104019. DOI: 10.1016/j.biocontrol.2019.104019.

Chiabrando, V., Giacalone, G. (2018). Kiwifruit under plastic covering: impact on fruit quality and on orchard microclimate. *Journal of Food, Nutrition and Agriculture* **1**, 1-6.

Choi, S., Jayaraman, J., Segonzac, C., Park, H., Park, H., Han, S., Sohn, K. (2017). *Pseudomonas syringae* pv*. actinidiae* type III effectors localized at multiple cellular compartments activate or suppress innate immune responses in *Nicotiana benthamiana*. *Frontiers in Plant Science* **8**, 2157.

Chouhan, S., Sharma, K., Guleria, S. (2017). Antimicrobial activity of some essential oils-present status and future perspectives. Medicines 4(3), 58. DOI: 10.3390/medicines4030058.

Clay, N.K., Adio, A.M., Denoux, C., Jander, G, Ausubel, F.M. (2009). Glucosinolate metabolites required for an *Arabidopsis* innate immune response. *Science* **323**(5910), 95-101.

Collina, M., Donati, I., Bertacchini, E., Brunelli, A., Spinelli, F. (2016). Greenhouse assays on the control of the bacterial canker of kiwifruit (*Pseudomonas syringae* pv. *actinidiae*). *Journal of Berry Research* **6**, 407-415.

Compant, S., Samad, A., Faist, H., Sessitsch, A. (2019). A review on the plant microbiome: Ecology, functions, and emerging trends in microbial application. *Journal of Advanced Research* **19**, 29-37.

Cornish, D.A., Yu, J., Oldham, J., Benge, J., Max, W., Vanneste, J. (2015). *In vitro* inhibition of *Pseudomonas syringae* pv. *actinidiae* by wound protectants. *New Zealand Plant Protection* **68**, 332-339.

Costa, G., Donati, I., Mauri, S., Graziani, S., Cellini, A., Buriani, G., Fiorentini, L., Rocchi, L., Giacomuzzi, V., Spinelli, F. (2013). Influence of orchard management on kiwifruit bacterial disease. Proceedings of the I International Symposium on Bacterial Canker of Kiwifruit (Psa), New Zealand, 19-22 Nov 2013.

Cotru, R., Renzi, M., Taratufolo, M.C., Mazzaglia, A., Balestra, G.M., Stănică, F. (2013). *Actinidia arguta* ploidy level variation in relation to *Pseudomonas syringae* pv. *actinidiae* susceptibility. *Lucrări Ştiinţifice* **56**, 1-12.

Couvin, D., Bernheim, A., Toffano-Nioche, C., Touchon, M., Michalik, J., Néron, B., Rocha, E., Vergnaud, G., Gautheret, D., Pourcel, C. (2018). CRISPRCasFinder, an update of CRISRFinder, includes a portable version, enhanced performance and integrates search for Cas proteins. *Nucleic Acids Research* **46**, 246-251.

Cunty, A., Poliakoff, F., Rivoal, C., Cesbron, S., Fischer-Le Saux, M., Lemaire, C., Jacques, M.A., Manceau, C, Vanneste, J.L. (2015). Characterisation of *Pseudomonas syringae* pv. *actinidiae* (Psa) isolated from France and assignment of Psa biovar 4 to a de novo pathovar: *Pseudomonas syringae* pv. *actinidifoliorum pv. nov. Plant Pathology* **64**, 582-596.

Currie, M., Martin, P., Blattmann, M., Gordon, B., Patterson, K. (2014). Final report on growing tolerant cultivars in a Psa environment, VI1296. A report prepared for ZESPRI Group Limited. SPTS No. 9766. Plant Food Research, Auckland, New Zealand. Available at: http://www.kvh.org.nz/vdb/document/99012 [Last accessed 16 January 2021].

Dangl, J.L., Jones, J.D. (2001). Plant pathogens and integrated defence responses to infection. *Nature* **411**, 826-833.

Daranas, N., Roselló, G., Cabrefiga, J., Donati, I., Francés, J., Badosa, E., Spinelli, F., Montesinos, E., Bonaterra, A. (2019). Biological control of bacterial plant diseases with *Lactobacillus plantarum* strains selected for their broad-spectrum activity. *The Annals of Applied Biology* **174**, 92-105.

Datson, P., Nardozza, S., Manako, K., Herrick, J., Martinez-Sanchez, M., Curtis, C. (2015). Monitoring the *Actinidia* germplasm for resistance to *Pseudomonas syringae* pv. *actinidiae. Acta Horticulturae* **1095**, 181-184.

de Jong, H., Reglinski, T., Elmer, P., Wurms, K., Vanneste, J.L., Guo, L.F., Alavi, M. (2019). Integrated use of *Aureobasidium pullulans* strain CG163 and acibenzolar-s-methyl for management of bacterial canker in kiwifruit. *Plants*, 8(8), 287. DOI: 10.3390/plants8080287.

de Ollas, C., Hernando, B., Arbona, V., Gómez-Cadenas A. (2013) Jasmonic acid transient accumulation is needed for abscisic acid increase in citrus roots under drought stress conditions. *Physiologia Plantarum* **147**, 296-306.

Deak, K.I., Malamy, J. (2005). Osmotic regulation of root system architecture. *The Plant Journal* **43**(1), 17-28.

Debenham, M., Seelye, J., Mullan, A. (2013). An *in vitro* repository for clonal kiwifruit germplasm. *Acta Horticulturae* **1113**, 93-98.

DGAV, Direção-Geral de Alimentação e Veterinária (2014). Plano de Ação Nacional para o Controlo da *Pseudomonas syringae* pv. *actinidiae* do Kiwi (PSA). Available at: http://srvbamid.dgv.min-agricultura.pt/xeov21/attachfileu.jsp?look_parentBoui=5020213&att_display=n&att_download=y [Last accessed in 16 January 2021].

Di Lallo, G.D., Evangelisti, M., Mancuso, F., Ferrante, P., Marcelletti, S., Tinari, A., Superti, F., Migliore, L., D'Addabbo, P., Frezza, D., Scortichini, M., Thaller, M. (2014). Isolation and partial characterization of bacteriophages infecting *Pseudomonas syringae* pv. *actinidiae*, causal agent of kiwifruit bacterial canker. *Journal of Basic Microbiology* **54**(11), 1210-1221. DOI: 10.1002/jobm.201300951.

Dietrich, R., Ploss, K., Heil, M. (2004). Constitutive and induced resistance to pathogens in *Arabidopsis thaliana* depends on nitrogen supply. *Plant, Cell & Environment* **27**(7), 896-906.

Ditommaso, A., Watson, A.K. (1995). Impact of a fungal pathogen, *Colletotrichum coccodes* on growth and competitive ability of *Abutilon theophrasti*. *New Phytologist* **131**(1), 51-60.

Dixon, R.A., Achnine, L., Kota, P., Liu, C.J., Srinivasa, M.S., Wang, L.J. (2002). The phenylpropanoid pathway and plant defence-a genomics perspective. *Molecular Plant Pathology* **3**, 371-390.

Do, K., Chung, B., Joa, J. (2016). D-PSA-K: A model for estimating the accumulated potential damage on kiwifruit canes caused by bacterial canker during the growing and overwintering seasons. *Plant Pathology Journal* **32**, 537-544.

Donati, I., Buriani, G., Cellini, A., Mauri, S., Costa, G., Spinelli, F. (2014). New insights on the bacterial canker of kiwifruit (*Pseudomonas syringae* pv. *actinidiae*). *Journal of Berry Research* **4**, 53-67.

Donati, I., Cellini, A., Buriani, G., Mauri, S., Kay, C., Tacconi, G., Spinelli, F. (2018). Pathways of flower infection and pollen-mediated dispersion of *Pseudomonas syringae* pv. *actinidiae*, the causal agent of kiwifruit bacterial canker. *Horticulture Research* **5**, 56. DOI: 10.1038/s41438-018-0058-6.

Donati, I., Cellini, A., Sangiorgio, D., Vanneste, J.L., Scortichini, M., Balestra, G.M., Spinelli, F. (2020). *Pseudomonas syringae* pv. *actinidiae*: Ecology, Infection Dynamics and Disease Epidemiology. *Microbial Ecology* **80**, 81-102.

Dong, O., Ronald, P. (2019). Genetic engineering for disease resistance in plants: recent progress and future perspectives. *Plant Physiology* **180**, 26-38.

Dordas, C. (2008). Role of nutrients in controlling plant diseases in sustainable agriculture. A review. *Agronomy for Sustainable Development* **28**, 33-46.

DRAPC, Direção Regional de Agricultura e Pescas do Centro (2015). Relatório da execução do plano de ação nacional para o controlo da *Pseudomonas syringae* pv. *actinidiae* do kiwi (Psa) na DRAPcentro. Available at: https://www.drapc.gov.pt/base/documentos/relatorio_psa_kiwi_2015.pdf [Last accessed in 16 January 2021].

DRAPN, Direção Regional de Agricultura e Pescas do Norte (2013). Plano de ação nacional para o controlo da *Pseudomonas syringae* pv. *actinidiae* do kiwi (PSA). Available at: http://www.drapnorte.gov.pt/drapn/conteudos/lca/PAN-PSA%20KIWI_2013.pdf [Last accessed in 16 January 2021].

Dreo, T., Pirc, M., Ravnikar, M., Zezlina, I., Poliakoff, F., Rivoal, C., Nice, F., Cunty A. (2014). First report of *Pseudomonas syringae* pv. *actinidiae*, the causal agent of bacterial canker of kiwifruit in Slovenia. *Plant Disease* **98**(11), 1578.

Eitas, T.K., Nimchuk, Z., Dangl, J. (2008). *Arabidopsis TAO1* is a TIR-NB-LRR protein that contributes to disease resistance induced by the *Pseudomonas syringae* effector *AvrB*. *Proceedings of the National Academy of Sciences* **105**, 6475-6480.

EPPO, European and Mediterranean Plant Protection Organization (2012). Pest Risk Analysis for *Pseudomonas syringae* pv. *actinidiae*. Available at: https://gd.eppo.int/download/doc/1255_pra_exp_PSDMAK.pdf [Last accessed in 16 January 2021].

EPPO, European and Mediterranean Plant Protection Organization (2014). PM 7/120 (1) *Pseudomonas syringae* pv. *actinidiae*. *EPPO Bulletin* **44 (3)**, 360-375.

EPPO, European and Mediterranean Plant Protection Organization (2018). Reporting Service Articles. https://gd.eppo.int/taxon/PSDMAK/reporting [Last accessed in 16 January 2021].

EPPO, European and Mediterranean Plant Protection Organization (2020). *Pseudomonas syringae pv. actinidiae* Distribution. Available at: https://gd.eppo.int/taxon/PSDMAK/distribution [Last accessed in 16 January 2021].

ESRI, Environmental Systems Research Institute (2014). ArcGIS desktop help 10.2 geostatistical analyst. Available at http://resources.arcgis.com/en/help/main/10.2/index.html [Last accessed in 16 January 2021]

Eulgem, T., Tsuchiya, T., Wang, X., Beasley, B., Cuzick, A., Tör, M., Zhu, T., Mcdowell, J.H., Holub, E., Dangl, J. (2007). *EDM2* is required for *RPP7*-dependent disease resistance in *Arabidopsis* and affects *RPP7* transcript levels. *The Plant Journal: for Cell and Molecular Biology*, **49**(5), 829-839.

Euring, D., Loefke, C., Teichmann, T., Polle, A. (2012). Nitrogen fertilization has differential effects on N allocation and lignin in two Populus species with contrasting ecology. *Trees* **26**, 1933-1942.

Everett, K.R., Pushparajah, I.P.S., Vergara, M., Shahjahan, K., Parry, B., Casonato, S. (2016). Monitoring effectiveness of wound protectants against Psa. A report prepared for ZESPRI Group Limited. SPTS No. 12997. Plant Food Research, Auckland, New Zealand. Available at: https://www.kvh.org.nz/vdb/document/105229 [Last accessed in 16 January 2021].

Everett, K.R., Shahjahan, K., Pushparajah, I.P.S., Ramos, L., Parry, B., Hasna, L., Middleditch, C., Vergara, M.J. (2017). Monitoring effectiveness of wound protectants against Psa: Part 2. A report prepared for ZESPRI Group Limited. SPTS No. 15809. Plant Food Research, Auckland, New Zealand. Available at: http://www.kvh.org.nz/vdb/document/104230 [Last accessed in 16 January 2021].

FAOSTAT, Food and Agriculture Organization statistical database (2021). Available at: http://www.fao.org/faostat/en/#data/QC/visualize [Last accessed in 16 January 2021]

Félix, A., Cavaco, M. (2004). Caracterização do ecossistema agrário da cultura da actinídea (*Actinidia deliciosa* A. CHEV) (*Actinidiaceae*). VII-Encontro Nacional de Proteção Integrada, Coimbra (Portugal).

Ferguson, A.R. (2013). Kiwifruit: the wild and the cultivated plants. *Advances in Food and Nutrition Research*, **68**, 15-32.

Ferrante, P. Scortichini, M. (2009). Identification of *Pseudomonas syringae pv. actinidiae* as causal agent of bacterial canker of yellow kiwifruit (*Actinidia chinensis* Planchon) in central Italy. Journal of Phytopathology **157**(11-12), 768-770.

Ferrante, P., Fiorillo, E., Marcelletti, S., Marocchi, F., Mastroleo, M., Simeoni, S., Scortichini, M. (2012). The importance of the main colonization and penetration sites of *Pseudomonas syringae* pv. *actinidiae* and prevailing weather conditions in the development of epidemics in yellow kiwifruit, recently observed in central Italy. Journal of Plant Pathology **94**, 455-461.

Ferrante, P., Scortichini, M. (2014). Frost promotes the pathogenicity of *Pseudomonas syringae pv. actinidiae* in *Actinidia chinensis* and *A. deliciosa* plants. Plant Pathology **63**(1), 12-19.

Figueira, D., Garcia, E., Ares, A., Tiago, I., Veríssimo, A., Costa, J. (2020). Genetic diversity of *Pseudomonas syringae* pv*. actinidiae*: Seasonal and spatial population dynamics. *Microorganisms* **8**, 931.

Fister, A., Landherr, L., Maximova, S., Guiltinan, M. (2018). Transient expression of CRISPR/Cas9 machinery targeting *TcNPR3* enhances defense response in *Theobroma cacao*. *Frontiers in Plant Science* **9**, 268. DOI: 10.3389/fpls.2018.00268.

Flores, O., Retamales, J., Núñez, M., León, M., Salinas, P., Besoain, X., Yañez, C., Bastías, R. (2020). Characterization of bacteriophages against *Pseudomonas syringae* pv*. actinidiae* with potential use as natural antimicrobials in kiwifruit plants. *Microorganisms* **8**, 974. DOI: 10.3390/microorganisms8070974.

Frampton, R.A., Taylor, C., Moreno, A.V., Visnovsky, S.B., Petty, N.K., Pitman, A., Fineran, P.C. (2014). Identification of Bacteriophages for biocontrol of the kiwifruit canker phytopathogen *Pseudomonas syringae* pv*. actinidiae*. *Applied and Environmental Microbiology* **80**, 2216 - 2228.

Froud, K., Beresford, R.M., Cogger, N. (2017). Risk factors for kiwifruit bacterial canker disease development in 'Hayward' kiwifruit blocks. *Australasian Plant Pathology* **46**, 421-431.

Fujikawa, T., Hatomi, H., Sawada, H. (2020). Draft genome sequences of 10 strains of *Pseudomonas syringae* pv*. actinidiae* biovar 1, a major kiwifruit bacterial canker pathogen in Japan. *Microbiology Resource Announcements* 9, e00759-20. DOI: 10.1128/mra.00759-20.

Fujikawa, T., Sawada, H. (2016). Genome analysis of the kiwifruit canker pathogen *Pseudomonas syringae* pv*. actinidiae* biovar 5. Scientific Reports **6**, 21399. DOI: 10.1038/srep21399.

Fujikawa, T., Sawada, H. (2019). Genome analysis of *Pseudomonas syringae* pv*. actinidiae* biovar 6, which produces the phytotoxins, phaseolotoxin and coronatine. Scientific Reports **9**, 3836. DOI: 10.1038/s41598-019-40754-9.

Fukushima, R.S., Hatfield, R.D. (2001). Extraction and isolation of lignin for utilization as a standard to determine lignin concentration using the acetyl bromide spectrophotometric method. *Journal of Agricultural and Food Chemistry* **49**(7), 3133-3139.

Gallego-Giraldo, L., Posé, S., Pattathil, S., Peralta, A.G., Hahn, M.G., Ayre, B.G., Sunuwar, J., Hernandez, J., Patel, M., Shah, J., Rao, X., Knox, J.P., Dixon, R.A. (2018). Elicitors and defense gene induction in plants with altered lignin compositions. *New Phytologist* **219**(4), 1235-1251.

Gao, Q., Zhu, S., Kachroo, P., Kachroo, A. (2015). Signal regulators of systemic acquired tolerance. *Frontiers in Plant Science* **6**, 228. DOI: 10.3389/fpls.2015.00228.

Garbin, L.M., Dillenburg, R.L. (2008). Effects of different nitrogen sources on growth, chlorophyll concentration, nitrate reductase activity and carbon and nitrogen distribution in *Araucaria angustifoli*. *Brazilian Journal of Plant Physiology* **20**(4): 295-303.

Gaskin, R., Manktelow, D., Cook, S. May, B., Horgan, D., van Leeuwen, R. (2016). Novel technologies to deliver protectant sprays to strung canopies. A report prepared for ZESPRI Group Limited. Plant Protection Chemistry NZ, Rotorua, New Zealand. Available at: http://www.kvh.org.nz/vdb/document/103507 [Last accessed in 16 January 2021].

Gavanji, S., Larki, B., Zand, A.J., Mohammadi, E., Mehrasa, M., Taraghian, A.H. (2012). Comparative effects of propolis of honey bee on pathogenic bacteria. *African Journal of Pharmacy and Pharmacology* **6**, 2408-2412.

Genka, H., Baba, T., Tsuda, M., Kanaya, S., Mori, H., Yoshida, T., Noguchi, M., Tsuchiya, K., Sawada, H. (2006). Comparative analysis of argK-tox clusters and their flanking regions in phaseolotoxin-producing *Pseudomonas syringae* pathovars. *Journal of Molecular Evolution* **63**, 401-414.

Gill, S., Tuteja, N. (2010). Reactive oxygen species and antioxidant machinery in abiotic stress tolerance in crop plants. *Plant Physiology and Biochemistry* **48**(12), 909-930.

Gloser, V., Gloser, J. (2000). Nitrogen and base cation uptake in seedlings of *Acer pseudoplatanus* and *Calamagrostis villosa* exposed to an acidified environment. *Plant and Soil* **226**, 71-77.

Gnanamanickam, S.S. (2006). *Plant-associated bacteria*. Springer, Netherlands. DOI: 10.1007/978-1-4020-4538-7.

Gong, B., Li, X., VandenLangenberg, K., Wen, D., Sun, S., Wei, M., Li, Y., Yang, F., Shi, Q., Wang, X. (2014). Overexpression of S-adenosyl-L-methionine synthetase increased tomato tolerance to alkali stress through polyamine metabolism. *Plant Biotechnology Journal* **12**(6): 694-708.

Groen, S., Whiteman, N. (2014). The Evolution of ethylene signaling in plant chemical ecology. *Journal of Chemical Ecology* **40**, 700-716.

Guan, X., Zhao, H., Xu, Y., Wang, Y. (2010). Transient expression of glyoxal oxidase from the Chinese wild grape *Vitis pseudoreticulata* can suppress powdery mildew in a susceptible genotype. *Protoplasma* **248**, 415-423.

Guginski-Piva, C.A., Santos, I., Júnior, A., Heck, D., Flores, M.F., Pazolini, K. (2015). Propolis for the control of powdery mildew and the induction of phytoalexins in cucumber. *Idesia (arica)* **33**, 39-47.

Guo, S., Zhou, Y., Shen, Q., Zhang, F. (2007). Effect of ammonium and nitrate nutrition on some physiological processes in higher plants - growth, photosynthesis, photorespiration, and water relations. *Plant Biology* **9**, 21-29.

Gupta, K.J., Brotman, Y., Segu, S., Zeier, T.E., Zeier, J., Persijn, S., Cristescu, S.M., Harren, F.J., Bauwe, H., Fernie, A.R., Kaiser, W.M., Mur, L.A. (2013). The form of nitrogen nutrition affects resistance against *Pseudomonas syringae* pv. *phaseolicola* in tobacco. *Journal of Experimental Botany* **64**(2), 553-568.

Gupta, N., Bajpai, M., Majumdar, R.S., Mishra, P. (2015). Response of Iodine on antioxidant levels of *Glycine max* L. grown under Cd stress. *Advances in Biological Research* **9**, 40-48.

Gupta, N., Debnath, S., Sharma, S., Sharma, P., Purohit, J. (2017). Role of nutrients in controlling the plant diseases in sustainable agriculture, In: Meena, V., Mishra, P., Bisht, J., Pattanayak, A. (Eds.), *Agriculturally Important Microbes for Sustainable Agriculture*, Springer, Singapore, pp. 33-46.

Hachiya, T., Sakakibara, H. (2017). Interactions between nitrate and ammonium in their uptake, allocation, assimilation, and signaling in plants. *Journal of Experimental Botany* **68**(10), 2501-2512.

Han, H.S., Koh, Y., Hur, J., Jung, J. (2004). Occurrence of the *strA-strB* streptomycin resistance genes in *Pseudomonas* species isolated from kiwifruit plants. *Journal of Microbiology* **42**(4), 365-368.

Hanley, Z. (2018) Kiwifruit (*Actinidia* spp.) breeding, In Al-Khayri, J., Jain, S., Johnson, D. (Eds), *Advances in Plant Breeding Strategies: Fruits*, Vol. 3. Springer, pp. 377-401.

Hashem, M., Moharam, A.M., Zaied, A.A., Saleh, F. (2010). Efficacy of essential oils in the control of cumin root rot disease caused by *Fusarium* spp. *Crop Protection* **29**, 1111-1117.

Hatfield, R.D., Grabber, J.H., Ralph, J, Brei, K. (1999). Using the acetyl bromide assay to determine lignin concentrations in herbaceous plants: some cautionary notes. *Journal of Agricultural and Food Chemistry* **47**(2), 628-632.

Hauck, P., Thilmony, R., He, S.Y. (2003). A *Pseudomonas syringae* type III effector suppresses cell wall-based extracellular defense in susceptible Arabidopsis plants. *Proceedings of the National Academy of Sciences of the United States of America* **100**(14), 8577-8582.

Hawkesford, M., Horst, W., Kichey, T., Lambers, H., Schjoerring, J., Møller, I.S., White, P. (2012). Functions of macronutrients, In: Marschner, P. (Ed.), *Marschner's Mineral Nutrition of Higher Plants* Ed 3. Academic Press, Massachusetts, USA, pp. 135-189.

Haynes, R.J., Goh, K.M. (1978). Ammonium and nitrate nutrition of plants. *Biological Reviews* **53**, 465-510.

Hee Lee, Y., Choi, C.W., Kim, S., Yun, J.G., Chang, S.W., Kim, Y.S., Hong, J. (2012). Chemical pesticides and plant essential oils for disease control of tomato bacterial wilt. *Plant Pathology Journal* **28**, 32-39.

Hill, R., Stark, C., Cummings, N., Elmer, P., Hoyte, S. (2015). Use of beneficial microorganisms and elicitors for control of *Pseudomonas syringae* pv*. actinidiae* in kiwifruit (*Actinidia* spp.). *Acta Horticulturae* **1095**, 137-144.

Hirano, S.S., Upper, C.D. (1990). Population biology and epidemiology of *Pseudomonas syringae*. *Annual Review of Phytopathology* **28**, 155-177.

Hoffland, E., Jeger, M.J., van Beusichem, M.L. (2000). Effect of nitrogen supply rate on disease resistance in tomato depends on the pathogen. *Plant and Soil* **218**, 239-247.

Holaskova, E., Galuszka, P., Frebort, I., Oz, M. (2015). Antimicrobial peptide production and plant-based expression systems for medical and agricultural biotechnology. *Biotechnology Advances* **33**, 1005-1023.

Holmes, A. (2012). Effect of soil nutrition and composition on the susceptibility of Hayward and Hort16A to *Pseudomonas syringae* pv*. actinidiae*. ZESPRI Group, Tauranga, New Zealand. Available at: http://www.kvh.org.nz/vdb/document/91481 [Last accessed in 16 January 2021].

Hoopen, F.T., Cuin, T.A., Pedas, P., Hegelund, J.N., Shabala, S., Schjoerring, J.K., Jahn, T.P. (2010). Competition between uptake of ammonium and potassium in barley and *Arabidopsis* roots: molecular mechanisms and physiological consequences. *Journal of Experimental Botany* **61**(9), 2303-2315.

Horchani, F., Hajri, R., Aschi-Smiti, S. (2010). Effect of ammonium or nitrate nutrition on photosynthesis, growth, and nitrogen assimilation in tomato plants. *Journal of Plant Nutrition and Soil Science* **173**(4), 610-617.

Hossain, M.A., Munemasa, S., Uraji, M., Nakamura, Y., Mori. I.C., Murata, Y. (2011). Involvement of endogenous abscisic acid in methyl jasmonate induced stomatal closure in *Arabidopsis*. *Plant Physiology* **156**, 430-438.

Howard, D.D., Chambers, A.Y., Logan, J. (1994). Nitrogen and fungicide effects on yield components and disease severity in wheat. *Journal of Production Agriculture* **7**, 448-454.

Hoyte, S., Reglinski, T., Elmer, P.,Mauchline, N., Stannard, K, Casonato, S. (2015). Developing and using bioassays to screen for Psa resistance in New Zealand kiwifruit. *Acta Horticulturae* **1095**, 171-180.

Huang, H., Liu, Y. (2014). Natural hybridization, introgression breeding, and cultivar improvement in the genus *Actinidia*. *Tree Genetics Genome* **10**, 1113-1122.

Huang, H., Wang, Y., Zhang, Z., Jiang, Z., Wang, S. (2004). *Actinidia* germplasm resources and kiwifruit industry In China. *HortScience* **39**, 1165-1172.

Huang, S., Ding, J., Deng, D., Tang, W., Sun, H., Liu, D., Zhang, L., *et al*. (2013). Draft genome of the kiwifruit *Actinidia chinensis*. *Nature Communications* **4**, 2640. DOI: 10.1038/ncomms3640.

Huang, Z.A., Jiang, D.A., Yang, Y., Sun, W.J., Jin, S.H. (2004). Effects of nitrogen deficiency on gas exchange, chlorophyll fluorescence, and antioxidant enzymes in leaves of rice plants. *Photosynthetica* **42**, 357-364.

Huber, D., Römheld, V., Weinmann, M. (2012a). Relationship between nutrition, plant diseases and pests, In: Marschner, P. (Ed.), *Marschner's Mineral Nutrition of Higher Plants*, Ed 3. Academic Press, Massachusetts, pp. 283-298.

Huber, D.M., Jones, J.B. (2012b). The role of magnesium in plant disease. *Plant and Soil* **368**, 73-85.

Ibrahim, M.H., Jaafar, H.Z.E., Rahmat, A., Rahman, Z.A. (2011). Effects of nitrogen fertilization on synthesis of primary and secondary metabolites in three varieties of kacip fatimah (*Labisia pumila* Blume). *International Journal of Molecular Sciences* **12**(8), 5238-5254.

Ide, Y., Kusano, M., Oikawa, A., Fukushima, A., Tomatsu, H., Saito, K., Hirai, M., Fujiwara, T. (2011). Effects of molybdenum deficiency and defects in molybdate transporter *MOT1* on transcript accumulation and nitrogen/sulphur metabolism in *Arabidopsis thaliana*. *Journal of Experimental Botany* **62**(4): 1483-1497.

INE, Instituto Nacional de Estatísticas (2018). Estatísticas Agrícolas 2018. Available at: https://www.ine.pt/ngt_server/attachfileu.jsp?look_parentBoui=383057785&att_display=n&att_download=y [Last accessed 16 January 2021].

Ishiga, T., Sakata, N., Nguyen, V.T., Ishiga, Y. (2020). Flood inoculation of seedlings on culture medium to study interactions between *Pseudomonas syringae* pv. *actinidiae* and kiwifruit. *Journal of General Plant Pathology* **86**, 257-265.

Iterson, M.V., Boer, J.M., Menezes, R. (2010). Filtering, FDR and power. *BMC Bioinformatics* **11**, 450-450.

Jaganathan, D., Ramasamy, K., Sellamuthu, G., Jayabalan, S., Venkataraman, G. (2018). CRISPR for crop improvement: an update review. *Frontiers in Plant Science* **9**, 985.

Jaski, J., Telaxka, F., Moura, G., Franzener, G. (2019). Green propolis ethanolic extract in bean plant protection against bacterial diseases. *Ciência Rural* **49**(6), e20180597. DOI: 10.1590/0103-8478CR20180597.

Jayaraman, J., Yoon, M., Applegate, E.R., Stroud, E.A., Templeton, M. (2020). *AvrE1* and *HopR1* from *Pseudomonas syringae* pv. *actinidiae* are additively required for full virulence on kiwifruit. *Molecular Plant Pathology* **21**, 1467-1480.

Ji, K., Kai, W., Zhao, B., Sun, Y., Yuan, B., Dai, S., Li, Q., Chen, P., Wang, Y., Pei, Y., Wang, H., Guo, Y., Leng, P. (2014). *SlNCED1* and *SlCYP707A2*: key genes involved in ABA metabolism during tomato fruit ripening. *Journal of Experimental Botany* **65**, 5243-5255.

Johnson, C., Boden, E., Arias, J. (2003). Salicylic acid and *NPR1* induce the recruitment of trans-activating TGA factors to a defense gene promoter in *Arabidopsis*. *The Plant Cell* **15**, 1846-1858.

Jung, Y., Kang, K. (2014). Application of antimicrobial peptides for disease control in plants. *Plant Breeding and Biotechnology* **2**, 1-13.

Kammann, C., Schmidt, H., Messerschmidt, N., Linsel, S., Steffens, D., Mueller, C., Koyro, H., Conte, P., Stephen, J. (2015). Plant growth improvement mediated by nitrate capture in co-composted biochar. *Scientific Reports* **5**, 11080. DOI: 10.1038/srep11080.

Kang, L., Wang, Y., Uppalapati, S.R., Wang, K., Tang, Y., Vadapalli, V., Venables, B., Chapman, K., Blancaflor, E., Mysore, K. (2008). Overexpression of a fatty acid amide hydrolase compromises innate immunity in *Arabidopsis*. *The Plant Journal: for Cell and Molecular Biology* **56**(2), 336-349.

Kennelly, M., Cazorla, F., de Vicente, A., Ramos, C., Sundin, G. (2007). *Pseudomonas syringae* diseases of fruit trees: progress toward understanding and control. *Plant Disease* **91**, 4-17.

Khandan, H.A., Gallipoli, L., Mazzaglia, A. (2013). Predicting the potential global distribution of *Pseudomonas syringae* pv. *actinidiae* (Psa). *New Zealand Plant Protection* **66**, 184-193.

Kim, K., Son, K.I., Koh, Y. (2018). Adaptation of the New Zealand Psa risk model for forecasting kiwifruit bacterial canker in Korea. *Plant Pathology* **67**, 1208-1219.

Kinnersley, A.M., Turano, F. (2000). Gamma aminobutyric acid (GABA) and plant responses to stress. *Critical Reviews in Plant Sciences* **19**(6): 479-509.

Kisaki, G., Tanaka, S., Ishihara, A., Igarashi, C., Morimoto, T., Hamano, K., Endo, A., *et al*. (2018). Evaluation of various cultivars of *Actinidia* species and breeding source *Actinidia rufa* for resistance to *Pseudomonas syringae* pv*. actinidiae* biovar 3. *Journal of General Plant Pathology* **84***,* 399-406.

Ko, S., Lee, Y., Cha, K., Park, K., Park, I., Kim, Y. (2002). An improved method for testing pathogenicity of *Pseudomonas syringae* pv*. actinidiae* causing bacterial canker of kiwifruit. *Research in Plant Disease* **8**(4), 250-253.

Koh, Y. (1994). Outbreak and spread of bacterial canker in kiwifruit. *Korean Journal of Plant Pathology* **10**, 68-72.

Koh, Y., Park, S., Lee, D. (1996). Characteristics of bacterial canker of kiwifruit occurring in Korea and its control by trunk injection. *Plant Pathology Journal* **12**, 324-330.

Koh, Y.J., Kim, G.H., Jung, J.S., Lee, Y.S., Hur, J.S. (2010). Outbreak of bacterial canker on Hort16A (*Actinidia chinensis* Planchon) caused by *Pseudomonas syringae* pv*. actinidiae* in Korea. *New Zealand Journal of Crop and Horticultural Science* **38**, 275-282.

Kolomiets, M.V., Chen, H., Gladon, R.J., Braun, E.J., Hannapel, D.J. (2000). A leaf lipoxygenase of potato induced specifically by pathogen infection. *Plant Physiology* **124**, 1121-1130.

Kopka, J., Schauer, N., Krueger, S., Birkemeyer, C., Usadel, B., Bergmüller, E., Dörmann, P., Weckwerth, W., Gibon, Y., Stitt, M., Willmitzer, L., Fernie, A.R., Steinhauser, D. (2005). GMD@CSB.DB: the golm metabolome database. *Bioinformatics* **21**, 1635-1638.

Kulbat, K., 2016. The role of phenolic compounds in plant resistance Ed 2 Vol 8. Institute of General Food Chemistry, Lodz University of Technology, Wolczanska, pp. 97-108.

KVH, Kiwifruit Vine Health (2016). A Review of research and development undertaken on Psa. A report prepared for ZESPRI Group Limited. Kiwifruit Vine Health (KVH), Mt. Maunganui, New Zealand. Available at: http://www.kvh.org.nz/vdb/document/103504 [Last accessed 16 January 2021].

KVH, Kiwifruit Vine Health (2018). Psa-V best practice guide. A report prepared for Kiwifruit Vine Health. KVH, Mt. Maunganui, New Zealand. Available at: https://www.kvh.org.nz/vdb/document/101436 [Last accessed 16 January 2021].

Lamichhane, J.R., Osdaghi, E., Behlau, F., Köhl, J., Jones, J.B., Aubertot, J. (2018). Thirteen decades of antimicrobial copper compounds applied in agriculture. A review. *Agronomy for Sustainable Development* **38**, 1-18.

Lastdrager, J., Hanson, J., Smeekens, S. (2014). Sugar signals and the control of plant growth and development. *Journal of Experimental Botany* **65**(3), 799-807

Łata, B. (2014). Variability in enzymatic and non-enzymatic antioxidants in red and green-leafy kale in relation to soil type and N-level. *Scientia Horticulturae* **68**, 38-45.

Lattanzio, V. (2013). Phenolic Compounds: Introduction, In: K.G Ramawat, J.M., Mérillon (Eds) *Natural Products*, Springer-Verlag: Berlin Heidelberg, pp. 543-580.

Lea, U.S., Slimestad, R., Smedvig, P., Lillo, C. (2006). Nitrogen deficiency enhances expression of specific MYB and bHLH transcription factors and accumulation of end products in the flavonoid pathway. *Planta* **225**, 1245-1253.

Lee, Y., Kim, J., Kim, G.H., Choi, E.D., Koh, Y., Jung, A.J. (2017). Biovars of *Pseudomonas syringae* pv*. actinidiae* strains, the causal agent of bacterial canker of kiwifruit, isolated in Korea. *Research in Plant Disease* **23**(1), 35-41.

Lee, Y.S., Kim, G.H., Song, Y.-R., Oh, C.-S., Koh, Y.J., Jung, J.S. (2020). Streptomycin resistant isolates of *Pseudomonas syringae* pv*. actinidiae* in Korea. *Research in Plant Disease* **26**, 44-47.

Lei, Y., Jing, Z., Li, L. (2015). Selection and evaluation of a new kiwifruit rootstock hybrid for bacterial canker resistance. *Acta Horticulturae* 1096, 413-420.

Li, H.S. (2000). Principles and techniques of plant physiological biochemical experiment. Beijing: Higher Education Press.

Li, T., Fan, P., Yun, Z., Jiang, G., Zhang, Z., Jiang, Y. (2019). β-Aminobutyric Acid Priming Acquisition and Defense Response of Mango Fruit to Colletotrichum gloeosporioides Infection Based on Quantitative Proteomics. *Cells* **8,** 1029. DOI: 10.3390/cells8091029.

Li, T., Spalding, M., Weeks, D., Yang, B. (2012). High-efficiency TALEN-based gene editing produces disease-resistant rice. *Nature Biotechnology* **30**, 390-392.

Li, Y., Cheng, H., Fang, S., Qian, Z. (2001). Prevalent forecast of kiwifruit bacterial canker caused by *Pseudomonas syringae* pv*. actinidiae*. *Ying Yong Sheng Tai Xue Bao* **12**(3), 355-358.

Li, Y., Wang, X., Zeng, Y., Liu, P. (2020). Metabolic profiling reveals local and systemic responses of kiwifruit to *Pseudomonas syringae* pv*. actinidiae*. *Plant Direct* **4**(12), e00297. DOI: 10.1002/pld3.297.

Lima, R.P., Silva, G.C., Dantas, A.L., Dantas, R.L., Sousa, A.S., Melo, R.D., Silva, S.D. (2018). Ascorbic acid redox metabolism in 'Paluma' guava under nitrogen fertilization. *Acta Horticulturae* **1194**, 389-396.

Lisec, J., Schauer, N., Kopka, J., Willmitzer, L., Fernie, A. (2006). Gas chromatography mass spectrometry-based metabolite profiling in plants. *Nature Protocols* **1**, 387-396.

Liu, P., Xue, S., He, R., Hu, J., Wang, X., Jia, B., Gallipoli, L., Mazzaglia, A., Balestra, G.M., Zhu, L. (2016). *Pseudomonas syringae* pv*. actinidiae* isolated from non-kiwifruit plant species in China. *European Journal of Plant Pathology* **145**, 743-754.

Livak, K.J, Schmittgen, T.D. (2001). Analysis of relative gene expression data using real-time quantitative PCR and the 2(-Delta Delta C(T)). *Methods* **25**, 402-408.

Lorenzo, O., Piqueras, R., Sanchez-Serrano, J.J., Solano, R. (2003). Ethylene response factor1 integrates signals from ethylene and jasmonate pathways in plant defense. *Plant Cell* **15**, 165-178.

Lovato, A., Pignatti, A., Vitulo, N., Vandelle, E., Polverari, A. (2019). Inhibition of virulence-related traits in *Pseudomonas syringae* pv*. actinidiae* by gunpowder green tea extracts. *Frontiers in Microbiology* **10**, 2362. DOI: 10.3389/fmicb.2019.02362.

Lu, X., Tintor, N., Mentzel, T., Kombrink, E., Boller, T., Robatzek, S., Schulze-Lefert, P., Saijo, Y. (2009). Uncoupling of sustained MAMP receptor signaling from early outputs in an *Arabidopsis* endoplasmic reticulum glucosidase II allele. *Proceedings of the National Academy of Sciences* **106**, 22522-22527.

Lu, Y, Yao, J.F. (2018). Chloroplasts at the crossroad of photosynthesis, pathogen infection and plant defense. *International Journal of Molecular Sciences* **19**(12), E3900. DOI: 10.3390/ijms19123900.

Lu, Y.X., Li, C.J., Zhang, F.S. (2005). Transpiration, potassium uptake and flow in Tobacco as affected by nitrogen forms and nutrient levels. *Annals of Botany* **95**(6), 991-998.

Luedemann, A., Strassburg, K., Erban, A., Kopka, J. (2008). TagFinder for the quantitative analysis of gas chromatography-mass spectrometry (GC-MS)-based metabolite profiling experiments. *Bioinformatics* **24**, 732-737.

Maes, W., Baert, A., Huete, A., Minchin, P.E., Snelgar, W., Steppe, K. (2016). A new wet reference target method for continuous infrared thermography of vegetations. *Agricultural and Forest Meteorology* **226**, 119-131.

Maes, W., Minchin, P., Snelgar, W., Steppe, K. (2014). Early detection of Psa infection in kiwifruit by means of infrared thermography at leaf and orchard scale. *Functional Plant Biology* **41**, 1207-1220.

Mahlein, A. (2016). Plant disease detection by imaging sensors - Parallels and specific demands for precision agriculture and plant phenotyping. *Plant Disease* **100**(2), 241-251.

Mahlein, A., Rumpf, T., Welke, P., Dehne, H., Plümer, L., Steiner, U., Oerke, E. (2013). Development of spectral indices for detecting and identifying plant diseases. *Remote Sensing of Environment* **128**, 21-30.

Marcon, M., Cacioppo, O., Tacconi, G. (2015). Osiris: new pedoclimatic web monitoring system for irrigation, management and PSA control. *Acta Horticulturae* **1096**, 409-412.

Marinova, D., Ribarova, F, Atanassova, M. (2005). Total phenolics and total flavonoids in bulgarian fruits and vegetables. *Journal of Chemical Technology and Metallurgy* **40**, 255-260.

Mariotti, F., Tomé, D., Mirand, P.P., (2008). Converting Nitrogen into Protein - Beyond 6.25 and Jones' Factors. *Critical Reviews in Food Science and Nutrition* **48**, 177-184.

Mattarelli, P., Epifano, F., Minardi, P., Vito, M.D., Modesto, M., Barbanti, L., Bellardi, M. (2017). Chemical composition and antimicrobial activity of essential oils from aerial parts of *Monarda didyma* and *Monarda fistulosa* cultivated in Italy. *Journal of Essential Oil Bearing Plants* **20**, 76-86.

Mauch-Mani, B., Baccelli, I., Luna, E., Flors, V. (2017). Defense priming: an adaptive part of induced resistance. *Annual Review of Plant Biology* **68**, 485-512.

Mauri, S., Cellini, A., Buriani, G., Donati, I., Costa, G., Spinelli, F. (2016). Optimization of cultural practices to reduce the development of *Pseudomonas syringae* pv*. actinidiae*, causal agent of the bacterial canker of kiwifruit. *Journal of Berry Research* **6**(4), 355-371.

McAtee, P.A., Brian, L.A., Curran, B., Linden, O.V., Nieuwenhuizen, N.J., Chen, X., Henry-Kirk, R.A., Stroud, E.A., Nardozza, S., Jayaraman, J., Rikkerink, E.H., Print, C.G., Allan, A.C, Templeton, M.D. (2018). Re-programming of *Pseudomonas syringae* pv*. actinidiae* gene expression during early stages of infection of kiwifruit. *BMC genomics* **19**, 822. DOI: 10.1186/s12864-018-5197-5.

McCann, H.C., Li, L., Liu, Y., Li, D., Pan, H., Zhong, C., Rikkerink, E., Templeton, M., Straub, C., Colombi, E., Rainey, P., Huang, H. (2017). Origin and evolution of the kiwifruit canker pandemic. *Genome Biology and Evolution* **9**, 932-944.

McCann, H.C., Rikkerink, E.H., Bertels, F., Fiers, M., Lu, A., Rees-George, J., Andersen, M., Gleave, A., Haubold, B., Wohlers, M., Guttman, D., Wang, P., Straub, C., Vanneste, J., Rainey, P., Templeton, M. (2013). Genomic analysis of the kiwifruit pathogen *Pseudomonas syringae* pv*. actinidiae* provides insight into the origins of an emergent plant disease. *PLoS Pathogens*, **9**(7), e1003503. DOI: 10.1371/journal.ppat.1003503.

Melotto, M., Underwood, W.R., Koczan, J., Nomura, K., He, S. (2006). Plant stomata function in innate immunity against bacterial invasion. *Cell* **126**, 969-980.

Miao, L., Genjia, T., Yao, L. (2009). Relationships between the concentrations of phenolics, soluble proteins in plants of kiwifruit cultivars and their resistance to kiwifruit bacterial canker by *Pseudomonas syringae* pv*. actinidiae*. *Plant Protection* **35**(1), 37-41.

Miao, L., Genjia, T., Yao, L., Lian, X. (2005). Resistance mechanism of kiwifruit cultivars to *Pseudomonas syringae* pv. *actinidae*. *Acta Phytopathologica Sinica* **32**(1):37-42.

Michelotti, V., Lamontanara, A., Buriani, G., Orrù, L., Cellini, A., Donati, I., Vanneste, J.L., Cattivelli, L., Tacconi, G, Spinelli, F. (2018). Comparative transcriptome analysis of the

interaction between *Actinidia chinensis* var. *chinensis* and *Pseudomonas syringae* pv. *actinidiae* in absence and presence of acibenzolar-S-methyl. *BMC Genomics* **19**(1), 585. DOI: 10.1186/s12864-018-4967-4.

Mills, T., Boldingh, H., Blattmann, P., Green, S., Meekings, J. (2008). Nitrogen application rate and the concentration of other macronutrients in the fruit and leaves of gold kiwifruit. *Journal of Plant Nutrition* **31**, 1656-1675.

Misra, R.C., Sandeep, Kamthan, M., Kumar, S., Ghosh, S. (2016). A thaumatin-like protein of *Ocimum basilicum* confers tolerance to fungal pathogen and abiotic stress in transgenic *Arabidopsis*. *Scientific Reports* **6**, 25340. DOI: 10.1038/srep25340.

Mittler, R., Vanderauwera, S., Gollery, M, Van Breusegem, F. (2004). The reactive oxygen gene network in plants. *Trends in Plant Science* **9**, 490-498.

Mohanty, S., Hughes, D., Salathé, M. (2016). Using deep learning for image-based plant disease detection. *Frontiers in Plant Science* **7**, 1419. DOI: 10.3389/fpls.2016.01419.

Monchiero, M., Gullino, M., Pugliese, M., Spadaro, D., Garibaldi, A. (2015). Efficacy of different chemical and biological products in the control of *Pseudomonas syringae* pv. *actinidiae* on kiwifruit. *Australasian Plant Pathology* **44**, 13-23.

Mori, Y., Kuwano, Y., Tomokiyo, S., Kuroyanagi, N., Odahara, K. (2019). Inhibitory effects of Moso bamboo (*Phyllostachys heterocycla* f. *pubescens*) extracts on phytopathogenic bacterial and fungal growth. *Wood Science and Technology* **53**, 135-150.

Mortazavi, A., Williams, B.A., Mccue, K., Schaeffer, L., Wold, B. (2008). Mapping and quantifying mammalian transcriptomes by RNA-Seq. *Nature Methods* **5**, 621-628.

Morton, A. (2013). Kiwifruit (*Actinidia* spp.) vine and fruit responses to nitrogen fertiliser applied to the soil or leaves. PhD Thesis in Fruit Science, Massey University (New Zealand). Available at: https://mro.massey.ac.nz/handle/10179/6856 [Last accessed in 16 January 2021].

Mounier, E., Pervent, M., Ljung, K., Gojon, A., Nacry, P. (2014). Auxin-mediated nitrate signaling by *NRT1.1* participates in the adaptive response of *Arabidopsis* root architecture to the spatial heterogeneity of nitrate availability. *Plant, Cell & Environment* **37**, 162-174.

Mowat, A., Hoyte, S., Holmes, A.W., Elmer, P., Reglinski, T., Miller, S.A., Saunders, S.J. (2015). Effect of nitrogen source on the susceptibility of two kiwifruit seedling genotypes to bacterial canker. *Acta Horticulturae* **1095**, 161-167.

Mucyn, T.S., Clemente, A., Andriotis, V.M., Balmuth, A.L., Oldroyd, G.E., Staskawicz, B.J, Rathjen, J.P. (2006). The tomato NBARC-LRR protein Prf interacts with Pto kinase *in vivo* to regulate specific plant immunity. *Plant Cell* **18**, 2792-2806.

Munene, R., Changamu, E.O., Korir, N.K., Gweyi-Onyango, J. (2017). Effects of different nitrogen forms on growth, phenolics, flavonoids and antioxidant activity in amaranth species. *Tropical Plant Research* **4**, 81-89.

Mur, L.A.J., Simpson, C., Kumari, A., Gupta, A.K., Gupta, K.J. (2016). Moving nitrogen to the centre of plant defence against pathogens. *Annals of Botany* **119**(5), 703-709.

Na, L., Li, Z., Xiangxiang, M., Ara, N., Jinghua, Y., Mingfang, Z. (2014). Effect of nitrate/ammonium ratios on growth, root morphology and nutrient elements uptake of watermelon (*Citrullus* l*anatus*) seedlings. *Journal of Plant Nutrition* **37**(11), 1859-1872.

Napoleão, T.A., Soares, G., Vital, C.E., Bastos, C., Castro, R., Loureiro, M.E., Giordano, A. (2017). Methyl jasmonate and salicylic acid are able to modify cell wall but only salicylic acid alters biomass digestibility in the model grass *Brachypodium distachyon*. *Plant Science* **263**, 46-54.

Nardozza, S., Boldingh, H.L., Osorio, S., Höhne, M., Wohlers, M., Gleave, A.P., MacRae, E.A., Richardson, A.C., Atkinson, R.G., Sulpice, R., Fernie, A.R., Clearwater, M.J. (2013).

Metabolic analysis of kiwifruit (*Actinidia deliciosa*) berries from extreme genotypes reveals hallmarks for fruit starch metabolism. *Journal of Experimental Botany* **64**, 5049-5063.

Nardozza, S., Martinez-Sanchez, M., Curtis, C., Datson, P., Montefiori, M. (2015). Screening *Actinidia* germplasm for different levels of tolerance, or resistance, to Psa (*Pseudomonas syringae* pv*. actinidiae*). *Acta Horticulturae* **1096**, 351-356.

Neves, N. (2008). Informação Botânica; In: Antunes, D. (Ed), *Kiwi: da produção à comercialização*. Universidade do Algarve, pp. 29-39.

Ni, P., Wang, L., Deng, B., Jiu, S., Ma, C., Zhang, C., Almeida, A., Wang, D., Xu, W., Wang, S. (2020). Combined application of bacteriophages and carvacrol in the control of *Pseudomonas syringae* pv*. actinidiae* planktonic and biofilm forms. *Microorganisms* **8**(6), 837. DOI: 10.3390/microorganisms8060837.

Novaes, E., Osorio, L., Drost, D.R., Miles, B., Boaventura-Novaes, C., Benedict, C., Dervinis, C., Yu, Q., Sykes, R., Davis, M., Martin, T.A., Peter, G., Kirst, M. (2009). Quantitative genetic analysis of biomass and wood chemistry of Populus under different nitrogen levels. *The New Phytologist*, **182(4)**, 878-890.

Nunes da Silva, M., Machado, J., Balestra, G.M., Mazzaglia, A., Vasconcelos, M., Carvalho, S.M.P. (2019). Exploring the expression of defence-related genes in *Actinidia* spp. after infection with *Pseudomonas syringae* pv*. actinidiae* and pv. *actinidifoliorum*: first steps. *European Journal of Horticultural Science* **84**, 206-212.

Nunes da Silva, M., Vasconcelos, M., Gaspar, M., Balestra, G.M., Mazzaglia, A., Carvalho, S.M.P. (2020). Early pathogen recognition and antioxidant system activation contributes to *Actinidia arguta* tolerance against *Pseudomonas syringae* pathovars *Actinidiae* and *actinidifoliorum*. *Frontiers in Plant Science* **11**, 1022. DOI: 10.3389/fpls.2020.01022.

Ochoa-Díaz, M.M., Daza-Giovannetty, S., Gómez-Camargo, D. (2018). Bacterial genotyping methods: from the basics to modern. *Methods in Molecular Biology* **1734**, 13-20.

Oliveras, À., Baró, A., Montesinos, L., Badosa, E., Montesinos, E., Feliu, L., Planas, M. (2018). Antimicrobial activity of linear lipopeptides derived from BP100 towards plant pathogens. *PLoS ONE* **13**, e0201571. DOI: 10.1371/journal.pone.0201571.

Ollas, C., Hernando, B., Arbona, V., Gomez-Cadenas, A. (2013). Jasmonic acid transient accumulation is needed for abscisic acid increase in citrus roots under drought stress conditions. *Physiologia Plantarum* **147**, 296-306.

Ordóñez, R., Zampini, I., Moreno, M., Isla, M. (2011). Potential application of Northern Argentine propolis to control some phytopathogenic bacteria. *Microbiological Research* **166**, 578-584.

Ortigosa, A., Gimenez-Ibanez, S., Leonhardt, N., Solano, R. (2019). Design of a bacterial speck resistant tomato by CRISPR/Cas9-mediated editing of SlJAZ2. *Plant Biotechnology Journal* **17**, 665-673.

Pacheco, C., Calouro, F., Vieira, S., Santos, F., Neves, N., Curado, F., Franco, J., Rodrigues, S., Antunes, D. (2008). Influence of nitrogen and potassium on yield, fruit quality and mineral composition of kiwifruit. *International Journal of Energy and Environment* **2**(1), 9-15.

Park, J., Bae, S., Kim, J. (2015). Cas-Designer: a web-based tool for choice of CRISPR-Cas9 target sites. *Bioinformatics* **31**, 4014-4016.

Park, J., Lim, J., Yu, J., Oh, C. (2018). Genomic features and lytic activity of the bacteriophage PPPL-1 effective against *Pseudomonas syringae* pv*. actinidiae*, a cause of bacterial canker in kiwifruit. *Journal of Microbiology and Biotechnology* **28**, 1542-1546.

Pattemore, D., Goodwin, R., McBrydie, H., Hoyte, S., Vanneste, J. (2014). Evidence of the role of honey bees (*Apis mellifera*) as vectors of the bacterial plant pathogen *Pseudomonas syringae*. *Australasian Plant Pathology* **43**, 571-575.

Pedersen, I.F., Sorensen, P., Rasmussen, J., Withers, P.J.A., Rubaek, G.H. (2019). Fertilizer ammonium:nitrate rations determine phosphorus uptake by young maize plants. *Journal of Plant Nutrition and Soil Science* **182**, 541-551.

Peng, A., Chen, S., Lei, T., Xu, L., He, Y., Wu, L., Yao, L., Zou, X. (2017). Engineering canker-resistant plants through CRISPR/Cas9-targeted editing of the susceptibility gene *CsLOB1* promoter in citrus. *Plant Biotechnology Journal* **15**, 1509-1519.

Petriccione, M., Di Cecco, I., Arena, S., Scaloni, A, Scortichini, M. (2013). Proteomic changes in *Actinidia chinensis* shoot during systemic infection with a pandemic *Pseudomonas syringae* pv*. actinidiae* strain *Journal of Proteomics* **78**, 461-476.

Petriccione, M., Mastrobuoni, F., Zampella, L., Scortichini, M. (2015). Reference gene selection for normalization of RT-qPCR gene expression data from *Actinidia deliciosa* leaves infected with *Pseudomonas syringae* pv*. actinidiae*. *Scientific Reports* **5**, 16961. DOI: 10.1038/srep16961.

Petriccione, M., Salzano, A.M., Di Cecco, I., Scaloni, A., Scortichini, M. (2014). Proteomic analysis of the *Actinidia deliciosa* leaf apoplast during biotrophic colonization by *Pseudomonas syringae* pv*. actinidiae*. *Journal of Proteomics* **101**, 43-62.

Pieterse, C.M., Does, D.V., Zamioudis, C., Leon-Reyes, A., Wees, S.V. (2012). Hormonal modulation of plant immunity. *Annual Review of Cell and Developmental Biology* **28**, 489-521.

Pietrzak, U., McPhail, D. (2004). Copper accumulation, distribution and fractionation in vineyard soils of Victoria, Australia. *Geoderma* **122**, 151-166.

Pinheiro, L., Pereira, C., Frazão, C., Balcão, V., Almeida, A. (2019). Effciency of phage ϕ6 for biocontrol of *Pseudomonas syringae* pv. *syringae*: an *in vitro* preliminary study. *Microorganisms* **7**(9), 286. DOI: 10.3390/microorganisms7090286.

Pinosa, F., Buhot, N., Kwaaitaal, M., Fahlberg, P., Thordal-Christensen, H., Ellerström, M., Andersson, M. (2013). *Arabidopsis* phospholipase Dδ is involved in basal defense and nonhost resistance to powdery mildew fungi. *Plant Physiology* **163**, 896-906.

Pinto, V.A. (2018). Avaliação do potencial do ácido salicílico e do metil jasmonato contra o cancro bacteriano do kiwi causado pela *Pseudomonas syringae* pv*. actinidiae* (Psa). Master's Thesis, Faculty of Sciences, Faculty of Porto, 100 pp. Available at: https://hdl.handle.net/10216/118820 [Last accessed in 16 January 2021].

Pobiega, K., Kraśniewska, K., Derewiaka, D., Gniewosz, M. (2019). Comparison of the antimicrobial activity of propolis extracts obtained by means of various extraction methods. *Journal of Food Science and Technology* **56**, 5386-5395.

Pucci, N., Laura, O., Vanessa, M., Valentina, L., Angela, B., Massimo, P. Stefania, L. (2018). essential oils with inhibitory capacities on *Pseudomonas syringae* pv*. actinidiae*, the causal agent of Kiwifruit Bacterial Canker. *Asian Journal of Plant Pathology* **12**, 16-26.

Purahong, W., Orrù, L., Donati, I., Perpetuini, G., Cellini, A., Lamontanara, A., Michelotti, V., Tacconi, G., Spinelli, F. (2018). Plant microbiome and its link to plant health: host species, organs and *Pseudomonas syringae* pv*. actinidiae* infection shaping bacterial phyllosphere communities of kiwifruit plants. *Frontiers in Plant Science* **9**, 1563. DOI: 10.3389/fpls.2018.01563.

Qadir, O., Siervo, M., Seal, C.J., Brandt, K. (2017). Manipulation of contents of nitrate, phenolic acids, chlorophylls, and carotenoids in lettuce (*Lactuca sativa* L.) via contrasting responses to nitrogen fertilizer when grown in a controlled environment. *Journal of Agricultural and Food Chemistry* **65**(46), 10003-10010.

Qin, Z., Zhang, J., Jiang, Y., Wang, R., Wu, R. (2020). Predicting the potential distribution of *Pseudomonas syringae* pv*. actinidiae* in China using ensemble models. *Plant Pathology* **69**, 120-131.

Qu, F., Ye, X., Morris, T. (2008). *Arabidopsis DRB4*, *AGO1*, *AGO7*, and *RDR6* participate in a *DCL4*-initiated antiviral RNA silencing pathway negatively regulated by *DCL1*. *Proceedings of the National Academy of Sciences* **105**, 14732-14737.

R Core Team. (2019). R: a language and environment for statistical computing. R Foundation for Statistical Computing, Vienna, Austria. https://www.R-project.org/

Raab, T.K., Terry, N. (1994). Nitrogen-source regulation of growth and photosynthesis in *Beta vulgaris* L. *Plant Physiology* **105**, 1159-1166.

Rajniak, J., Barco, B., Clay, N.K., Sattely, E. (2015). A new cyanogenic metabolite in *Arabidopsis* required for inducible pathogen defense. *Nature* **525**, 376-379.

Ramírez-Carrasco, G., Martínez-Aguilar, K., Alvarez-Venegas, R. (2017). Transgenerational defense priming for crop protection against plant pathogens: a hypothesis. *Frontiers in Plant Science* **8**, 696. DOI: 10.3389/fpls.2017.00696.

Raza, K., Mishra, A. (2012). A novel anticlustering filtering algorithm for the prediction of genes as a drug target. *American Journal of Biomedical Engineering* **2**(5), 206-211.

Reglinski, T., Vanneste, J., Wurms, K., Gould, E., Spinelli, F., Rikkerink, E. (2013). Using fundamental knowledge of induced resistance to develop control strategies for bacterial canker of kiwifruit caused by *Pseudomonas syringae* pv*. actinidiae*. *Frontiers in Plant Science* **4**, 24. DOI: 10.3389/fpls.2013.00024.

Reis, A.R., Favarin, J.L., Gratao, P.L., Capaldi, F.R., Azevedo, R.A. (2015). Antioxidant metabolism in coffee (*Coffea arabica* L.) plants in response to nitrogen supply. *Theoretical and Experimental Plant Physiology* **27**, 203-213.

Renzi, M., Copini, P., Taddei, A., Rossetti, A., Gallipoli, L., Mazzaglia, A., Balestra, G.M. (2012). Bacterial canker on kiwifruit in Italy: anatomical changes in the wood and in the primary infection sites. *Phytopathology* **102**(9), 827-840.

Rezzonico, E., Flury, N., Meins, F., Beffa, R. (1998). Transcriptional down-regulation by abscisic acid of pathogenesis-related beta-1,3-glucanase genes in tobacco cell cultures. *Plant Physiology* **117**(2), 585-592.

Rigsby, C.M., Shoemaker, E., Mallinger, M.M., Orians, C.M., Preisser, E.L. (2019). Conifer responses to a stylet-feeding invasive herbivore and induction with methyl jasmonate: impact on the expression of induced defences and a native folivore. *Agricultural and Forest Entomology* **21**(2), 227-234.

Rinaldo, A., Ayliffe, M. (2015). Gene targeting and editing in crop plants: a new era of precision opportunities. *Molecular Breeding* 35, 40. DOI: 10.1007/s11032-015-0210-z.

Rinallo, C., Modi, G. (2002). Content of oxalate in *Actinidia deliciosa* plants grown in nutrient solutions with different nitrogen forms. *Biologia Plantarum* **45**(1), 137-139.

Robinson, M., McCarthy, D.J., Smyth, G. (2010). edgeR: a bioconductor package for differential expression analysis of digital gene expression data. *Bioinformatics* **26**, 139-140.

Rossetti, A., Mazzaglia, A., Muganu, M., Paolocci, M., Sguizzato, M., Esposito, E., Cortesi, R., Balestra, G.M. (2017). Microparticles containing gallic and ellagic acids for the biological control of bacterial diseases of kiwifruit plants. *Journal of Plant Diseases and Protection* **124**, 563-575.

Saei, A., Hoeata, K., Krebs, A., Sutton, P., Herrick, J., Wood, M., Gea, L. (2018). The status of *Pseudomonas syringae* pv. *actinidiae* (Psa) in the New Zealand kiwifruit breeding programme in relation to ploidy level. *Acta Horticulturae* **1218**, 293-298.

Santiago, J., Rodrigues, A., Saez, A., Rubio, S., Antoni, R., Dupeux, F., Park, S., Márquez, J.A., Cutler, S., Rodríguez, P.L. (2009). Modulation of drought resistance by the abscisic acid receptor *PYL5* through inhibition of clade A *PP2Cs*. *The Plant Journal: for Cell and Molecular Biology* **60**(4), 575-588.

Santoni, F., Paolini, J., Barboni, T., Costa, J. (2014). Relationships between the leaf and fruit mineral compositions of *Actinidia deliciosa* var. Hayward according to nitrogen and potassium fertilization. *Food Chemistry* **147**, 269-271.

Santos, C.S., Roriz, M., Carvalho, S.M.P., Vasconcelos, M.W. (2015). Iron partitioning at an early growth stage impacts iron deficiency response in soybean plants (*Glycine max* L.). *Frontiers in Plant Science* **6**, 325. DOI: 10.3389/fpls.2015.00325.

Sartori, A., Bevilacqua, D., Terlizzi, M., Cintio, A.D., Rosato, T., Caboni, E., Ferrante, P., Scortichini, M., Cipriani, G. (2015). EMS mutagenesis and selection of genotypes resistant or tolerant to *Pseudomonas syringae* pv*. actinidiae*. *Acta Horticulturae* **1096**, 221-228.

Sawada, H., Fujikawa, T. (2019). Genetic diversity of *Pseudomonas syringae* pv*. actinidiae*, pathogen of kiwifruit bacterial canker. *Plant Pathology* **68**, 1235-1248.

Sawada, H., Kondo, K., Nakaune, R. (2016). Novel biovar (biovar 6) of *Pseudomonas syringae* pv*. actinidiae* causing bacterial canker of kiwifruit (*Actinidia deliciosa*) in Japan. *Japanese Journal of Phytopathology* **82**, 101-115.

Sawada, H., Miyoshi, T, Ide, Y. (2014). Novel MLSA group (Psa5) of *Pseudomonas syringae* pv*. actinidiae* causing bacterial canker of kiwifruit (*Actinidia chinensis*) in Japan. *Japanese Journal of Phytopathology* **80**, 171-184.

Schauer, N., Steinhauser, D., Strelkov, S., Schomburg, D., Allison, G., Moritz, T., Lundgren, K., Roessner-Tunali, U., Forbes, M.G., Willmitzer, L., Fernie, A.R., Kopka, J. (2005). GC-MS libraries for the rapid identification of metabolites in complex biological samples. *FEBS Letters* **579**, 1332-1337.

Schmittgen, T.D., Zakrajsek, B.A. (2000). Effect of experimental treatment on housekeeping gene expression: validation by real-time, quantitative RT-PCR. *Journal of Biochemical and Biophysical Methods* **46**, 69-81.

Sciubba, F., Cocco, M.E., Angori, G., Spagnoli, M., Salvador, F.R., Engel, P., Delfini, M. (2019). NMR-based metabolic study of leaves of three species of *Actinidia* with different degrees of susceptibility to *Pseudomonas syringae* pv*. actinidiae*. *Natural Product Research* **34**, 2043-2050.

Scortichini, M. (2014). Field efficacy of chitosan to control *Pseudomonas syringae* pv*. actinidiae*, the causal agent of kiwifruit bacterial canker. *European Journal of Plant Pathology* **140**, 887-892.

Scortichini, M. (2016). Field efficacy of a zinc-copper-hydracid of citric acid biocomplex compound to reduce oozing from winter cankers caused by *Pseudomonas syringae* pv*. actinidiae* to *Actinidia* spp. *Journal of Plant Pathology* **98**, 651-655.

Scortichini, M., Marcelletti, S., Ferrante, P.I., Petriccione, M., Firrao, G. (2012). *Pseudomonas syringae* pv*. actinidiae*: a re-emerging, multi-faceted, pandemic pathogen. *Molecular Plant Pathology*, **13**(7), 631-40.

Serizawa, S., Ichikawa, T. (1993a). Epidemiology of bacterial canker of kiwifruit. *Japanese Journal of Phytopathology* **59**(4), 452-459.

Serizawa, S., Ichikawa, T. (1993b). Epidemiology of bacterial canker of kiwifruit, 3: The seasonal changes of bacterial population in lesions and of its exudation from lesion. *Japanese Journal of Phytopathology* ***59***, 469-476.

Serizawa, S., Ichikawa, T. (1993c). Epidemiology of bacterial canker of kiwifruit. 2. The most suitable times and environments for infection on new canes. *Japanese Journal of Phytopathology* **59**(4), 460-468.

Serizawa, S., Ichikawa, T. (1993d). Epidemiology of bacterial canker of kiwifruit. 4. Optimum temperature for disease development on new canes. *Japanese Journal of Phytopathology* **59**(6), 694-701.

Serizawa, S., Ichikawa, T., Suzuki, H. (1994). Epidemiology of bacterial canker of kiwifruit. 5. Effect of infection in fall to early winter on the disease development in branches and trunk after winter. *Japanese Journal of Phytopathology* **60**(2), 237-244.

Serizawa, S., Ichikawa, T., Takikawa, Y., Tsuyumu, S. (1989). Occurrence of bacterial canker of kiwifruit in Japan: description of symptoms, isolation of the pathogen and screening of bactericides. *Japanese Journal of Phytopathology* **55**, 427-436.

Sevengor, S., Yasar, F., Kusvuran, S, Ellialtioglu, S. (2011). The effect of salt stress on growth, chlorophyll content, lipid peroxidation and antioxidative enzymes of pumpkin seedling. *African Journal of Agricultural Research* **6**(21), 4920-4924.

Shanmugam, A., Kathiresan, K., Nayak, L. (2016). Preparation, characterization and antibacterial activity of chitosan and phosphorylated chitosan from cuttlebone of *Sepia kobiensis* (Hoyle, 1885). *Biotechnology Reports* **9**, 25-30.

Sharma, P., Jha, A.B., Dubey, R.S, Pessarakli, M. (2012). Reactive oxygen species, oxidative damage, and antioxidative defense mechanism in plants under stressful conditions. *Journal of Botany* **2012**, 217037. DOI: 10.1155/2012/217037.

Simonetti, G., Pucci, N., Brasili, E., Valletta, A., Sammarco, I., Carnevale, E., Pasqua, G., Loreti, S. (2020). *In vitro* antimicrobial activity of plant extracts against *Pseudomonas syringae* pv. *actinidiae* causal agent of bacterial canker in kiwifruit. *Plant Biosystems - An International Journal Dealing with all Aspects of Plant Biology* **154**, 100-106.

Song, Y., Choi, M., Choi, G., Park, I., Oh, C. (2016). Antibacterial activity of cinnamaldehyde and estragole extracted from plant essential oils against *Pseudomonas syringae* pv. *actinidiae* causing bacterial canker disease in kiwifruit. *The Plant Pathology Journal* **32**, 363-370.

Song, Y., Sun, L., Lin, M., Chen, J., Qi, X., Hu, C., Fang, J. (2019). Comparative transcriptome analysis of resistant and susceptible kiwifruits in response to *Pseudomonas syringae* pv. *actinidiae* during early infection. *PLoS ONE*, 14(2), e0211913. DOI: 10.1371/journal.pone.0211913.

Soylu, E.M., Kurt, Ş., Soylu, S. (2010). *In vitro* and *in vivo* antifungal activities of the essential oils of various plants against tomato grey mould disease agent *Botrytis cinerea*. *International Journal of Food Microbiology*, 143(3), 183-189.

Spinelli, F., Donati, I., Vanneste, J.L., Costa, M, Costa, G. (2011). Real time monitoring of the interactions between *Pseudomonas syringae* pv. *actinidiae* and *Actinidia* species. *Acta Horticulturae* **913**, 461-466.

Stefani, E., Giovanardi, D. (2012). Dissemination of *Pseudomonas syringae pv. actinidiae* through pollen and its epiphytic life on leaves and fruits. *Phytopathologia Mediterranea* **50**(3), 489-496.

Stefaniak, J., Przybył, J., Latocha, P., Łata, B. (2020). Bioactive compounds, total antioxidant capacity and yield of kiwiberry fruit under different nitrogen regimes in field conditions. *Journal of the Science of Food and Agriculture* **100**, 3832-3840.

Stefaniak, J., Stasiak, A., Latocha, P., Łata, B. (2019). Seasonal changes in macronutrients in the leaves and fruit of kiwiberry: nitrogen level and cultivar effects. *Communications in Soil Science and Plant Analysis* **50**, 2913-2926.

Stella de Freitas, T.F., Stout, M.J., Santana, J. (2019). Effects of exogenous methyl jasmonate and salicylic acid on rice resistance to *Oebalus pugnax*. *Pest Management Science* **75**(3):744-752.

Stewart, A., Hill, R., Stark, C. (2011). Desktop evaluation on commercially available microbial-based products for control or suppression of *Pseudomonas syringae* pv. *actinidiae*. Report No 1. Bio-Protection Research Centre, Lincoln University, Lincoln, New Zealand. Available at: https://www.kvh.org.nz/vdb/document/481 [Last accessed in 16 January 2021].

Sumanta, N., Haque, C.I., Nishika, J., Suprakrash, R. (2014). Spectrophotometric analysis of chlorophylls and carotenoids from commonly grown fern species by using various extracting solvents. *Research Journal of Chemical Sciences* **4**, 63-69.

Sun, L., Fang, J., Zhang, M., Qi, X., Lin, M., Chen, J. (2020). Molecular cloning and functional analysis of the *NPR1* homolog in kiwifruit (*Actinidia eriantha*). *Frontiers in Plant Science* **11**, 551201. DOI: 10.3389/fpls.2020.551201.

Tabatabaei, S.J., Fatemi, L., Fallahi, E. (2006). Effect of ammonium: nitrate ratio on yield, calcium concentration, and photosynthesis rate in strawberry. *Journal of Plant Nutrition* **29**, 1273-1285.

Taheri, P, Kakooee, T. (2017). Reactive oxygen species accumulation and homeostasis are involved in plant immunity to an opportunistic fungal pathogen. *Journal of Plant Physiology* **216**, 152-163.

Tahir, J., Hoyte, S., Bassett, H., Brendolise, C., Chatterjee, A., Templeton, K., Deng, C., *et al*. (2019). Multiple quantitative trait loci contribute to resistance to bacterial canker incited by *Pseudomonas syringae* pv*. actinidiae* in kiwifruit (*Actinidia chinensis*). *Horticulture Research* **6**, 101. DOI: 10.1038/s41438-019-0184-9.

Tamura, K., Imamura, M., Yoneyama, K., Kohno, Y., Takikawa, Y., Yamaguchi, I., Takahashi, H. (2002). Role of phaseolotoxin production by *Pseudomonas syringae* pv*. actinidiae* in the formation of halo lesions of kiwifruit canker disease. *Physiological and Molecular Plant Pathology* **60**, 207-214.

Tang, P., Xu, Q., Shen, R., Yao, X. (2019a). Phylogenetic relationship in *Actinidia* (*Actinidia*ceae) based on four noncoding chloroplast DNA sequences. *Plant Systematics and Evolution* **305**, 787-796.

Tang, S., Prodhan, Z., Biswas, S., Le, C., Sekaran, S. (2018). Antimicrobial peptides from different plant sources: Isolation, characterisation, and purification. *Phytochemistry* **154**, 94-105.

Tang, W., Sun, X., Yue, J., Tang, X., Jiao, C., Yang, Y., Niu, X., Miao, M., Zhang, D., Huang, S., Shi, W.L., Li, M., Fang, C., Fei, Z., Liu, Y. (2019b). Chromosome-scale genome assembly of kiwifruit *Actinidia eriantha* with single-molecule sequencing and chromatin interaction mapping. *GigaScience* **8**, 1-10.

Taylor, J., Mowat, A., Bollen, A., Whelan, B. (2014). Early season detection and mapping of *Pseudomonas syringae* pv. *actinidae* infected kiwifruit (*Actinidia* sp.) orchards. *New Zealand Journal of Crop and Horticultural Science* **42**, 303-311.

Teh, O., Hatsugai, N., Tamura, K., Fuji, K., Tabata, R., Yamaguchi, K., Shingenobu, S., Yamada, M., Hasebe, M., Sawa, S., Shimada, T., Hara-Nishimura, I. (2015). BEACH-domain proteins act together in a cascade to mediate vacuolar protein trafficking and disease resistance in *Arabidopsis*. *Molecular Plant* **8**(3), 389-398.

Toda, Y., Okura, F. (2019). How convolutional neural networks diagnose plant disease. *Plant Phenomics* **2019**, 9237136. DOI: 10.34133/2019/9237136.

Tomatsu, H., Takano, J., Takahashi, H., Watanabe-Takahashi, A., Shibagaki, N., Fujiwara, T. (2007). An *Arabidopsis thaliana* high-affinity molybdate transporter required for efficient uptake of molybdate from soil. *Proceedings of the National Academy of Sciences* **104**, 18807-18812.

Ton, J., Flors, V., Mauch-Mani, B. (2009). The multifaceted role of ABA in disease resistance. *Trends Plant Science* **14**, 310-317.

Tontou, R., Gaggìa, F., Baffoni, L., Devescovi, G., Venturi, V., Giovanardi, D., Stefani, E. (2016a). Molecular characterisation of an endophyte showing a strong antagonistic activity against *Pseudomonas syringae* pv*. actinidiae*. *Plant and Soil* **405**, 97-106.

Tontou, R., Giovanardi, D., Ferrari, M., Stefani, E. (2016b). Isolation of bacterial endophytes from *Actinidia chinensis* and preliminary studies on their possible use as antagonists against *Pseudomonas syringae* pv*. actinidiae*. *Journal of Berry Research* **6**, 395-406.

Tripathi, D., Raikhy, G., Kumar, D. (2019). Chemical elicitors of systemic acquired resistance - Salicylic acid and its functional analogs. *Current Plant Biology* **17**, 48-59.

Tripathi, D.K., Singh, S., Mishra, S., Chauhan, D.K., Dubey, N. (2015). Micronutrients and their diverse role in agricultural crops: advances and future prospective. *Acta Physiologiae Plantarum* **37**, 1-14.

Truman, W., Torres de Zabala, M., Grant, M. (2006). Type III effectors orchestrate a complex interplay between transcriptional networks to modify basal defence responses during pathogenesis and resistance. *The Plant Journal* **46**, 14-33.

Tsabarducas, V., Chatzistathis, T., Therios, I., Patakas, A. (2017). How nitrogen form and concentration affect growth, nutrient accumulation and photosynthetic performance of *Olea europaea* L. (cv. "Kalamon"). *Scientia Horticulturae* **218**, 23-29.

Tyson, J., Curtis, C., Manning, M., Dobson, S., McKenna, C. (2016). Preliminary investigations of the risk of plant debris as a *Pseudomonas syringae* pv*. actinidiae* inoculum source. *New Zealand Plant Protection* **69**, 11-16.

Tyson, J., Rees-George, J., Curtis, C., Manning, M., Fullerton, R. (2012). Survival of *Pseudomonas syringae* pv*. actinidiae* on the orchard floor over winter. *New Zealand Plant Protection* **65**, 25-28.

Ushiyama, K., Suyama, K., Kita, N., Aono, N., Fujii, H. (1992). Isolation of kiwifruit canker pathogen, *Pseudomonas syringae* pv*. actinidiae* from leaf spot of tara vine (*Actinidia arguta* Planch.). *Japanese Journal of Phytopathology* **58**, 476-479.

Vaerman, J.L., Saussoy, P., Ingargiola, I. (2004). Evaluation of real-time PCR data. *Journal of Biological Regulators & Homeostatic Agents* **18**, 212-214.

Valente, L.M., Custódio, M., Batista, S., Fernandes, H., Kiron, V. (2019). Defatted microalgae (*Nannochloropsis* sp.) from biorefinery as a potential feed protein source to replace fishmeal in European sea bass diets. *Fish Physiology and Biochemistry* **45**(3), 1067-1081.

van Esse, H., Reuber, T., van der Does, D. (2020). Genetic modification to improve disease resistance in crops. *New Phytologist* **225**, 70-86.

van Hulten, M., Pelser, M., van Loon, L., Pieterse, C., Ton, J. (2006). Costs and benefits of priming for defense in *Arabidopsis*. *Proceedings of the National Academy of Sciences of the United States of America* **103**, 5602-5607.

Vanneste, J. (2017). The scientific, economic, and social impacts of the New Zealand outbreak of bacterial canker of kiwifruit (*Pseudomonas syringae* pv*. actinidiae*). *Annual Reviews of Phytopathology* **55**, 377-399.

Vanneste, J., Moffat, B., Oldham, J. (2012). Survival of *Pseudomonas syringae* pv*. actinidiae* on *Cryptomeria japonica*, a non-host plant used as shelter belts in kiwifruit orchards. *New Zealand Plant Protection* **65**, 1-7.

Vanneste, J., Reglinski, T., Yu, J., Cornish, D.A. (2015). Multiplication and movement of *Pseudomonas syringae* pv*. actinidiae* in kiwifruit plants. *Acta Horticulturae* **1095**, 117-122.

Vanneste, J., Yu, J., Cornish, D., Max, S., Clark, G. (2011). Presence of *Pseudomonas syringae* pv*. actinidiae*, the causal agent of bacterial canker of kiwifruit, on symptomatic and asymptomatic tissues of kiwifruit. *New Zealand Plant Protection* **64**, 241-245.

Vanneste, J.L., Cornish, D.A., Yu, J, Stokes, A. (2014). First report of *Pseudomonas syringae* pv*. actinidiae* the causal agent of bacterial canker of kiwifruit on *Actinidia arguta* vines in New Zeal. *Plant Disease* **98**, 418.

Vanneste, J.L., Yu, J., Cornish, D.A., Tanner, D.J. Windner, R., Chapman, J.R., Taylor, R.K., Mackay, J.F, Dowlut, S. (2013). Identification, virulence, and distribution of two biovars of *Pseudomonas syringae* pv*. actinidiae* in New Zealand. *Plant Disease* **97**, 708-719.

Varkonyi-Gasic, E., Wang, T., Voogd, C., Jeon, S., Drummond, R.S., Gleave, A., Allan, A. (2019). Mutagenesis of kiwifruit CENTRORADIALIS-like genes transforms a climbing woody perennial with long juvenility and axillary flowering into a compact plant with rapid terminal flowering. *Plant Biotechnology Journal* **17**, 869 - 880.

Vavala, E., Passariello, C., Pepi, F., Colone, M., Garzoli, S., Ragno, R., Pirolli, A., Stringaro, A., Angiolella, L. (2016). Antibacterial activity of essential oils mixture against PSA. *Natural Product Research* **30**, 412-418.

Vincent, J.G., Vincent, H.W., Morton, J. (1944). Filter paper disc modification of the oxford cup penicillin determination. *Proceedings of the Society for Experimental Biology and Medicine* **55**, 162-164.

Vu, T.T., Kim, H., Tran, V.K., Vu, H.D., Hoang, T., Han, J.W., Choi, Y., Jang, K., Choi, G., Kim, J. (2017). Antibacterial activity of tannins isolated from *Sapium baccatum* extract and use for control of tomato bacterial wilt. *PLoS ONE* **12**, e0181499. DOI: 10.1371/journal.pone.0181499.

Wang, F., Li, J., Ye, K., Liu, P., Gong, H., Jiang, Q., Qi, B., Mo, Q. (2019). An *in vitro Actinidia* bioassay to evaluate the resistance to *Pseudomonas syringae* pv*. actinidiae*. *The Plant Pathology Journal* **35**, 372-380.

Wang, F.-M., Mo, Q.-H., Ye, K.-Y., Gong, H.-J., Qi, B.-B., Liu, P.-P-, Jiang, Q.-S., LI, J.-W. (2020a). Evaluation of the wild *Actinidia* germplasm for resistance to *Pseudomonas syringae* pv*. actinidiae*. *Plant Pathology* **69**, 979-989.

Wang, M.Y., Siddiqi, M.Y., Glass, D.M. (1996). Interaction between K^+ and NH_4^+: Effects on ion uptake by rice roots. *Plant, Cell & Environment* **19**, 1037-1046.

Wang, R., Li, Q., He, S., Liu, Y., Wang, M., Jiang, G. (2018c). Modeling and mapping the current and future distribution of *Pseudomonas syringae* pv*. actinidiae* under climate change in China. *PLoS ONE, 13*., e0192153. DOI: 10.1371/journal.pone.0192153.

Wang, T., Jia, Z., Zhang, J., Liu, M., Guo, Z., Wang, G. (2020b). Identification and analysis of NBS-LRR Genes in *Actinidia chinensis* genome. *Plants* **9**(10), 1350. DOI: 10.3390/plants9101350.

Wang, T., Lin-Wang, K. (2007). High throughput transformation of *Actinidia*: a platform for kiwifruit functional genomics and molecular breeding. *Transgenic Plant Journal* **1**, 175-184.

Wang, T., Wang, G., Jia, Z.-H., Pan, D.-L., Zhang, J.-Y., Guo, Z.-R. (2018a). Transcriptome analysis of kiwifruit in response to *Pseudomonas syringae* pv*. actinidiae* infection. *International Journal of Molecular Sciences* **19**(2), 373. DOI: 10.3390/ijms19020373.

Wang, X., Below, F.E. (1998). Accumulation and partitioning of mineral nutrients in wheat as influenced by nitrogen form. *Journal of Plant Nutrition* **21**, 49-61.

Wang, Z., Liu, Y., Li, D., Li, L., Zhang, Q., Wang, S., Huang, H. (2017a). Identification of circular RNAs in kiwifruit and their species-specific response to bacterial canker pathogen invasion. *Frontiers in Plant Science* **8**, 413. DOI: 10.3389/fpls.2017.00413.

Wang, Z., Liu, Y., Li, L., Li, D., Zhang, Q., Guo, Y., Wang, S., Zhong, C, Huang, H. (2017b). Whole transcriptome sequencing of *Pseudomonas syringae* pv*. actinidiae*-infected kiwifruit plants reveals species-specific interaction between long non-coding RNA and coding genes. *Scientific Reports* **7**, 4910. DOI: 10.1038/s41598-017-05377-y

Wang, Z., Wang, S., Li, D., Zhang, Q., Li, L., Zhong, C., Liu, Y., Huang, H. (2018b). Optimized paired-sgRNA/Cas9 cloning and expression cassette triggers high-efficiency multiplex genome editing in kiwifruit. *Plant Biotechnology Journal* **16**, 1424-1433.

Warnes, G.R., Bolker, B., Bonebakker, L., Gentleman, R., Huber, W., Liaw A., Thomas L., Maechler, M., Magnusson, A., Moeller, S., Schwartz, M., Venables, B. (2020). gplots: various r programming tools for plotting data. R package version 3.0.3. https://CRAN.R-project.org/package=gplots.

Weingart, H., Ullrich, H., Geider, K, Volksch B. (2001). The role of ethylene production in virulence of *Pseudomonas syringae* pvs. *glycinea* and *phaseolicola*, *Phytopathology* **91**, 511-518.

Wicaksono, W., Jones, E., Casonato, S., Monk, J., Ridgway, H. (2018). Biological control of *Pseudomonas syringae* pv*. actinidiae* (Psa), the causal agent of bacterial canker of kiwifruit, using endophytic bacteria recovered from a medicinal plant. *Biological Control* **116**, 103-112.

Wilson, L., Hetzel, S., Pockrandt, C., Reinert, K., Bauer, C. (2019). VARSCOT: variant-aware detection and scoring enables sensitive and personalized off-target detection for CRISPR-Cas9. *BMC Biotechnology* **19**, 40. DOI: 10.1186/s12896-019-0535-5.

Woldemariam, M.G., Onkokesung, N., Baldwin, I.T., Galis, I. (2012). Jasmonoyl-l-isoleucine hydrolase 1 (*JIH1*) regulates jasmonoyl-l-isoleucine levels and attenuates plant defenses against herbivores. *The Plant Journal* **72**(5), 758-767.

Wurms, K., Gould, E., Chee, A., Taylor, J.T., Curran, B., Reglinski, T. (2017b). Elicitor induction of defence genes and reduction of bacterial canker in kiwifruit. *New Zealand Plant Protection* **70**, 272-284.

Wurms, K., Hardaker, A.J., Chee, A.A., Bowen, J., Phipps, J.E., Taylor, J., Jensen, D., Cooney, J., Wohlers, M., Reglinski, T. (2017a). Phytohormone and putative defense gene expression differentiates the response of 'Hayward' kiwifruit to Psa and Pfm infections. *Frontiers in Plant Science* **8**, 1366. DOI: 10.3389/fpls.2017.01366.

Xiong, L., Lee, H., Ishitani, M., Zhu, J. (2002). Regulation of osmotic stress-responsive gene expression by the *LOS6*/*ABA1* locus in *Arabidopsis*. *The Journal of Biological Chemistry* **277**, 8588-8596.

Xue, J., Fan, Y., Su, B., Fuentes, S. (2019). Assessment of canopy vigor information from kiwifruit plants based on a digital surface model from unmanned aerial vehicle imagery. *International Journal of Agricultural and Biological Engineering* **12**, 165-171.

Yang, S., Peng, L., Cheng, Y., Chen, F., Pan, S. (2010). Control of citrus green and blue molds by Chinese propolis. *Food Science and Biotechnology* **19**, 1303-1308.

Yasuda, M., Ishikawa, A., Jikumaru, Y., Seki, M., Umezawa, T., Asami, T., Maruyama-Nakashita, A., Kudo, T., Shinozaki, K., Yoshida, S., Nakashita, H. (2008). Antagonistic interaction between systemic acquired resistance and the abscisic acid-mediated abiotic stress response in *Arabidopsis*[W]. *The Plant Cell* **20**, 1678-1692.

Yin, Y., Ni, P., Deng, B., Wang, S., Xu, W., Wang, D. (2019). Isolation and characterisation of phages against *Pseudomonas syringae* pv*. actinidiae*. *Acta Agriculturae Scandinavica, Section B — Soil & Plant Science* **69**, 199 - 208.

Yoon, M., Rikkerink, E. (2019). *Rpa1* mediates an immune response to *avrRpm1*$_{Psa}$ and confers resistance against *Pseudomonas syringae* pv*. actinidiae*. *The Plant Journal: for Cell and Molecular Biology* **102**(4), 688-702.

Yoshioka, H., Sugie, K., Park, H., Maeda, H., Tsuda, N., Kawakita, K., Doke, N. (2001). Induction of plant gp91 *phox* homolog by fungal cell wall, arachidonic acid, and salicylic acid in potato. *Molecular Plant-Microbe Interactions* **14**(6), 725-736.

Young, J. (2012). *Pseudomonas syringae* pv*. actinidiae* in New Zealand. *Journal of Plant Pathology* **94**, 5-10.

Yu, J.G., Lim, J.A., Song, Y., Heu, S.G., Kim, G.H., Koh, Y., Oh, C. (2016). Isolation and characterization of bacteriophages against *Pseudomonas syringae* pv*. actinidiae* causing

bacterial canker disease in kiwifruit. *Journal of Microbiology and Biotechnology* **26**(2), 385-393.

Yusuf, Y., Durdane, Y., Servet, A. (2005). Antifungal activity of Turkish propolis against *Phytophthora* species. *Plant Pathology Journal* **4**, 58-60.

Zebarth, B., Tai, H.H., Luo, S., Millard, P., Koeyer, D.D., Li, X., Xiong, X. (2012). Effect of nitrogen form on gene expression in leaf tissue of greenhouse grown potatoes during three stages of growth. *American Journal of Potato Research* **89**, 315-327.

Zhang, F., Niu, J., Zhang, W., Chen, X., Li, C., Yuan, L., Xie, J. (2010b). Potassium nutrition of crops under varied regimes of nitrogen supply. *Plant and Soil* **335**(1-2), 21-34.

Zhang, H., Li, H., Feng, J., Xiao, J., Song, G., Xie, M. (2013). Investigation and analysis of infection caused by *Pseudomonas syringae* pv. *actinidiae* and its affecting factors in Zhejiang province. *Acta Agriculturae Zhejiangensis* **25**, 832-835.

Zhang, J., Du, X., Wang, Q., Chen, X., Lv, D., Xu, K., Qu, S., Zhang, Z. (2010a). Expression of pathogenesis related genes in response to salicylic acid, methyl jasmonate and 1-aminocyclopropane-1-carboxylic acid in *Malus hupehensis* (Pamp.) Rehd. *BMC Research Notes* **3**, 208. DOI: 10.1186/1756-0500-3-208.

Zhang, S., Yang, Q, Ma, R. (2007). *Erwinia carotovora* ssp. *carotovora* infection induced "defense lignin" accumulation and lignin biosynthetic gene expression in Chinese cabbage (*Brassica rapa* L. ssp. *pekinensis*). J. Integr. *Plant Biology* **49**(7), 993-1002.

Zhang, Y., Zhong, C., Liu, Y., Zhang, Q., Sun, X., Li, D. (2017). Agronomic trait variations and ploidy differentiation of kiwiberries in northwest China: implication for breeding. *Frontiers in Plant Science*, **8**, 711. DOI: 10.3389/fpls.2017.00711.

Zhao, J., Devaiah, S., Wang, C., Li, M., Welti, R., Wang, X. (2013). *Arabidopsis* phospholipase Dβ1 modulates defense responses to bacterial and fungal pathogens. *The New Phytologist* **199**(1), 228-240.

Zhao, S., Hong, W., Wu, J., Wang, Y., Ji, S., Zhu, S., Wei, C., Zhang, J., Li, Y. (2017). A viral protein promotes host *SAMS1* activity and ethylene production for the benefit of virus infection. *eLife* **6**, e27529. 10.7554/eLife.27529.

Zheng, X., Spivey, N.W., Zeng, W., Liu, P., Fu, Z.Q., Klessig, D.F., He, S.Y, Dong, X. (2012). Coronatine promotes *Pseudomonas syringae* virulence in plants by activating a signalling cascade that inhibits salicylic acid accumulation. *Cell Host & Microbe* **11**, 587-596.

Zhishen, J., Mengcheng, T., Jianming, W. (1999). The determination of flavonoid concentrations in mulberry and their scavenging effects on superoxide radicals. *Food Chemistry* **64**, 555-559.

Zoysa, G., Cameron, A., Hegde, V., Raghothama, S., Sarojini, V. (2015). Antimicrobial peptides with potential for biofilm eradication: synthesis and structure activity relationship studies of battacin peptides. *Journal of Medicinal Chemistry* **58**, 625-639.